

Organoselenium Chemistry: Role of Intramolecular Interactions[†]

Anna J. Mukherjee,[‡] Sanjio S. Zade,[§] Harkesh B. Singh,^{*,‡} and Raghavan B. Sunoj[‡]

Department of Chemistry, Indian Institute of Technology Bombay, Powai, Mumbai 400 076, India, and Department of Chemical Sciences, Indian Institute of Science Education and Research Kolkata, Mohanpur 741252, Nadia, West Bengal, India

Received October 26, 2009

Contents

1. Introduction	4357	5. Intramolecularly Coordinated Organoselenium Compounds as Glutathione Peroxidase Mimics	4399
2. Intramolecularly Coordinated Organoselenium Compounds: Hypervalency	4359	6. Theoretical Models for Interpretation of Nonbonding Interactions	4407
2.1. Intramolecular Nonbonded Se...N Interactions	4359	7. Summary	4412
2.2. Transannular Se...N Interactions	4366	8. Acknowledgments	4412
2.3. Se...O Nonbonded Intramolecular Interactions and Se...O Transannular Interactions	4367	9. References	4412
2.4. The Se...H "Hydrogen Bond"	4374		
2.5. Other Types of Nonbonded Interaction	4375		
2.5.1. Se...Halogen	4375		
2.5.2. Se...S Interactions	4378		
2.5.3. Se...Se Interactions	4378		
3. Intramolecularly Coordinated Organoselenium Compounds as Ligands	4380		
3.1. Neutral Ligands	4381		
3.2. Anionic Ligands	4385		
4. Intramolecularly Coordinated Organoselenium Compounds in Organic Synthesis	4387		
4.1. Asymmetric Selenoxide Elimination and [2,3]-Sigmatropic Rearrangement	4387		
4.2. Methoxyselenylation and Oxselenylation	4389		
4.3. Catalytic Methoxyselenylation	4394		
4.4. Azidoselenenylation	4394		
4.5. Carboselenenylation	4394		
4.6. Asymmetric Selenocyclization	4394		
4.7. Organoselenium Compounds with Se...N Interaction as Oxidizing Agents	4396		
4.8. Asymmetric Hydrosilylation	4397		
4.9. Selective Hydrogenation Catalysts	4398		
4.10. Miscellaneous	4398		
4.10.1. Selenoxide Catalyzed Bromination of Organic Substrates with Sodium Bromide and Hydrogen Peroxide	4398		
4.10.2. Hydroxyselenation of Allylic Alcohols	4398		
4.10.3. Influence of a Hydroxy Group in Asymmetric Reduction of Selenides: Enantioselective Synthesis of Naturally Occurring Monoterpenes	4398		
4.10.4. Selenoxides as Leaving Groups: Epoxide Synthesis	4399		
4.10.5. Stereoselective Isoquinoline Alkaloid Synthesis with New Diselenides	4399		

1. Introduction

In 1836 the first organoselenium compound, diethyl selenide, was prepared by Löwig,¹ and it was isolated in the pure form in 1869.² Early selenium chemistry involved the synthesis of simple aliphatic compounds such as selenols (RSeH), selenides (RSeR), and diselenides (RSeSeR); however, because of their malodorous nature, these compounds were difficult to handle. This, combined with the instability of certain derivatives and difficulties in purification, meant that selenium chemistry was slow to develop. By the 1950s, the number of known selenium compounds had increased significantly, but it was not until the 1970s, when several new reactions leading to novel compounds with unusual properties were discovered, that selenium chemistry began to attract more general interest.^{3–9} Aryl-substituted compounds were synthesized that were found to be less volatile and more pleasant to handle than the earlier aliphatic compounds. Compounds containing selenium in high oxidation states are relatively easy to manipulate using modern techniques.^{4c} Organoselenium chemistry has now become a well-established field of research, and recent advances have been brought about by the potential technical applications of selenium compounds. Today selenium compounds find application in many areas including organic synthesis,⁴ biochemistry,⁵ xerography,⁶ the synthesis of conducting materials⁷ and semiconductors,⁸ and ligand chemistry.^{4c,9} Many of these aspects of selenium chemistry are well-covered elsewhere in the literature; however, the subject of hypervalency has not attracted much attention and is the focus of this review.¹⁰

In organic compounds, selenium is usually found in a divalent state with two covalently bonded substituents and two lone pairs of valence electrons. By bonding in this way, selenium is able to complete its octet of electrons, thus giving it a noble gas configuration. It has been found, however, that in the solid state and in solution selenium frequently further interacts with a nearby heteroatom or heteroatoms (O, N, S, etc.), producing a pseudo-high-valent selenium species.¹¹ This phenomenon can be explained by assuming a nonbonded interaction between divalent selenium and a heteroatom derived from the hypervalent nature of selenium. The nonbonded

* Corresponding author.

[†] Dedicated to late Professor William R. McWhinnie, Department of Chemical Engineering and Applied Chemistry, Aston University, Birmingham B4 7ET, U.K.

[‡] Indian Institute of Technology Bombay.

[§] Indian Institute of Science Education and Research Kolkata.



Anna Mukherjee graduated in Chemistry in 1999 from the University of Wales, Swansea, and completed her M.Sc. project work under the supervision of Professor C. P. Morley. She then worked under the supervision of Professor H. B. Singh at the Indian Institute of Technology, Bombay, on intramolecular interactions. She received her Ph.D. degree from the University of Bristol (2004), under the supervision of Professor R. P. Evershed, where she continued to work on a Wellcome Trust Research Fellowship in Bioarchaeology until July 2007. Since then Anna has worked in the water industry as a drinking water quality scientist.



Sanjio S. Zade received his M.Sc. in chemistry from Amravati University in 1997. He received his Ph.D. from the Indian Institute of Technology, Bombay (1999–2004), under the supervision of Prof. H. B. Singh. He spent his postdoctoral period in the research group of Prof. Michael Bendikov at the Weizmann Institute of Science, Israel (Feinberg fellowship) (2004–2006). He then joined as a lecturer at the M. S. University, Baroda, in 2006. He currently holds a position of Assistant Professor in Chemistry at Indian Institute of Science Education and Research, Kolkata, since 2007. His research interests include the development of new π -conjugated systems and their applications as materials for organic electronics.

interactions involving a divalent selenium can be categorized into two types, structures **1** and **2** (Figure 1).¹²

In the first type, **1**, selenium weakly donates the lone pair to atom X (X = Pt, Hg, etc.) located just above the divalent Se plane, and in the second type, **2**, selenium partially accepts a lone pair of electrons from atom Y (Y = O, N, etc.) located at the backside of one of the covalent bonds. This type of interaction is responsible for the linearity of the C–Se \cdots Y bonds. In **2** the nucleophiles interact with the low-lying antibonding orbital of the selenium moiety (σ^* C–Se). This is responsible for the electrophilicity of selenium compounds. In this review, only interactions of type **2** will be discussed.

Organoselenium derivatives stabilized by intramolecular nonbonded Se \cdots Y (Y = H, N, O, S, Se, I, Cl, F) interactions are extremely versatile and have attracted considerable current interest. They find many applications, the most important of which are outlined below:



Harkesh B. Singh, born in 1956 in UP, India, obtained his Ph.D. (1979) at Lucknow University with Prof. T. N. Srivastava. In 1979, he moved to the U.K. and did a second Ph.D. at Aston University, Birmingham, under the supervision of Prof. W. R. McWhinnie (1979–1983). After a brief stay at the Indian Institute of Technology, Delhi, as Pool Scientist with Prof. B. L. Khandelwal, he joined the Indian Institute of Technology, Bombay, in 1984 as a lecturer and rose through the ranks to become a full professor in 1995. He is a Fellow of the National Academy of Sciences (FNASc), Allahabad; Indian Academy of Sciences (FASc), Bangalore; and the Royal Society of Chemistry (FRSC). He has been a Visiting Scientist at the University of California, Santa Barbara (Prof. Fred Wudl's laboratory), under the BOYS-CAST scheme. His research objectives are centred around design, synthesis, and structural studies of novel organometallic derivatives of sulphur, -selenium, and -tellurium and their applications.



Dr. Raghavan B. Sunoj obtained his Ph.D. in organic chemistry under the guidance of Professor Jayaraman Chadrachekhar from the Indian Institute of Science Bangalore in the year 2001. Subsequently, he took up a postdoctoral assignment to work with Professor Christopher M. Hadad at the Department of Chemistry, The Ohio State University, Columbus, Ohio (U.S.A.). He joined the Department of Chemistry, IIT Bombay, in the year 2003, where he is currently working as an associate professor. Sunoj has won several national recognitions such as Indian National Science Academy Young Scientist award 2006 and the National Academy of Sciences India Platinum Jubilee Young Scientist award 2008. He is currently a young associate of the Indian Academy of Sciences Bangalore. Sunoj's research interests include the applications of computational chemistry to organic, inorganic, and organometallic reactivity problems. The emphasis has been on mechanism and stereoselectivity with an objective toward exploring the fundamental factors responsible for stereoselectivity in asymmetric reactions promoted by organic and organometallic reagents. The role of microsolvation in stereoselective organic reactions is another key area of his research activity. Quantification of intramolecular and intermolecular weak interactions as well as electronic structure studies on transition metal and main group systems are also currently pursued. Sunoj has extensively interacted with a variety of experimental groups toward rationalizing interesting experimental observations using computational chemistry techniques.

(a) The synthesis of novel, hypervalent, stable organoselenium compounds in which selenium exists as a pseudo-

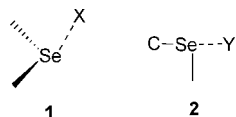


Figure 1. Two categories of the nonbonded interactions involving a divalent selenium.

high-valent species. The hypervalent nature of selenium is thought to be responsible for its high bioactivity as well as the specific redox activity of organoselenium compounds.

(b) Use as electrophilic and nucleophilic reagents in asymmetric synthesis. The intramolecular $\text{Se} \cdots \text{Y}$ interaction induces conformational rigidity in the molecule and is assumed to play a dominant role in chirality transfer.

(c) Use as ligands in chiral and achiral catalysis.

(d) Use as ligands for the isolation of monomeric metal chalcogenolates precursors for metal organic chemical vapor deposition (MOCVD) of semiconductors.

(e) Use as synthetic models for the glutathione peroxidase family of enzymes where the $\text{Se} \cdots \text{N}$ interactions play a major role in the stabilization of the key intermediate, selenenic acid.

The first section of this review will be dedicated to the pseudo-high-valent nature of the selenium atom. We will discuss the various types of intramolecular nonbonding interactions that can be seen in organoselenium compounds. The focus is on this type of interaction between selenium and nitrogen atoms; however, other interactions such as $\text{Se} \cdots \text{O}$, $\text{Se} \cdots \text{H}$, $\text{Se} \cdots \text{F}$, and $\text{Se} \cdots \text{Se}$ will also be mentioned in some detail. In section 2, we will present the use of intramolecularly coordinated organoselenium compounds as ligands. Neutral and anionic ligands will be discussed in detail as well their use as catalysts in organic synthesis, and their role as precursors to MOCVD semiconductor materials will be reported. Section 3 is dedicated to the synthetic applications of intramolecularly coordinated organoselenium compounds, a field that is well-established and rapidly expanding. Many types of reactions are extensively discussed, including asymmetric selenoxide elimination, [2,3]-sigmatropic rearrangement, asymmetric selenocyclization, methoxyselenenylation and oxyselenenylation, asymmetric electrophilic addition, hydrosilylation, and the use of this type of compound as oxidizing agents. Section 4 describes the role of selenium compounds in biological processes and the use of organoselenium compounds as models for the mammalian enzyme glutathione peroxidase (Gp.).

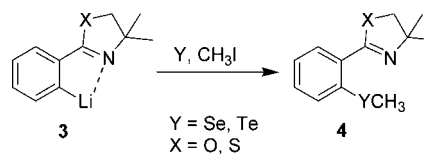
It is felt that a comprehensive review of this type is both timely and necessary and will act as a bridge between developing work in the field of selenium chemistry and two recent reviews in the tellurium field by Singh et al.¹³ and McWhinnie et al.¹⁴

2. Intramolecularly Coordinated Organoselenium Compounds: Hypervalency

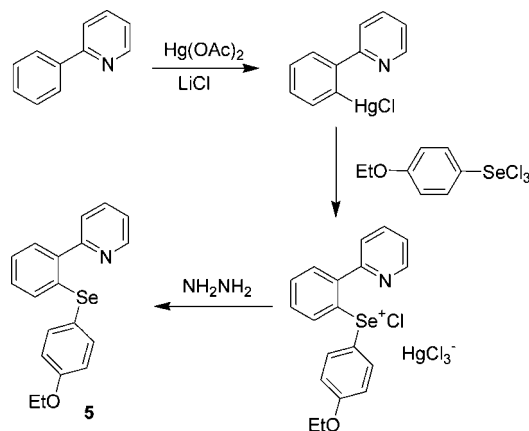
2.1. Intramolecular Nonbonded $\text{Se} \cdots \text{N}$ Interactions

The first examples of intramolecularly coordinated organoselenium compounds incorporating a $\text{Se} \cdots \text{N}$ interaction appear to have been reported by Christiaens et al. in 1984.¹⁵ It was reported that *ortho*-lithiated oxazoline intermediates **3** could be reacted with elemental selenium or tellurium and iodomethane to produce new *ortho*-chalcogenated oxazolines **4** in high yield (Scheme 1). The intermediate was stabilized

Scheme 1



Scheme 2



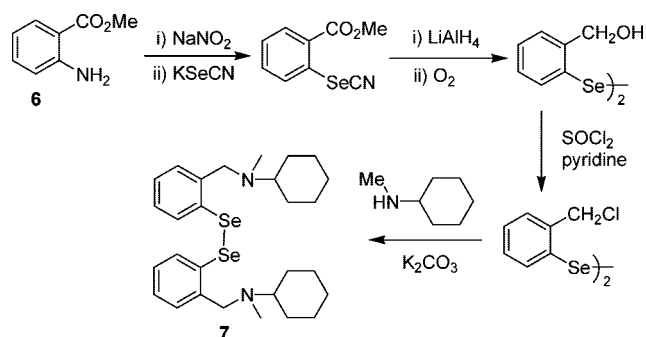
by interaction with the lone pair of electrons on the nitrogen atom. Although no crystal structure or NMR spectroscopic data were presented in order to confirm the presence of a $\text{Se} \cdots \text{N}$ intramolecular nonbonded interaction, the organochalcogen derivatives are presumably stabilized by $\text{Y} \cdots \text{N}$ ($\text{Y} = \text{Se}, \text{Te}$) intramolecular interaction.

In a study by McWhinnie and co-workers, the crystal structure of *p*-ethoxyphenyl-2-(2-pyridyl)phenyl selenide, **5**, was reported.¹⁶ Compound **5** has a suitably positioned nitrogen atom to form a five-membered chelate ring. The compound was synthesized using mercuration (Scheme 2).¹⁷ The geometry of the $\text{Se}(\text{II})$ atom was found to be consistent with the presence of two stereochemically active lone pairs of electrons. The $\text{Se} \cdots \text{N}$ separation of 2.813(6) Å was found to be greater than the sum of the covalent radii (1.87 Å) but significantly less than the sum of the van der Waals radii (3.5 Å)¹⁸ for these atoms. However, the geometric evidence showed that the nitrogen atom was directed away from the selenium atom, thus indicating that there was no significant selenium-to-nitrogen bonding. A similar situation was reported for the analogous tellurium compound.¹⁷

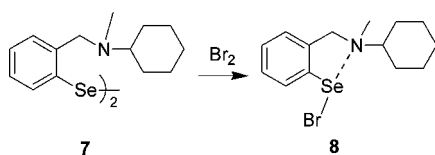
Iwaoka et al. in 1992 reported the first direct observation of intramolecular interaction between a divalent selenium and a tertiary amine with the use of single-crystal X-ray analysis and NMR spectroscopy.¹⁹ The compound studied was 2,2'-diselenobis(*N*-cyclohexyl-*N*-methylbenzylamine), **7**. It was synthesized from methyl anthranilate, **6**, as shown in Scheme 3.

For compound **7**, the atomic distances of $\text{Se} \cdots \text{N}$ were found to be 2.78 Å and 2.96 Å, respectively, both significantly shorter than the sum of the corresponding van der Waals radii. Bond angles for $\text{Se}-\text{Se} \cdots \text{N}$ (172° and 165°) indicated an approximate linear alignment of the four atoms ($\text{N} \cdots \text{Se}-\text{Se} \cdots \text{N}$). These structural parameters clearly indicate that a nonbonded interaction between selenium and the tertiary amine exists in the solid state. The results of X-ray analysis for **7** were in agreement with the previous suggestion that nucleophiles approach Se in the selenide plane along a vector defined by the σ^* ($\text{C}-\text{Se}$) orbital on the back side of one of the selenide bonds.²⁰ The ¹H NMR

Scheme 3



Scheme 4



spectrum, however, did not give any evidence for such a $\text{Se}\cdots\text{N}$ interaction in solution, and this was presumed to be due to poor electrophilicity of the divalent selenium. Compound **7** was oxidized using equimolar bromine to afford the selenyl bromide **8** (Scheme 4). The ^1H NMR spectrum of **8** strongly suggested the presence of intramolecular $\text{Se}\cdots\text{N}$ interaction in solution.

Tomoda et al. claimed the first X-ray crystal structure of areneselenenyl chloride stabilized by the stereoelectronic effect of an intramolecular nitrogen atom.²¹ Diselenide **9** was synthesized from 2,2'-diselenobis(benzylchloride), bis[2-(2-pyridyl)ethyl]amine, and triethylamine. It can act as a catalyst in olefin conversion to allylic ethers or esters in the presence of a copper(II) ion.²² However, this compound may not be a true example of an areneselenenyl chloride since the compound was crystallized as the Cu(II) complex, **10**. The electronic structure of such hypervalent selenium species was discussed based on ab initio MO calculations and natural bond orbital (NBO) analysis using a model selenenyl chloride with a tertiary amino group. The observed short interatomic distance between selenium and the amino nitrogen clearly illustrated the existence of a strong nonbonded interaction between the two atoms. The distance was found to be only 0.35 Å longer than the standard $\text{Se}-\text{N}$ (sp^3) single-bond length and about 1.3 Å shorter than the van der Waals contact. A linear arrangement of the $\text{Se}-\text{Cl}$ covalent bond and the coordinating nitrogen was observed, which, in theory, should allow the effective orbital interaction between the nitrogen lone pair and the σ^* orbital of the $\text{Se}-\text{Cl}$ bond. The nature of the $\text{N}\cdots\text{Se}-\text{Cl}$ interaction was proposed to be a 3-center 4-electron bond. The electronic structure around the selenium atom itself was most similar to the $\text{S}_{\text{N}}2$ (second-order nucleophilic substitution) transition state at a divalent selenium. Tomoda et al. have also investigated the nature of intramolecular nonbonded interactions in 2-selenobenzylamine derivatives (**11**–**17**) using ^1H , ^{77}Se , and ^{15}N NMR spectroscopy.¹² According to their NMR spectral properties, compounds **11**–**17** can be classified into three groups. The first group, containing compounds **12**–**14**, shows a strong $\text{Se}\cdots\text{N}$ interaction. The second group contains **15** and **16** and possesses $\text{Se}\cdots\text{N}$ interactions of intermediate strength, and the third group, containing **11** and **17**, has only weak (or no) $\text{Se}\cdots\text{N}$ interaction. This classification supported the correlation between the strength of the $\text{Se}\cdots\text{N}$ interaction

Chart 1

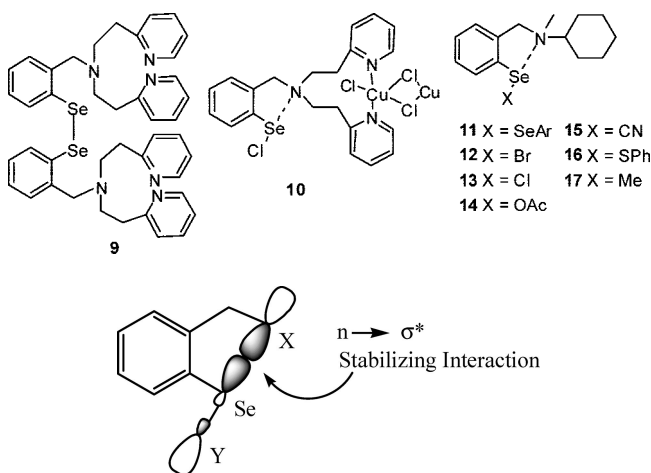
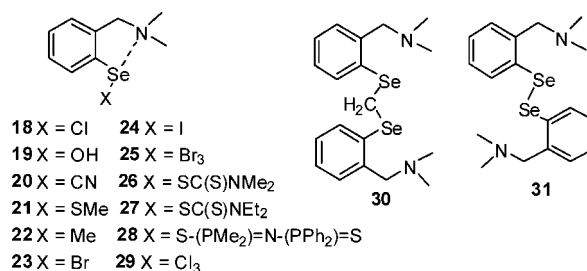
Figure 2. Orbital overlap for the $\text{Se}\cdots\text{N}$ interaction.

Chart 2



and the relative electrophilicity of the selenium moiety ($\text{Se}-\text{X}$) bond.

This observed correlation suggested that the $\text{Se}\cdots\text{N}$ interaction represented the initial stage or near transition state of the electrophilic reaction of a divalent selenium with a nitrogen lone pair, once again indicating orbital interaction between the nitrogen lone pair (n_{N}) and the low-lying antibonding orbital ($\sigma^*_{\text{Se}-\text{X}}$) of the selenium moiety (Figure 2). The electron delocalization from n_{N} to $\sigma^*_{\text{Se}-\text{X}}$ may cause kinetic activation or weakening of the $\text{Se}-\text{X}$ bond, whereas it provides thermodynamic stabilization for the $\text{X}-\text{Se}\cdots\text{N}$ system.

A large downfield shift of ^{15}N NMR spectra and a significant enhancement of $J_{\text{Se}-\text{N}}$ coupling constants were observed with an increase in $\text{Se}\cdots\text{N}$ interaction. The NMR evidence led to two postulates:

(1) The strength of the $\text{Se}\cdots\text{N}$ interaction increases with the increase in the electrophilic reactivity of the selenium moiety.

(2) The $\text{Se}\cdots\text{N}$ interaction mostly arises from the orbital interaction between the selenium and the nitrogen.

Kaur et al. have obtained a crystal structure for the bromo-derivative **23**.²³ A typical T-shaped, 10- Se -3 selane geometry was found around Se with strong noncovalent $\text{Se}\cdots\text{N}$ interaction. Kaur et al. showed the existence of $\text{Se}\cdots\text{N}$ interactions in the corresponding tribromide, RSeBr_3 , **25**, in solution. The compound was found to equilibrate between coordinated and noncoordinated forms.

The ^1H NMR spectra of these compounds showed that, at ambient temperature, there was no evidence of significant $\text{Se}\cdots\text{N}$ interaction except in the case of **25**, where selenium is bonded to the maximum number of electronegative groups and is most electrophilic. Compound **25** was only partially soluble in CDCl_3 , so the ^1H NMR spectra were recorded in

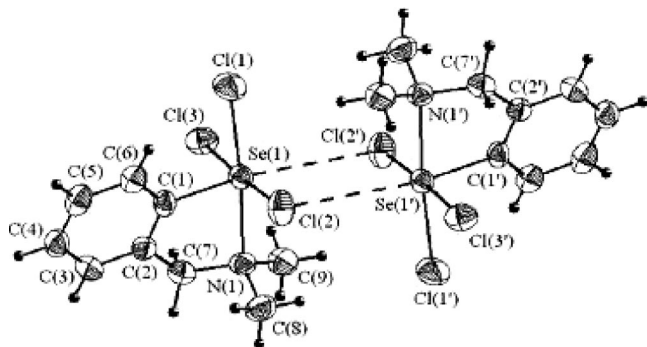


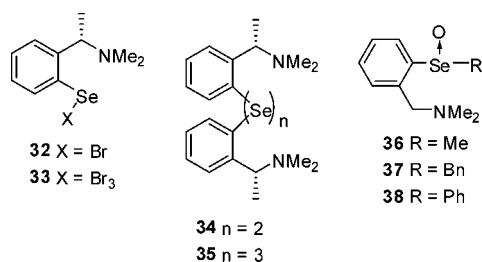
Figure 3. Molecular structure of **29**. Reprinted with permission from ref 25. Copyright 2005 Elsevier.

CDCl_3 , $\text{Me}_2\text{SO}-d_6$, and a mixture of both. Interpretation of the results suggested that **25** exists in two forms having an intramolecularly coordinated and noncoordinated sp^3 nitrogen. In CDCl_3 , only the coordinated form was seen, and in $\text{Me}_2\text{SO}-d_6$, the noncoordinated form was seen because the solvent replaced the coordinated nitrogen atom. The ^{77}Se NMR resonances were found to occur in the expected range.²⁴ For the monohalides **23** and **24**, a large deshielding was observed with respect to the diselenide and the trend noted was RSeBr ($\delta 987$) $>$ RSeI ($\delta 818$). For compound **24**, no peaks were seen for the diselenide, thus indicating higher stability resulting from intramolecular coordination. Crystal structures obtained for compounds **23** and **27** were found to be iso-structural with a typical 10-Se-3 selane T-shaped geometry seen around selenium with strong nonvalent $\text{Se}\cdots\text{N}$ interaction. The three-coordinate Se was bonded to a carbon atom and a bromine atom and showed a $\text{N}\cdots\text{Se}$ separation that was well within the sum of van der Waals radii for N and Se reported by Pauling.¹⁸ Kulcsar et al. recently reported some new compounds in this series, which include selenenyl dithiocarbamate and dithioimiddiphosphinate **26–28** along with Se(IV) , selenium trichloride **29**.²⁵ The structures of **18** and **26–29** have been reported. All the structures showed strong $\text{Se}\cdots\text{N}$ nonbonded interactions; additionally, Se(IV) selenium trichloride **29** exists as a dimer through $\text{Se}\cdots\text{Cl}$ intramolecular interactions (Figure 3). Analogous chiral derivatives (**32–35**) were also synthesized from [(*S*)-*N,N*-dimethyl-1-phenethylamine] using similar methods to those for the achiral ligands described previously.^{23,26} The trend in ^1H NMR chemical shifts observed was found to be very similar to that of the analogous achiral compounds. There was no evidence for any strong $\text{Se}\cdots\text{N}$ interaction at ambient temperature except for selenenyl bromide **32**.

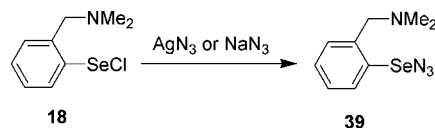
Optically active selenoxides have been extensively studied as key intermediates in asymmetric synthesis.^{4f–h} Isolation of an optically pure alkyl aryl selenoxide is very difficult since it readily undergoes racemization by atmospheric moisture, even though the aryl group possesses bulky substituents. In this regard, isolation of optically pure alkyl aryl and diaryl selenoxides **36–38** has been accomplished using intramolecular coordination of nitrogen of the dimethylamino group with selenium.²⁷

Recently, Klapötke et al. have successfully synthesized and structurally characterized selenenyl chloride **18** and azide **39** using diselenide **31** as a precursor.²⁸ Selenenyl chloride **18** has been synthesized by treating diselenide **31** with sulfur chloride. Subsequent reaction with NaN_3 or AgN_3 has afforded the selenenyl azide **39** (Scheme 5). This is the first report on the isolation and structural characterization of a stable selenenyl azide, which has, in turn, been possible

Chart 3



Scheme 5



by novel $\text{Se}\cdots\text{N}$ nonbonded interaction. Initially, a number of attempts have been made to isolate stable selenenyl azides by using a sterically demanding precursor such as RSeCl where $\text{R} = 2,4,6-(\text{CH}_3)_3\text{C}_6\text{H}_2$, $2,4,6-(\text{CF}_3)_3\text{C}_6\text{H}_2$, $2,4,6-(t\text{-Bu})_3\text{C}_6\text{H}_2$, $2,6-(\text{Mes})_3\text{C}_6\text{H}_3$, or $(\text{Me}_3\text{Si})_3\text{Si}$.²⁹ However, in situ ^{77}Se NMR studies exhibited that the use of such sterically demanding substituents did not prevent decomposition of the selenenyl azide to diselenide. The single-crystal X-ray structures of **18**, **24**, and selenenyl azide **39** (Figure 4) have showed the expected coordination of the aminomethyl nitrogen atom to selenium leading to five-membered heterocyclic zwitterions with a 3-coordinated selenium anion and 4-coordinated ammonium cation (3c-4e bond system), resulting in rather short $\text{Se}\cdots\text{N}$ distances of 2.135(4), 2.204(6), and 2.172(3) Å for **18**, selenenyl azide **39**, and **24**, respectively, which are comparable with the value reported for **23** (2.243(6) Å).

Organoselenium(IV) diazides $\text{R}_2\text{Se}(\text{N}_3)_2$ ($\text{R} = \text{Me}$, Et, *i*Pr, Ph, Mes ($2,4,6-(\text{Me})_3\text{C}_6\text{H}_2$), $2\text{-Me}_2\text{NCH}_2\text{C}_6\text{H}_4$) and triazides $\text{RSe}(\text{N}_3)_3$ ($\text{R} = \text{Me}$, *i*Pr, Ph, Mes, Tipp ($2,4,6-(i\text{Pr})_3\text{C}_6\text{H}_2$), Mes* ($2,4,6-(t\text{Bu})_3\text{C}_6\text{H}_2$), $2\text{-Me}_2\text{NCH}_2\text{C}_6\text{H}_4$) were synthesized from corresponding difluorides and trifluorides, respectively.³⁰ The organoselenium(IV) difluorides R_2SeF_2 ($\text{R} = \text{Me}$, Et, *i*Pr, Ph, Mes, Tipp, $2\text{-Me}_2\text{NCH}_2\text{C}_6\text{H}_4$) and trifluorides RSeF_3 ($\text{R} = \text{Me}$, *i*Pr, Ph, Mes, Tipp, Mes*, $2\text{-Me}_2\text{NCH}_2\text{C}_6\text{H}_4$) were synthesized by the reaction of organoselenides and -diselenides (R_2Se and R_2Se_2) with XeF_2 . Organoselenium(IV) difluorides and trifluorides are extremely moisture-sensitive. The reaction of the extremely reactive selenium difluoride with moisture furnishes the corresponding selenium oxide. As observed for Mes_2SeF_2 , in the case of $(2\text{-Me}_2\text{NCH}_2\text{C}_6\text{H}_4)_2\text{SeF}_2$, traces of water lead

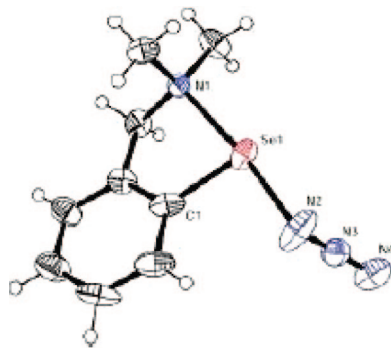
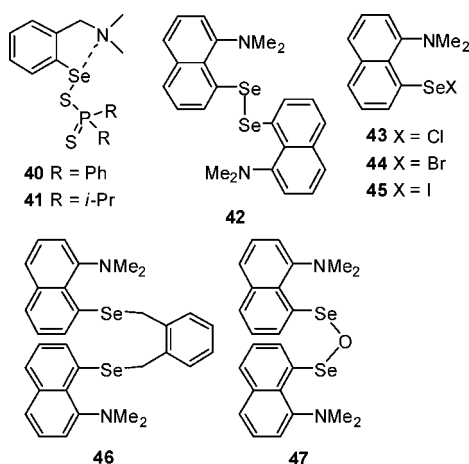


Figure 4. Molecular structure of **39**. Reprinted with permission from ref 28. Copyright 2004 American Chemical Society.

Chart 4



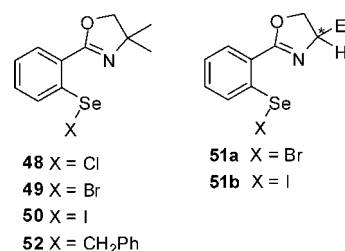
to formation of the selenium oxide, (2-Me₂NCH₂-C₆H₄)₂SeO·HF, as HF adduct. The selenium atom is pseudo-octahedrally coordinated with two virtually equal intramolecular Se···N contacts of 2.749(8) and 2.748(7) Å, respectively. These intramolecular contacts are considerably elongated compared to the reported molecular structure of 2-Me₂NCH₂C₆H₄SeN₃ (**39**).²⁸ The organoselenium azides are extremely temperature-sensitive materials, can only be handled at low temperatures, and decompose on warm-up with vigorous formation of dinitrogen.

Singh and co-workers have studied the synthesis, structure, and reactivity of organochalcogen compounds derived from 1-(*N,N*-dimethylamino)naphthalene and *N,N*-dimethylbenzylamine (**42–46**).³¹ All compounds were again synthesized using the *ortho*-lithiation methodology. The Se···N nonbonded interactions were found to be present in all the compounds in the solid state; however, in solution, the interactions were considered to be weak because the two methyl groups on the nitrogen in **42–46** were observed as a sharp singlet in ¹H NMR and ¹³C NMR spectra. This was thought to indicate a pyramidal inversion at the N-center of the NMe₂ group in solution. It was reported that the stability and reactivity of the compounds mainly depended on the strength of the Se···N interaction and the steric bulkiness of the ligand. The more rigid naphthalene based ligand showed different reactivity and bonding compared with the more flexible *N,N*-dimethylbenzylamine based ligand. For example, the strength of the Se···N nonbonded interactions in the *N,N*-dimethylnaphthylamine based compounds were found to be much stronger than interactions in *N,N*-dimethylbenzylamine based compounds. The diselenide **42** was chiral, whereas the corresponding benzyl derivative **22** was not. In both cases, the Se···N interaction was found to alter the Se···X bond length due to its *trans* influence.

Fujiyama et al. reported the presence of *peri*-Se···N interaction in the selenic anhydride, **47**, with 8-dimethylamino-1-naphthyl ligand.³² The crystal structure of **47** was determined by X-ray diffraction analysis. The Se···N contacts were found to be 2.420 and 2.447 Å, which are both shorter than the sum of the van der Waals radii (3.5 Å). The N···Se···O angles were 173.4° and 172.2°; this linear alignment demonstrated the hypervalent nature of selenium atoms. The X-ray data for **47** suggested that it was stabilized by the *peri*-participation of the two nitrogen atoms.

Recent work by Singh and co-workers has described intramolecular nonbonding interactions in a series of chiral and achiral organoselenium compounds derived from (4,4-

Chart 5



dimethyl-2-phenyl)oxazoline³³ and (*R*)-(4-ethyl)-2-phenyloxazoline³⁴ containing a sp² N donor atom. Compounds **48–52** were synthesized using the *ortho*-lithiation route.

¹H NMR spectra showed that the chemical shifts for methyl and methylene protons of the oxazoline ring mainly depended on the electronegativity of the atom bonded to selenium. The trend RSeCl > RSeBr > RSeI suggested a much stronger interaction for compound **48** in which the selenium was bonded to a highly electronegative chlorine atom. Compounds **48–50** were found to exhibit strong Se···N interactions. In contrast, compound **52** showed only a weak Se···N interaction. The signals due to –CH₂– protons were shifted slightly downfield, suggesting that the introduction of benzylic groups reduces the Se···N interaction. The molecular structures for compounds **51a** and **51b** (Figure 5) were obtained. They showed that the Se···N separations were much shorter than the van der Waals radii and the Se–X (X = Br, I) distances were significantly longer than the sum of the single-bond covalent radii for Se–X. This was attributed to the interaction between the nitrogen lone pair and the Se–X bond causing a significant charge transfer from nitrogen to Se–X. This considerably weakened the Se–X bond, thus increasing the possibility of nucleophilic attack on the selenium. The N···Se–X unit was found to be almost linear due to the Se···N interaction. It was observed that the deviation of the Se–X bond from the phenyl plane was significantly reduced. This was accompanied by an increase in Se–X bond length. The ⁷⁷Se NMR chemical shifts were found to be quite informative; the suggestion that Se···N nonbonding interaction results in a downfield shift of NMR peaks is now widely accepted, although the shift values do not correspond exactly with the strength of the interaction. In monohalides **48–50**, the trend of ⁷⁷Se NMR chemical shift was **48** > **49** > **50**, showing that the Se resonances become increasingly deshielded as the electronegativity of the attached atom increases. Interatomic distances were found to increase in the order **48** > **49** > **50**

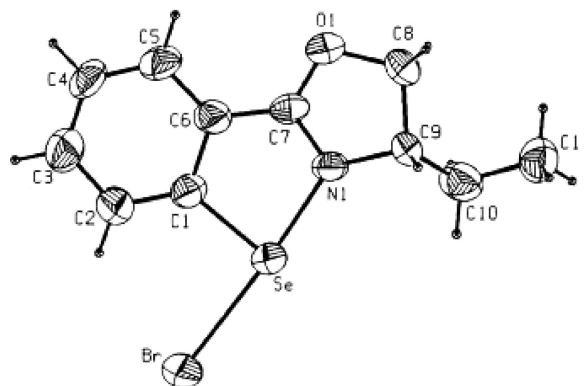
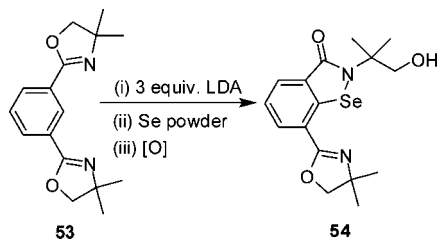


Figure 5. Molecular structure of **51a**. Reprinted with permission from ref 34. Copyright 1999 Elsevier.

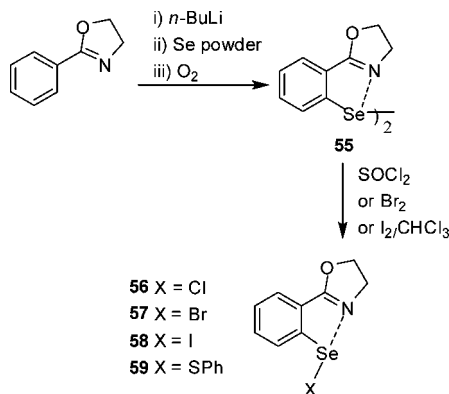


Figure 6. Resonance structures of oxazoline ring indicating contribution of the lone pair of electrons present on the oxygen atom.

Scheme 6

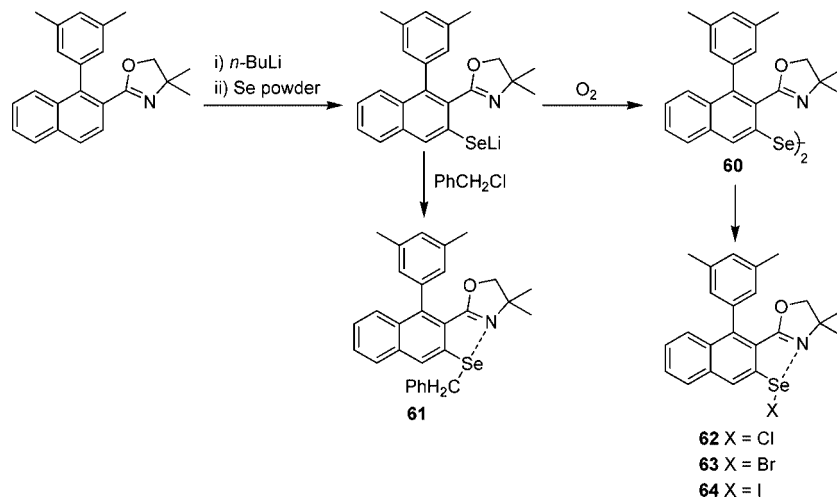


Scheme 7



> **52**, which was in accordance with the results from ^1H NMR chemical shift values. In all the compounds, the nitrogen atom present in the five-membered heterocyclic ring was found to interact directly with the Se atom to form another five-membered ring. It was suggested that $\text{Se}\cdots\text{N}$ interaction and the unusual stability of the compound may have arisen from the fact that the lone pair of electrons present on the oxygen atom may be involved in a resonance contribution with the π -systems, as shown in Figure 6. A correlation was also made between $\text{Se}\cdots\text{N}$ interaction and C—O distances in the oxazoline ring. For compounds **48–50** where the $\text{Se}\cdots\text{N}$ interaction is very strong, the C—O bond lengths lie somewhere between C—O and C=O.

Scheme 8



Selenazole **54** has been recently reported as a mimic of antithyroid drug.³⁵ The unusually cleaved product **54** was obtained by the reaction of 2,6-bis(4,4-dimethyl-2-oxazolin-2-yl)benzene with 3 equiv of lithium diisopropylamide (LDA), selenium insertion followed by oxidative workup (Scheme 6). The single crystal X-ray structure of **54** indicated the presence strong $\text{Se}\cdots\text{N}$ intramolecular interaction (2.601(2) Å) between selenium and nitrogen of the uncleaved-oxazoline ring.

To fine-tune the $\text{Se}\cdots\text{N}$ intramolecular interactions and study the consequent GPx activity, Singh and co-workers have reported the synthesis and characterization of bis[2-(2-oxazolinyl)phenyl] diselenide **55** and its halogen derivatives **56**, **57**, and **58**, incorporating the sterically unhindered 2-phenyl-2-oxazoline (Scheme 7).³⁶ The ^1H , ^{77}Se NMR spectroscopic studies as well as single-crystal X-ray structures are strongly indicative of the presence of $\text{Se}\cdots\text{N}$ intramolecular interactions. The Se—N distances [2.71(6), 2.76(6) Å for diselenide **55**, 1.98(2) Å for bromide **57**, and 2.01(4) Å for iodide **58**] are considerably shorter than the sum of their van der Waals radii and comparable to the related compounds incorporating (4,4-dimethyl-2-phenyl)-2-oxazoline. Organoselenenyl sulfides have been proposed as intermediates in the catalytic cycle of glutathione peroxidase mimics. Very few stable and structurally characterized selenenyl sulfides are reported in the literature. In the series of organoselenenyl compounds having sterically unhindered 2-phenyl-2-oxazoline, the related phenyl sulfide **59** has been synthesized by reacting diselenide **55** with benzenethiol. The selenenyl sulfide showed strong nonbonding $\text{Se}\cdots\text{N}$ (2.636(2) Å) interaction.³⁷

Singh and co-workers have extended the study on intramolecularly stabilized organoselenium compounds by using the substrate having both intramolecular coordinating and sterically demanding groups. For this purpose, 2-[1-(3,5-dimethylphenyl)-2-naphthyl]-4,5-dihydro-4,4-dimethyl-1,3-oxazole has been chosen as a precursor. The synthesis of corresponding diselenide **60** has been carried out by the well-known route, i.e., *ortho*-lithiation, selenium insertion into the C—Li bond followed by oxidative workup (Scheme 8).³⁸ Benzyl selenide **61** was obtained by treating corresponding in situ prepared lithium selenolate with benzyl chloride. Selenenyl halides **62**, **63**, and **64** have been also synthesized. The most interesting feature of the structure of diselenide **60** is the existence of both $\text{Se}\cdots\text{N}$ and $\text{Se}\cdots\text{O}$ interactions

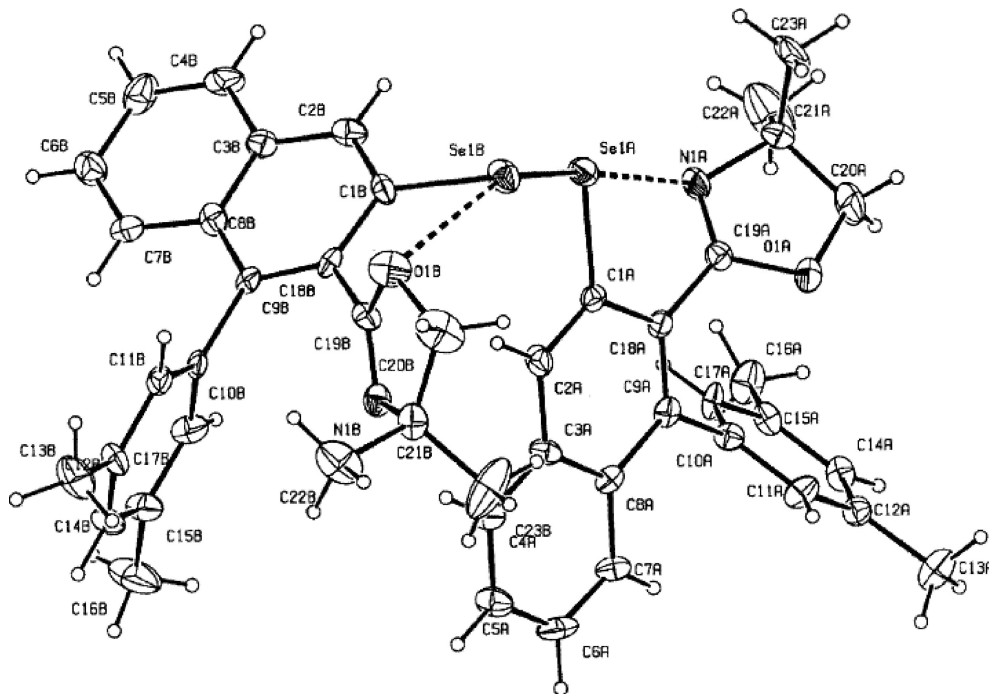
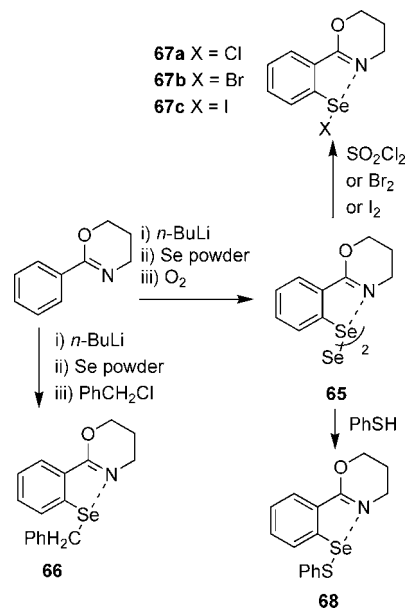


Figure 7. Molecular structure of **60**. Reprinted with permission from ref 38. Copyright 2004 American Chemical Society.

between selenium atoms and nitrogen/oxygen in the same molecule (Figure 7). This is the first report on such types of intramolecular interactions. In the several structures of selenium compounds incorporating 2-phenyloxazoline, only $\text{Se}\cdots\text{N}$ interactions were observed, and in no case was the $\text{Se}\cdots\text{O}$ interaction observed. The unusual intramolecular $\text{Se}\cdots\text{O}$ interaction in the structure of diselenide **60** has been explained on the basis of the different orientation of oxazoline ring due to steric crowding. One of the oxazoline rings is twisted in such a way that nitrogen of the ring is pointed away and oxygen is pointed toward the selenium atom. The $\text{Se}\cdots\text{N}$ [2.976(8) Å] and $\text{Se}\cdots\text{O}$ [2.9815 Å] distances are comparable with the reported examples. The strong nonbonded $\text{Se}\cdots\text{N}$ interactions were observed in the selenenyl bromide **63** and iodide **64** [Se–N distances 2.052(3) and 2.059(5) Å, respectively. The intermolecular $\text{Se}\cdots\text{X}$ (X = Cl, Br, I) interactions generally observed in the packing diagram of selenenyl halides are absent in the present case, possibly due to the presence of sterically demanding groups. Thus, these selenenyl halides can be considered as true monomers in the solid state.

To study the chelate ring size effect, Singh et al. have studied another substrate having coordinating nitrogen as a part of a six-membered heterocycle, oxazine.³⁹ The synthesis of diselenide has been attempted by the ortholithiation method. However, oxidative workup of lithium arylselenolate afforded triselenide **65** as the major product (Scheme 9). Interestingly, in previous reports by the group, similar reactions using ligands 2-phenyl-2-oxazoline, 4,4-dimethyl-2-phenyl-2-oxazoline, (*R*)-4-ethyl-4-hydro-2-phenyloxazoline with nitrogen as part of a five-membered oxazoline ring have afforded corresponding diselenides. Generally, bulky ligands such as dithiophenetriptycyl,⁴⁰ tris(trimethylsilyl)methyl,⁴¹ and 2,6-di[2,6-di(2,6-dimethylphenyl)tolyl]-4-*tert*-butylphenyl⁴² have been used to isolate triselenide or tetraselenide. In this case, triselenide **65** has been stabilized by intramolecular $\text{Se}\cdots\text{N}$ coordination (Figure 8). Benzyl selenide **66** was obtained by the treatment of benzyl chloride with the lithium arylselenolate solution. The corresponding halogen

Scheme 9



derivatives **67a–67c** have been synthesized by treating triselenide **65** with an excess of the appropriate halogenating reagent. The distances between selenium and nitrogen [2.562(18) and 2.569(14) Å for **65**, 2.777(16) and 2.686(9) Å for **66**, 1.964(3) and 1.975(3) Å for **67a**, 1.970(5) and 1.980(5) Å for **67b**, 1.971(3) Å for **67c**, 2.458(2) Å for **68**] indicated the presence of strong nonbonding $\text{Se}\cdots\text{N}$ interaction.

Jones and Ramirez de Arellano⁴³ have reported synthesis and structure of stable azobenzene based selenenyl chloride **69**. The $\text{Se}\cdots\text{N}$ bond length in **69** is 2.025(3) Å. The ⁷⁷Se-NMR shift (δ 884.09) found for **69** is in agreement with the expected deshielding effect on the ⁷⁷Se nucleus arising from the nitrogen coordination.

The first chiral diselenide **71** having an *ortho*-azomethine functional group has been synthesized by the reaction bis(*o*-

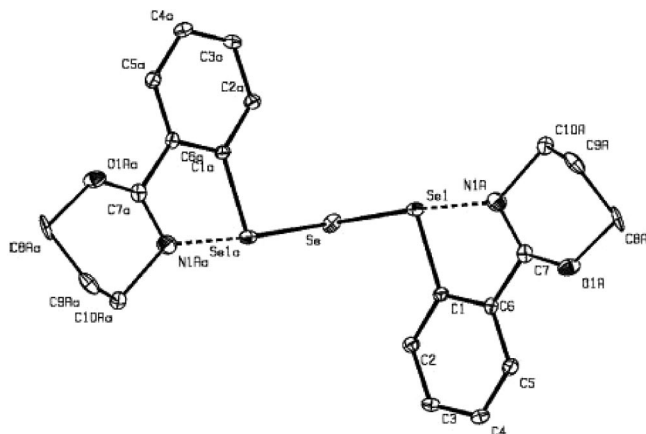
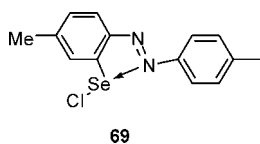
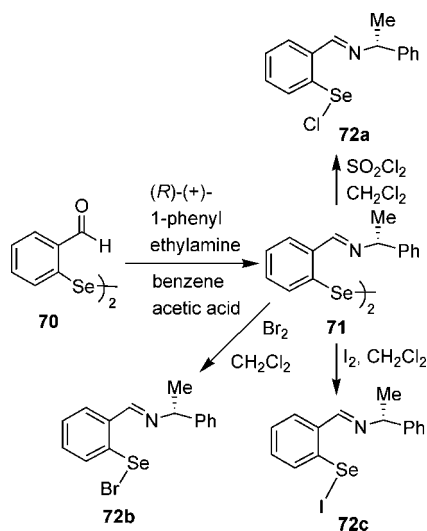


Figure 8. Molecular structure of **65**. Reprinted with permission from ref 39. Copyright 2004 American Chemical Society.

Chart 6



Scheme 10



formylphenyl) diselenide with chiral amine *R*(+)-(1-phenyl-ethylamine) (Scheme 10).⁴⁴ The chiral diselenide **71** was further characterized by derivatizing it into corresponding selenenyl halides **72a–72c**. The derivatives are characterized by single-crystal X-ray diffraction studies. In the solid state, all halogen derivatives revealed a strong $\text{Se}\cdots\text{N}$ intramolecular interaction, whereas the bromide derivative **72b** showed the strongest $\text{Se}\cdots\text{N}$ intramolecular interaction. Interestingly, the ^{77}Se NMR shift for **72b** (1006 ppm) is observed slightly more downfield than that of **72a** (1004 ppm).

Diselenides $[2\text{-}\{\text{O}(\text{CH}_2\text{CH}_2)_2\text{NCH}_2\}\text{C}_6\text{H}_4]_2\text{Se}_2$ (**73a**) and $[2\text{-}\{\text{MeN}(\text{CH}_2\text{CH}_2)_2\text{NCH}_2\}\text{C}_6\text{H}_4]_2\text{Se}_2$ (**73b**) and selenenyl halides $[2\text{-}\{\text{O}(\text{CH}_2\text{CH}_2)_2\text{NCH}_2\}\text{C}_6\text{H}_4]\text{SeX}$ ($\text{X} = \text{Cl}$ (**74a**), Br (**74b**), I (**74c**)) and $[2\text{-}\{\text{MeN}(\text{CH}_2\text{CH}_2)_2\text{NCH}_2\}\text{C}_6\text{H}_4]\text{SeI}$ (**74d**) were synthesized by a similar route, as shown in Scheme 7.⁴⁵ The solid-state molecular structures of **73a–73b**, **74a**, **74b**·HBr, **74c**, and **74d** were established by single-crystal X-ray diffraction. Because of the hypervalent nature ($\text{Se}\cdots\text{N}$ nonbonded interaction), in all cases T-shaped

Chart 7

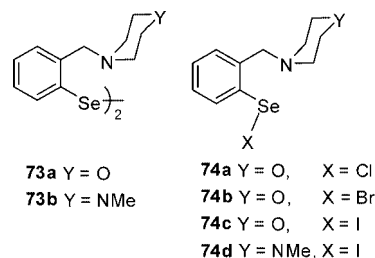
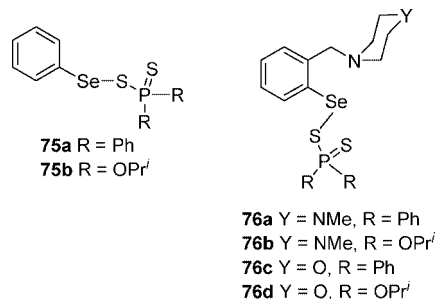


Chart 8

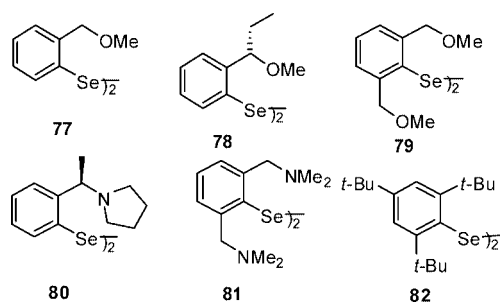


coordination geometries around Se were found. The H,Se-heteronuclear NMR correlations provided further evidence for the presence of the intramolecular $\text{N} \rightarrow \text{Se}$ interaction in solution for the organoselenium compounds. The variable-temperature NMR data suggest that these interactions in solution are stronger for the organoselenium(II) chloride and bromide and weaker in the cases of the iodides and diselenide derivatives. Dimeric associations between *R*- and *S*-**74c** isomers are formed through intermolecular $\text{Se}\cdots\text{I}$ interactions. For all compounds, except **73a**, supramolecular architectures were built through intermolecular contacts between hydrogen atoms and heavier electronegative (halogen, oxygen) atoms.

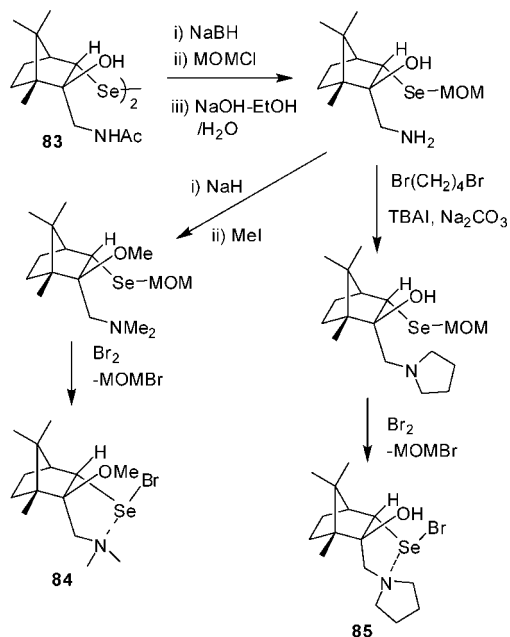
Arylselenium(II) derivatives of dithiophosphorus ligands of type $\text{ArSeSP}(\text{S})\text{R}_2$ [$\text{Ar} = \text{Ph}$, $\text{R} = \text{Ph}$ (**75a**), *Oi*-Pr (**75b**); $2\text{-}[\text{MeN}(\text{CH}_2\text{CH}_2)_2\text{NCH}_2]\text{C}_6\text{H}_4$, $\text{R} = \text{Ph}$ (**76a**), *Oi*-Pr (**76b**); $2\text{-}[\text{O}(\text{CH}_2\text{CH}_2)_2\text{NCH}_2]\text{C}_6\text{H}_4$, $\text{R} = \text{Oi-Pr}$ (**76d**)] were prepared by redistribution reactions between Ar_2Se_2 and $[\text{R}_2\text{P}(\text{S})\text{S}]_2$.⁴⁶ The derivative $[2\text{-}\{\text{O}(\text{CH}_2\text{CH}_2)_2\text{NCH}_2\}\text{C}_6\text{H}_4]\text{SeSP}(\text{S})\text{Ph}_2$ (**76c**) was obtained by the salt metathesis reaction between $[2\text{-}\{\text{O}(\text{CH}_2\text{CH}_2)_2\text{NCH}_2\}\text{C}_6\text{H}_4]\text{SeCl}$ and $\text{NH}_4\text{S}_2\text{PPh}_2$. The single-crystal X-ray diffraction studies showed that, in compounds **76a**, **76b**, and **76d**, the N atom is intramolecularly coordinated to the selenium center with $\text{Se}\cdots\text{N}$ distances of 2.463(4), 2.529(3), and 2.557(7) Å, respectively, resulting in a T-shaped geometry (hypervalent 10- Se -3 species). The NMR data suggest a considerable weakness of the intramolecular $\text{N}\cdots\text{Se}$ interaction, which allows a fast conformational change of the six-membered piperazinyl or morpholinyl ring. The dithiophosphorus ligands act as anisobidentate in **75a** and monodentate in **76a**, **76b**, and **76d**. Supramolecular architectures based on intermolecular $\text{S}\cdots\text{H}$, $\text{N}\cdots\text{H}$, and $\text{O}\cdots\text{H}$ contacts between molecular units are formed in the hypervalent derivatives **76a**, **76b**, and **76d**, respectively, while in the compounds **75a** the molecules are associated into polymeric chains through either $\text{Se}\cdots\text{S}$ (3.590(2) Å) contacts, with no further interchain interactions.

Because of high instability, an air-stable selenenyl fluoride has not been isolated so far; however, ArSeF equivalents such as $\text{Ar}_2\text{Se}_2/\text{XeF}_2$,⁴⁷ $\text{Ar}_2\text{Se}_2/\text{Et}_3\text{N}\cdot 3\text{HF}$,⁴⁸ $\text{ArSe}-\text{YMe}/\text{XeF}_2$ ($\text{Y} = \text{Si, Ge, Sn, Pb}$),⁴⁹ $\text{ArSeOTf}/\text{Et}_3\text{N}\cdot 3\text{HF}$,⁵⁰ $\text{ArSe}-\text{Br}/$

Chart 9



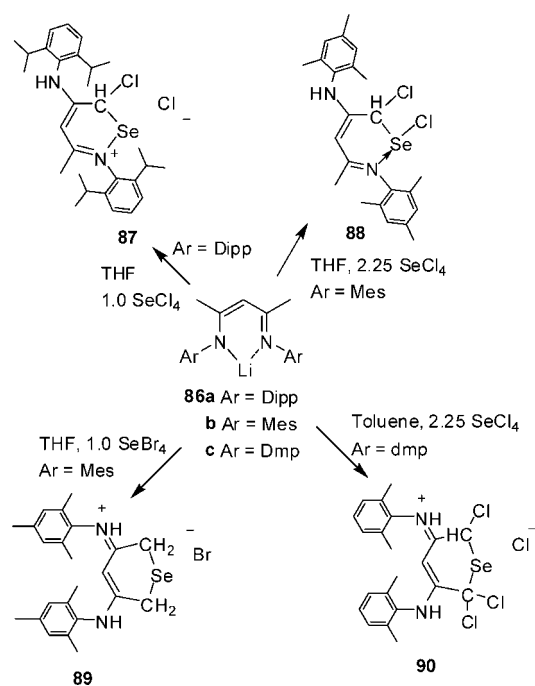
Scheme 11



AgF/ultrasound,⁵¹ PhSeCl/AgF/CH₃CN,⁵² *N*-phenylselenophthalimide (NPSP)/Py·9HF,⁵³ and NPSP/Et₃N·3HF⁵⁴ were used in different applications including addition reactions with alkenes and acetylenes. To detect the active arylselenenyl fluoride, ⁷⁷Se and ¹⁹F NMR spectroscopy has been carried out on the reaction mixtures of corresponding diselenides/trimethylsilyl selenides and XeF₂ at low temperature (−20 to −40 °C).⁵⁵ The diselenides **77–79** with mono- and dimethoxy substitution in close proximity of selenium and diselenides without internally interacting groups did not show formation of selenenyl fluorides; instead the signals corresponding to pseudo-trigonal-bipyramidal selenenium trifluoride were obtained. Diselenides **31** and **80** with dialkylaminomethyl substitution afforded the selenenyl fluoride and selenium trifluoride in 1.25:1 and 2.5:1 ratio, respectively. However, the stabilization of arylselenenyl fluoride with two dialkylaminomethyl substitutions using diselenide **81** produced the selenenium salt with HF₂[−] anion. In this case, use of the sterically bulky diselenide **82** is more useful to obtain a pure selenenyl fluoride.

Back and co-workers have prepared aliphatic selenenyl bromide (1*R*)-2-endo-(dimethyl)methyl-2-exo-methoxy-3-endo-camphorylselenenyl bromide **84** and its 2-endo-(pyrrolidenyl)methyl analogue **85** from (1*R*)-2-endo-acetamidomethyl-2-exo-methoxy-3-endo-camphoryl diselenide **83** (Scheme 11).⁵⁶ The crystal structures of both selenenyl bromides indicated that both compounds have strong N–Se interactions, with N–Se interatomic distances of ca. 2.1 Å, which, in turn, diminish the electrophilic character of the

Scheme 12



selenium atoms. As a result, both compounds have an unusual lack of reactivity in electrophilic oxyseleenylation and cyclization reactions.

Treatment of SeX₄ (X = Cl, Br) with Dippnacnac **86a** (nacnac = [N(Ar)C(Me)₂CH][−], Ar = Dipp = 2,6-diisopropylphenyl), MesnacnacLi **86b** (Ar = Mes = C₆H₂Me₃-2,4,6), or DmpnacnacLi **86c** (Ar = Dmp = C₆H₃Me₂-2,6) afforded new Se^{II} six-membered heterocycles, [DippnacnacHCl₂Se]⁺Cl[−] (**87**), [MesnacnacHCl₂SeCl]⁺Cl[−] (**88**), [MesnacnacH₂Se]⁺Br[−] (**89**), and [DmpnacnacH₂Cl₃Se]⁺Cl[−] (**90**) (Scheme 12).⁵⁷ Each of the complexes was proposed to have formed from the initial reaction of SeX₄ with the C–C double bond that resulted from the enamine form of the ligand, giving rise to a Se–C single bond. Subsequent nucleophilic attack by either the more distant nitrogen atom or the remaining C–C double bond of the enamine form resulted in the Se heterocycle. The crystal structure of **88** revealed an Se–N bond length of 1.980(2) Å, which is longer than a nominal Se–N single bond that usually lies in the range 1.8245–1.846 Å but comparable with values for complexes that showed Se–N intramolecular interactions. The Se–Cl bond in **88** [2.5799(7) Å] is fairly long and can be attributed to an effective overlap between the nitrogen lone pair with the σ*-orbital of the Se–Cl bond, which is favorable because of the N–Se–Cl angle that is close to linear (177.84°).

2.2. Transannular Se···N Interactions

Transannular interaction in bifunctional molecules is a fundamental phenomenon that is observed in many cyclic compounds. If a cationic species is generated on one group in such compounds, then the other functional group can interact in order to stabilize the cationic species. This results in the generation of a transannular bond. The formation of such a transannular bond can cause a conformational change in a molecule, leading to a new functional group.⁵⁸ Fujihara and co-workers have reported much work on hypervalent selenium compounds containing transannular Se···N interactions. For example, the reaction of **91a** with *tert*-butyl

Scheme 13

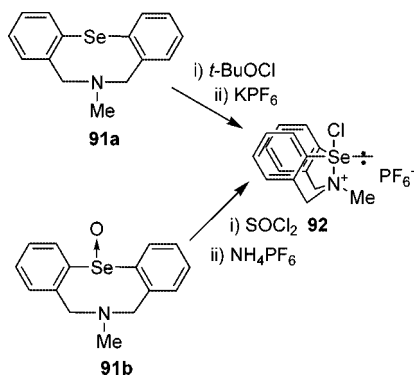
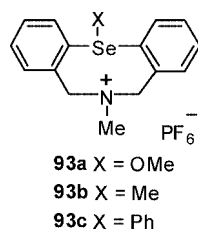


Chart 10



hypochlorite (*t*-BuOCl) and the reaction of selenoxide **91b** with SOCl₂ afforded the corresponding chloroselenenane **92**, which contained a transannular Se...N bond^{58,59} (Scheme 13).

Compound **92** was the first example of an isolable σ -ammonioselenane with a chlorine ligand or a methyl or phenyl group at the apical position, although the analogous sulfur compound had previously been reported.⁶⁰ The crystal structure of **92** showed that the Se...N distance (2.191 Å) was significantly shorter than the sum of van der Waals radii, confirming the presence of the transannular bond. Compound **92** was further reacted to produce compounds **93a–93c**.

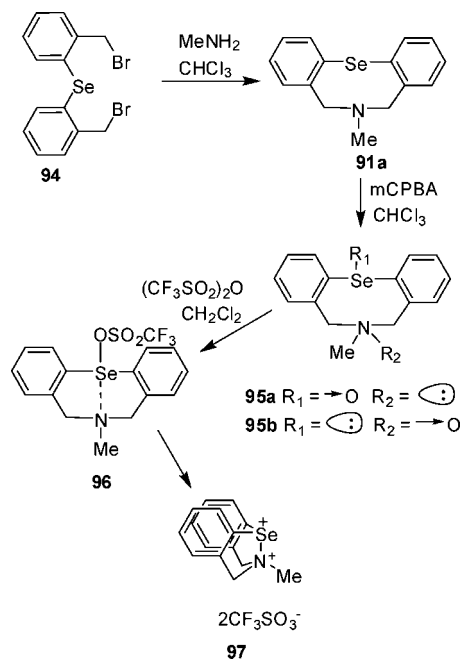
The selenanes **92** and **93a–93c** were a new type of hypervalent selenium compound because in general σ -selenanes bear two electronegative groups such as oxygen or halogen atoms at the apical positions. In 1990 Fujihara and co-workers reported the first example of a dication containing a transannular Se...N bond (Scheme 14).⁶¹

Compound **97** was obtained as a stable crystalline salt and was characterized by spectroscopic and chemical methods. It was also found to act as an oxidizing agent. Further work by Fujihara's group reported a new type of isolable cyclic diazaselenurane **99** stabilized by a three-center transannular interaction between selenium and two nitrogen atoms (Scheme 15).⁶²

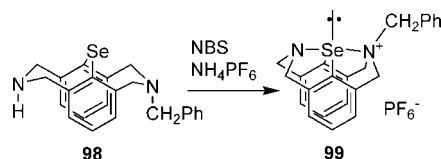
The conformation of **99** was found to be fixed as a twin boat form by the transannular bond between selenium and two amino groups. Evidence for the existence of the N–Se–N⁺ bond was derived from ¹⁵N and ⁷⁷Se NMR spectra of the ¹⁵N labeled selenurane.

The first selenenium and tellurenum cations stabilized by two intramolecular amino groups have been synthesized and structurally characterized.⁶³ Synthesis of selenenium cation **100** has been accomplished by Se-demethylation of 2,6-bis[(dimethylamino)methyl]phenyl methyl selenide with *t*-BuOCl in anhydrous MeOH, followed by conversion into the PF₆⁻ salt upon treatment with KPF₆. The cation showed short intramolecular Se...N contacts of 2.154 and 2.180 Å and the N...Se...N angle of 161.9°, which is strongly distorted from a linear arrangement. The X-ray data sug-

Scheme 14



Scheme 15



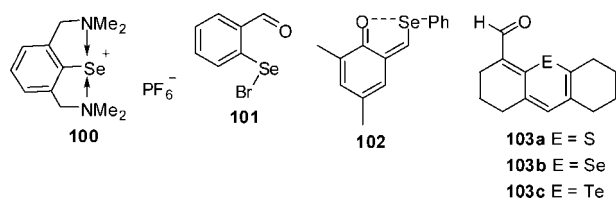
gested that the selenenium cation **100** was considered to be stabilized by the neighboring-group participation of the two nitrogen atoms.

2.3. Se...O Nonbonded Intramolecular Interactions and Se...O Transannular Interactions

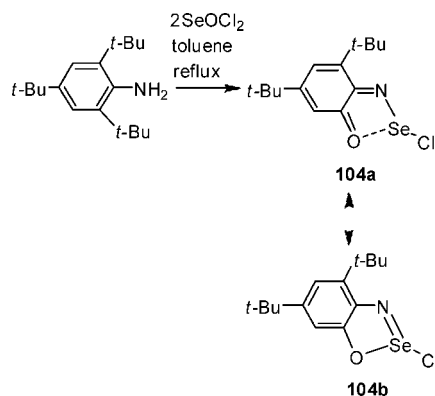
In 1975, Baiwir et al. reported the structure of *o*-formylphenylselenenyl bromide, **101**, as determined by three-dimensional X-ray analysis.⁶⁴ Compound **101**, obtained by direct bromination, was found to have a selenium oxygen separation of 2.305 Å, indicating Se...O interaction and the tendency to form a five-membered chelate ring. Two years later, X-ray evidence for partial Se...O bonding in selenoimines was documented.⁶⁵ Compound **102**, derived from 2,4-xyleneol, was revealed to have a *syn* geometry and a Se...O separation of 2.575 Å. This value represented a 45% increase in the Se–O single bond length of 1.77 Å. Close and co-workers reported the presence of strong O...E (E = Se, Te) interactions in **102** and **103**.⁶⁶ In contrast, compound **103a** only seemed to show a weak S...O interaction. Experimental evidence (IR, ¹⁸O labeling, dipole moments, and ¹H and ¹³C NMR) suggested that, in aldehydes **103a**, **103b**, and **103c**, there was a partial covalent O...E bonding in the order Te > Se > S.

During a study to investigate Se–N multiple bonds Roesky and co-workers synthesized the unexpected product **104** in an attempt to prepare a N=Se=O derivative (Scheme 16).⁶⁷ The quinone structure **104a** was found to predominate, and X-ray data showed the Se...O distance to be 2.079 Å. Compound **104** can be compared to compound **102**; however, Se–N and Se...O distances were much shorter in **104**.

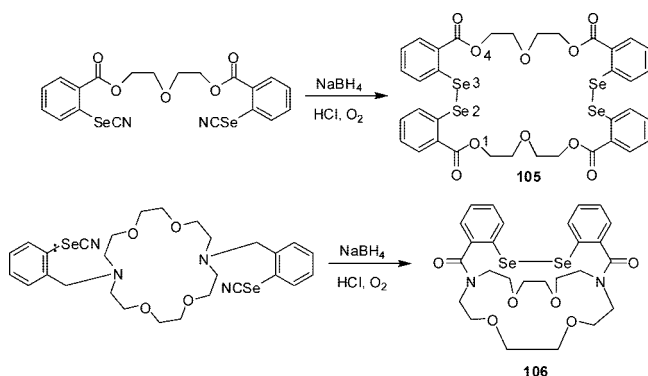
Chart 11



Scheme 16



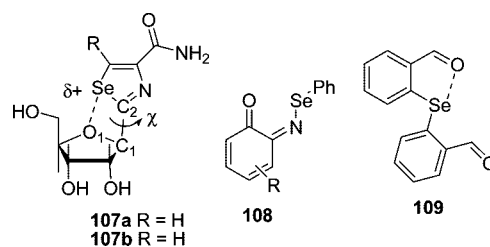
Scheme 17



Tomoda et al. reported work on the incorporation of Se–Se bonds into crown-ether host molecules (Scheme 17). In 1990, they carried out the first synthesis of this class of host molecules, **105** and **106**, and determined their structures by X-ray analysis.⁶⁸ The most interesting feature of the structure of **105** was the unusual proximity of the atoms Se(2) and O(1) (2.65 Å) and O(4) and Se(3) (2.71 Å). These short contacts suggested the existence of strong attractive interactions between the atoms. The four atoms O(1)–Se(2)–Se(3)–O(4) showed almost linear alignment, thus demonstrating the hypervalent property of selenium, which probably leads to the conformational stability of the macrocyclic system. The molecular structure of **106** also displayed short interatomic Se···O distances.

Selenazofurin, **107a** (2-β-D-ribofuranosylselenazole-4-carboxamide, NSC 340847), is the selenium analogue of thiazofurin, an antitumor agent. Selenazofurin has also been found to exhibit chemotherapeutic behavior. Goldstein et al. reported that the X-ray crystal structures of **107a** and its 5-amino derivative, **107b**, indicated the presence of short contacts between the selenium atom and the furanose oxygen, O1.⁶⁹ Compound **107b** had a longer Se···O contact than **107a** (3.314 Å and 3.012 Å, respectively), but both were shorter than the sum of Se and O van der Waals radii (3.4 Å). These interactions were proposed to be electrostatic in nature. The ⁷⁷Se NMR data and X-ray studies suggested that

Chart 12



in **107a** the Se atom carries a positive charge in a partially delocalized selenazole ring and in **107b** there is a decrease in positive charge on the Se resulting in a decrease in the attractive component of the Se···O1 interaction. Later, a series of quantum-mechanical based computational studies were performed in order to confirm the origin of the Se···O interaction in **107a** and **107b**.⁷⁰ These studies indicated that the Se···O contacts were the result of nonbonded interactions (vide infra).

A study by Barton et al. in 1993 further supported the idea of unusual attractive interactions between a chalcogen and an oxygen atom.⁷¹ The reaction of benzeneseleninic anhydride and hexamethyldisilazane gave a reactive intermediate, oligomeric (RSeN)₄, which oxidized a phenol to the selenoiminoquinone **108**. The spectroscopic and crystallographic studies showed that the oxygen atom of the carbonyl group was involved in an attractive interaction with the selenium atom.

During a study on Se,N-containing macrocyclic ligand, Singh et al. went on to solve the structure of monoselenide **109**.⁷² The crystal structure displayed a Se···O distance that was shorter (2.812 Å, Figure 9) than the sum of van der Waals radii; the other O atom was directed away from selenium and, therefore, is not coordinated. In further studies, diselenide **70** has been characterized structurally.³⁷ In the crystal structure of **70**, the asymmetric unit comprises two crystallographically independent molecules. Se···O distances of 2.720, 2.751, 2.729, and 2.725 Å indicate the presence of stronger intramolecular nonbonded interactions compared to the corresponding monoselenide. The nearly linear arrangement of O···Se–Se···O strongly confirms the presence of nonbonding interaction.

The selenium···nitrogen interaction is the preferred nonbonded interaction in the selenium compounds having *ortho*-oxazole ring. Recently, Singh and co-workers have reported the Se···O interaction preferred over the Se···N interaction

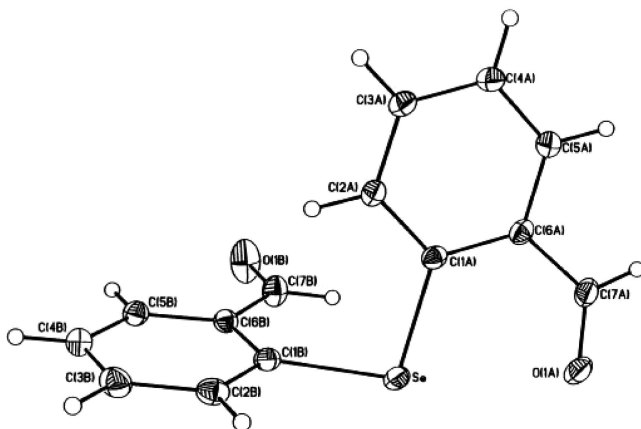
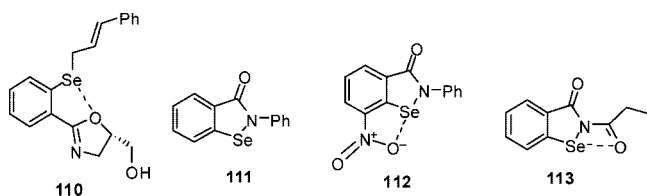
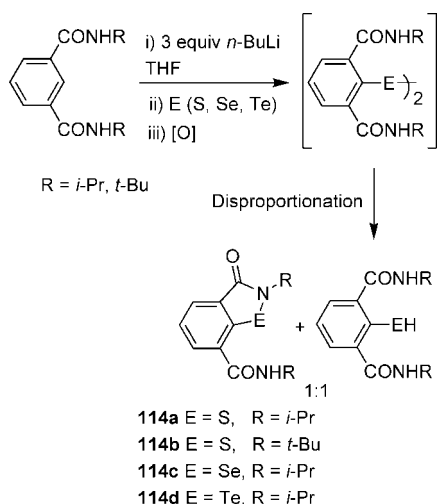


Figure 9. Molecular structure of **109**. Reprinted with permission from ref 72. Copyright 2001 Elsevier.

Chart 13



Scheme 18



in diselenide **60** for steric reasons.³⁸ Similar observation (Se–O distance = 2.709 Å) has been obtained by Carter et al. for the structure of oxazole containing selenide **110** during the study of selenium oxidation with in situ [2,3]-sigmatropic rearrangement (SOS reaction).⁷³ The probable reason for the reversal of interaction in compound **110** was suggested as the participation of the nitrogen in intermolecular hydrogen bonding with the free hydroxyl of another molecule. Such a change in the nature of intramolecular interaction between oxazole and selenium was also observed in ⁷⁷Se NMR studies.

Ebselen **111** (2-phenylbenziselenazol-3(2H)-one) is a well-known glutathione peroxidase (GPx) mimic.³¹ In order to modify its catalytic activity, a number of attempts have been reported in literature by changing the substituent at 2-phenyl by another substituent as well as introducing an additional substituent at 7-position. Concerning this, 7-nitro-2-phenylbenziselenazol-3(2H)-one **112** has been reported with enhanced GPx like catalytic activity.⁷⁴ The distance between selenium and one of the nitrogens of the nitro group [2.562(4) Å] was found to be significantly less than the sum of their van der Waals radii. The other examples include 2-propionylbenziselenazol-3(2H)-one **113**, which has exhibited Se···O interaction (Se–O distance = 2.806 Å).⁷⁵

Scheme 19

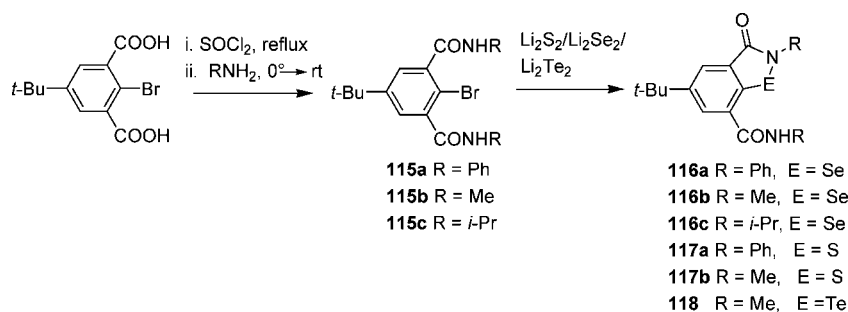
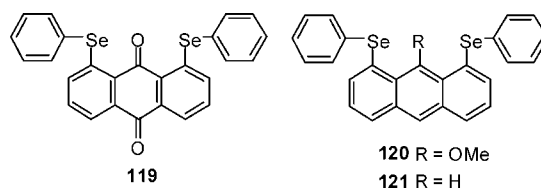


Chart 14



Recently, Kersting and DeLion have reported a new synthetic route to prepare 7-carbamoyl substituted ebselen derivatives including sulfur and tellurium analogues (**114a–114d**) (Scheme 18).⁷⁶ The synthesis has been accomplished by the reaction of isophthalamide with *n*-BuLi and chalcogen insertion followed by oxidative workup. Crystal structure of **114c** has exhibited strong Se···O interaction, whereas tellurium analogue **114d** has exhibited additional π – π stacking.

Singh et al. have reported convenient one-pot synthesis of 5-*tert*-butyl and 7-carbamoyl containing ebselen derivatives (**116a–116c**) (Scheme 19).⁷⁷ An attempt to synthesize diselenide by treating the precursor bromo compounds (**115a–115c**) with dilithium diselenide unexpectedly resulted in the formation of ebselen derivatives. Compounds **116a** and **116b** are isostructural with parent ebselen with the additional Se···O interaction similar to that observed for the compound **105**.

Five C–Se···O···Se–C atoms have been shown to align linearly for 1,8-bis(phenylselenanyl)anthraquinone (**119**) and 9-(methoxy)-1,8-bis(phenylselenanyl)anthracene (**120**).⁷⁸ In contrast to **119** and **120**, in the crystal structure of 1,8-bis(phenylselenanyl)anthracene (**121**), C–Se···H···Se–C atoms were not aligned. The linear alignment has been analyzed by the 5c-6e model. Observed nonbonded Se···O distances of 2.67–2.74 Å were found to be about 0.7 Å shorter than the sum of their van der Waals radii. The formation of C–Se···O···Se–C 5c-6e system has been explained by effective connection of two nonbonded $n_{\text{px}}(\text{O}) \cdots \sigma^*(\text{Se}-\text{C})$ 3c-4e system through $n_{\text{px}}(\text{O})$. Similarly, the $n_{\text{px}}(\text{O}) \cdots \sigma^*(\text{Se}-\text{C})$ 3c-4e has been observed in **124**, which stabilizes the structure.⁷⁹

A set of new $\delta(^{77}\text{Se})$ NMR parameters has been proposed as a standard for the planar (**pl**) orientational effect (Scheme 20) of *p*-YC₆H₄ (Ar) in ArSeR, employing 9-(arylselenanyl)-tritylenes (**122**, *p*-YC₆H₄SeTpc).⁸⁰ The Se–C_R bond in ArSeR is placed on the Ar plane in **pl** and it is perpendicular (**pd**) to the plane in **pd**. Large upfield shifts were observed for Y = NMe₂, OMe, and Me (–22 to –6 ppm) and large downfield shifts were observed for Y = COOEt, CN, and NO₂ (19–37 ppm), relative to Y = H, with small upfield and moderate downfield shifts by Y of halogens (–1 ppm for Y = F and 4 ppm for Y = Cl and Br). This must be the

Scheme 20

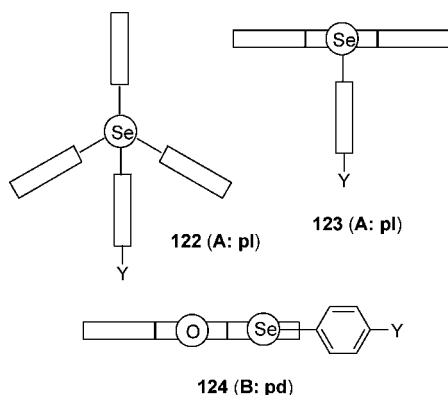
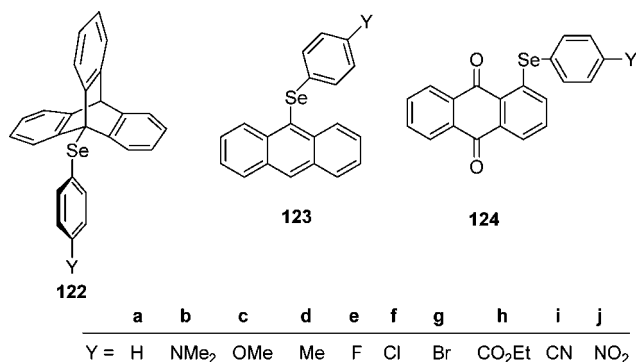


Chart 15



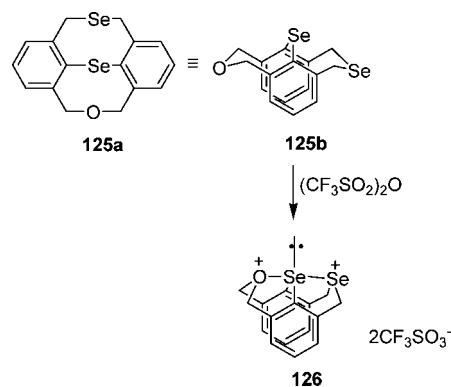
result of the $p(\text{Se})-\pi(\text{C}_6\text{H}_4)-p(\text{Y})$ conjugation in **122** (**pl**). While the character of $\delta(\text{Se})$ in **122** (**pl**) is very similar to that in 9-(arylselanyl)anthracenes (**123** (**pl**)), it is very different from that of 1-(arylselanyl)anthraquinones (**124** (**pd**)). Similarly, that of **124** (**B: pd**) is the hypervalent 3c-4e interaction of the $n_p(\text{O})\cdots\sigma^*(\text{Se}-\text{C})$ type. The $p-\pi$ conjugation of the $p(\text{Se})-\pi(\text{Atc})-\pi(\text{C}=\text{O})$ type assists strongly to stabilize **124** (**B: pd**) in addition to the hypervalent 3c-4e interaction in **124** (**B: pd**). The driving force to stabilize **124** (**B: pd**) is very strong. Structures of various ArSeR in solutions are determined from the viewpoint of the orientational effect based on the standard $\delta(\text{Se})$ of **122**–**124**. While the structure of 2-methyl-1-(arylselanyl)naphthalenes is concluded to be all **pl** in solutions, those of 8-chloro- and 8-bromo-1-(arylselanyl)naphthalenes are all **pd**, except for $\text{Y} = \text{COOEt}$, CN , and NO_2 . The equilibrium between **pd** and **pl** contributes to those with $\text{Y} = \text{COOEt}$, CN , and NO_2 . The structure of 1-(arylselanyl)naphthalenes changes depending on Y . The structures of ArSeMe and ArSeCOPh were shown to be **pl** and **pd**, respectively, in solutions. Those of ArSePh and ArSeAr seem to change depending on Y . Sets of $\delta(\text{Se})$ of **122** and **123** must serve as the standard for **pl** and that of **124** does for **pd** in solutions.

Fujihara et al. reported their findings on a three-center transannular interaction between oxygen and two selenium atoms in a new diselenocine (Scheme 21).⁸¹

The transannular $\text{O}\cdots\text{Se}$ contact in **126** was found to be remarkably shorter than the sum of the van der Waals radii of the two elements. The X-ray structure was obtained showing that the $\text{O}\cdots\text{Se}-\text{Se}$ bond angle was roughly colinear. This was the first reported example of transannular hypercoordination between oxy- and diseleno-groups.

Although several areneseleonic acids stabilized by coordination to *o*-nitro,⁸² carbonyl,⁸³ or amino⁸⁴ groups have

Scheme 21



previously been reported, they were observable only in solution. Reich and co-workers disputed some of the reported selenenic acids, stating that they were actually selenenic anhydrides or seleninic acids.⁸⁵ Saiki et al. have recently reported the existence of a nonbonding interaction between Se and O in the crystal structure of the first isolable selenenic acid in the solid state, **127**.⁸⁶ Compound **127** was characterized using NMR and IR spectroscopy, fast atom bombardment (FAB) mass spectrometry, and elemental analysis. The structure was also elucidated by X-ray crystallography (Figure 10). The $\text{Se1}\cdots\text{O3}$ distance was reported to be 2.64 Å, significantly shorter than the sum of the corresponding van der Waals radii (3.42 Å).⁸⁷ Atoms O3 , Se1 , and O1 are arranged almost linearly. These parameters infer the existence of a nonbonding interaction between Se1 and O3 atoms in the solid state.

Chandrasekaran et al. have developed a general synthetic methodology for the synthesis of conformationally locked,

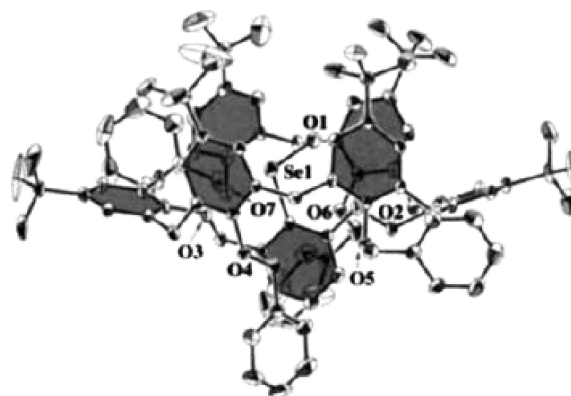
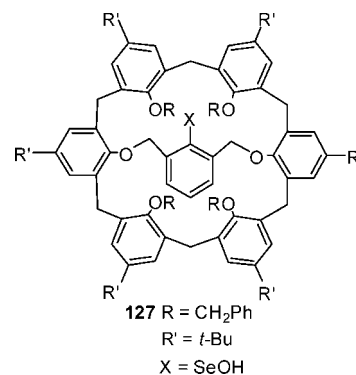
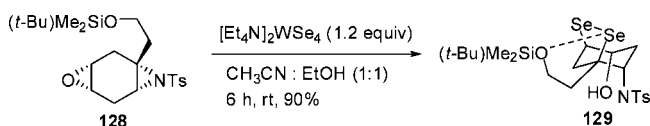


Figure 10. Molecular structure of **127**. Reprinted with permission from ref 86. Copyright 1997 Wiley Interscience.

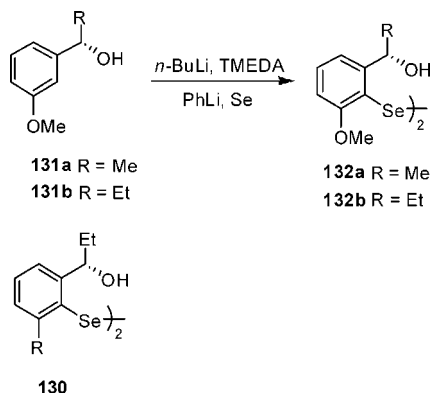
Chart 16



Scheme 22



Scheme 23

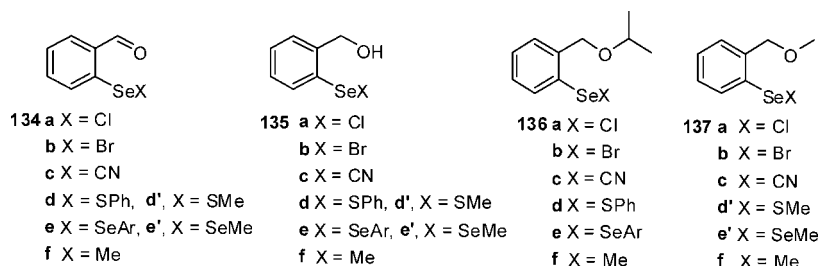


bridged diselena-bicyclo[3.2.1]octane derivatives by regio- and stereospecific nucleophilic ring-opening of *cis*-1,4-aziridino epoxides (Scheme 22).⁸⁸ The UV-vis spectrum of **129** shows a blue shift (414 nm) compared to the diselenide. The ⁷⁷Se NMR of **129** shows a difference of 147 ppm between the two selenium signals, whereas the difference between the selenium signals in other conformationally locked diselenides is only 10–70 ppm. This can be attributed to an Se...O (Se...O distances, 2.843 Å, and Se–Se...O2 bond angle, 166.4°) nonbonding interaction in **129**.

Wirth and co-workers investigated stereoselective reactions using chiral selenium compounds.⁸⁹ They developed readily available chiral diselenides of type **130** (Scheme 23). It was shown that the oxygen atom in the chiral side chain in close proximity to the selenium was responsible for the efficient transfer of chirality.⁹⁰

X-ray analysis of **132a** was performed, and its structure was found to be substantially different from other diselenides bearing heteroatom-containing side chains. In other structures, a strong interaction between the heteroatom of the side chain and the selenium was found. In the structure of **132a**, a strong interaction with the oxygen of the methoxy group was observed while the distance from the selenium to the oxygen in the side chain was found to be greater than the sum of the van der Waals radii (Se...O mean distance 2.977 Å). The selenenyl triflate, **133**, derived from compound **132a** (Scheme 24), represented a more efficient reagent for stereoselective selenenylation reaction. X-ray diffraction structure and nuclear Overhauser effect (NOE) measurements of **132a** were found to underline the assumption that the increased transfer of chirality was due to the forced interaction of the *ortho*-oxygen atom with the selenium.

Chart 17



Scheme 24

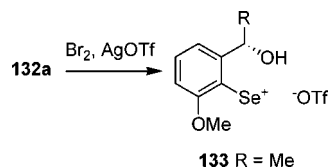


Table 1. ¹⁷O and ⁷⁷Se NMR Chemical Shifts for **134**, **135**, and **136**

X	134		135		136		
	δ_{O}^a	δ_{Se}^b	δ_{O}^a	δ_{Se}^b	δ_{O}^a	δ_{Se}^b	
a	Cl	493.0	1114.1	24.9	987.1	54.8	986.5
b	Br	515.9	1029.5	23.2	839.5	55.2	857.8
c	CN	548.0	426.7	22.0	314.5	44.6	315.1
d	SPh	556.6	621.7	16.0	501.8	44.4	503.8
e	SeAr	559.3	458.5	13.3	433.2	39.0	412.0
f	Me	561.6	259.5	10.6	157.2	39.0	166.6

^a ¹⁷O NMR spectra were measured for the corresponding ¹⁷O-enriched compounds at 67.70 MHz in CDCl₃ at 298 K with D₂O as an external standard. ^b ⁷⁷Se NMR spectra were measured at 95.35 MHz in CDCl₃ at 298 K with Me₂Se as an external standard.

Recent work by Tomoda et al. provided the first systematic NMR evidence for Se...O interactions.⁹¹ From the viewpoint of the electronegativity scale, it was expected that the interaction between selenium and oxygen (Se...O) may be of intermediate strength. However, the results of earlier publications on the mechanism of Se...O interactions were variable, thus leaving the actual mechanism uncertain. In that study, compounds **134a–134f**, **135a–135f**, and **136a–136f** were synthesized and analyzed by ¹⁷O and ⁷⁷Se NMR spectroscopy (Table 1).

The experimental data shown in Table 1 strongly suggested that the conformation with a Se...O interaction is a major conformer in solution for three series of model compounds (**134a–134f**, **135a–135f**, and **136a–136f**) and should be the one that has a close atomic contact between the Se and O atom. Within series **134**, a monotonous downfield shift of δ_O was observed from **a** to **f** (δ_O = 493.0 → 561.6), while exactly the opposite trend was apparent for series **135** (δ_O = 24.9 → 10.6) and **136** (δ_O = 55.2 → 39.0). The compounds in series **134** possessed a sp² hybridized oxygen, and those in series **135** and **136** carried a sp³ hybridized oxygen. Comparison of ⁷⁷Se chemical shifts (δ_{Se}) between compounds **134**, **135**, and **136** possessing the same substituents, X, revealed that **134a–134f** were considerably downfield shifted from those for the corresponding **135a–135f** and **136a–136f**, suggesting the presence of strong magnetic anisotropic effects on the Se atoms of series **134a–134f** from the intramolecular carbonyl group that must locate in close proximity to the Se atom.

In conformer **A**, the O–Se–X angle is nearly 180° and there is a close O...Se contact, whereas in conformer **B**,

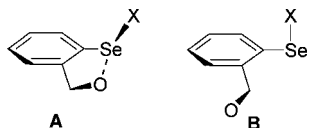


Figure 11. Two conformers of organoselenium compound with heteroatom (O) in proximity of the selenium center. In conformer **A**, the O–Se–X angle is nearly 180° and there is a close O···Se contact, whereas in conformer **B**, the Se–X bond is almost perpendicular to the plane of the phenyl ring without any contact.

the Se–X bond is almost perpendicular to the plane of the phenyl ring and, thus, there is no Se···O contact (Figure 11). In summary, the experimental data was in full accord with the existence of attractive nonbonded Se···O interactions, the most likely mechanism of which was the orbital interaction between the oxygen lone pair and the low-lying $\sigma^*_{\text{Se-X}}$ antibonding orbital. Possible enhanced strength of the Se···O interaction in series **134** compared to series **135** and **136** could be explained in terms of π -conjugation between the formyl group and the phenyl ring in **134**, which may lead to free rotation about the C(Ph)–CH bond, generating a stable conformation of **134** with a Se···O distance that is shorter than those for **135** and **136**. These results were further corroborated by the recent work of Singh et al., where the single crystal of **135e** showed the existence of only one Se···O nonbonded interaction in solid state while the other oxygen is pointing away from the second selenium atom (Figure 12). As expected with the sp^3 oxygen atom, the Se···O interaction is weak and the Se–Se···O bond angle is 166° with Se···O distance of 3.008 Å.⁹²

Selenenic acid is a highly reactive species formed during the catalytic cycle of glutathione peroxidase (GPx) and sigmatropic recation. There has been a long-standing interest in stabilization and isolation of selenenic acid. To date, only three examples of isolated and structurally characterized selenenic acid have appeared in the literature.^{40,42,86} Selenenate esters can be considered as a protected form of the

selenenic acid. Recently, Singh et al. reported the first example of isolation and structural characterization of cyclic selenenate ester **139** stabilized by Se···O interaction.⁹³ The reaction of diselenide **138** with halogenating reagent ($\text{SO}_2\text{Cl}_2/\text{Br}_2/\text{I}_2$) followed by quenching with water unexpectedly afforded the novel selenenate ester **139** (Scheme 25). Diselenide **138** was synthesized by the treatment of the precursor bromo compound with disodium diselenide. The Se···O distances (2.604 and 2.465 Å) are considerably shorter than the sum of their van der Waals radii (Figure 13). Further studies on bis-*ortho*-substituted (formyl or phenylcarbamoyl substituted) organoselenium compounds (**138**, **140**, **141**, and **142**) reveal an interesting fact that, in contrast to organoselenium compounds having only one *ortho*-formyl or alkyl/arylcarbamoyl substitution, bis-*ortho*-substituted organoselenium compounds do not show any Se···O interactions in their single-crystal X-ray structures.⁹⁴ Consequently, a marked difference has been observed in their chemical reactivity. For example, the reactions with halogenating reagents afforded selenenate ester instead of the expected selenenyl halides (Scheme 25).^{93,94} The selenenyl halides are not stable and react with traces of water and give selenenic acid, which further undergoes intramolecular reaction to give selenenate ester. Although a recent publication by Wada et al. describes the synthesis of compounds such as **143a** and **143b**,⁹⁵ there is no mention of any interaction between the *ortho*-methoxy group and the selenium atom.

Ferrocenyl selenides **144a**–**144f** have been synthesized by lithiation of *N,N*-diisopropyl ferrocenecarboxamide followed by quenching with appropriate aryl/alkyl diselenide, except **144g**, which was synthesized directly by treating benzyl chloride with lithium *N,N*-diisopropyl ferrocenecarboxamide selenolate in one-pot reaction (Scheme 26).⁹⁶ Selenides **144a**–**144c** have been structurally characterized by single-crystal X-ray diffraction studies. All three selenides do not show any Se···N interaction in the solid state. Only **144c** shows considerable Se···O interaction in the solid state.

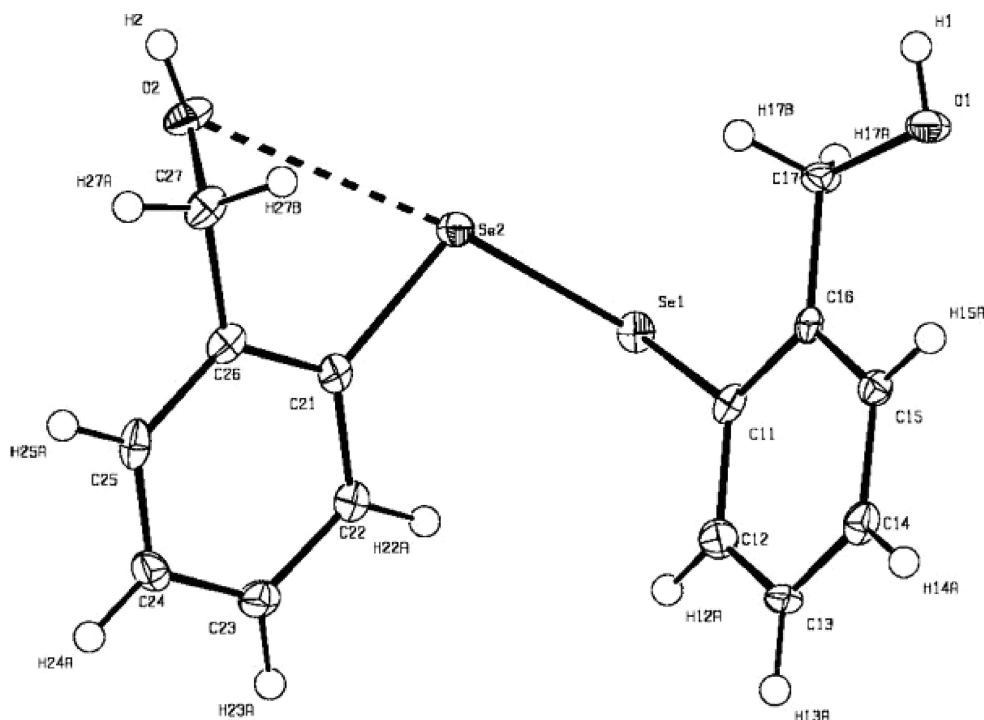
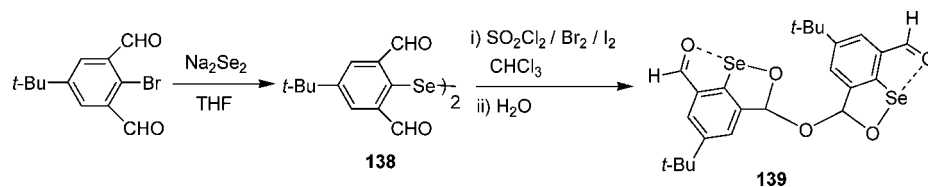


Figure 12. Molecular structure of **135e**. Reprinted with permission from ref 92. Copyright 2005 American Chemical Society.

Scheme 25



This observation is in contrast to strong Se \cdots N interaction observed for related oxazoline based ferrocenyl/phenyl selenide. This has been explained on the basis of the resonating structures shown in Scheme 27. Owing to the charged nature of the resonance structures of **144c'** and **144c''**, one may expect O to be an electron donor, which, in

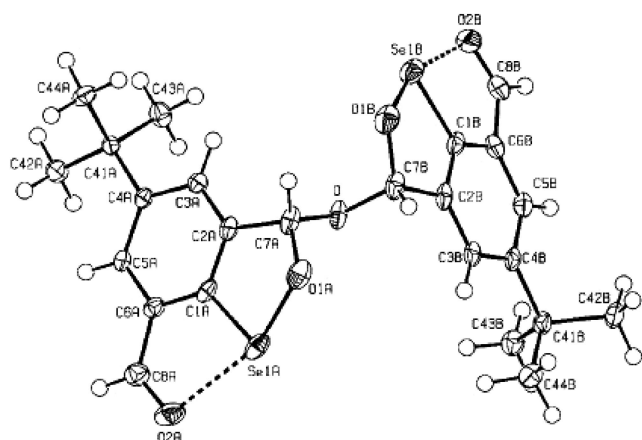


Figure 13. Molecular structure of **139**. Reprinted with permission from ref 93. Copyright 2004 Wiley Interscience.

Chart 18

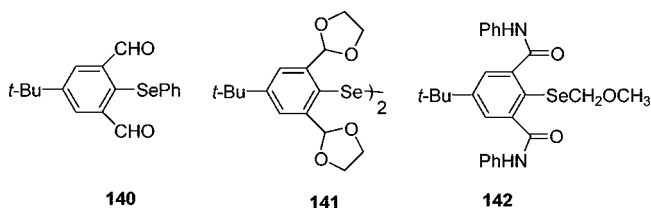


Chart 19

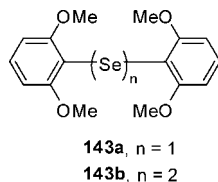
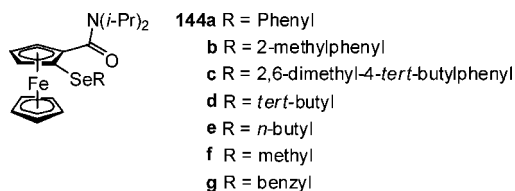
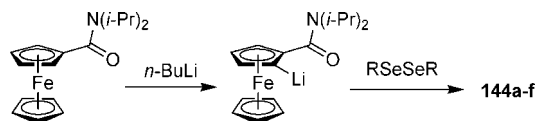


Chart 20



Scheme 26



Scheme 27

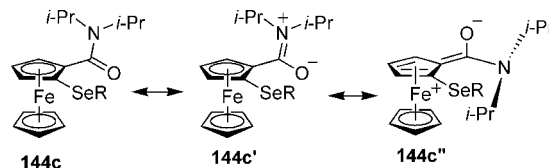
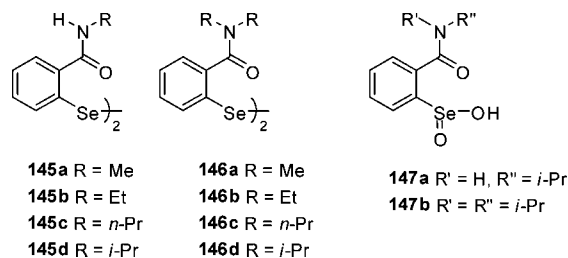


Chart 21

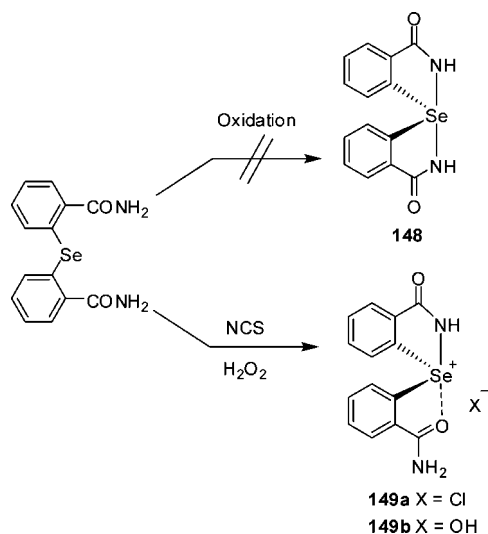


turn, reduces the possibility of any intramolecular interaction of the nitrogen atom with selenium. Another detrimental factor for Se...N interaction may be steric crowding by the isopropyl groups attached to nitrogen.

Bhabak and Mugesh have synthesized a series of secondary and tertiary amide-substituted diselenides and studied their GPx-like antioxidant activities.⁹⁷ Single-crystal X-ray diffraction studies on compounds **146a** and **146d** were performed to understand the nature of Se...O/N interactions in these compounds. The X-ray structures of **146a** and **146d** revealed that the carbonyl oxygen atoms interact with selenium, leading to the formation of O...Se–Se...O arrangements. The Se...O distances in compound **146a** (2.793 and 2.852 Å) are shorter than those of **146d** (3.053 and 3.264 Å), suggesting that the bulkier *tert*-amino group decreased Se...O nonbonded interactions. A similar observation was obtained for the single-crystal X-ray structures of compounds **147a** and **147b** which revealed that the Se...O interactions in compound **147a** are much stronger than those of **147b**, indicating that the substitution of the free N–H group by an *N*-alkyl substituent reduces the strength of Se...O interactions in the seleninic acid.

The oxidation of 2,2-selenobis(benzamide) with *N*-chlorosuccinimide or hydrogen peroxide afforded the corresponding stable azaselenonium chloride **149a** and hydroxide **149b**, respectively, rather than the corresponding spirodiazaselenurane **148** (Scheme 28).⁹⁸ The structures were characterized by spectroscopic and X-ray crystallographic methods. Each contains a covalent N–Se bond, as well as a noncovalent interaction between the selenium atom and the carbonyl oxygen atom of the other amide moiety. In the case of **149**, the electronegative oxygen and nitrogen atoms occupied the apical positions of a distorted trigonal bipyramid, in which the N(axial)–Se–O(axial) bond angle of 169.00(9) is roughly linear. The Se–O bond distances of 2.311(2) and 2.492(14) Å are significantly longer than the typical covalent value of 1.76 Å. This indicates a strong interaction between Se and O, rather than a covalent bond. The treatment of the

Scheme 28



azaselenonium chloride with an excess of potassium hydride in DMSO- d_6 afforded the corresponding spirodiazaselenurane species, which proved to be hydrolytically unstable but was characterized by NMR spectroscopy.

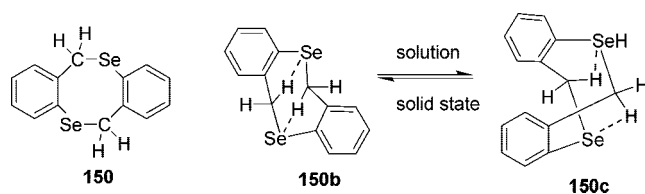
The syntheses of the triorganochalcogenium dinitramide salts $[\text{Ph}_3\text{Te}][\text{N}(\text{NO}_2)_2]$, $[\text{Me}_3\text{Te}][\text{N}(\text{NO}_2)_2]$, $[\text{Ph}_3\text{Se}][\text{N}(\text{NO}_2)_2]$, $[\text{Me}_3\text{Se}][\text{N}(\text{NO}_2)_2]$, $[\text{Ph}_3\text{S}][\text{N}(\text{NO}_2)_2]$, and $[\text{Me}_3\text{S}][\text{N}(\text{NO}_2)_2]$ and their characterization by multinuclear NMR spectroscopy, vibrational spectra, and single-crystal structures were studied by Klapötke et al.⁹⁹ In contrast to telluronium salt, selenonium salt consists of isolated cation–anion pairs with only monodentate chalcogen–oxygen contacts. The intermolecular selenium–oxygen distance is 2.979(4) Å, significantly shorter than the sum of the selenium–oxygen van der Waals radii. This intermolecular contact leads to distorted trigonal-bipyramidal coordination (AX_4E) around the selenium atom. This is in contrast to the structure of telluronium salt and likely an effect of the smaller size of a selenium atom compared to a tellurium atom. The same behavior has been reported previously for the comparable azide salts $[\text{Ph}_3\text{Te}]\text{N}_3$ and $[\text{Ph}_3\text{Se}]\text{N}_3$.¹⁰⁰

2.4. The $\text{Se}\cdots\text{H}$ “Hydrogen Bond”

The first observation of intramolecular $\text{Se}\cdots\text{H}-\text{C}$ “hydrogen bond” was reported by Tomoda et al. in 1994.¹⁰¹ The $\text{Se}\cdots\text{H}-\text{C}$ nonbonded interaction was found in compound diselenocin **150**, obtained unexpectedly from the reduction of 2,2′-diselenobis(benzyl chloride)¹⁹ with sodium borohydride in methanol during the synthesis of a glutathione peroxidase model.¹⁰² Compound **150** was shown to exist as two conformers **150b** and **150c** (Scheme 29).⁸⁴

A unique feature of the molecular structure was the unusually short interatomic distances between selenium and one of the two benzylic hydrogens on the nonbonded benzylic carbon atom. Solid-state IR spectral measurements

Scheme 29

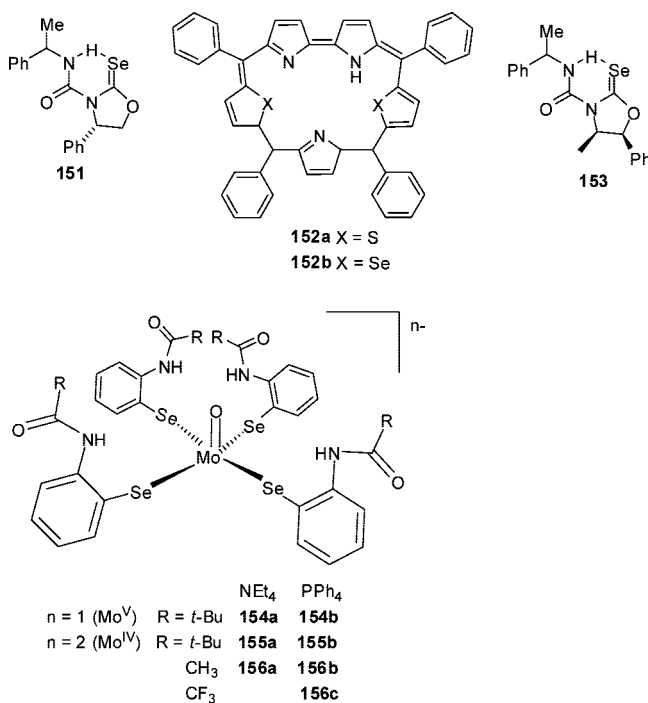


demonstrated that the $\text{Se}\cdots\text{H}$ van der Waals contact present was an attractive one. Further confirmation of the $\text{Se}\cdots\text{H}-\text{C}$ interaction in **150** was obtained by the determination of a spin–spin coupling constant between the two atoms involved in the interaction. From the experimental work undertaken, it was not possible to precisely define the nature of the forces involved in the $\text{Se}\cdots\text{H}-\text{C}$ interaction but the experiments showed a significant interaction which could be classed as a “hydrogen bond”. As selenium is not highly electronegative and the C–H bond is essentially nonpolar, it was thought that the interaction was not of an electrostatic nature.

In 1996 Tomoda et al. further investigated the $\text{Se}\cdots\text{H}-\text{C}$ bond in order to unambiguously demonstrate that it was a hydrogen bond and not merely caused by van der Waals repulsion.¹⁰² The deuterium-induced isotope effects of the $\text{Se}\cdots\text{H}-\text{C}$ nonbonded interaction in **150** were investigated. The IR spectroscopic behavior of the deuterated compound was compared with a reference compound (benzyl- α,α - d_2 phenylselenide). The $\text{Se}\cdots\text{H}-\text{C}$ interactions in both compounds **150b** and **150c** were found to cause a decrease in the low wavenumber shift of ν_1 . The ^{77}Se NMR results indicated an upfield isotope shift caused by the throughspace $\text{Se}\cdots\text{H}-\text{C}$ interaction ($\Delta\delta = 0.44$ ppm for **150b** and 0.25 ppm for **150c**). These results clearly suggested that the interaction was an attractive one. Further evidence for the presence of a $\text{Se}\cdots\text{H}-\text{C}$ interaction was reported by Wu and co-workers.¹⁰³ They presented results signaling the potential for significant hydrogen selenium bonding interactions with biomacromolecular systems containing either selenomethionine or selenocystein. The oxazolidin-2-selone **151** and its derivatives represent a new class of chiral derivatizing agents (CDA) with enhanced sensitivity and have $\text{N}-\text{H}\cdots\text{Se}$ bonding with $^1J_{\text{Se}-\text{H}}$ coupling constant ~ 12 – 13 Hz. Narayanan et al. described the first structural characterization of two core-modified sapphyrins, **152a** and **152b**.¹⁰⁴ These have been shown to self-assemble in the solid state to form a supramolecular ladder held together by weak $\text{S}\cdots\text{H}-\text{C}$ and $\text{Se}\cdots\text{H}-\text{C}$ hydrogen bonding interactions. The first X-ray crystal structures of **152a** and **152b** revealed that the replacement of the pyrrole NH groups by S or Se changed the π -electron delocalization. The bond lengths in the macrocycle were altered compared to those of free thiophene or selenophene fragments. Singh et al. have reported the $\text{Se}\cdots\text{H}-\text{C}$ intermolecular hydrogen bonding interactions in the crystal structure of diselenide **138** and monoselenide **140**.⁹⁴ The packing diagram of monoselenide exhibited the formation of a centrosymmetric pair of molecules by the pair of such $\text{Se}\cdots\text{H}-\text{C}$ intermolecular hydrogen bonding interactions.

Silks and co-workers have also recently reported the presence of $\text{Se}\cdots\text{H}$ interaction during a study of the synthesis and applications of chiral selenones.¹⁰⁵ During the course of their work, they measured both the proton coupled and decoupled ^{77}Se NMR spectra of a number of selenone amine adducts. The results of these experiments on compound **153** lead to the conclusion that the amine adduct assumed an *anti*-carbonyl relationship and that the N–H must be hydrogen bonded to the selenium atom of the selenocarbonyl. Moreover, the selenium was found to be weakly interacting with the water arising from CDCl_3 , which was not dried prior to use. These results signified the potential for significant selenium hydrogen bonding interactions within biomacromolecular systems.

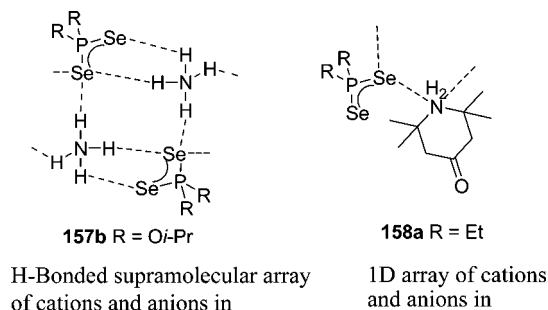
Chart 22



Recently, Okamura et al. have studied $\text{Se} \cdots \text{H}-\text{N}$ hydrogen bonds in molybdenum areneselenolate **154**–**156**, and the hydrogen bonds were detected directly by $^{77}\text{Se}-^1\text{H}$ nuclear spin–spin coupling.¹⁰⁶ The $\text{Se} \cdots \text{H}-\text{N}$ hydrogen bonds facilitated the isolation of the first example of monooxomolybdenum(IV) areneselenolate **155**–**156** in the reduced state. In the crystal structures of **156a** and **156c**, although the direction of the amide NH is not so desirable, the large $4p\pi$ orbital of the selenium atom enables the formation of $\text{Se} \cdots \text{H}-\text{N}$ hydrogen bond. The ^{77}Se NMR spectrum of **155a** showed a doublet at 303 ppm with coupling constant $^1J(^{77}\text{Se}-^1\text{H}) = 5.4$ Hz (spin–spin coupling constant). The relatively small J coupling constant of **155a** in comparison with the observed $^{77}\text{Se}-^1\text{H}$ spin–spin coupling constant of ca. 12–13 Hz in selone¹⁰³ indicates weak spin–spin coupling through the hydrogen bond. The $^{77}\text{Se}-^1\text{H}$ correlated spectroscopy (COSY) clearly indicates that the $^{77}\text{Se}-^1\text{H}$ coupling occurs through the $\text{Se} \cdots \text{H}-\text{N}$ hydrogen bond and not via the other pathway. Reduction of the Mo(V) complex (**154b**) to Mo (IV) (**155a**) resulted in a low wavenumber shift of $\nu(\text{NH})$ by 35 cm^{-1} in the IR spectrum. The enhancement of $\text{Se} \cdots \text{H}-\text{N}$ hydrogen bonds by the reduction of the molybdenum center is explained by the increase of the electron density on selenium, which is ascribed to the decrease of the electron donation to the metal ion. Molecular orbital (MO) calculations with 3-21G** showed that three of four amide NH groups were located to form intraligand $\text{Se} \cdots \text{H}-\text{N}$ hydrogen bonds; however, one amide group is distinguishable from the other three. The $\text{Se} \cdots \text{H}-\text{N}$ hydrogen bond stabilizes the Mo–Se bond by decreasing the antibonding character of the Mo–Se bond.

Hydrogen bonding in the form of $\text{N}-\text{H} \cdots \text{Se}$ interaction has been observed in the crystal structure of *N*-phenyl-*N'*-benzoylselenourea ($\text{C}_6\text{H}_5\cdot\text{NH}\cdot\text{CSe}\cdot\text{NH}\cdot\text{CO}\cdot\text{C}_6\text{H}_5$).¹⁰⁷ A short $\text{N}-\text{H} \cdots \text{Se}$ contact of 3.83 Å indicative of hydrogen bonding was observed in a grouping with $\text{N}-\text{H}$ (1.08 Å) and $\text{Se} \cdots \text{H}$ (2.94 Å). The $\text{N}-\text{H} \cdots \text{Se}$ angle of 140° was attributed to hydrogen bonding, resulting in *N*-phenyl-*N'*-benzoylselenourea crystallizing as a centrosymmetric, hydrogen bonded

Chart 23



dimer. The hydrogen bonding ability of *N*-phenyl-*N'*-benzoylselenourea was thought to be caused by a partial negative charge on the Se atom. A further example of $\text{N}-\text{H} \cdots \text{Se}$ bonding was reported by Bensch et al.¹⁰⁸ The complex anion $[\text{Mn}_4(\text{en})_9(\text{SbSe}_4)_4]^{4-}$ ($\text{en} = 1,2$ -diaminoethane) was prepared by the reaction of elemental manganese, antimony, and selenium under mild solvothermal conditions. $\text{N}-\text{H} \cdots \text{Se}$ hydrogen bonding was observed between the selenium center of the SbSe_4^{3-} anion and an amino hydrogen of a chelate ligand bound to manganese. The $\text{Se} \cdots \text{H}$ distance was 2.614 Å, which is less than the sum of van der Waals radii for the atoms. The $\text{N}-\text{H} \cdots \text{Se}$ angle was 176.1° .

Liu et al. reported the structural characterization of ammonium salt of the diselenophosphate (dsep) ligand, $\text{NH}_4\text{Se}_2\text{P}(\text{O}i\text{Pr})_2$, **157b**.¹⁰⁹ $\text{NH}_4\text{Se}_2\text{P}(\text{O}i\text{Pr})_2$ exhibits a 1D supramolecular chain produced by the H-bonding between the NH moieties and Se atoms ($\text{N}-\text{H} \cdots \text{Se}$) of the dsep ligand. In addition, the $\text{NH}_4\text{Se}_2\text{P}(\text{OR})_2$ ligands serve as an ammonia source in the Fe powder catalyzed condensation of acetone with ammonia to form 2,2,6,6-tetramethyl-4-oxopiperidinium salts of the dsep ligand, $[\{\text{H}_2\text{N}(\text{CH}_2)_2(\text{CMe}_2)_2\text{CO}\}\{\text{Se}_2\text{P}(\text{OR})_2\}]$ (**158a** R = Et, **158b** R = *i*-Pr), of which the former (R = Et) was structurally characterized. The structural elucidation of $[\{\text{H}_2\text{N}(\text{CH}_2)_2(\text{CMe}_2)_2\text{CO}\}\{\text{Se}_2\text{P}(\text{OEt})_2\}]$ **158a** could enable us to demonstrate the H-bonding interactions of cationic oxopiperidinium and anionic dsep ligand in the solid state. The N atom of the oxopiperidinium ring in **158a**, which is in chair conformation, is slightly closer to the Se1 atom of the anionic unit as evident from nonbonding distances of $\text{Se1} \cdots \text{N}$ (3.454(5) Å) compared to $\text{Se2} \cdots \text{N}$ (3.589(4) Å). Se of the diselenophosphate unit forms H-bonding with two hydrogen atoms on N atoms of neighboring oxopiperidinium cations in the crystal lattice. The H-bonding leads to the formation of a one-dimensional supramolecular array. The $\text{Se} \cdots \text{H}$ distances are within the reported range. The H-bonding of Se1 to two cationic units resulted in a slightly larger P1–Se1 bond length.

2.5. Other Types of Nonbonded Interaction

2.5.1. $\text{Se} \cdots \text{Halogen}$

Nakanishi et al. have been interested in the nonbonded interactions between a fluorine atom, with its small size of valence orbitals, and other heteroatoms in close proximity such as a selenium atom in compounds like **159b**.¹¹⁰ The X-ray crystallographic structure of **159b** showed alignment of the fluorine, selenium, and carbon atoms ($\angle \text{F}-\text{Se}-\text{C} = 175.0^\circ$, Figure 14). The nonbonded distance between the F and Se atoms was found to be shorter than the sum of the van der Waals radii for the two atoms by 0.6 Å. Two possible types of interaction were proposed. One was the interaction

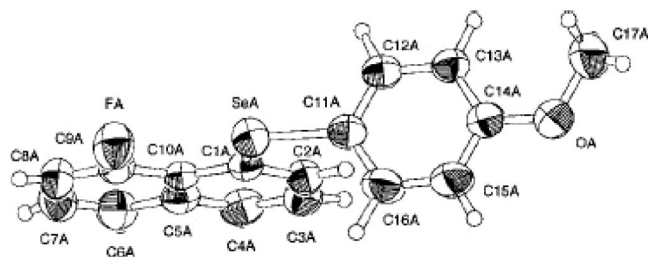
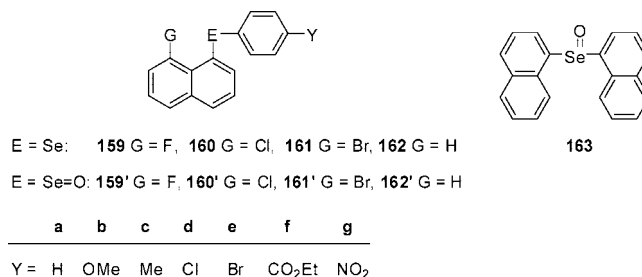


Figure 14. Molecular structure of **159b**. Reprinted with permission from ref 110b. Copyright 2002 American Chemical Society.

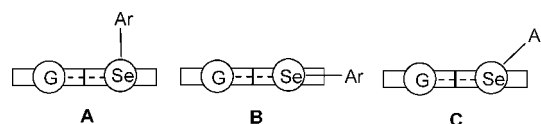
of the π -framework of the naphthalene ring cooperated by the p-type orbitals of fluorine and selenium atoms. The other was the $n_{\text{F}}-\sigma^*(\text{Se}-\text{C})$ type interaction, which was strongly suggested by the linear alignment of the $\text{F}\cdots\text{Se}-\text{C}$ atoms in **159b** as described above. The group has recently extended the investigations to other related derivatives of the type 8-G-1-($p\text{-C}_6\text{H}_4\text{Se}$) C_{10}H_6 ($\text{G} = \text{Cl}, \text{Br}; \text{Y} = \text{H}, \text{OMe}, \text{Me}, \text{etc.}$).^{110b} The single-crystal X-ray structures of **160b–160d** and **161d**, **161g** revealed similar interactions to that observed for compound **159b**, i.e., the nearly linear arrangement $\text{G}\cdots\text{Se}-\text{C}$ moiety. The $\text{Se}-\text{C}$ bond of $p\text{-C}_6\text{H}_4\text{Se}$ in 8-G-1-($p\text{-C}_6\text{H}_4\text{Se}$) C_{10}H_6 was almost perpendicular to the naphthyl plane in crystal structures of **159–161**, which is in contrast to the structure of **162**. This has been ascribed to the nonbonded $\text{G}\cdots\text{Se}-\text{C}$ 3c-4e interaction, which has been further supported by ab initio MO calculations (vide infra). Introduction of oxygen at Se, i.e., oxidation of Se to the corresponding selenoxide, changed the structures in different conformation where $\text{Se}-\text{C}_{\text{Ar}}$ and $\text{Se}-\text{O}$ bonds are perpendicular to and parallel to the naphthyl plane, respectively;¹¹¹ two factors have been proposed to be responsible for the resulting structures on the basis of X-ray structures and quantum chemical (QC) calculations. The origin of the O dependence (the structural change by O at Se is called O dependence) is the nonbonded $n_{\text{p}}(\text{O})\cdots\pi(\text{Nap})$ interactions, whereas G dependence (the structural change by G at 8-position is called G dependence) is the nonbonded $n_{\text{p}}(\text{G})\cdots\sigma^*(\text{Se}-\text{O})$ 3c-4e interactions. The latter interactions align the $\text{G}\cdots\text{Se}-\text{O}$ atoms linearly. Structural features of compounds **159'–162'** are of the same type, whereas, in compound **163**, both naphthyl rings are perpendicular to the $\text{Se}-\text{O}$ bond as a result of the double $n_{\text{pz}}(\text{O})\cdots\pi_{\text{z}}(\text{Nap})$ and $n_{\text{py}}(\text{O})\cdots\pi_{\text{y}}(\text{Nap})$ interactions. The nonbonded $n_{\text{p}}(\text{G})\cdots\sigma^*(\text{Se}-\text{O})$ 3c-4e interactions are very weak except for $\text{G} = \text{Br}$. QC calculations showed that the energy-lowering effect of the O dependence is estimated to be 20 kJ mol^{-1} and the G dependence of the nonbonded $n_{\text{p}}(\text{Br})\cdots\sigma^*(\text{Se}-\text{O})$ 3c-4e interaction in **161'** is close to that value, if the steric repulsion between Br and Se is contained in the G dependence. The G dependence must be larger in an order of $\text{F} < \text{Cl} < \text{Br}$. On the other hand, the steric repulsion of G also increases in an order of $\text{H} < \text{F} < \text{Cl} < \text{Br}$.

Structures of 1-(arylethynylselanyl)naphthalenes [1-($p\text{-YC}_6\text{H}_4\text{C}\equiv\text{CSe}$) C_{10}H_7 : **164**, $\text{Y} = \text{H}$ (a), OMe (b), Me (c), Cl (e), CN (h), NO_2 (i)] have been determined by X-ray crystallographic analysis.¹¹² The structures are of type A for **164a–164c**, bearing Y that is a nonacceptor, and type B for **164e**, **164h**, and **164i**, having Y that is a strong acceptor. The $\text{Se}-\text{C}_{\text{sp}}$ bond is perpendicular to the naphthyl plane in type A, but is in the plane in type B; and type C is intermediate between A and B (Scheme 30). The Y dependence observed in **164** is just the opposite to the case of

Chart 24



Scheme 30



1-(arylselanyl)naphthalenes [1-($p\text{-YC}_6\text{H}_4\text{Se}$) C_{10}H_7] **159–162**. This can be ascribed to “ethynyl effect”, which controls the structures of **164**. The structures of **164h** and **164i** are planar or almost planar. The energy-lowering effect by the parallel direction between $n_{\text{p}}(\text{Se})$ and $n_{\text{p}}(\text{Y})$ must be responsible for the observations if Y is a strong acceptor. The parallel direction between $n_{\text{p}}(\text{Se})$ and $n_{\text{p}}(\text{Y})$ operates to lower the energy if Y is an acceptor, but it destabilizes the system for donor Y groups. Therefore, the origin of the ethynyl effect is explained in terms of how widely the electron in $n_{\text{p}}(\text{Se})$ extends over the π -framework under the conditions. Crystal packing effects, such as the formation of dimers, also play an important role in determining the structures of **164**. The dimer formation in **164a–164c** substantially stabilizes the structures. The π -stacking of naphthyl groups may also contribute to the dimer formation. Compound **164** exists in type A form in solutions, with some equilibration with type B. The ethynyl effect that controls the fine structures of **164** is also observed in solution. The results are well-supported by QC calculations on the structures, energy profiles, and the evaluation of electron affinity. The NMR chemical shifts corroborate the behavior of **164** in solution.

Furthermore, 8-G-1-($p\text{-YC}_6\text{H}_4\text{C}\equiv\text{CSe}$) C_{10}H_6 [**164'** ($\text{G} = \text{Cl}$) and **164''** ($\text{G} = \text{Br}$): $\text{Y} = \text{H}$ (a), OMe (b), Me (c), F (d), Cl (e), CN (f), NO_2 (g)] have been prepared, and their NMR spectra have been measured. Structures have been determined by X-ray crystallographic analysis for **164'b**, **164'e**, and **164'g**, which are all type B (B), where the $\text{Se}-\text{C}_{\text{sp}}$ bond is placed in the naphthyl plane.¹¹³ The compounds having $\text{Se}-\text{C}_{\text{sp}}$ bond perpendicular to the naphthyl plane are called type A. Structures around the $p\text{-YC}_6\text{H}_4$ (Ar) group are pd (perpendicular) for $\text{Y} = \text{OMe}$ (**164'b**) and Cl (**164'e**) and pl (planar) for $\text{Y} = \text{NO}_2$ (**164'g**), where the $\text{Se}-\text{C}_{\text{Nap}}$ bond is placed in the aryl plane in pl and perpendicular to the plane in pd. The **164b** (A: pd) structure changes dramatically on going to **164'b** (B: pd) with $\text{G} = \text{Cl}$ at the 8-position. The G dependence arises from the energy-lowering effect of the $n_{\text{p}}(\text{Cl})\cdots\sigma^*(\text{Se}-\text{C}_{\text{sp}})$ 3c-4e interaction. Structures are both (B: pd) for **164e** and **164'e** and both (B: pl) for **164g** and **164'g**. One may realize that the structures are unchanged by $\text{G} = \text{Cl}$ in place of $\text{G} = \text{H}$ for $\text{Y} = \text{Cl}$ and NO_2 at a first glance. However, the B structures in **164'e** and **164'g** must be much more stabilized by the G dependence of the $n_{\text{p}}(\text{Cl})\cdots\sigma^*(\text{Se}-\text{C}_{\text{sp}})$ 3c-4e interaction or the $\text{G}\cdots\text{Se}-\text{C}_{\text{sp}}-\text{C}_{\text{sp}}-\text{C}_{\text{sp}2}$ 5c-6e type interaction. The structures of **164'** and **164''** have been examined in solution as well as by NMR parameters.

Chart 25

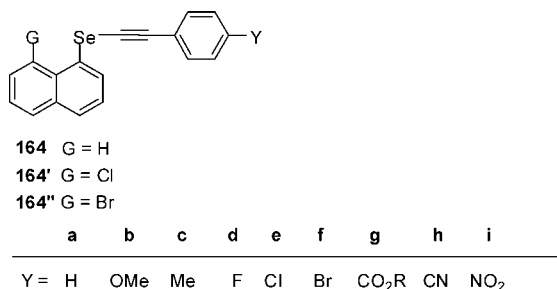
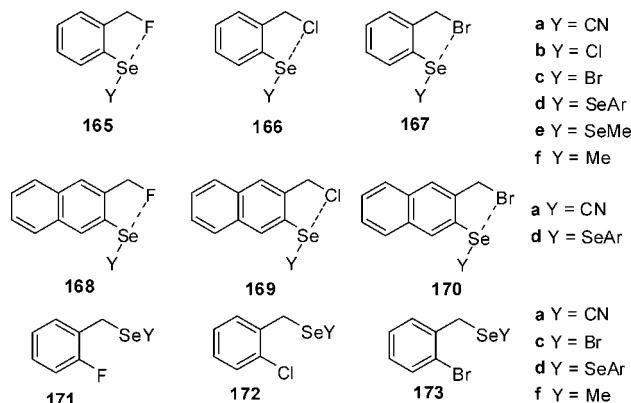
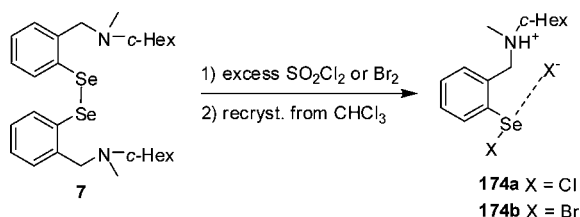


Chart 26



Scheme 31

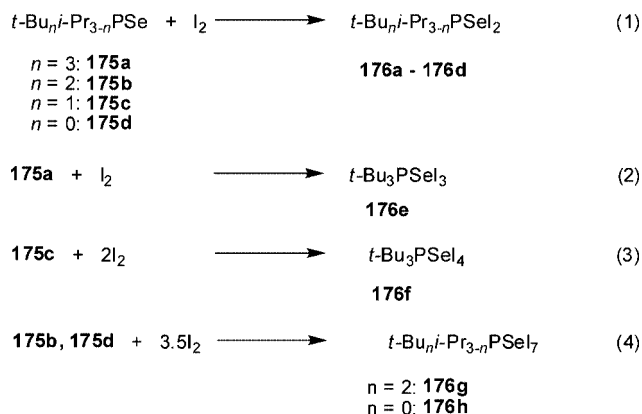


The results show that **164'** and **164''** are quite similar to each other and the structures are predominantly type B, with some equilibrium between pd and pl around the aryl groups in solution. QC calculations support these observations.

Tomoda and co-workers have also studied nonbonded Se...F interactions in a series of *O*-selenobenzylfuramide derivatives.¹¹⁴ Furthermore, three series of selenenyl halides (**165**–**167**; **168**–**170**; and **171**–**173**) have been synthesized, and the strength of Se...X interaction has been established on the basis of ⁷⁷Se NMR.¹¹⁵ It is shown that the magnitude of the downfield shift of ⁷⁷Se NMR can be used as a quantitative probe for measuring the strength of nonbonded Se...X interactions.^{114a,116} On the basis of ⁷⁷Se NMR analysis of the first two series, it is concluded that the strength of Se...X interactions decreases in the order of Se...F > Se...Cl > Se...Br. Because of much lower basicity of halogens in the third series (**171**–**173**), Se...X interactions have not been observed. It is worth noting that electron correlation would also be one of the more important factors in Se...X interactions.

When diselenide **7** was treated with an excess of SO₂Cl₂ or Br₂, arylselenenyl chloride **174a** and bromide **174b** stabilized by hypervalent coordination with a halide anions were obtained by recrystallization from CHCl₃ (Scheme 31).¹¹⁷ The significant close contacts [2.676(2) Å, Se1...Cl2, and 2.769(2) Å, Se1...Br2] between the counter-halides and

Scheme 32



the divalent selenium atom were observed. A subsequent elongation of Se1–Cl1 and Se1–Br1 bonds [2.307(2) Å, Se1–Cl1, and 2.474(2) Å, Se1–Br1] also has been observed. The geometry around selenium was T-shaped with linear arrangement of Cl1–Se1–Cl2 and Br1–Se1–Br2.

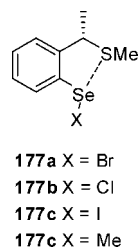
The reactions of trialkylphosphane selenides $t\text{Bu}_n i\text{Pr}_{3-n}\text{PSe}$ ($n = 3$, **175a**; $n = 2$, **175b**; $n = 1$, **175c**; $n = 0$, **175d**) with iodine were studied with the help of heteronuclear NMR spectroscopy, vibrational spectroscopy, and X-ray crystal structure determinations.¹¹⁸ The compounds, though, are not organoselenium in a strict sense and exhibit interesting intra- and intermolecular secondary interactions. The reaction of **175a** with 1 equiv of iodine provides, after crystallization from dichloromethane/pentane, solid **175b**, which consists of pairs of molecular adducts $t\text{Bu}_3\text{PSe} \cdots \text{I} \cdots \text{I}$, together with chains of alternating $[(t\text{Bu}_3\text{PSe})_2\text{I}]^+$ and I_3^- ions (Scheme 32). The addition of iodine to **175b**, **175c**, and **175d** in a 1:1 molar ratio furnishes ionic solids with the formulation $[(t\text{Bu}_n i\text{Pr}_{3-n}\text{PSe})_2\text{I}]^+[\text{I}_3]^-$ ($n = 2$, **176b**; $n = 1$, **176c**; $n = 0$, **176d**). Compounds **176a**–**176d** exhibit supramolecular structures based on various kinds of weak Se...I and Se...Se interactions. In **176a**, the uncharged molecules form dimers through Se...Se contacts, while the anions and cations assemble to form chains through linear P–Se...I anion contacts. The ionic compounds **176b** and **176d** consist of the same type of chains, although they are not isotypic to each other. The two independent formula units of **176c** are topologically different; whereas one forms cation–anion chains analogous to those of **176b** and **176d**, the other forms cation chains through Se...Se contacts. Though the Se...I contacts between the latter chains and triiodide anions are very long, these seem to be structurally significant. These contacts, which are well above the sum of the van der Waals radii, have been proposed as *tertiary contacts*. On using more than 1 equiv of I₂, compounds corresponding to the formulation $t\text{Bu}_n i\text{Pr}_{3-n}\text{PSeI}_x$ ($x = 3$, $n = 3$: **176e**; $x = 4$, $n = 1$: **176f**; $x = 7$, $n = 2$ and 0: **176g** and **176h**) were isolated as single crystals. Ionic **176e** contains pairs of cations $[(t\text{Bu}_3\text{PSe})_2\text{I}]^+$, connected by Se...Se contacts, located between corrugated layers of polymeric I_3^- anions. Compound **176f** consists of two independent formula units $t\text{Bu}i\text{Pr}_2\text{PSeI}_2 \cdot \text{I}_2$, which could, however, be regarded as $t\text{Bu}i\text{Pr}_2\text{PSeI}^+ \cdot \text{I}^- \cdot \text{I}_2$ because of the long I–I distance adjacent to Se. To a fair approximation, the packing of the two units is independent; unit 1 forms dimers $(\cdots\text{Se} \cdots \text{I} \cdots \text{I} \cdots \text{I} \cdots)_2$, whereas the same motif in unit 2 forms chains. The structural subunits are linked through further contacts involving terminal iodine atoms from $t\text{Bu}i\text{Pr}_2\text{PSeI} \cdots \text{I}$ units, which thereby form μ_3 -bridging units, and by additional I–I...Se

contacts. In **176g**, iodide-bridged cations $[t\text{Bu}_2\text{iPrPSeI}\cdots\text{I}\cdots\text{ISePiPr}t\text{Bu}_2]^+$ are anchored to a polyiodide network of formal composition $\text{I}_{11-} = [\text{I}^-](\text{I}_2)_5$ through $\text{I}\cdots\text{I}$ contacts. Except for one $\text{I}\cdots\text{I}$ contact, the polyiodide is two-dimensional, although highly puckered. In **176h**, $[\text{iPr}_3\text{PSeI}]^+$ cations and I_2 molecules exhibit weak $\text{I}\cdots\text{I}$ interactions with I^- units from puckered square-net-like polyiodide layers. Trialkylphosphane selenides interact with various amounts of iodine, giving $\text{Se}\cdots\text{I}$ bonds in adducts with the composition R_3PSeI_x ($x = 2-7$). The solid compounds exhibit a number of weak intermolecular “soft–soft” interactions (>3 Å), namely, the expected variety of $\text{I}\cdots\text{I}$ interactions, but also $\text{Se}\cdots\text{I}$ interactions between cations and anions, and attractive $\text{Se}\cdots\text{Se}$ interactions between molecules and between cations. In general, these interactions in supramolecular networks can be rationalized in terms of unsymmetric $3c-4e$ systems and of $n \rightarrow \sigma^*$ overlap. In solution, the complexes are kinetically labile with respect to rapid R_3PSe ligand exchange analogous to halogen transfer reactions in systems $\text{R}_3\text{P}/\text{R}_3\text{PX}_2$ ($\text{X} = \text{Br}, \text{I}$) and $\text{R}_3\text{PSe}/\text{R}_3\text{PSeBr}_2$. Iodine coordination leads to significant downfield shifts in the ^{77}Se NMR signals. As in several other cases of donor–acceptor adducts with iodine, the molecular species $\text{R}_3\text{PSe}-\text{I}-\text{I}$ are energetically close to the ionic species $(\text{R}_3\text{PSe})_2\text{I}^+[\text{I}_3]^-$. Excess I_2 favors formation of R_3PSeI^+ cations that behave as soft electrophiles interacting with polyiodide anions.

2.5.2. $\text{Se}\cdots\text{S}$ Interactions

Tiecco and co-workers have established novel $\text{Se}\cdots\text{S}$ interactions using achiral/chiral sulfur-containing electrophilic selenium reagents for efficient asymmetric syntheses.¹¹⁹ Spectroscopic and chemical evidence demonstrate that the observed high selectivity of the asymmetric reactions is associated with a nonbonding selenium–sulfur interaction. It was suggested that these excellent results were due to the fact that the selenium–sulfur interaction is more efficient than the interactions between selenium–oxygen or –nitrogen. More recently, in order to have unambiguous experimental evidence for the existence of this $\text{Se}-\text{S}$ interaction, X-ray analysis of selenenyl halides **177a** and **177b** was reported by the same group.¹²⁰ Compounds **177a** and **177b** are isostructural; the coordination geometry around the selenium atom is T-shaped with a bond angle of $178.86(5)^\circ$ for **177a** and $177.74(4)^\circ$ for **177b**. The distance between Se and S [$2.497(7)$ Å for **177a** and $2.344(2)$ Å for **177b**] is significantly shorter than the sum of the van der Waals radii (3.7 Å), and this demonstrates that an intramolecular interaction between selenium and sulfur exists. The shorter distance observed in compound **177b** compared with that of compound **177a** seems to indicate a stronger interaction when the counterion is chlorine, and this observation is consistent with the calculated covalency factor χ for bromide (0.826) and chloride (0.902) derivatives. Further, it is supported by the solution ^1H , ^{13}C , and ^{77}Se NMR spectral data. Comparison of the Overhauser dipolar correlations for arylselenenyl chloride **177c** and arylmethyl selenide **177d** deduced a greater conformational rigidity for compound **177c** than that observed in **177d**. This is very likely due to the interaction between the selenium and sulfur atoms, which is not only present in the crystal form but also present in CDCl_3 solutions as well. Dependencies of the chemical shifts for the methyl and the methine protons and carbons on the electronegativity of the halogen attached to the selenium atom additionally confirm these interactions in solution. In agreement with

Chart 27



previous observations in other arylselenenyl halides, the trend in the chemical shift values is $\text{RSeCl} > \text{RSeBr} > \text{RSeI}$, and this suggests that the strongest $\text{Se}-\text{S}$ interaction occurs in the case of chloride **177c**. The upfield shift in ^{77}Se NMR of compound **177b** (750 ppm) and **177c** (797 ppm) compared to the corresponding unsubstituted PhSeBr (867 ppm) and PhSeCl (1044 ppm) is contradictory to the previous observations.^{11b,91b}

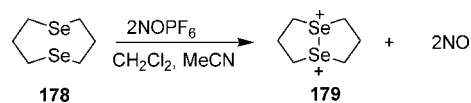
2.5.3. $\text{Se}\cdots\text{Se}$ Interactions

The diselenide PF_6^- salt $[\text{R}_2\text{Se}^+-\text{Se}^+\text{R}_2]$, **179**, was first isolated by Fujihara and co-workers.¹²¹ Compound **179** was synthesized by a two-electron oxidation of the bis-selenide **178** with nitrosonium hexafluorophosphate (NO^+PF_6^-) (Scheme 33). Compound **179** contained a transannular Se^+-Se^+ bond; this was thought to be the first example of a clear-cut transannular interaction between two selenium atoms in medium-sized cyclic bis(selenides).

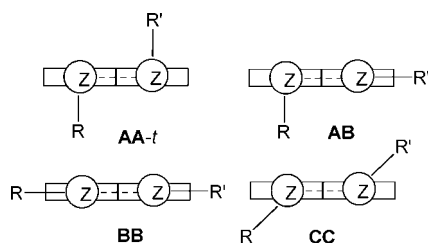
Chivers et al. have reported a synthetic protocol for the *tert*-butyl-substituted dichalcogenoimidodiphosphinates $[\text{Na}(\text{tmeda})\{(\text{EP}t\text{Bu}_2)_2\text{N}\}]$ ($\text{E} = \text{S}, \text{Se}, \text{Te}$).¹²² The two-electron oxidation of $[\text{Na}(\text{tmeda})\{(\text{EP}t\text{Bu}_2)_2\text{N}\}]$ ($\text{E} = \text{S}, \text{Se}, \text{Te}$) with iodine produced the salts $[(\text{EP}t\text{Bu}_2)_2\text{N}]^+\text{X}^-$ ($\text{E} = \text{S}, \text{X} = \text{I}_3$; $\text{E} = \text{Se}, \text{X} = \text{I}$; $\text{E} = \text{Te}, \text{X} = \text{I}$), which were characterized by X-ray crystallography. In contrast to the linear chains formed in $[(\text{EP}t\text{Pr}_2)_2\text{N}]^+\text{I}^-$, the *tert*-butyl derivatives $[(\text{SeP}t\text{Bu}_2)_2\text{N}]^+\text{I}^-$ exist as dimeric structures in which two five-membered $[(\text{SeP}t\text{Bu}_2)_2\text{N}]^+$ cations are associated by $\text{Se}\cdots\text{Se}$ contact of $3.466(2)$ Å and a selenium atom of each cation is linked to an iodine atom.

Fujihara et al. have also reported *peri*-interactions between selenium atoms in dinaphthol[1,8-b,c]-1,5-diselenocin, **180**, and 1,8-bis(methylseleno)naphthalene, **181**.¹²³ Compound **180** has been prepared as a nonplanar aromatic molecule possessing the possibility of a *peri*- $\text{Se}\cdots\text{Se}$ interaction and the interaction between the p-orbitals of the selenium atoms and the naphthalene π -system. To confirm the presence of the *peri*- $\text{Se}\cdots\text{Se}$ interaction, cyclic voltammetry (CV) was used to study the electrochemical oxidation of **180** and **181**. One reversible oxidation peak was observed at the oxidation potential $+0.33$ V for **180** and $+0.48$ V for **181**. The facile oxidation of **180** and **181** and the unusual stability of their cationic species were ascribed to *peri*- $\text{Se}\cdots\text{Se}$ interaction. The compounds were also found to exhibit interesting properties induced by the interaction between selenium atoms. They later reported *peri*-selenium participation in the seleno-Pummerer reaction of 1,8-bis(methylseleno)naphthalene, **181**, and naphthol[1,8-b,c]-1,5-diselenocin, **182a**.¹²⁴

Scheme 33



Scheme 34



Unusual seleno-Pummerer reactions of the diseleno *peri*-bridged naphthalenes, **181** and **182a**, were observed. The fact that the reactions proceeded under mild conditions was attributed to the interaction between the two selenium atoms. Evidence to support such an interaction was found from the ^{77}Se NMR data. Proton-decoupled ^{77}Se NMR spectra of the unsymmetrical diselenonaphthalenes showed satellite peaks due to ^{77}Se – ^{77}Se coupling. Large coupling constants of $J_{\text{Se-Se}} = 203\text{ Hz}$ for **182a** and $J_{\text{Se-Se}} = 310\text{ Hz}$ for **183a** were observed.

Homonuclear $\text{Z}\cdots\text{Z}$ ($\text{Z} = \text{O}, \text{S}, \text{Se}, \text{and Te}$) interactions have been investigated employing naphthalene 1,8-positions in 1,8-(MeZ) $_2\text{C}_{10}\text{H}_6$, 1-MeZ-8-PhZC $_{10}\text{H}_6$, and 1,8-(PhZ) $_2\text{C}_{10}\text{H}_6$.¹²⁵ Two types of structures were detected for **181**, **182a**, and **182b** (Scheme 34): CC for **181** (BB and CC structures were observed for the corresponding O and S analogues, respectively) and **182a** (AB structure was observed for the corresponding O and S analogues, respectively) and AB for **182b** (AB structure was observed for the corresponding O and S analogues and CC was observed for the corresponding Te analogue) by X-ray crystallographic analysis. The following controlling factors for the structures are considered: (a) The double $\text{p}(\text{O})$ – $\pi(\text{Nap})$ conjugations determine the structure of BB for the oxygen analogue of **181**. The $\text{p}(\text{Z})$ – $\pi(\text{Nap})$ conjugations in BB become weaker in the order $\text{Z} = \text{O} > \text{S} > \text{Se} > \text{Te}$. (b) The hypervalent $\text{n}_\text{p}(\text{Z})\cdots\sigma^*(\text{Z}-\text{C})$ 3c–4e interactions ($\text{Z} = \text{S}, \text{Se}, \text{and Te}$) operate in AB, which stabilizes the system. The $\text{p}(\text{Z})$ – $\pi(\text{Nap}/\text{Ph})$ conjugations also support stabilization of AB. (c) Structure type CC is formed by the distortion of BB. The donor–acceptor interactions of $\text{n}_\text{s}(\text{Z})\cdots\sigma^*(\text{Z}-\text{C})$ and $\text{n}_\text{p}(\text{Z})\cdots\sigma^*(\text{Z}-\text{C})$ substantially stabilize CC. The disappearance of the nodal plane in $\pi^*(\text{Z}\cdots\text{Z}, \text{HOMO})$ in CC contributes to stabilize CC, where the nodal plane appears apparently in BB. The relative stability of CC increases in the order $\text{Z} = \text{O} \ll \text{S} < \text{Se} < \text{Te}$. (d) Structure type AA-*t* is constructed by $\sigma(2\text{c}-4\text{e})$. AA-*t* of the symmetric structure is a local minimum. The stability decreases as AA-*t* becomes unsymmetrical.

X-ray crystallographic analysis of 8-methylselanyl-1-(methylselenenyl)naphthalene (**182a** (LO)) and 1,8-bis-(methylselenenyl)-naphthalene **182b** (OO) revealed that the three $\text{Se}\cdots\text{Se}=\text{O}$ atoms in **182a** (LO) and the four $\text{O}=\text{Se}\cdots\text{Se}=\text{O}$ atoms in **182b** (OO) align linearly. Two $\text{C}(\text{Me})$ – Se bonds are perpendicular to the naphthyl plane and opposite to each other. All $\text{Se}=\text{O}$ bonds are placed in the naphthyl plane. The superior tendency for the $\text{Se}=\text{O}$ bonds to stay in the naphthyl plane (O dependence) must be the driving force for the fine structures of **182a** (LO) and **182b** (OO). The noncovalent $\text{n}_\text{p}(\text{Se})\cdots\sigma(\text{Se}-\text{O})$ 3c–4e interactions operate effectively to stabilize the structure of **182a** (LO). On the other hand, there is no $\text{n}_\text{p}(\text{Se})$ in **182b** (OO). Therefore, noncovalent $\text{n}_\text{p}(\text{Se})\cdots\sigma(\text{Se}-\text{O})$ 3c–4e interactions cannot operate. The driving force for the structure

Chart 28

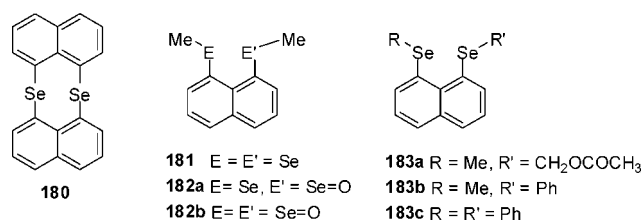
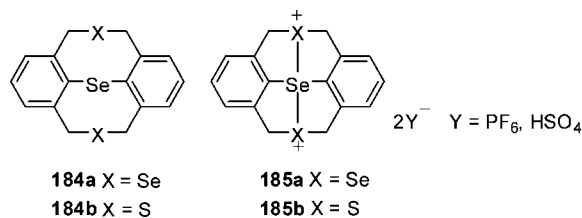
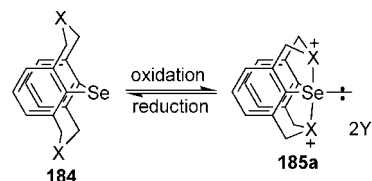


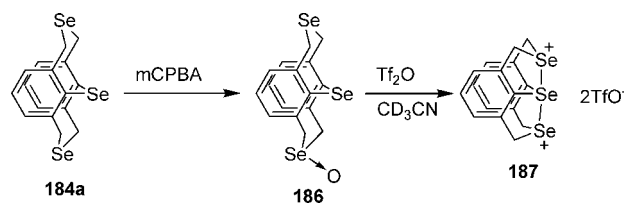
Chart 29



Scheme 35



Scheme 36



of **182b** (OO) must mainly come from the O dependence for each $\text{Se}-\text{O}$ bond in **182b** (OO), since the G dependence cannot operate without $\text{n}_\text{p}(\text{Se})$. Although the nonbonded $\text{Se}\cdots\text{Se}$ distances are less than the sum of van der Waals radii by ca. 0.65 \AA , the $\sigma(4\text{c}-4\text{e})$ interaction seems not so important.

Further work by Fujihara et al. reported that transannular bond formation can occur between three chalcogen atoms (Se, S).¹²⁶ This multicenter chalcogenide participation was found to provide a new type of hypervalent σ -selenurane with two apical selenonio, **185a**, or sulfonio ligands, **185b**.

The selenurane dication, **185a**, was found to undergo a reversible two-electron reduction, which was accompanied by a conformational change between chair and boat forms (Scheme 35).

Furukawa et al. reported the X-ray crystallographic analysis of the dication salt of 1,11-(methanoselenomethano)-5H,7H-dibenzo[b,g][1,5]-diselenocin, **184a**.¹²⁷ This showed that the dication had a selenium atom in a trigonal bipyramidal bonding environment. An ab initio calculation for the dication revealed that the positive charge was exclusively carried by the three selenium atoms. The central Se atom was found to carry a more positive charge than the two apical selenium atoms, thus indicating that the two apical $\text{Se}-\text{Se}$ bonds were highly polarized as in the neutral hypervalent molecules having a three-center four-electron (3c–4e) bond (Scheme 36).

The X-ray analysis of **187** clearly revealed that, in the solid state, the conformation was a distorted boat–boat form fixed

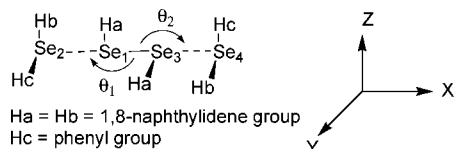
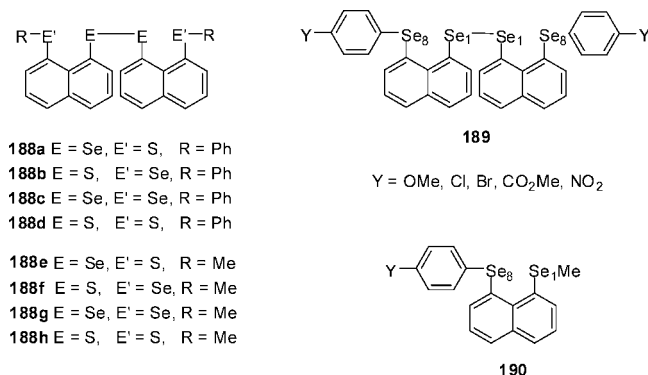


Figure 15. Linear alignment of four selenium atoms in the compound bis[8-(phenylselanyl)naphthyl]diselenide where two naphthyl planes were almost perpendicular to each other.

Chart 30



by the three-center transannular bond between the three selenium atoms. These facile structural changes in the redox reactions were ascribed to the stabilization of the oxidized species by multicenter chalcogenide participation, i.e., the formation of selenurane dications and the destabilization by transannular lone pair–lone pair repulsion of the neutral boat forms derived from reduction of the dications.

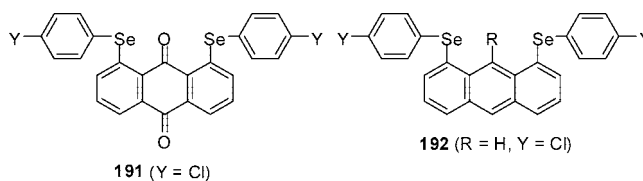
In 1996 Nakanishi et al. reported the linear alignment of four selenium atoms in the compound bis[8-(phenylselanyl)naphthyl]diselenide **188**.¹²⁸ The X-ray crystallographic analysis (Figure 15) showed that the two naphthyl planes were almost perpendicular to each other. The naphthyl groups were arranged in such a way that the four selenium atoms were almost linear, although they could rotate about the C(1)–Se(1) and/or C(17)–Se(3) bonds, thus avoiding steric repulsion with the Se–Se bond. MO calculations were performed on a simplified model of **188**. The results showed that the bond could be regarded as a four-center six-electron (4c-6e) bond.

As an extension to this study, novel properties owing to the linear 4c-6e Se₄ bond have been investigated.¹²⁹ An inverse substituent effect on the ⁷⁷Se NMR chemical shifts of the diselenide Se atoms in **189** bearing substituents at the phenyl *para*-positions was noted when compared to those in 1-(methylselena)-8-(phenylselena)naphthalene and its *para*-substituted derivatives, **190**.

The ⁷⁷Se NMR chemical shifts of diselenide Se atoms versus those of arylselanyl groups in **189** and **190** were plotted. Compound **190** showed a regular correlation that was attributed to the lone pair–lone pair interaction between Se atoms, whereas **189** showed an inverse correlation that could not be explained by lone pair–lone pair interaction. It was proposed to be due to the 4c-6e interaction of the four linear selenium atoms constructed by the p-orbitals of the outside selenium atoms with the σ* orbital of the inside Se–Se bond.¹³⁰

More recently, Nakanishi et al. reported the synthesis and reactivity of **188a–188d**. Interestingly, compounds **188a** and **188d** did not undergo borohydride reduction.¹³¹ The reactivity was explained on the basis of the stability of the produced anions. The stability of the anions, in turn, depends on the

Chart 31



conformational arrangement of the E–E–C bonds and the resulting 3c-4e and 5c-6e bonding systems. Theoretical calculations have been carried out on the compounds **188e–188h** as models for **188a–188d**. The formation of n_p(E')...σ*(E–E)...n_p(E') 4c-6e from linear combination of double n_p(E)...σ*(E'–C) 3c-4e in **188e** was predicted to be more stable by 21 kJ mol^{−1} than orthogonal combination (discrete n_p(E)...σ*(E'–C) 3c-4e) at the MP2 level. However, **188f** with double n_p(S)...σ*(Se–C) 3c-4e is predicted to be more stable in orthogonal combination by 18 kJ mol^{−1} if calculated at the same level. The reactivity of **188e–188h** derived from **188a–188d** could be related to the stability of the intermediate anions [1-(8-MeE'C₁₀H₆)E[−]], produced by the reduction of **188e–188h**. On the basis of the conformation of the transition state, QC calculations predicted E–E bonds in **188f** and **188g** must be reduced more easily than in the cases of **188d** and **188h**, which corresponds to experimental observation in **188b** and **188c**, respectively, of which E–E bonds reduced easily.

Further, the 5c-6e interactions were illustrated by taking examples of anthraquinone and anthracene derivatives **119–121**, **191**, and **192**.¹³² The X-ray crystal structures of **119** and **120** showed linear arrangement of C–Se...O...Se–C, whereas in **120**, C–Se...H...Se–C was obtained in nonlinear arrangement. The energy-lowering effect of the extended hypervalent σ*(C–Se)...n_p(O)...σ*(Se–C) 5c-6e interaction is the main factor for the linear arrangement in **120** and **121**. The contribution of the extended π-conjugation between π(C=O) and n_p(Se) through π-framework of anthracene also plays an additional role in **119**.

In a report by Schiemenz, the presence of *peri*-interactions in naphthalenes is strongly disputed.¹³³ It was argued that van der Waals radii should only be used to describe intermolecular interactions and not for intramolecular atomic distances. It was suggested that *peri*-substituted naphthalenes force substituents into close proximity in terms of steric hindrance, thus acting as a spacer and preventing electronic interaction. Schiemenz contradicted the work by Nakanishi et al.,¹¹⁰ stating that, in a *peri*-fluorine/selenium-substituted naphthalene, there are inefficient donor substituents and a poor acceptor substituent in the *peri*-positions. The F–Se bond distance and residual angle indicated repulsion of the *peri* substituents and not attractive nonbonded interaction as suggested by others.

3. Intramolecularly Coordinated Organoselenium Compounds as Ligands

The chemistry of selenium ligands is a subject of growing interest as a result of both their increasing accessibility and the realization that they may display significantly different properties from their sulfur analogues.⁹ Metal complexes with neutral or anionic ligands containing selenium and nitrogen donors such as chalcogenols (REH), chalcogenolates (RE[−]), chalcogenoethers (RER), and dichalcogenides (REER) have been extensively reviewed. They are interesting for several

reasons. They can give insight into the competitive coordination behavior between the “hard” and “soft” Lewis bases, nitrogen and selenium, toward the same metal center.¹³⁴ They are also potential precursors for MOCVD deposition of semiconductors,¹³⁵ and they have possible applications as cytostatic drugs when coordinated to platinum.¹³⁶ In such ligands, often the selenium is three or four bonds away from the heteroatom, leading to the possibility of intramolecular interaction and chelate ring formation. In this part, the presence of this type of interaction in a range of organoselenium ligands will be discussed, whether proven or merely postulated.

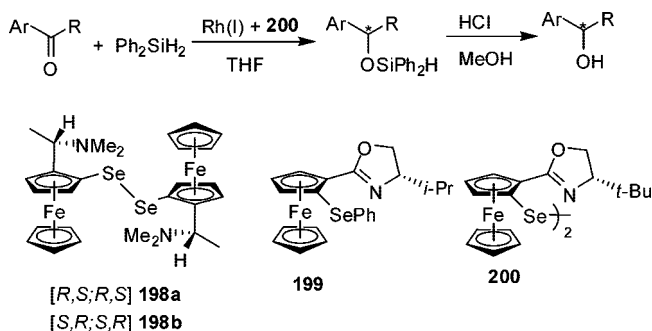
3.1. Neutral Ligands

In 1989 Brubaker et al. reported the synthesis of a new series of chiral ligands with potential chalcogen (S, Se)···N coordination.¹³⁷ The ligands were of the type (*R,S*)-(C₅H₄-ER) Fe-(C₅H₃-1-CH-MeNMe₂-ER) where E = S, **193**, or Se, **194**, and R = Me, Ph, Bz, 4-tolyl, and 4-chlorophenyl. The compounds were prepared by stepwise lithiation. These ligands were found to chelate platinum and palladium dichloride. The palladium complexes could be used as selective catalysts for the reduction of conjugated dienes to monoenes. Ligands **193a–193e** and **194a–194e** have three coordination sites, one nitrogen atom and two selenium (or sulfur) atoms. Therefore, there are three possible structures for the complexes, **195–197**.

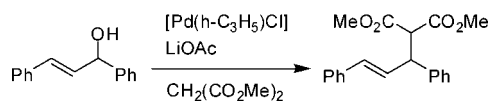
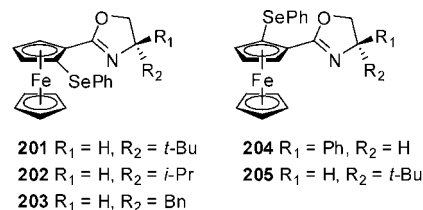
In 1992 Tomoda et al. reported the first use of organoselenium reagents in the catalytic conversion of alkenes into allylic compounds.²² The organoselenium compounds used were 2,2'-diselenobis {*N,N*-di[2-(2-pyridyl)ethyl]benzylamine}, **9**, and 2,2'-diselenobis(*N*-cyclohexyl-*N*-methylbenzylamine), **7**. Compounds having internal tertiary amines were used in the hope that a Se···N interaction would stabilize the molecule, thus avoiding the disproportionation of the selenenic acid intermediate.

In 1994 Uemura et al. described the first example of a transition metal catalyzed asymmetric reaction using organic dichalcogenides as chiral ligands.¹³⁸ The chiral compound (*R,S*)-di[2-(1-dimethylaminoethyl)ferrocenyl]diselenide was found to work effectively as a ligand for the rhodium(I)-catalyzed asymmetric hydrosilylation of several alkyl aryl ketones¹³⁹ (Scheme 37). Uemura et al. also reported work on the design of a chiral ligand for transition metal catalyzed enantioselective reduction of ketones.¹⁴⁰ One of the ligands investigated was **199**.¹⁴¹ It was prepared and applied to the hydrosilylation of acetophenone with a catalytic amount of [Rh(COD)Cl]₂ in Et₂O at 25 °C. However, the enantiomeric excess (ee) of 1-phenylethanol obtained by acid hydrolysis

Scheme 37



Scheme 38



of the hydrosilylation product was found to be only 13% (*R*). Related diselenide **200** has been used as catalyst precursor in the asymmetric addition of diethyl- and diphenylzinc to various aldehydes, yielding synthetically useful secondary alcohol.¹⁴²

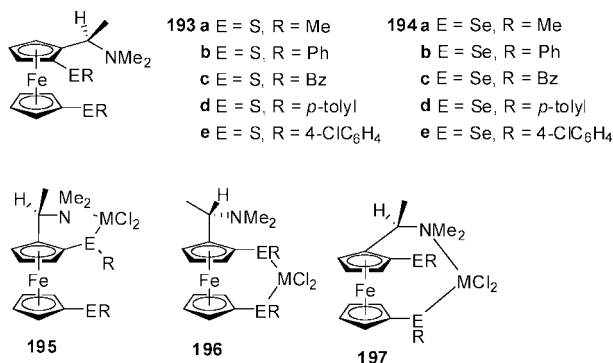
More recently, Hou and co-workers¹⁴³ have reported synthesis of a series of planar chiral selenide ligands **201–205** derived from ferrocenyl oxazolines and applied in a palladium catalyzed allylic substitution reaction (Scheme 38). Ligand **201** with *tert*-butyl as the substituent achieved the best yield and enantioselectivity.

Uemura and co-workers later prepared optically active [*R,S*; *R,S*]- and [*S,R*; *S,R*]-bis[(dimethylamino)ethyl]ferrocenyl]dichalcogenides (Fc*SeSeFc*)¹⁴⁴ for use in asymmetric selenoxide elimination,^{114a} [2,3]-sigmatropic rearrangement,^{108,145} and nucleophilic ring-opening of *meso*-epoxides.¹⁴⁶ They were also used as ligands for catalytic asymmetric reactions as described previously. Several diferrocenyl diselenides were prepared from [*R,S*; *R,S*]-bis[2-[1-(dimethylamino)ethyl]ferrocenyl]diselenide, **198a** (Scheme 39). The effectiveness of the various ligands **198a** and **206–210** for the Rh(I)-catalyzed hydrosilylation of ketones was examined. The results showed that the presence of a (dimethylamino)ethyl moiety on the ferrocene ring was most important for highly enantioselective hydrosilylations.

Khanna and co-workers reported the synthesis of 3-aminopropyl(aryl)selenide, **211**, and its complexes with palladium(II) and platinum(II), **212** and **213**, respectively.¹⁴⁷ IR and NMR data showed that the aminopropyl selenides were heterobifunctional ligands coordinating through Se and N to the metal center. The geometry of the metal atom in the complex was square planar with the Cl atoms adopting *cis*-positions.

Jones and co-workers studied the reactivity of newly prepared organoselenium derivatives toward palladium dichloride.¹⁴⁸ Crystal structures of **69** and **214** were obtained. The geometry of the diselenide **214** was found to offer various

Chart 32



Scheme 39

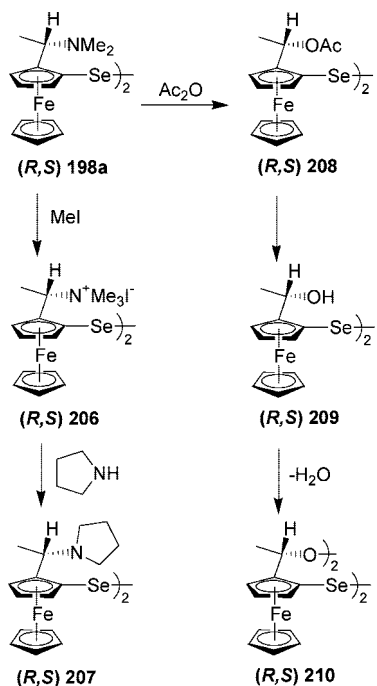
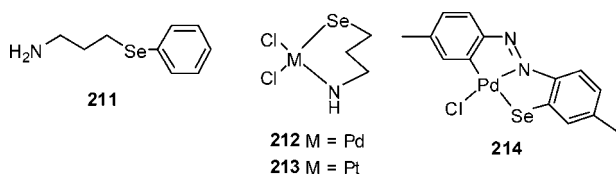
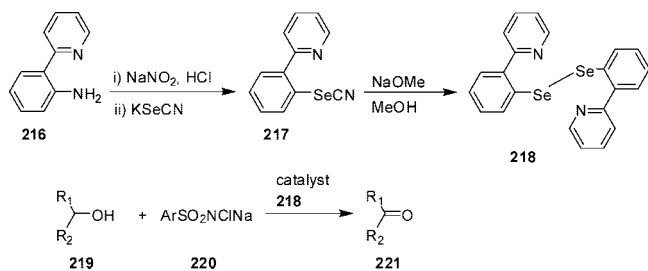


Chart 33



Scheme 40



possibilities for coordination. Complex **214** was shown to form two chelate 5-membered rings by coordination through *o*-carbon, nitrogen, and selenium.

The ligand 2,2'-dipyridyl diselenide (PySeSePy), **215**, contains two sets of N/Se donor atoms. It was first synthesized in 1962;¹⁴⁹ however, its crystal structure and coordination chemistry were first reported by Jones et al. in 1996.⁹⁶

Onami and co-workers¹⁵⁰ have reported the synthesis of bis[2-(2-pyridyl)phenyl]diselenide **218** from 2-(2-pyridyl)-aniline **216** as shown in Scheme 40. It was found to be an efficient catalyst for the oxidation of alcohols where *N*-chloro-4-chlorobenzenesulfonamide sodium salt was oxidant. It is proposed that *ortho*-substitution on benzene ring, which could hypercoordinate with selenium, is essential for a rapid catalytic reaction.

New chiral diselenides derived from [(*S*)-*N,N*-dimethyl-1-phenylethylamine] were synthesized by Kaur in 1996.²⁶ The procedures are given in Scheme 41. NMR spectra showed that there was no evidence for any strong Se \cdots N interaction at ambient temperature, except in the case of

Scheme 41

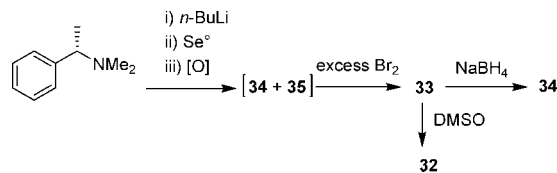
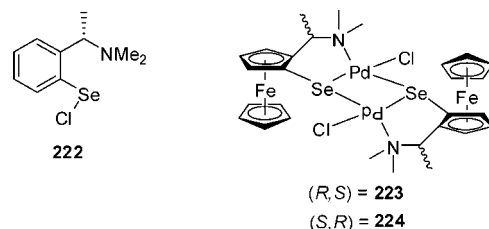
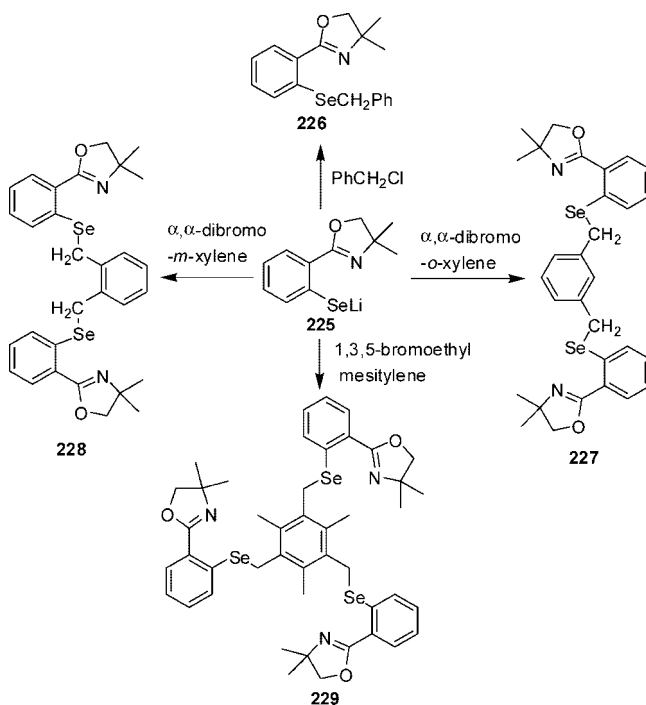


Chart 34



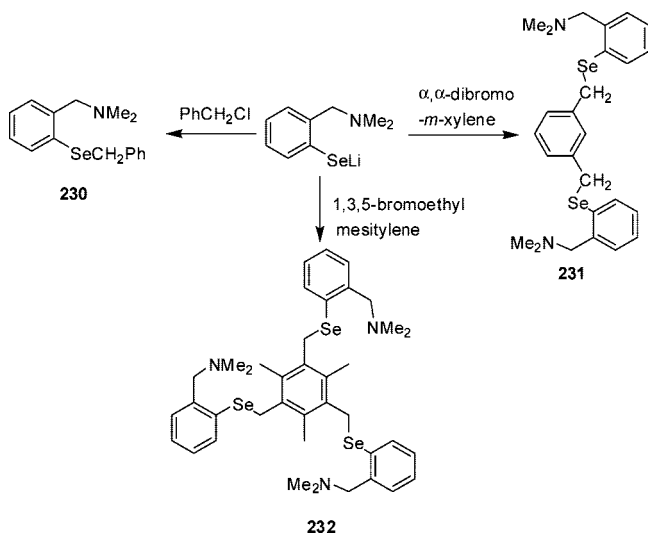
Scheme 42



compound **32**. The spectrum of compound **32** was found to imply the presence of strong Se \cdots N interaction. Addition of Pd(COD)Cl₂ to a solution of **32** afforded a mixture that, upon recrystallization from dichloromethane/hexane (80:20), gave yellow crystals of R*SeCl (Chart 34) rather than the expected Pd(II) selenolate complex. Organoselenyl chloride, presumably, results from the redox reaction of **32** with Pd(COD)Cl₂, where diselenide **32** is reduced to selenolate (R*Se⁻) and oxidized to R*SeCl **222**. In this case, the selenolate complex could not be isolated in pure form. However, analogous reactions of **198a** and **198b** with a Pd(II) chloride complex afforded the selenolate complexes **223** and **224** as the major products.

In general, arylbenzyl and aryl allyl selenides are unstable and decompose readily to give coupled hydrocarbon products and free selenium. However, the unsymmetrical selenides are useful synthetic reagents in heterocyclic chemistry. Singh et al. synthesized a series of this type of compound **226–229** (Scheme 42) along with novel benzylic compounds **230–232** (Scheme 43).³¹ These compounds were found to

Scheme 43



be slightly unstable but were suitable for satisfactory analysis and NMR spectroscopy.

Selenides **226–229** were analyzed by ^1H NMR spectroscopy. They were found to have only a weak $\text{Se}\cdots\text{N}$ interaction. The signals due to $-\text{CH}_2-$ protons were shifted downfield, which suggested that the introduction of benzylic groups had reduced the interaction. The same trend was observed for compounds **230–232**. The ^{77}Se chemical shifts for these benzylic compounds were shifted relatively upfield due to the presence of benzylic groups, which were covalently bonded to the Se atom and could not accept further electron density from selenium.

Recently, Singh et al. have reported synthesis and complexation studies of bis[(4,4-dimethyl-2-phenyl)oxazoliny]

Scheme 44

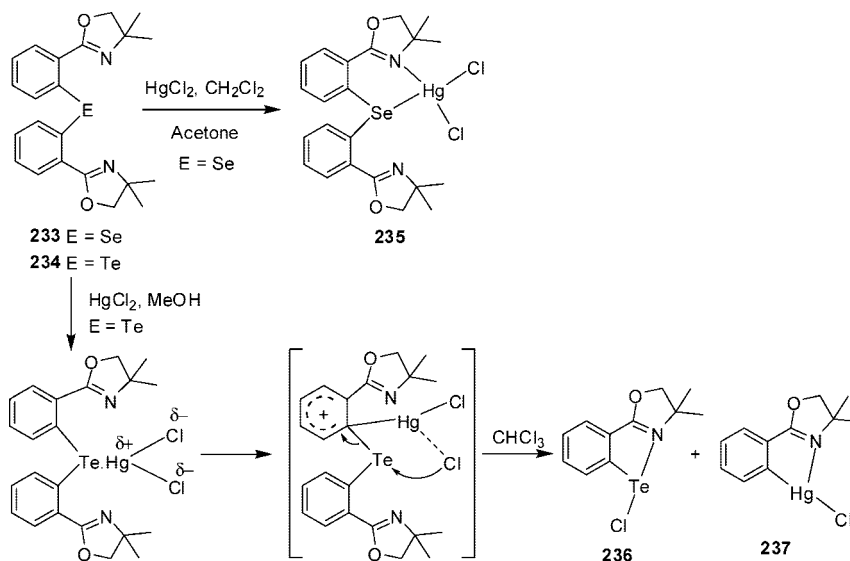
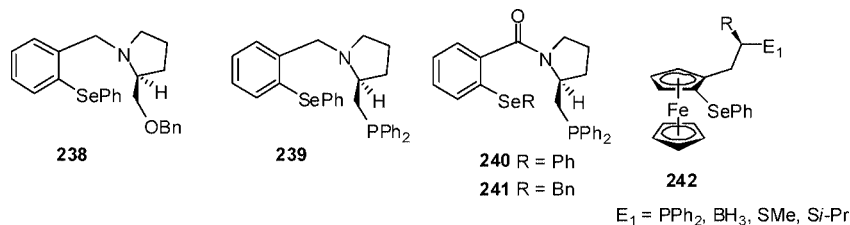


Chart 35

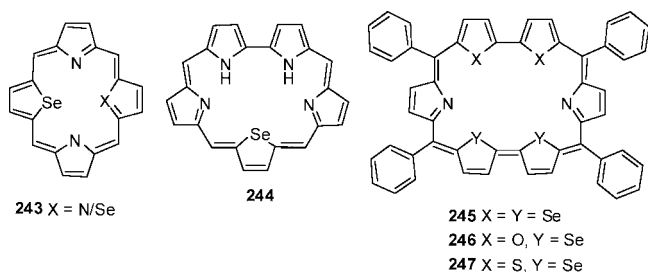


selenide **233** and its tellurium analogue **234**.¹⁵¹ The reaction of $\text{Pd}(\text{COD})\text{Cl}_2$ with these two ligands afforded the insoluble polymeric complexes; however, reaction of monoselenide afforded the 1:1 [**233**· HgCl_2] complex **235** on treatment of HgCl_2 . Only one of the nitrogen atoms coordinates to give tetrahedral mercury complex. In contrast to the selenide **233**, reaction of telluride **234** with HgCl_2 afforded the transmetalated products (4,4-dimethyl-2-phenyl)oxazoliny tellurium chloride **236** and (4,4-dimethyl-2-phenyl)oxazoliny mercuric chloride **237** (Scheme 44).

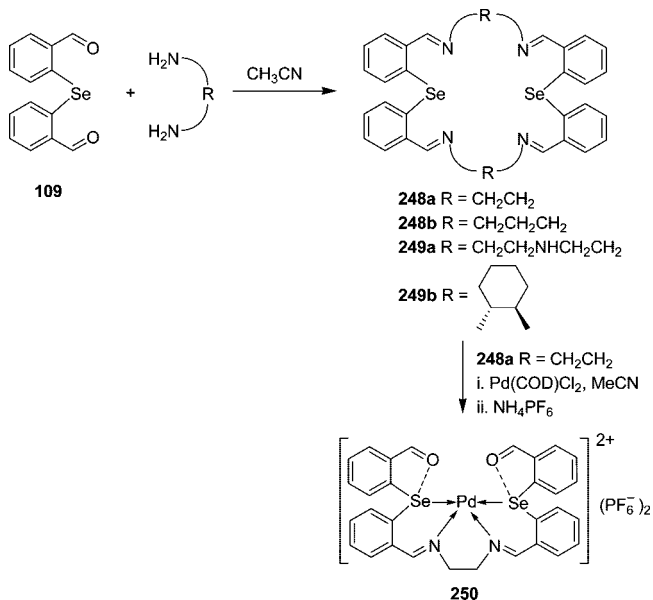
Hiroi et al. described new chiral ligands derived from (*S*)-proline having organoselenenyl groups, **238–241**.¹⁵² This type of ligand was found to be useful in palladium catalyzed asymmetric synthesis. Enders and co-workers have reported a simple asymmetric synthetic method for planar chiral ferrocenyl ligands of type **242**.¹⁵³ The ligand has a stereogenic center at the β -position of the side chain.

There have been many reports on selenium-containing porphyrins, such as compound **243** in the literature.¹⁵⁴ The porphyrin skeleton plays an important role in many biological and catalytic systems. Its metal complexes can be used as catalysts in oxidative dehydrogenation and symmetry forbidden reactions. By modifying the structure of this type of molecule, the catalytic activity can be altered. Catalytic activity depends on the central metal atom and on the substituents in the *p*-phenyl positions. If the two pyrrole NH groups positioned opposite each other are replaced by chalcogen atoms, electrons are drained from the porphyrin ring and the chalcogens take part in direct bonding interaction across the ring. The first example of a selenium-containing saphyrin **244** was reported in 1995 by Sessler et al.¹⁵⁵ More recently the synthesis, structures, and spectral and electrochemical properties of modified rubyrins containing Se_4N_2 , **245**, SeO_2N_2 , **246**, and $\text{Se}_2\text{S}_2\text{N}_2$, **247** were reported.¹⁵⁶ Optical

Chart 36



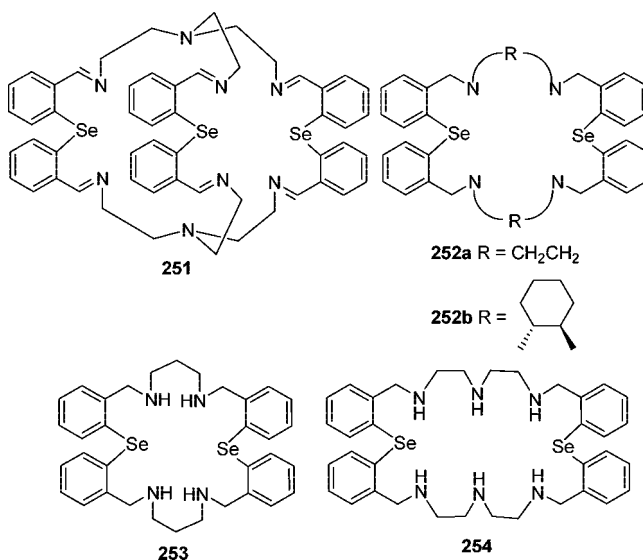
Scheme 45



and electrochemical analysis showed that the substitution of heteroatoms altered the cavity size and the electronic structure of the ring. The rubyrins were found to form stable complexes with anions such as F^- , N_3^- , and PO_4^{3-} .

Macrocyclic ligands contain at least three donor atoms with a ring size of at least nine atoms. Mixed selenium and nitrogen donor macrocycles are attractive synthetic targets for several reasons. First, these ligands contain “hard” and “soft” binding sites in close proximity within the same macrocyclic cavity; they can, therefore, coordinate both “hard” and “soft” guest ions or molecules and should also allow coordination of two guests simultaneously. Selenium in a macrocycle is useful for structural investigation using ^{77}Se NMR (this is not possible for sulfur, oxygen, or nitrogen containing macrocycles). Selenium has a greater σ -donating ability than N, O, and S, which may influence complexation properties. Finally incorporation of selenium, which is a larger atom, into macrocyclic ligands should change the size of the cage cavity, thus leading to interesting coordination behavior. These properties prompted Panda to work on the preparation and characterization of novel selenium containing aza-macrocycles.⁷² The macrocyclic ligands were prepared from the precursor bis(*o*-formylphenyl) selenide, **109**, which itself was synthesized from *o*-bromotoluene. 22-, 24-, and 28-membered macrocyclic Schiff base type ligands (**248–249**) were isolated in high yield (Scheme 45). The intramolecular nonbonded interaction is the important aspect for these template-free syntheses of Schiff base selenaza macrocycles. The resulting macrocycle **248a** showed the two $\text{Se}\cdots\text{N}$ nonbonded interactions with the distances of 2.723 and 2.729 Å, which are slightly shorter than that observed

Chart 37

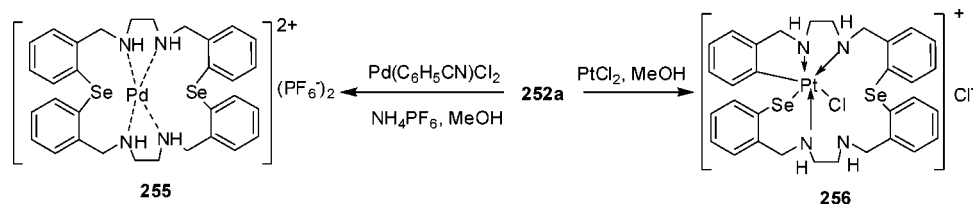


in **248b** (2.773 Å) where only one interaction is present.¹⁵⁷ These interactions lead to the interesting reactivity of these macrocycles toward complexation with different metal ions. Reaction of **248a** with $\text{Pd}(\text{COD})\text{Cl}_2$ unexpectedly resulted in complex **250**, where one arm of the macrocycle hydrolyzed into two formyl groups. The crystal structure of complex **250** showed the weak nonbonded $\text{Se}\cdots\text{O}$ interactions (2.855 Å). Extending the series, Singh et al. reported new selenaza **249b** macrocycle and its reduced form **252b** by replacing ethylenediamine by cyclohexylenediamine.¹⁵⁸ The resulting macrocycle has shown the strength of non-bonded interaction comparable to that observed in **248a**. The macrocycle has shown usual reactivity toward the metal ion $\text{Ni}(\text{II})$ and $\text{Co}(\text{II})$.

Intramolecular $\text{Se}\cdots\text{N}$ interaction is an important feature in the structure of macrocycles as it reduces the unfavorable lone pair–lone pair repulsion between nitrogen atoms. The macrocyclic cryptand, **251**, was also synthesized from the [2 + 3]-condensation of **109** using cesium metal ions as a template. Compounds **248** and **249** were reduced using sodium borohydride to generate their tetraamino derivatives (**252–254**). These were assumed to be more stable and capable of coordinating with a range of transition metal cations.

All the compounds prepared were characterized using elemental analysis, IR, mass spectrometry, and ^1H , ^{13}C , and ^{77}Se NMR. X-ray crystal structures were obtained for compounds **248–249a**. The observation of different chemical shift positions in the ^{77}Se NMR spectra of the compounds was attributed to the varying extent of $\text{Se}\cdots\text{N}$ interaction in each case. The maximum downfield shift was seen for **248b**, suggesting that this had the strongest interaction; the signal for **251** was shifted upfield compared with **248a** and **248b**, thus showing weaker $\text{Se}\cdots\text{N}$ coordination. If the shift values for **248a** and **248b** are compared with those found for **252a** and **253**, a significant decrease is observed, indicating a better shielding of the selenium nucleus in the tetraamines. This could be attributed to better $\text{Se}\cdots\text{N}$ coordination in the tetraamines, but it is more likely to be due to delocalization of the selenium lone pair in **252** and **253**. The structure of compound **249b** showed a $\text{Se}\cdots\text{N}$ distance of 2.814 Å, which is shorter than the sum of van der Waals radii (3.5 Å) but greater than the covalent radii

Scheme 46



sum (1.87 Å). Slightly weaker Se...N interaction (3.01 Å) has been observed in the crystal structure of macrocycle **252a**.¹⁵⁹ The ligating properties of the reduced Schiff base selenoaza macrocycle **252a** have been studied by treating with Pd(II), Hg(II), Ni(II), Cu(II), and Pt(II) (Scheme 46).^{159,160} The reaction of **253** with $\text{Pd}(\text{C}_6\text{H}_5\text{CN})\text{Cl}_2$ afforded the complex **255**. The solid-state structure of **255** showed the coordination of Pd(II) to only hard N donor atoms; however, the studied solution ⁷⁷Se NMR revealed the coordination to selenium in solution. In contrast to the reaction of $\text{Pd}(\text{C}_6\text{H}_5\text{CN})\text{Cl}_2$, the reaction of **252a** with PtCl_2 afforded the novel cationic Pt(IV) metallamacrocyclic complex **256** via the oxidative addition of C–Se bond to Pt(II). The facile oxidative addition may be facilitated by the more polar nature of C–Se bond, which resulted from the N → Se intramolecular interaction present in **252a** (Figure 16). Ligating property of macrocycle **254** has been studied toward Pd(II).¹⁵⁹

The coordination behavior of the 28-membered selenoaza macrocycle **254** has been studied with Hg(II) and Pb(II) (Scheme 47).¹⁶¹ The reaction of $\text{Hg}(\text{OCOCH}_3)_2$ with **254** afforded a novel mercurous complex **257**, where the mercurous ion was fully trapped inside the macrocyclic cavity. Complex **257** is the first example of a structurally characterized mercurous cation complex of a monocycle where Hg_2^{2+} is trapped inside the cavity of the monocycle. The mechanism of the formation of mercurous ion, though not clear, can be explained on the basis of the presence of HgO impurity with Hg(0), and the reaction of Hg(II) and Hg(0) strongly favors Hg_2^{2+} . The reaction of $\text{Pb}(\text{OAc})_2$ with **254** afforded a binuclear complex **258**. In both cases, the selenium–metal interaction has not been observed. This noninteraction between the Se donor atoms and the metal atoms in case of both the complexes may be explained in terms of the conformational requirement of the ligand around the metal.

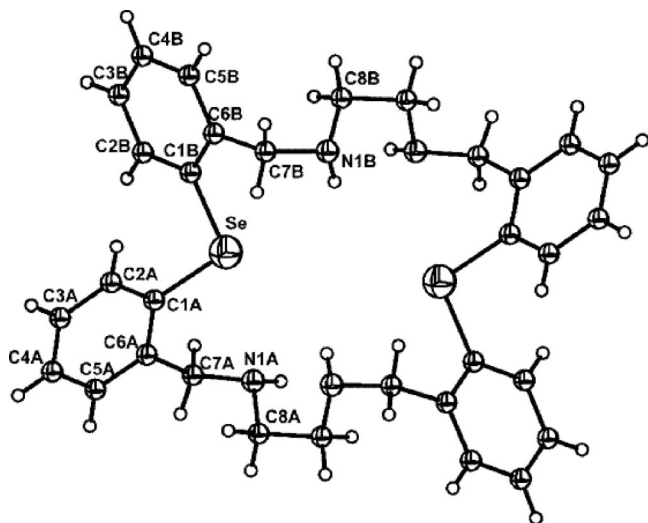
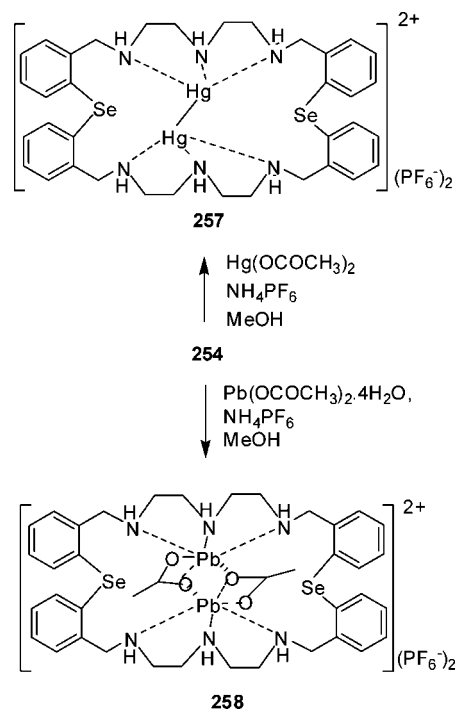


Figure 16. Molecular structure of **252a**. Reprinted with permission from ref 159. Copyright 2006 Wiley Interscience.

Scheme 47



3.2. Anionic Ligands

Up until 1992, metal complexes with selenolate (RSe^-) and tellurolate (RTe^-) ligands had been relatively little studied.^{9a,b,162} However, they are of current interest as precursors for metal chalcogenides.¹⁶³ Gornitzka et al. reported that the stability of alkali metal chalcogenolates could be greatly increased by chelation.¹⁶⁴ Crystalline lithium chalcogenolates were readily prepared by incorporation of a Li–E (E = Se, Te) unit into a six-membered chelate system (Scheme 48).

Compounds **261** and **262** were isolated in high yield. Compound **260** was used to obtain crystals of $[\text{Li}(\text{dme})][\text{CpFe}\{\text{C}_5\text{H}_3(\text{CH}_2\text{NMe}_2)\text{Te}\}]$, and the structure was determined by X-ray analysis. The Li–Te unit was found to be stabilized by intramolecular chelate formation.

Metal organic chemical vapor deposition (MOCVD) is a relatively recently developed technique used for the manufacture of electronic devices. It is an attractive technology requiring the availability of high-purity, volatile organometallic derivatives of the semiconductor, which are then decomposed thermally or photochemically over the substrate to produce high-quality films. The importance of chalcogenolates

Scheme 48

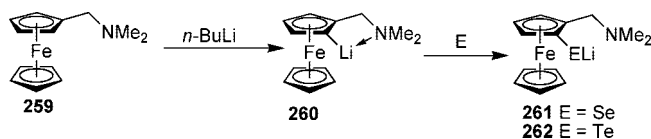
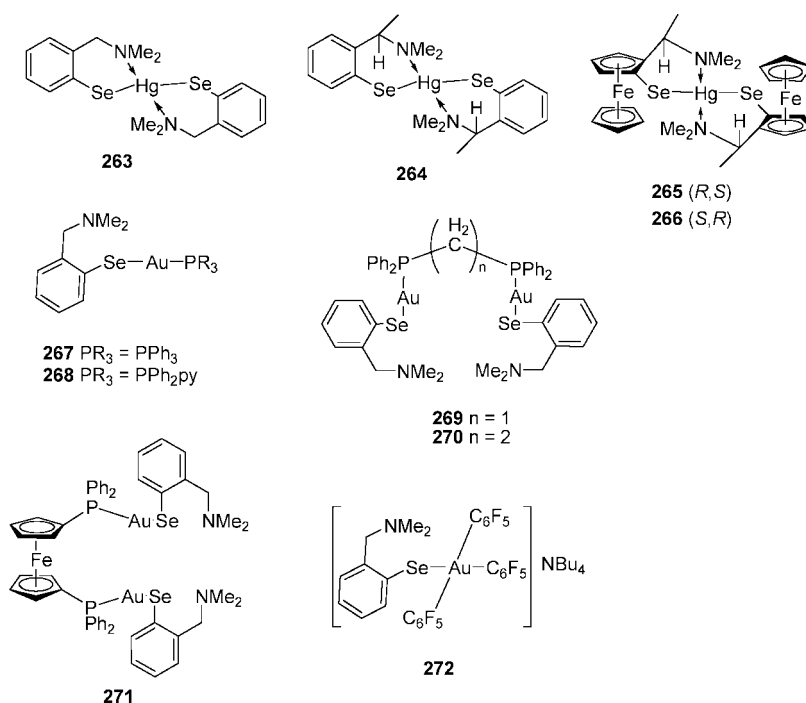


Chart 38



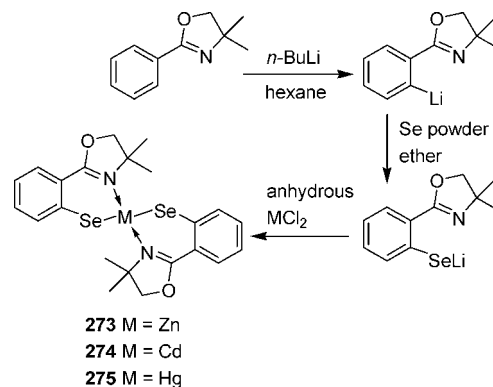
genide semiconductors has led to much current interest in the synthesis of novel organochalcogenide precursors for MOCVD. The bisdiethyldithiocarbamates are effective precursors for materials such as CdS, and good quality films can be deposited. However, attempts to use the analogous selenium compounds led to films that were heavily contaminated with elemental selenium.

Kaur and co-workers reported on the synthesis of monomeric, hydrocarbon-soluble mercury(II) selenolates, $\text{Hg}(\text{Se}-\text{C}_6\text{H}_4\text{CH}_2\text{NMe}_2)_2$ **263**, $\text{Hg}[(S)-\text{Se}-\text{C}_6\text{H}_4\text{CH}(\text{Me})\text{NMe}_2)_2$ **264**, $\text{Hg}[(R,S)-(\text{Se}-\text{C}_6\text{H}_4\text{CH}(\text{Me})\text{NMe}_2)_2\text{Fe}(\text{C}_5\text{H}_5)]_2$ **265**, and $\text{Hg}[(S,R)-(\text{Se}-\text{C}_6\text{H}_4\text{CH}(\text{Me})\text{NMe}_2)_2\text{Fe}(\text{C}_5\text{H}_5)]_2$ **266**, stabilized by internal chelation, forming a six-membered ring with Hg.^{26b} Crystal structures for compounds **263** and **266** were obtained; in both cases, the Hg atom was four-coordinate. The organoselenolate $2-(\text{Me}_2\text{NCH}_2)\text{C}_6\text{H}_4\text{Se}^-$ moiety has been further exploited to get Au(I) and Au(III) complexes **267–272**.¹⁶⁵ In the crystal structure of ferrocenyl gold selenolate **271**, one of the nitrogens is not involved in any intramolecular interactions to selenium or gold, and the other nitrogen atom is twisted toward the selenium atom with a short distance of 3.265 Å, which could be considered a weak intramolecular interaction, although packing forces may also be responsible. The vector of this interaction is placed trans to the Se–Au bond, and thus, the overall coordination around the selenium can be described as T-shaped.

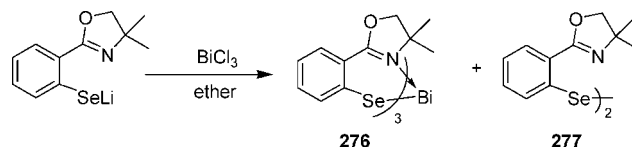
Singh et al. recently succeeded in preparing examples of zinc, **273**, cadmium, **274**, and mercury, **275**, selenolate complexes that were isolable and have been well-characterized.¹⁶⁶ The more rigid 4,4-dimethyl-2-phenyloxazoline substrate was used. Use of the phenyloxazoline ligand in the preparation of the novel “helically” chiral zinc selenolate, **273**, was described (Scheme 49).

Crystal structures for compounds **273**, **274**, and **275** were obtained. Compound **273** was found to be the first example of a helically chiral zinc complex derived from a bidentate selenolate ligand. All three complexes were monomeric, and the degree of association was controlled by the internal

Scheme 49

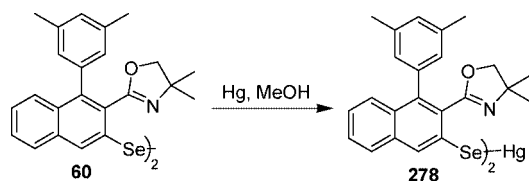


Scheme 50



chelation of the oxazoline ligand. These ligands have application in the preparation of helically chiral metal complexes. The compound **274**¹⁶⁶ and sulfur analogue¹⁶⁷ were used for the preparation of cadmium selenide and cadmium sulfide nanoparticles as single-source precursors by thermolysis in tri-*n*-octyl phosphine oxide.¹⁶⁸ The use of the metal chalcogenolates stabilized by intramolecular coordination for the preparation of respective metal chalcogenide nanoparticles by thermolysis method is thus demonstrated. The first example of a structurally characterized monomeric bismuth selenolate was recently reported by Singh et al.¹⁶⁹ Compound **276** was obtained by metathesis (Scheme 50); the diselenide **277** was also produced. The crystal structure of **276** showed that there were no close intermolecular contacts and that the lone pair of electrons located on the bismuth was stereochemically active.

Scheme 51



Recently, Singh et al. reported the isolation and structural characterization of mercury selenolate **278** derived from diselenide **60**, which incorporates the ligand having both sterically more bulky and intramolecularly coordinating groups.¹⁷⁰ Using the same ligand, the first isolation and characterization of a novel air-stable mercury telluroate has been also reported (Scheme 51).

Jain and co-workers have reported a series of Zn(II), Pd(II), and Pt(II) complexes of chalcogenolate ligands $\text{Me}_2\text{N}(\text{CH}_2)_n\text{E}^-$ (**279**, $n = 2$, $\text{E} = \text{Se}$; **280**, $n = 3$, $\text{E} = \text{Se}$; **281**, $n = 2$, $\text{E} = \text{Te}$; **282**, $n = 3$, $\text{E} = \text{Te}$) in a series of recent publications.¹⁷¹ The reaction of $\text{Me}_2\text{N}(\text{CH}_2)_3\text{Se}^-$ **280** ligand with Pd(II) and Pt(II) afforded considerably different modes of complexation from that of its lower homologue $\text{Me}_2\text{N}(\text{CH}_2)_2\text{Se}^-$ **279**. The γ -aminoselenolate ligand **280** can bind palladium and platinum as a simple selenolate, as a metal-metal bridging selenolate, or in N,Se-chelating or chelating bridging modes. The studies were extended by using $\text{Me}_2\text{NCH}(\text{Me})\text{CH}_2\text{E}^-$ **283** and $\text{Me}_2\text{NCH}_2\text{CH}(\text{Me})\text{E}^-$ **284** ligands.¹⁷² The precursor diselenides $(\text{Me}_2\text{NCH}(\text{Me})\text{CH}_2\text{Se})_2$ **285** and $(\text{Me}_2\text{NCH}_2\text{CH}(\text{Me})\text{Se})_2$ **286** have a “skew” structure and can show restricted rotation about Se-Se bond. For each diselenide, three distereomers are expected: (*R,R*), (*S,S*), and a meso form. Thus, each molecule is expected to display two resonances [(*R,R*)/(*S,S*) and meso] for the selenium atoms in the ^{77}Se NMR spectrum. However, each signal in the ^{77}Se NMR spectrum appeared as two closely spaced lines (ca. 1 ppm separation). It has been attributed to the presence of intramolecular interactions between Se and N. The $\text{Se}\cdots\text{N}$ distances of about 2.8 Å are significantly shorter than sum of their van der Waals radii.

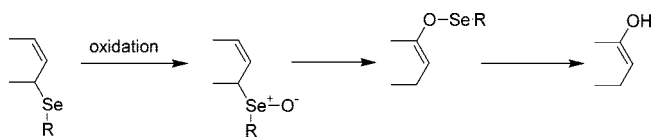
4. Intramolecularly Coordinated Organoselenium Compounds in Organic Synthesis

Over the last few decades, organoselenium based methodology has become an established tool in organic synthetic techniques. Organoselenium moieties can act as either nucleophiles or electrophiles under mild conditions and can easily be incorporated into a wide variety of substrates. Because of these attractive features, the use of organoselenium compounds in organic synthesis is a subject that has been reviewed extensively.^{4g,h,173} The organoselenium reagents having intramolecular coordinating groups have been extensively used in several organic transformations. The intramolecular coordination of selenium with a heteroatom such as oxygen or nitrogen leads to the formation of a heterocycle in a fixed conformation, thus increasing the stereoselectivity. Examples of transformations, where coordination by the heteroatom with selenium plays a vital role, are described in the following section.

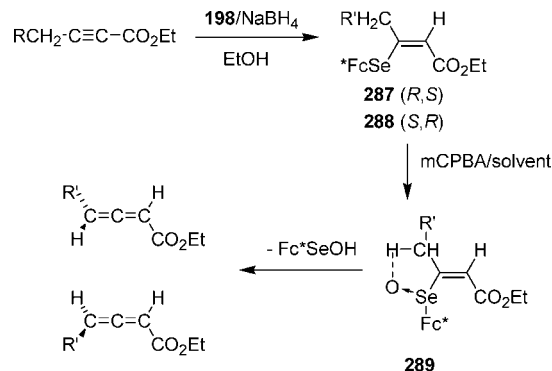
4.1. Asymmetric Selenoxide Elimination and [2,3]-Sigmatropic Rearrangement

The [2,3]-sigmatropic rearrangement of selenium oxides to an allylic carbon is one of the most common reactions

Scheme 52



Scheme 53



used for indirect functionalization by the transfer of a group from selenium to a carbon electrophile (Scheme 52).¹⁷⁴ These rearrangements involve the formation of a Se-C bond at an allylic position to a double bond to yield a selenoether, which can then be oxidized. The allylic selenoxide then undergoes spontaneous [2,3]-sigmatropic rearrangement to yield the selenenic ester, which can be cleaved to give the desired alcohol under mild acidic conditions.¹⁷⁵

Chiral selenoxides resulting from enantioselective oxidation of prochiral selenides or from diastereoselective oxidation of selenides containing a chiral moiety have been applied to selenoxide elimination and [2,3]-sigmatropic rearrangement.¹⁷⁶ Uemura et al. reported the first example of asymmetric selenoxide elimination leading to chiral allenecarboxylic derivatives (Scheme 53).¹³⁸ Two optically active ferrocenyl diselenides, **198a** and **198b**, each possessing two chiral centers, were prepared by the lithiation route and applied to induce highly enantioselective selenoxide elimination, producing axially chiral allenecarboxylic esters.

The best enantioselectivity (up to 89% ee) was obtained by the use of CH_2Cl_2 as the solvent at low temperature and in the presence of a molecular sieve to remove any trace of water. From the results of this reaction, it was postulated that

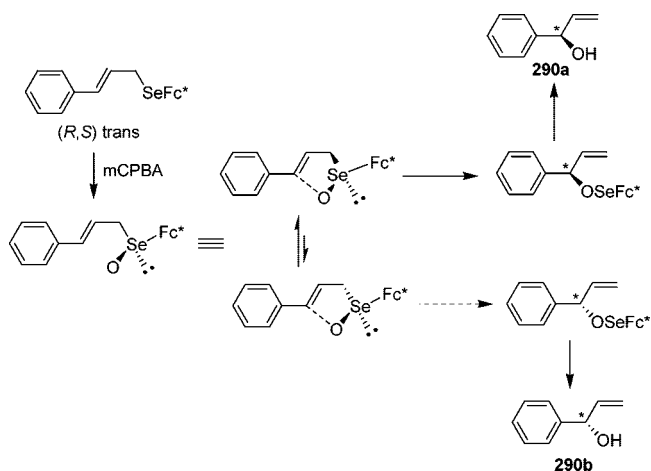
(1) The initial oxidation step proceeded with high diastereoselectivity.

(2) The intermediate chiral selenoxides were stabilized by steric, electronic, and/or coordination effects of the 1-(dimethylamino)ethyl moiety, which diminished the racemization of the selenoxides.

(3) In the intermediate selenoxides, a high diastereoselective hydrogen abstraction from the methylene protons (asymmetric selenoxide elimination) occurred with almost no loss of optical purity.

The X-ray structural elucidation of compound **198b** was reported by Uemura a year later.¹⁴⁶ No evidence of any $\text{Se}\cdots\text{N}$ nonbonded interaction was found; the atomic distances between Se and N were larger than the sum of their van der Waals radii. The ^1H NMR data confirmed that no $\text{Se}\cdots\text{N}$ interaction was present. The X-ray crystal structure of **198a** was reported by Singh et al.¹⁷⁷ The compound was not seen to have any $\text{Se}\cdots\text{N}$ interaction in the solid state as $\text{Se}\cdots\text{N}$ bond lengths (3.697 and 4.296 Å) were greater than

Scheme 54



the sum of the van der Waals radii (3.54 Å) for both atoms. It was, however, thought that the nitrogen atoms present may come closer to the selenium atom in solution. Diselenides **198a** and **198b** were also applied to the asymmetric [2,3]-sigmatropic rearrangement to produce chiral allylic alcohols **290**; they were found to be good reagents giving high ee values. The steric course of the reaction was proposed (Scheme 54).

Uemura et al. also investigated possible [2,3]-sigmatropic rearrangement in allylic telluroxides.¹⁷⁸ However, unlike in the analogous selenoxides, the ee values of the allylic alcohols obtained were found to be low under a variety of conditions. This was attributed to the rapid epimerization of chiral telluroxides through the achiral dihydrates and/or analogous intermediates.

Recently, Carter et al. have reported a vanadium-catalyzed selenide oxidation with in situ [2,3]-sigmatropic rearrangement using only 10 mol % of VO(acac)₂ with either cumene hydroperoxide (CHP) or *tert*-butyl hydroperoxide (TBHP) (Scheme 55).⁷³ The reaction proceeded rapidly and cleanly to provide the resultant allylic alcohol in good yield. A broad spectrum of aryl, allylic selenides has been screened to

Scheme 55

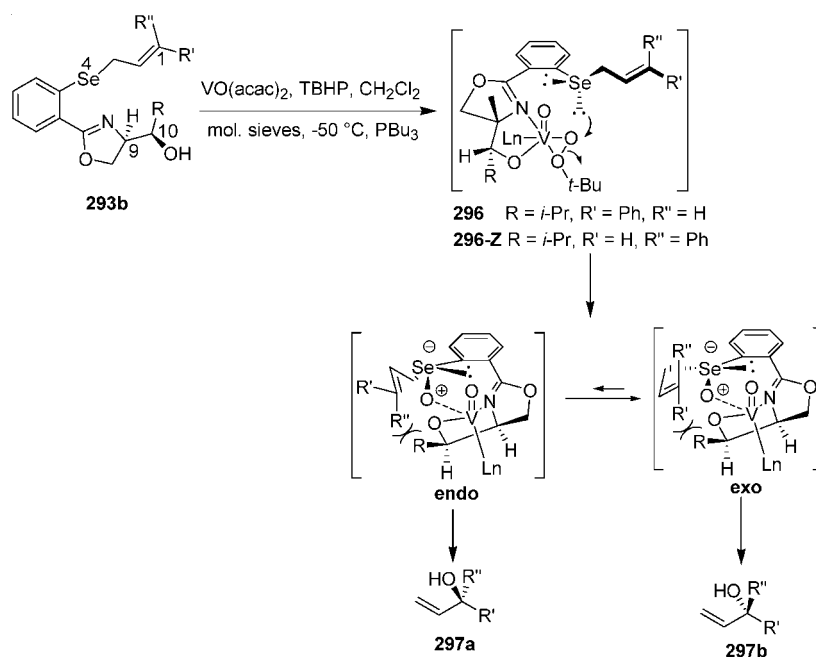
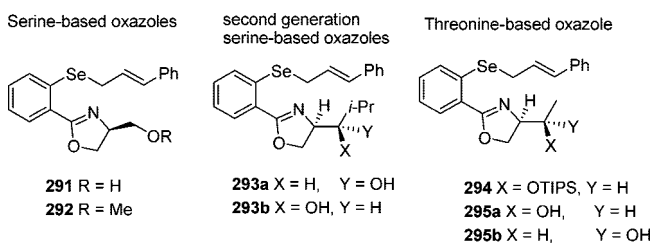


Chart 39

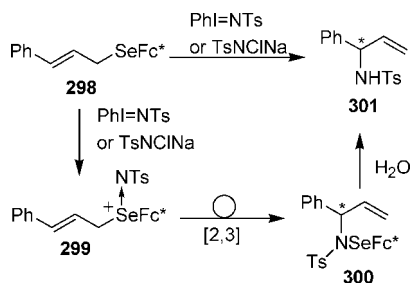


demonstrate the generality of the methodology. The serine based (**291** and **292**), second-generation serine based (**293**), and threonine based (**294** and **295**) chiral oxazolines have been used to prepare the precursor allylic selenides (Chart 39). Selenide **293b** was found to be the most efficient precursor for the asymmetric selenide oxidation in situ [2,3]-sigmatropic rearrangement. It has been proposed that the chirality transfer observed in the product allyl alcohol was the result of a net 1,9- and/or 1,10-induction, as shown in Scheme 55. Authors have mentioned that the recovery of the chiral auxiliary from the substrate such as selenide **293b** should be possible. Treatment of the diselenide byproduct produced in the reaction sequence with the reducing agents, such as NaBH₄, should generate the necessary nucleophile for alkylation with the corresponding allyl halide.

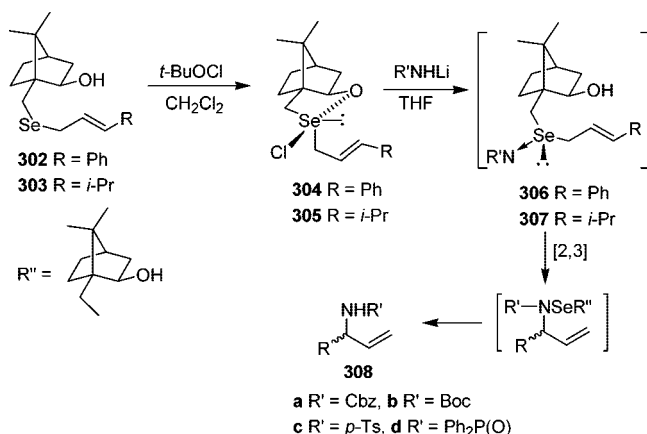
Selenimides are the nitrogen analogues of selenoxides. These were found to undergo the same [2,3]-sigmatropic transformation.¹⁷⁹ Chiral allylic amines (of type **301**) were obtained by the asymmetric imination of chiral cinnamyl ferrocenyl selenides (*E* and *Z*) **298** (derived from diselenide **198a**, **198b**) with [*N*-(toluene-*p*-sulfonyl)imino]phenyl iodine (PhI=NTs) or chloramine-T (TSNClNa) (Scheme 56). The products were found to have high ee values.

Kurose et al. reported that the nucleophilic reaction of allylic chloroselenuranes **302** and **303** with *N*-protected amines followed by the [2,3]-sigmatropic rearrangement of the resulting chiral allylic selenimides **306** and **307** proceeded in a highly stereoselective fashion, resulting in chiral *N*-protected allylic amines **308**.¹⁸⁰ Evidence for an *endo* transition state was described (Scheme 57). The proposed

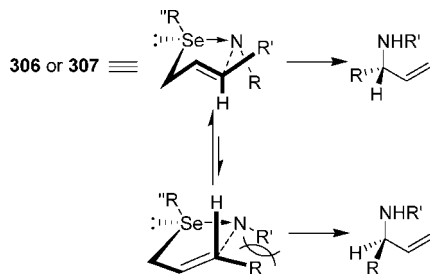
Scheme 56



Scheme 57



Scheme 58



stereochemical course of the asymmetric [2,3]-sigmatropic rearrangement of the allylic selenimides is depicted in Scheme 58. Recently, it has been shown that the direct catalytic enantioselective imidation of organic selenide can be carried out.¹⁸¹ Furthermore, the direct imidation of selenide into the corresponding optically active selenimide can be affected by the in-built *ortho*-coordinating chiral auxiliary such as chiral oxazolines.

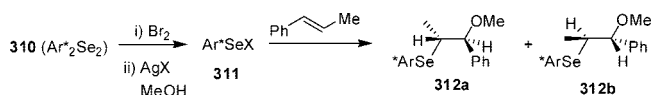
It was concluded that this [2,3] sigmatropic rearrangement proceeded predominantly via the *endo* transition state, which is stabilized by the intramolecular interaction between selenium and nitrogen.

4.2. Methoxyselenenylation and Oxyseleenylation

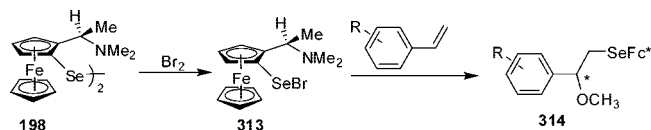
Functionalization of alkenes by the use of selenium compounds offers attractive possibilities for synthetic organic chemistry. One of the most important reactions of this type is methoxyselenenylation^{4a,b,182} and its more recently discovered asymmetric variant. Several chiral selenium compounds have been designed for asymmetric methoxyselenenylation. However, the syntheses can be complex, involving many steps, and often have low overall yields.

The first asymmetric methoxyselenenylation reaction of various alkenes was reported by Tomoda et al. in 1988.¹⁸³

Scheme 59



Scheme 60



The chirality-inducing agents used were optically active binaphthyl compounds that contained one selenium atom. The optical yield obtained was low, and attempts to improve it failed. It was thought that the incorporation of a coordinating group, such as an amide group, at the 2-position in the binaphthyl skeleton would enhance the optical induction.¹⁸⁴ It was indeed found that the presence of the amide was effective in increasing the optical yield. Chirally modified amide groups were used as the X group, **309** (Chart 40). When open-chain chiral amide groups were used, the de (diastereomeric excess) was unexpectedly low (8%); however, when chiral proline groups were used, de values were increased up to 59%, and the highest de values (up to 79%) were observed when there were N-substituents in the proline ring having the (*S*)-configuration.

Tomoda et al. went on to report the synthesis of chiral selenium reagent **310**.¹⁸⁵ It was thought that the chirality of the pyrrolidine ring could be effectively transferred to the reaction site through the strong $\text{Se}\cdots\text{N}$ nonbonded interaction. The use of **310** as a chiral inducer in asymmetric methoxyselenenylation of various olefins was reported (Scheme 59).¹⁸⁶ It was found that a decrease in nucleophilicity of the counteranion (i.e., an increase in electrophilicity of the selenium reagent) could enhance the de of the reaction.

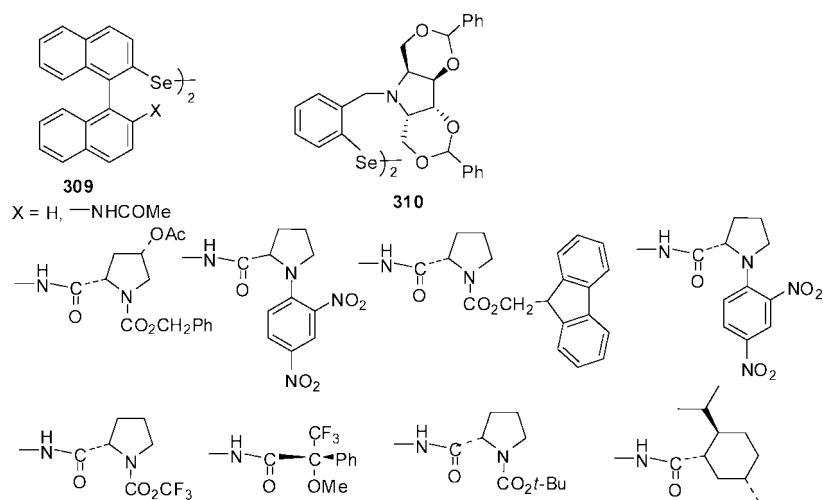
Fukuzawa et al. reported asymmetric methoxyselenenylation using a ferrocenyl based chiral selenium reagent (Scheme 60).¹⁸⁷ The precursor **198** could be readily prepared by the lithiation route from a commercially available ferrocenylamine, whereas previous chiral selenium reagents required multistep syntheses (Scheme 60).

Chiral diselenide **198** was converted to the ferrocenyl bromide, **313**, which in turn reacted with styrene derivatives at room temperature to give the β -methoxyselenium compound **314** as a single regioisomer. The diastereoselectivity was found to be very high compared with values obtained for binaphthyl and C_2 symmetrical phenyl based chiral Se compounds. It was found that addition of a catalytic amount of ZnI_2 further improved yields while maintaining high de values. It was also suggested that a sterically large group was necessary to achieve a high facial selectivity. Fukuzawa et al. later improved on this reaction by using the more electrophilic selenium triflate as the electrophile.¹⁸⁸

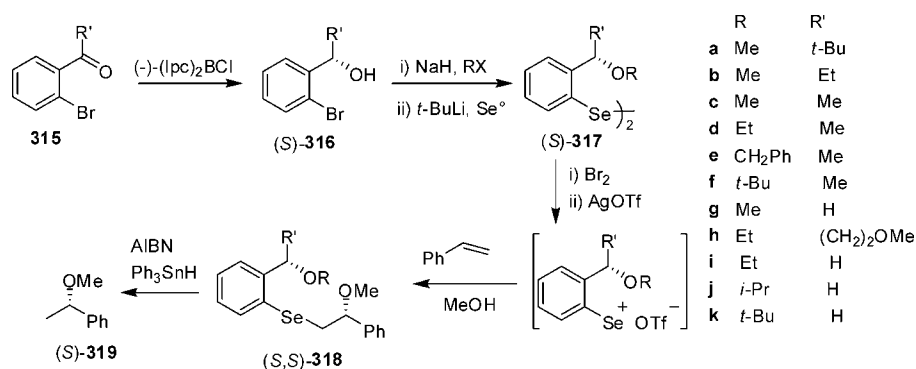
Wirth presented some new chiral diselenides **317** that were also readily accessible in a few steps (Scheme 61).¹⁸⁹ In the addition reaction to alkenes, diastereoselectivities of up to 88% were achieved. The selenium compounds synthesized in this way were suitable for use in further reactions as potential free radical precursors or for further functionalization.

Coordination of the oxygen of the OR group to the selenium cation led to the formation of a fixed conformation heterocycle. On addition of the alkene, the chirality was transferred to the newly formed asymmetric centers. For

Chart 40



Scheme 61



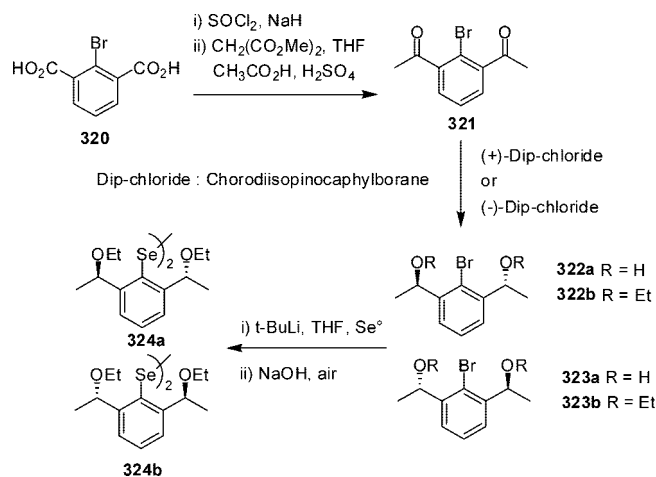
diselenide **317**, the ability of the oxygen to coordinate to Se was found to be influenced by the size of the substituent R. The larger the substituent, the weaker was the Se...O coordination and inducing effect on the newly formed stereocenter. Therefore, the highest diastereoselectivity on addition to styrene was observed when R = H. More recently, Wirth and co-workers prepared S and Te analogues of compound **317**; however, their cyclization reaction with unsaturated carboxylic acid gives disappointingly low selectivities.¹⁹⁰

A short and highly enantioselective synthesis of C₂ symmetrical (*R,R*) and (*S,S*)-bis[2,6-bis(1-ethoxyethyl)phenyl]diselenides **324** was reported by Déziel et al. (Scheme 62).¹⁹¹ The new synthetic route relied on the efficient asymmetric reduction of the diketone **321** with (+) or (–)-β-chlorodiisopinocampheylborane (Dip-chloride).

The original synthesis of **324** involved sequential conversion of each carboxylic acid in **320** to the desired chiral ethoxyethyl moiety.¹⁹² Déziel and co-workers went on to synthesize a more rigid analogue of compound **324**, which was the bis(tetrahydrofuran)yl based reagent **325**.¹⁹³ Reagent **325** was found to exert improved overall facial selectivity up to 98% de. It was one of the most effective chiral organoselenium reagents up to 1997. The element of C₂ symmetry was shown to be a key feature for high facial selectivity.

Tomoda et al. showed the importance of selenium reagents containing a strong Se...N interaction in asymmetric synthesis.¹⁹⁴ A new class of chiral Se reagents was synthesized based on the concept that the strong intramolecular interaction between an electrophilic Se and an optically modified

Scheme 62



tertiary amine would induce asymmetric induction in the reaction between the Se reagent and olefins. Compounds **325**–**327** have a heteroatom (O or N) at the position four bonds away from the selenium atom. The strong Se...N interaction in compound **326** may allow chiral sources on the nitrogen atom to come close to the reaction center in the transition state of the reaction. Because of this, distinct asymmetric induction is expected. It was assumed that the same type of Se...O interaction played a similar role in **317** and **327**.

Compound **328** is shown to exemplify how the strong Se...N interaction should allow the chiral source on R¹ and/or R² to come close to the reaction center, resulting in decent

Chart 41

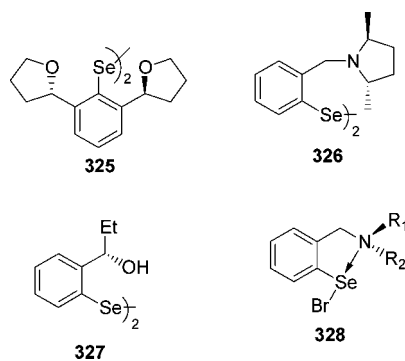
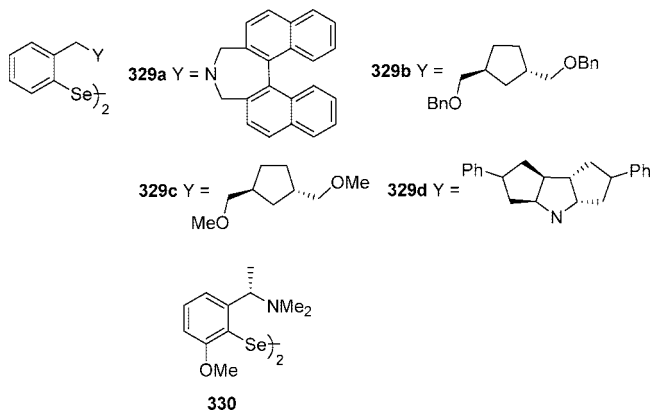


Chart 42



asymmetric induction. It was also expected that the strong $\text{Se} \cdots \text{N}$ interaction would dictate the molecular structure of the active Se reagent so that the reaction would proceed via a relatively confined transition state. These points were carefully considered when designing the asymmetric reactions. Chiral Se reagents **329** were synthesized using a 2-selenobenzene derivative and C_2 symmetrical cyclic amines. The diaryl diselenide **329d** was found to show the highest diastereoselectivities in both inter- and intramolecular asymmetric oxyseleenylation, when converted to a highly reactive electrophilic Se species by treatment with bromine and silver hexafluorophosphate under the optimum conditions.

Wirth et al. reported further work on the preparation of compounds **330** related to **317** with the incorporation of a methoxy group as a substituent on the ring.¹⁹⁵ The crystal structure for **132a** was obtained, showing that its structure was significantly different from other diselenides bearing heteroatom-containing side-chains. In other structures, strong interaction was found between selenium and the heteroatom of the side-chain; however, in **132a**, interaction with the oxygen of the methoxy group was observed. As a consequence of this, the hydrogen atom was placed in the plane of the benzene ring. The electrophilic methoxyselenenylation of styrene gave a de in excess of 96%. Thus, increased transfer of chirality was attributed to the forced interaction of the *ortho*-oxygen with selenium. This assumption was backed up by X-ray diffraction structure and NOE measurements. Chiral nitrogen-containing diselenides such as **34** were used in stereoselective oxyseleenylation–elimination reactions using peroxodisulfides to generate the electrophilic Se species. Chiral diselenides have also been described as useful ligands in various transformations including diethylzinc additions to aldehydes,¹⁹⁶ asymmetric hydrosilylation, and transfer hydrogenation reactions. Because of the low solubil-

Scheme 63

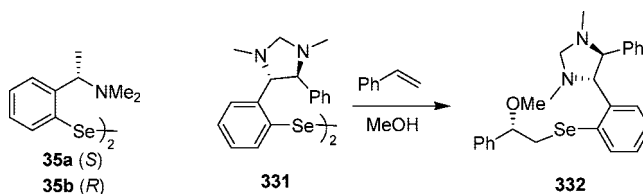
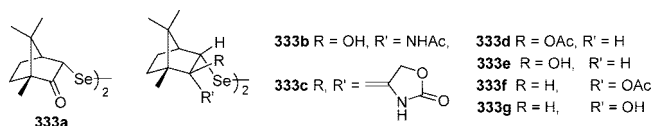
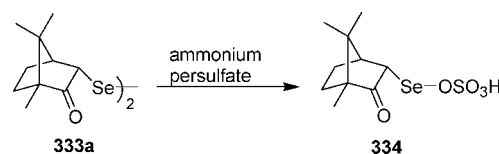


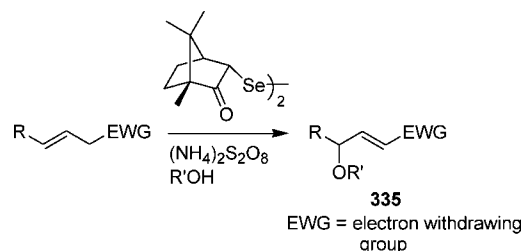
Chart 43



Scheme 64



Scheme 65



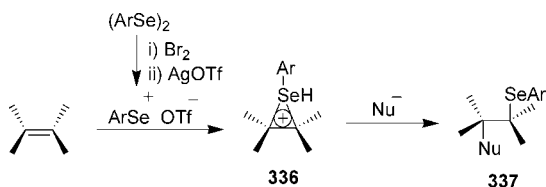
ity of the aryl selenium triflate under the reaction conditions for compound **34**, a more rigid diselenide, **331**, was designed.¹⁹⁷ This was assumed to give better selectivities and shorter reaction times. Diselenide **331** was then used for the methoxyselenenylation of styrene (Scheme 63). After the reaction, the addition product **332** was obtained in 98% yield. Therefore, a new chiral nitrogen-containing diselenide was synthesized, which could be used to facilitate methoxyselenenylations of styrene with high yields and high stereoselectivities even at room temperature.

More recently, a series of novel 3-camphor based diselenides were reported.¹⁹⁸ These differed in substitution at C_2 . The camphor seleno moiety was thought to be particularly suitable for the asymmetric methoxyselenenylation reaction because both antipodes of camphor are commercially available and diselenide **333a** could be prepared in one step as previously described. Diselenide **333a** was used as a starting material to prepare diselenides **333b–333g**.

Tiecco et al. reported that camphorselenenyl sulfate, **334**, could be easily prepared in situ in one step from **333a** and could be conveniently employed in the asymmetric selenomethoxylation of alkenes, giving moderate to good facial selectivity (Scheme 64).¹⁹⁹ Recently, Tiecco and co-workers reported camphor diselenide and ammonium persulfate induced oxyseleenylation–deselenenylation reactions of alkenes as a convenient one-pot synthesis for enantiomerically enriched allylic alcohols and ethers (of type **335**) (Scheme 65).²⁰⁰

The mechanistic course of the asymmetric methoxyselenenylation was investigated in detail by Wirth et al. in 1998.⁹⁰ In this type of reaction, seleniranium ions, **336**, formed by

Scheme 66



addition of chiral Se electrophiles to alkenes, are the intermediates (Scheme 66). Their formation is reversible. These heterocyclic three-membered intermediates are then attacked by a nucleophile from the *anti* side, leading to addition products **337**. Recently, Polschener and Seppelt have confirmed the formation of intermediate seleniranium ions by reporting the single-crystal X-ray studies of 1-phenyl-2,3-di-*tert*-butylseleniranium, 1-phenyl-2,3-diadamantylseleniranium, and 1-methyl-2,3-di-*tert*-butylseleniranium salts derived from the corresponding alkynes and $\text{PhSe}^+\text{SbCl}_6^-$ and $\text{MeSe}^+\text{SbCl}_6^-$.²⁰¹ The ^1H NMR study of the crossover experiment represents the first experimental observation of the formation of seleniranium ion.²⁰² The rapid olefin-to-olefin transfer of selenium cation represents one of the most likely pathways for racemization of enantiomerically enriched seleniranium ions and the most reasonable mechanistic rationale for the diastereoselectivity seen in selenylations with chiral, nonracemic selenylating reagents.

The stability of the seleniranium ion is strongly dependent on the $\text{Se}\cdots\text{heteroatom}$ interaction. This type of interaction in compounds such as **338** has been proven by the use of various experimental techniques such as X-ray crystallography, electron diffraction, ^1H NMR, ^{77}Se NMR spectroscopy, and NBO analysis. Because the formation of the seleniranium ion was found to be the determining step of stereochemistry, it was concluded that the reaction of the alkene with the chiral Se electrophile must lead preferentially to one seleniranium ion. Experimental observations showed that the different stabilities of the seleniranium ions were due to the rigidity of the system caused by $\text{Se}\cdots\text{O}$ interaction. Ab initio calculations were performed in order to investigate the structural and electronic properties of seleniranium ion intermediates. The four diastereoisomeric ions **338a–338d** were formed from the addition of styrene to a chiral Se electrophile of type **339**. There was found to be a strong correlation between the $\text{Se}\cdots\text{O}$ distances and the O–Se–alkene angle. In structures **338c** and **338d**, the alkene and the oxygen were arranged in an almost T-shaped fashion with the angle close to 180° . This would facilitate the interaction of the O lone pair with the antibonding molecular orbital of the selenium alkene bond. Therefore, stronger $\text{Se}\cdots\text{O}$ interactions and weaker Se–alkene bonds were found for **338c** and **338d** than for **338a** and **338b**. Because of the reversibility of the seleniranium ion formation, the stereoselectivity should be influenced by the relative stabilities of the ions **338a–338d**. In fact, the lowest energy was found for **338a** corresponding to *re*-attack, leading to the product with the (*R*) configuration at the new stereocenter. **338b** yielded the product with the opposite configuration and was found to be higher in energy (2.5 kcal/mol). Diastereoisomers **338c** and **338d** could not gain from π -stacking and energy differences of 5.4 and 7.4 kcal/mol, respectively, were calculated. Wirth also recently investigated the origin of stereoselectivities in asymmetric alkoxy selenenylations using computational methods.²⁰³ The stereoselectivities were rationalized by the relative stabilities of transition states for

Chart 44

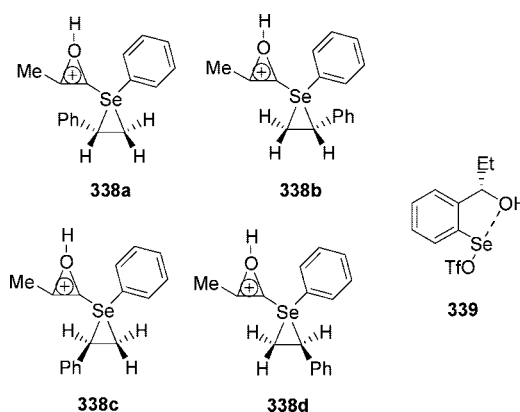


Chart 45

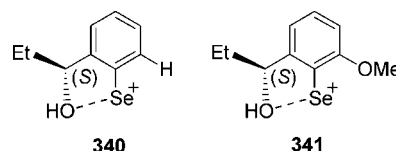


Table 2. Methoxyselenenylation Reaction of **342a–342g** with *trans*-Dec-5-ene

R*SeOTf	yield of product (%)	diastereomeric ratio
342a	88	94:6
342b	cyclization	
342c	65	66:34
342d	63	82:18
342e	51	85:15
342f	no reaction	
342g	no reaction	

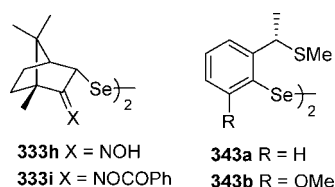
nucleophilic attack on seleniranium intermediates. A model to explain and predict stereoselectivities was developed.

More recently, Wirth et al. have reported the ab initio calculation results of the reactions of selenium nucleophiles **340** and **341** with different alkenes.²⁰⁴ From the computational results, it has been concluded that the coordination of the oxygen atom to the selenium is necessary for obtaining high stereoselectivity, and the higher experimental diastereomeric ratios with electrophile **341** in comparison with **340** can be explained neither by the stability of seleniranium ion intermediate nor by the strength of the side-chain coordination.

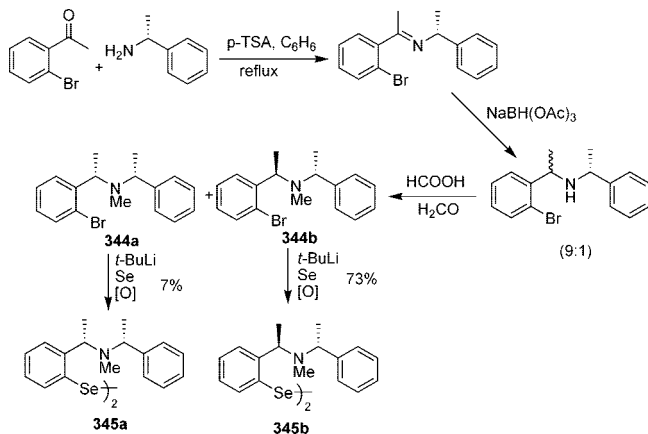
Comparison of the stereoselectivities afforded by *endo*- and *exo*-alcohol isomers (or their acetates) was expected to reveal the effects of $\text{O}\cdots\text{Se}$ coordination because *endo* isomers are more suitably oriented for such interactions. Diselenides **333a–333g** were converted in situ to the corresponding triflates, R^*SeOTf (**342a–342g**), and reacted with *trans*-dec-5-ene. The results are shown in Table 2. Compound **342a** provided the highest yield and the highest diastereomeric ratio. Because it was also produced in only one step, it is a very effective reagent for methoxyselenenylation reactions.

Diselenide **333a** has been converted into di[(1*R*)-2-oximino-*endo*-3-bornyl]diselenide **333h** and its benzoate derivative **333i**. The corresponding selenenyl triflates reacted with a variety of mono-, di-, and trisubstituted alkenes to afford the corresponding 1,2-addition product in a highly diastereoselective manner. Coordination effects between the substituents at 2-position of the camphor molecule and the positive selenium atom in the intermediate are believed to

Chart 46



Scheme 67

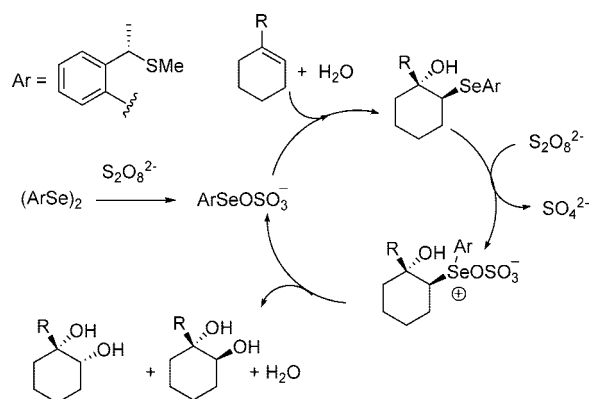


play an important role in determining the stereochemical outcome of methoxyselenenylation. Huang and co-workers reported the application of camphor based allyl methyl chiral selenonium ylide in asymmetric cyclopropanation as a new strategy for the highly stereoselective synthesis of chiral 1,2,3-cyclopropane.²⁰⁵ This strategy has the advantage of a facile synthesis and recyclability of chiral selenides, good yields, high generality, and controllable and very high diastereoselectivities and enantioselectivities.

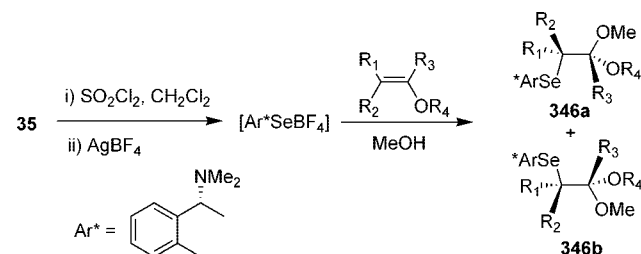
Recently, Tiecco et al. have reported the synthesis of new chiral sulfur containing diselenide, di-2-methoxy-6-[(1*S*)-1-(methylthio)ethyl]phenyl diselenide **343a**.^{119a} When treated with ammonium persulfate, this derivative is transformed into the corresponding selenenyl sulfate, which acts as a strong electrophilic reagent and adds to alkenes to afford the products of selenomethoxylation with excellent distereoselectivities. The presence of two substituents in both the *ortho*-positions to the selenium atom induced a greater conformational rigidity and a more efficient transfer of chirality. The kinetic resolution of racemic allylic alcohol has been achieved by treating allylic alcohol with 0.5 equiv of selenenyl triflate obtained from diselenide **343b** by methoxyselenenylation. The selenenyl triflate adds regioselectively to one of the enantiomers of the racemic mixture, and another enantiomer can be obtained in the enantiomerically pure form.^{119b} To confirm the role of heteroatom in stereoselective synthesis, Tiecco et al. carried out the methoxyselenenylation of styrene with 2-(1-methylpropyl)phenylselenenyl chloride and bromide; as expected, no diastereoselectivity was observed.¹²⁰

Tiecco et al. have, more recently, reported the synthesis of two new nitrogen containing diselenides **345a** and **345b**.²⁰⁶ These compounds were successfully employed for asymmetric methoxyselenenylation, hydroxyselenenylation, as well as cyclofunctionalization of olefins. Diselenides **345a** and **345b** were prepared by condensation of commercially available ketone and amine (Scheme 67). Starting from **345a**, all these addition processes occurred with good facial selectivity. Poor results were obtained, however, with **345b**.

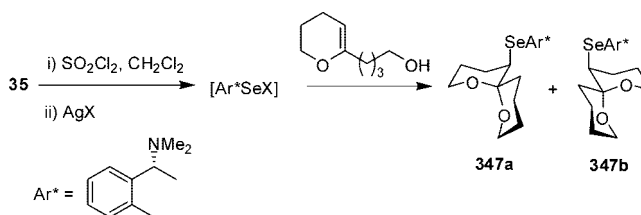
Scheme 68



Scheme 69



Scheme 70



Using chiral diselenide **343a**, a multistep, one-pot synthesis of diols has been demonstrated.²⁰⁷ The reaction was promoted by the $\text{ArSeOSO}_3\text{H}$ generated in situ from chiral diselenide and ammonium persulfate (Scheme 68). Using this strategy, 1-phenylcyclohexene stereospecifically converted in the corresponding *cis*-1,2-diol with excellent facial selectivity in high yield.

Uchiyama et al. have demonstrated asymmetric methoxyselenenylation of alkyl vinyl ethers (Scheme 69).²⁰⁸ Using (*R*)-(+)-*N,N*-dimethyl-1-phenethylamine diselenide **34**, this reaction afforded corresponding chiral acetals **346a** and **346b** with moderate to good distereoselectivity. The subsequent deselenenylation provided a new method of preparing enantiomerically enriched acetals in which acetal carbon was the only stereogenic center.

The intramolecular oxyseleenylation of 4-(3,4-dihydro-2*H*-pyran-6-yl)butan-1-ol (Scheme 70) leads to both enantiomers of 1,7-dioxaspiro[5.5]undecane **347a** and **347b**, the major pheromone components of the olive fruit fly.²⁰⁹

Regio- and diastereoselective methoxyselenenylation of the double bond attached to the *N,O*-ketalic of chiral perhydrobenzoxazines has been reported by achiral selenium reagent benzeneselenenyl chloride.²¹⁰ The diastereoselection can be rationalized by accepting the nonbonded interaction of the selenium to the oxygen atom of the heterocycle. Thus, it has been proposed that chiral perhydrobenzoxazines serve as excellent templates to promote methoxyselenenylation with total regio- and diastereoselectivity. Additionally, it is claimed that, depending on the reaction conditions, this

methodology yields better face discrimination than when chiral selenyl derivatives are used and offers the advantage of an easier purification of the mixtures of stereoisomers.

4.3. Catalytic Methoxyselenenylation

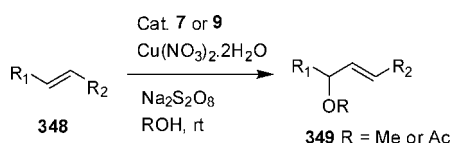
The first examples of the use of a catalytic amount of PhSeSePh to promote functional group transformations have been reported by Tiecco et al.²¹¹ Iwaoka and Tomoda reported their preliminary results on the catalytic conversion of alkenes into allylic ethers or esters using **7** and **9** as catalysts in 1992.²² This was the first time organoselenium reagents had been used in the catalytic conversion of alkenes **348** into allylic compounds **349** (Scheme 71). Diselenides having internal tertiary amines were used because it was thought that the Se...N interaction would stop disproportionation of the selenenic acid intermediate. Diselenide **7** was found to be a more efficient catalyst than **9**. Results were found to be comparable to similar reactions using electrochemical catalytic processes.

Kaur et al. have also used diselenides in the catalytic conversion of alkenes **350** into allylic acetates **351**.²³ Compound **31** was employed in a similar method to that of Iwaoka and Tomoda.²² The reaction is shown in Scheme 72.

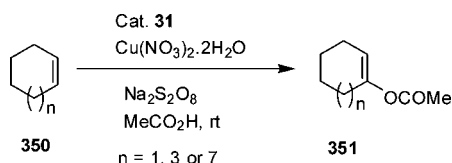
Wirth et al. reported a sequence of methoxyselenenylation and oxidative β -hydride elimination of alkenes using only catalytic amounts of chiral reagents (Scheme 73).²¹² Although the turnover numbers in the catalytic reaction described were still low, this was thought to be the highest enantiomeric excess reported for a catalytic asymmetric oxyseleenylation–elimination reaction.

Further, Wirth et al. reported the catalytic cyclization to obtain butenolides **353** from butenoic acids **352** using catalytic amounts of diphenyl diselenide and [bis(trifluoroacetoxy)iodo]benzene as stoichiometric oxidant in acetonitrile (Scheme 74).²¹³ For the asymmetric synthesis of butenolides, catalytic amounts of the chiral diselenides were employed. It was found that longer reaction times were required, lower

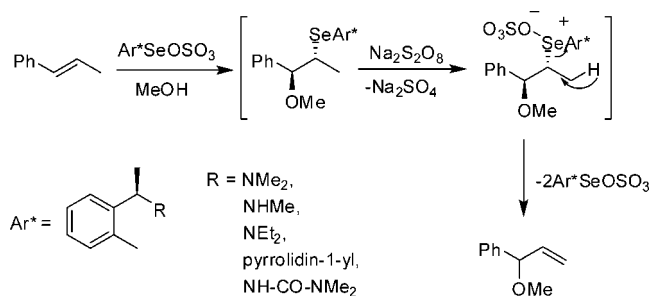
Scheme 71



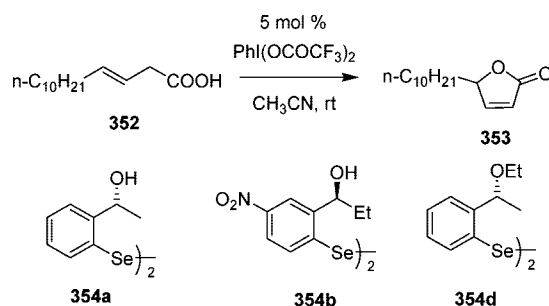
Scheme 72



Scheme 73



Scheme 74



yields were observed, and the enantioselectivity was low. The use of diselenides **354b** and **327** resulted in almost racemic product **353**, whereas with **354a**, the butenolide **353** was obtained with an enantiomeric ratio (er) of 57:43 (84% yield). Diselenide **354d** led to 61:39 er (46% yield) of **353** in the catalytic reaction.

4.4. Azidoselenenylation

Organic azides are versatile starting materials for the synthesis of a variety of nitrogen-containing compounds. The azido group can react with both nucleophilic and electrophilic reagents and can be used in 1,3-dipolar cycloaddition reactions. Recently, Tiecco et al. reported novel asymmetric azidoselenenylation of alkenes using chiral diselenide **333a**, **343a–343b**, **345b**, and **355**.^{119c} The excellent selectivity and yields obtained with the diselenide **343a–343b** compared to other diselenides indicate that the interaction of the selenium atom with the sulfur atom is stronger than its interaction with the other heteroatoms (oxygen or nitrogen). Better selectivity obtained for **343b** compared to **343a** can be ascribed to the presence of the additional methoxy group at the other *ortho*-position, which can induce a greater conformational rigidity to the chiral electrophilic reagent. The azidoselenenylation product thus obtained was further used for the synthesis of chiral oxazolines, aziridines, and triazoles (Scheme 75).

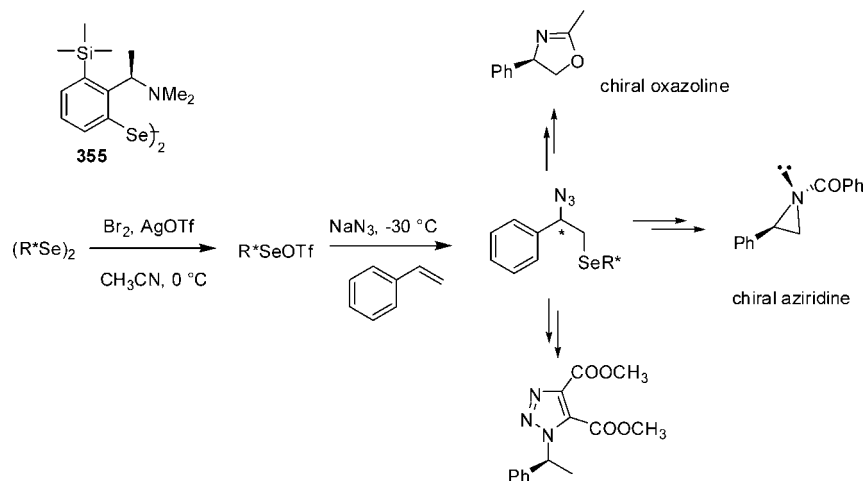
4.5. Carboselenenylation

Okamoto et al. have recently developed asymmetric carboselenenylation reaction of simple alkenes with aromatic compounds by using C₂-symmetric arbeselenenyl triflate **356** (Scheme 76).²¹⁴ The carbon–arben bond-forming reaction proceeds with high diastereoselectivity. This reaction is a convenient procedure for the preparation of chiral hydrocarbons that bear an aryl moiety at the stereogenic carbon atom and can be considered as a new type of asymmetric Friedel–Crafts alkylation reaction of aromatic compound with alkenes.

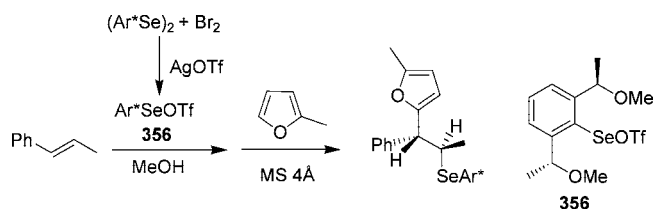
4.6. Asymmetric Selenocyclization

Recently, much work has been reported concerning asymmetric selenocyclizations in which diastereoselective cyclization has proved useful for the synthesis of heterocyclic compounds such as lactones, lactams, cyclic ethers, and nitrogen heterocycles.²¹⁵ Using organoselenium compounds as reagents for ring formation is attractive particularly when combined with further manipulation of the selenium group. The reaction generally involves the intramolecular trapping of the selenium species by suitably oriented nucleophile to yield different products depending on the linking chain (Scheme 77).²¹⁶

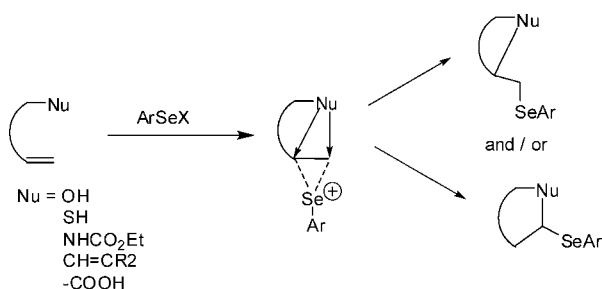
Scheme 75



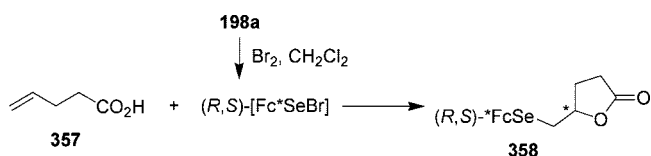
Scheme 76



Scheme 77



Scheme 78

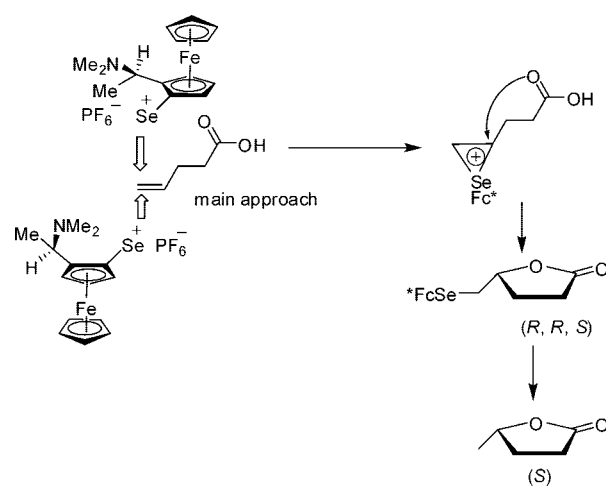


The first example of this cyclization was reported by Campos and Petragnani. It used a carboxylic group as the internal nucleophile; however, the reaction conditions were harsh and the reaction failed to find general application.²¹⁷ In all the products, the selenium position is either three or four bond lengths away from the heteroatom, thus leading to the possible intramolecular interactions.

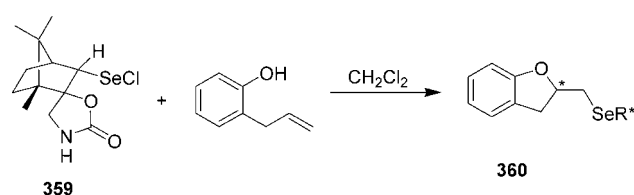
Uemura and co-workers reported the results of highly diastereoselective asymmetric selenocyclization of alkenes by the use of optically active chiral ferrocenyl selenyl bromide prepared in situ from diferrocenyl diselenide and bromine to give the corresponding chiral lactones, cyclic ethers, and nitrogen heterocyclic compounds, respectively (Scheme 78).²¹⁴ Moderate yields were obtained.

Very recently, Uemura et al. proposed a plausible reaction scheme for the cyclization where the chiral selenylating agent approached the $C=C$ double bond of the substrate from the least sterically congested direction, giving a chiral episele-

Scheme 79



Scheme 80

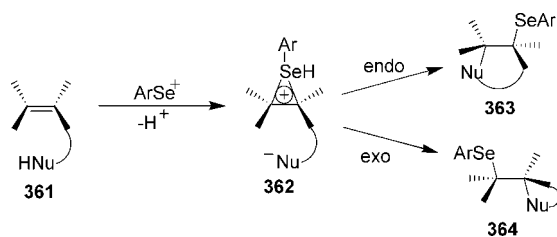


nonium ion. This was followed by intramolecular back-side attack of the nucleophile (Scheme 79).²¹⁸ The nature of the counteranions of the selenylating agent was found to profoundly affect the diastereoselectivity of the cyclization. Anions PF_6^- and BF_4^- were found to be superior for alkenoic acids, alkenols, and alkenyl urethanes, respectively.

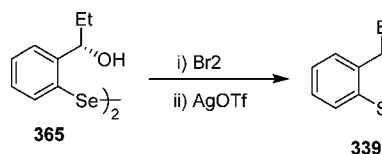
Back et al. have reported an effective cyclization of unsaturated alcohols and carboxylic acids with camphor based selenium electrophiles **359** (Scheme 80).²¹⁹ In general, monosubstituted and 1,2-disubstituted alkenes gave the best results. 1,1-Disubstituted cyclohexenyl systems gave poor diastereoselectivity.

The application of chiral selenium electrophiles in cyclizations of alkenes bearing an internal nucleophile was described by Wirth et al.²²⁰ The first step in the cyclization of alkenes, **361**, was the activation of the $C=C$ double bond by addition of a selenium electrophile, resulting in the formation of the seleniranium ion **362**. The ion was then attacked by the nucleophile from the *anti* side. The addition

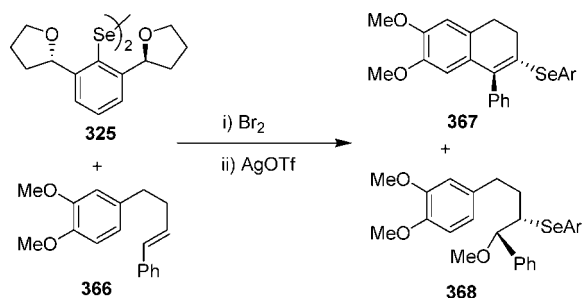
Scheme 81



Scheme 82



Scheme 83



can occur either by an *endo* or an *exo* pathway depending on ring size and the substitution pattern, leading to either product **363** or **364** (Scheme 81).

The cyclizations were performed using the chiral selenenyl triflate **339**, which was generated from diselenide **365**. Cyclizations leading to chiral tetrasubstituted carbon atoms were performed with good diastereoselectivities (Scheme 82).

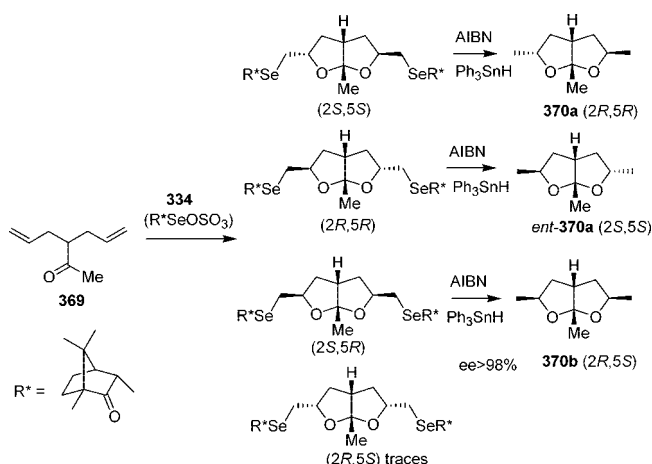
In 1998, Déziel and co-workers reported asymmetric arene–alkene cyclization mediated by a chiral organoselenium reagent, **325**. Compound **325** has selenium and oxygen atoms in very close proximity, allowing for the formation of $\text{Se}\cdots\text{O}$ intramolecular interaction. The cyclized product **367** was obtained with 98% diastereomeric excess. It was formed in a 1:1 ratio with product **368** (Scheme 83).²²¹

Chiral nonracemic camphorselenenyl sulfate **334** in situ synthesized from diselenide **333a** has been used for the double cyclization of bisalkenylketones to give 2,5,6-trisubstituted perhydrofuro[2,3-*b*]furans **370a** and **370b** with ee more than 98% (Scheme 84).²²² This simple procedure could have general application since it can be applied to the cyclization of several bisalkenylketones, thus leading to differently substituted perhydrofuro[2,3-*b*]furans. Moreover, the presence of the organoselenium function in the cyclization intermediates facilitates the introduction of several other groups to be easily affected.

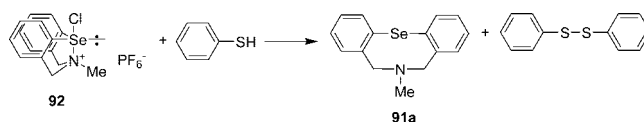
4.7. Organoselenium Compounds with $\text{Se}\cdots\text{N}$ Interaction as Oxidizing Agents

Several selenium cations (RSe^+) have been reported that are not only of structural importance but have been found to possess potential oxidant properties. Furukawa et al. reported the σ -selenane **92**, which is stabilized by a transannular $\text{Se}\cdots\text{N}$ bond.⁵⁸ This selenane was shown to behave as an oxidizing agent in the following reaction (Scheme 85).

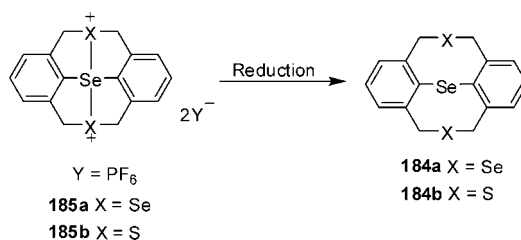
Scheme 84



Scheme 85



Scheme 86



Treatment of benzenethiol, with **92** in the presence of triethylamine in CH_3CN under an inert atmosphere and at room temperature, yielded diphenyl disulfide as the oxidation product in 88% yield and the selenazocine, **91a**, as the reduction product in 83% yield. The same group also reported new cyclic σ -selenuranes, **185a** and **185b**, which could be reduced, readily affording neutral **184a** and **184b** upon treatment with PhSH , Ph_3P , phenothiazine, or SmI_2 (i.e., **185a** and **185b** were acting as oxidizing agents) (Scheme 86).²²³

The use of the selenium functionality as a radical precursor has also been reported. Using this methodology, the first total syntheses of (+)-samin, **376** (Scheme 87),²²⁴ and (+)-membrane, **377** (synthesized in a similar manner),²²⁵ have been achieved using a sequence of addition and subsequent radical reactions. The electrophilic selenium compound **327** is presumably stabilized by $\text{Se}\cdots\text{O}$ interaction.

The use of chiral diselenides and their derivatives in the catalytic addition of organozinc reagents to aldehydes has been reported by Wirth.²²⁶ Nitrogen-containing selenium compounds **35**, **132b**, and **378–383** have been used as very efficient procatalysts for the asymmetric addition of diethylzinc to a variety of aldehydes; reactions were carried out in toluene at room temperature (Table 3). Diselenides **35**, **378**, **379**, and **381** have two alkylamino moieties and were found to be much more efficient catalysts compared with **132b** and **382**. A more detailed investigation of this reaction revealed that the diselenides act as procatalysts in the addition reactions; then after the addition of diethylzinc, the Se–Se bond is rapidly cleaved and catalytically active zinc selenolates are formed.

Scheme 87

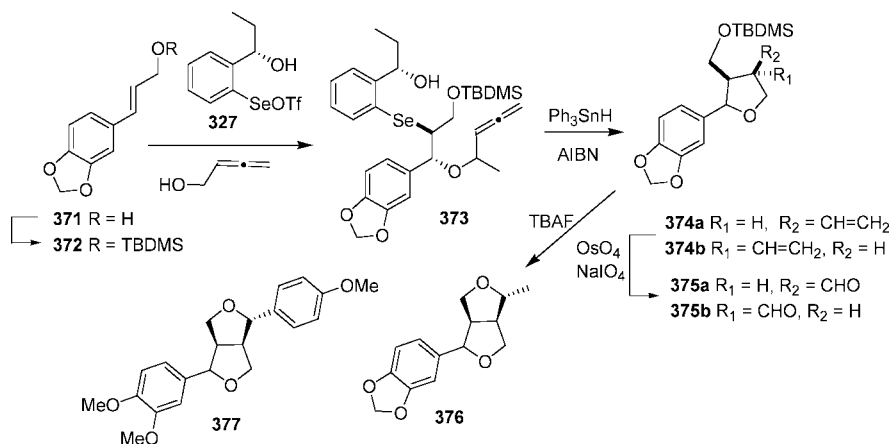


Table 3. Addition of Diethylzinc to Aldehyde in the Presence of a Catalytic Amount of Diselenide

catalyst	mol (%)	reaction time (h)	yield (%)	ee (%) configuration
34	1	12.5	82	93 (<i>R</i>)
130 (R = H)	5	13.5	10	15 (<i>S</i>)
378	1	13	57	91 (<i>S</i>)
379	1	22	91	96 (<i>S</i>)
380	1	14	23	27 (<i>R</i>)
381	1	12.5	71	92 (<i>R</i>)
382	5	13.5	32	8 (<i>R</i>)
383	5	13.5	1	8 (<i>R</i>)

Scheme 88

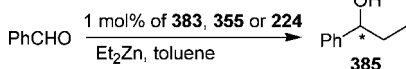
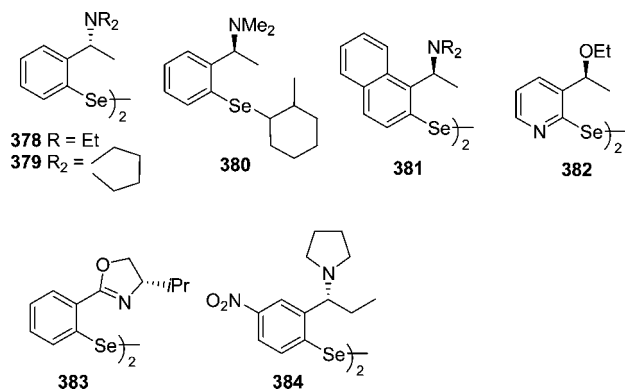


Table 4. Addition of Diethylzinc to Aldehyde in the Presence of a Catalytic Amount of Diselenide As Shown in Scheme 88

diselenide	yield of 385 (%)	ee of 385 (%)	configuration of 385
(<i>S,S,S,S</i>)- 224	89	97	<i>S</i>
(<i>R,R</i>)- 355	98	96	<i>S</i>
(<i>S,S</i>)- 355	95	96	<i>R</i>
(<i>R,R</i>)- 384	78	41	<i>S</i>

Wirth and co-workers recently reported the synthetic procedures for the preparation of new chiral, nonracemic nitrogen-containing diselenides **378**–**384**.¹⁹⁶ These compounds could be used efficiently as precursor catalysts in the diethylzinc addition to benzaldehyde, affording secondary alcohols **385** with high enantiomeric purities (up to 97% ee). Having already developed compounds of type **34**, compound **355** with a second *ortho*-substituent was prepared from

Chart 47



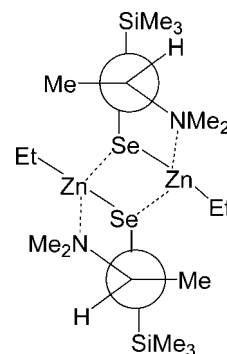
1-phenylethylamine in a few steps. Diselenide **331** was synthesized from (1*S*,2*S*)-1,2-diphenylethylenediamine, and **384** was prepared from 2-bromo-5-nitro-acetophenone. Diselenides **331**, **355**, and **384** were used in the diethylzinc addition to benzaldehyde (Scheme 88, Table 4).

It is interesting to compare the results of compounds **34** and **355**. The higher selectivity observed with compound **355** could well be an indication that the presence of the second *ortho*-substituent is pushing the nitrogen moiety of the chiral side-chain toward the selenium atom, thereby facilitating the coordination to zinc (Figure 17).

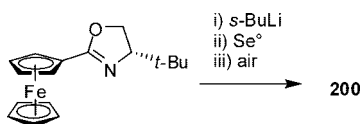
More recently, Bolm and co-workers have also reported catalytic asymmetric aryl transfer to aldehydes using oxazolonyl ferrocenyl diselenide **200**.²²⁷ The synthesis of **200** was accomplished by directed *ortho*-lithiation of (*S*)-2-ferrocenyl-4-*tert*-butoxazoline, followed by addition of selenium powder (Scheme 89). Asymmetric phenyl transfer to aldehydes in uniformly high yields and ee's of up to 85% were obtained when **200** was used as a catalyst (Scheme 90).

4.8. Asymmetric Hydrosilylation

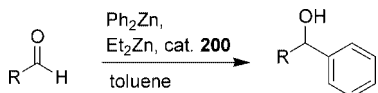
The transition metal catalyzed asymmetric hydrosilylation reaction of ketones has been extensively studied. In this reaction, phosphine ligands play an important role in stereoselection. Organochalcogen complexes with transition metal salts were originally thought to be unsuitable for this type of reaction. However, Uemura et al. have successfully employed chiral diferrocenyl dichalcogenides **198** for Rh(I) and Ir(I) catalyzed hydrosilylation reactions.^{138,141} The product yield and reaction rate were found to be affected by the nature of the alkyl and aryl groups of the ketone. They decreased as the bulkiness of the alkyl group increased, i.e.,

Figure 17. Interaction of chiral **355** with diethyl zinc.

Scheme 89



Scheme 90



$\text{Me} > \text{Et} > \text{Bu}^t$. Although the exact reaction mechanism has not been established, it was postulated that the first step was ligand exchange of the cyclooctadiene on the Rh(I) or Ir(I) complex with the dichalcogenide. This was followed by oxidative addition of diphenylsilane on Rh/Ir and subsequent coordination of the oxygen to Rh/Ir.

4.9. Selective Hydrogenation Catalysts

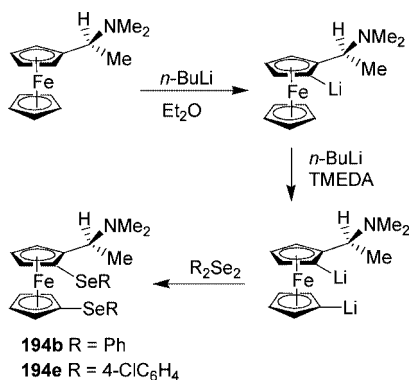
A series of ferrocenylamine selenides (**194a**, **194b**) have been prepared by the lithiation reaction of (*R*)-*N,N*-dimethyl-1-ferrocenylethylamine.^{137,228} The ferrocenyl sulfide and selenide derivatives were found to readily chelate platinum(II) and palladium(II) dichloride forming heterobimetallic complexes. The palladium ferrocenyl complexes were reported to be effective catalysts for the selective hydrogenation of dienes to monoenes under homogeneous conditions (Scheme 91).

4.10. Miscellaneous

4.10.1. Selenoxide Catalyzed Bromination of Organic Substrates with Sodium Bromide and Hydrogen Peroxide

Detty and co-workers have recently demonstrated the bromination of organic substrates using seleninic acid and selenoxide as a catalyst (Scheme 92).²²⁹ Here, arylseleninic acid or selenoxide catalyzes the oxidation of halide salts with H_2O_2 to give the corresponding positive halogen/hypohalous acid. Benzyl 2-((dimethylamino)methyl)phenyl selenoxide, **390**, which can form five-membered intramolecular coordination complex between the amine nitrogen atom and the selenium atom, was nearly 28 times more active as a catalyst than diphenyl selenoxide and 7 times more active than benzyl phenyl selenoxide.²³⁰ Formation of hydroxyperhydroxyselenane **389** is the rate-determining step for the catalytic activity of selenoxide. Under these reaction conditions, the protonated hydroxyselenonium species **388** is a likely intermediate that can add H_2O_2 to give the hydroxyperhydroxyselenane.

Scheme 91



Scheme 92

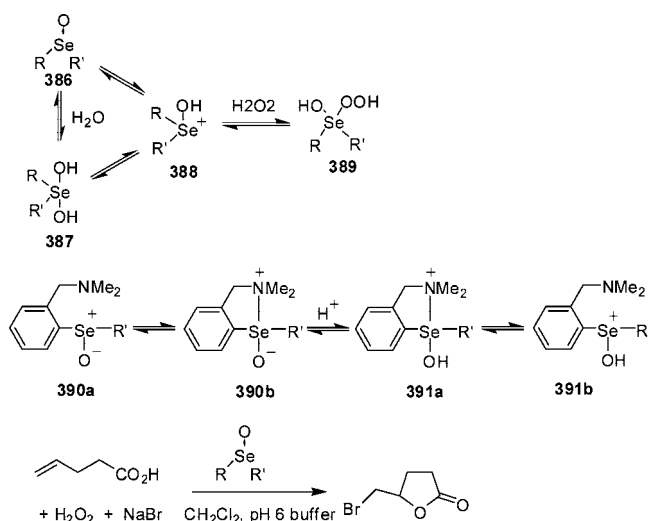
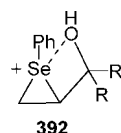


Chart 48



droxyselenane. The enhanced catalytic activity of selenoxide **390** may be due to the stabilization of hydroxyselenonium intermediate **391** by nonbonding interaction between Se and N.

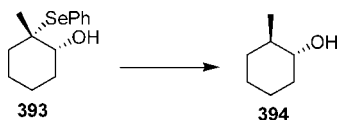
4.10.2. Hydroxyselenation of Allylic Alcohols

β -Hydroxyselenides, readily formed by the reaction of an alkene with phenylselenenyl phthalimide or phenylselenenyl chloride in the presence of water, are valuable intermediates in organic synthesis. This methodology was first applied to allylic alcohols by Cooper et al.²³¹ The reaction was found to proceed with a high degree of regio- and stereoselectivity. The formation of anti-Markovnikov “PhSeOH” adducts suggested that the allylic hydroxy group was directing the attack of water to the β -position of a reactive episelenonium ion intermediate, stabilized by $\text{Se}^+ \cdots \text{O}$ interaction, **392**. This also suggested that the addition of “PhSeOH” was reversible as the adducts did not isomerize to the thermodynamically more stable Markovnikov products. An interaction similar to that depicted in structure **392** has been proposed for the stereoselectivity observed in the kinetic resolution of allylic alcohols and in the methoxyselenenylation of α,β -unsaturated aldehydes.²³²

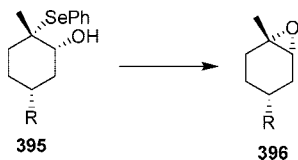
4.10.3. Influence of a Hydroxy Group in Asymmetric Reduction of Selenides: Enantioselective Synthesis of Naturally Occurring Monoterpenes

Ceccherelli et al. investigated the reductive cleavage of benzeneseleno groups in *trans*- β -hydroxyselenides to yield a stereogenic methyne center.²³³ When the reaction was carried out with lithium in diethylamine, the equilibrated carbanionic intermediate was found to trap the proton of the neighboring hydroxy group. This blocked the stereogenic center, thus giving a product with a predictable chirality (Scheme 93). Compound **393** has suitably positioned Se and O atoms for the formation of $\text{Se} \cdots \text{O}$ interaction.

Scheme 93



Scheme 94



4.10.4. Selenoxides as Leaving Groups: Epoxide Synthesis

Examination of the reactivity of β -hydroxyselenides by Ceccherelli et al. led to the discovery that these compounds can act as versatile precursors for the formation of epoxy-cyclohexanes.²³⁴ The *syn*-elimination of selenoxides is usually performed in polar aprotic solvents, leading to allylic alcohols; however, in the presence of strong alkali, it was reported that the methanolic solution of β -hydroxyselenoxides led to epoxides (Scheme 94).

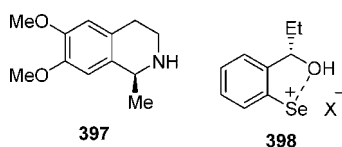
It was found that the tendency of the selenoxide group to behave as a leaving group in the presence of alkali was restricted to cyclic compounds in which the hydroxy and selenoxide groups had an *anti*-periplanar relationship.

4.10.5. Stereoselective Isoquinoline Alkaloid Synthesis with New Diselenides

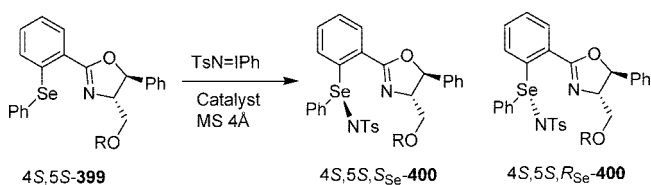
Intramolecular aminoselenenylation reactions lead to nitrogen-containing heterocycles that can be used as precursors for alkaloid synthesis. The selenium functionality remains present in addition products that, thus, can be used for further functionalizations. Wirth et al. used this strategy for the synthesis of tetrahydroisoquinoline alkaloids.²³⁵ Salsolidine, **397**, was chosen as a synthetic target. It was found that the counterion of the electrophilic selenium species, **398**, played an important role in the reaction, influencing yield and selectivity. Triflate was found to be the most suitable counterion.

Uemera and co-workers have reported diastereoselective imidation of diaryl selenides that contained intramolecularly coordinating chiral oxazolinyl moiety with [*N*-(*p*-toluenesulfonyl)imino]phenyliodinane (TsN=IPh) or chloramine-T trihydrate (Scheme 95).²³⁶

Chart 49



Scheme 95



5. Intramolecularly Coordinated Organoselenium Compounds as Glutathione Peroxidase Mimics

Glutathione peroxidase (GPx) is a mammalian enzyme that functions as an antioxidant.²³⁷ Any living organism that uses the reduction of oxygen to produce energy requires a mechanism for the removal of the highly reactive intermediates that are byproducts in the process. These intermediates, such as singlet oxygen, superoxide radicals, and peroxides, can cause damage to biomembranes and other cellular components.²³⁸ The selenoenzyme GPx functions as a catalyst for the reduction of hydroperoxides by glutathione, **401** (eq 1). It is for this reason that selenium is an important essential trace element in the diet of mammals.

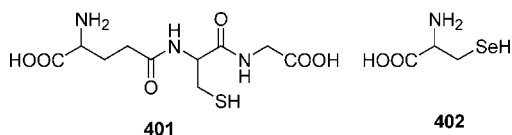


where GSH = reduced glutathione, GSSG = oxidized glutathione, and ROOH = any hydroperoxide.

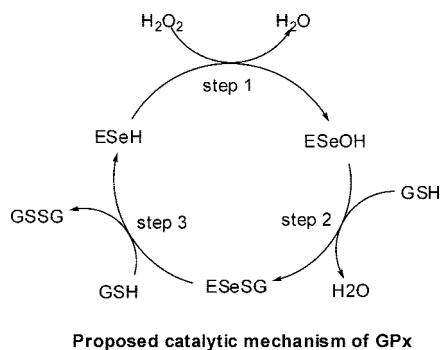
This reaction also stops further peroxide initiation of lipid peroxidation, thus protecting the integrity of the cell.²³⁹ There are three known classes of selenium-containing glutathione peroxidases:²⁴⁰ cytoplasmic glutathione peroxidase, plasma glutathione peroxidase, and phospholipid hydroperoxide glutathione peroxidase. All are mammalian enzymes and catalyze the above reaction. Cytoplasmic glutathione peroxidase is the most extensively studied of the three types; it was the first selenoenzyme to have been purified and is also the only one for which a three-dimensional structure has been elucidated.^{237f} This enzyme is a tetramer comprising four identical subunits ($M_r = 21\,000$ Da); each monomer consists of a single polypeptide chain containing 178 amino acid residues. The selenium of the selenocysteine **402** located in the active site of the enzyme is present as selenol and is structurally stabilized by hydrogen bridges to the amido group of the glutamine and imino group of tryptophane.

Recently, the crystal structure of human plasma glutathione peroxidase at 2.9 Å resolution was reported by Ren et al.²⁴¹ In this enzyme, selenium was found to exist in the form of seleninic acid (E–Se(O)OH) with two oxygen atoms bonded to the selenium. Although the two enzymes have similar overall active site structure, the environment close to the selenocysteine residues was found to differ significantly. The role of selenium in the GPx enzyme is to take part in a redox cycle that involves the selenolate anion (ESe[–]) as the active form, which reduces hydrogen peroxides and organic peroxides. Selenolate, which itself is oxidized to form selenenic acid (ESeOH) then reacts with reduced glutathione (GSH), forming a selenosulfide adduct (ESeSG). The active form of the enzyme is then regenerated by a second glutathione attacking selenosulfide, thereby forming oxidized glutathione (GSSG). During this process, 2 equiv of glutathione become oxidized to give disulfide and water and hydroperoxide is reduced to give the corresponding alcohol (Scheme 96).²⁴² A density functional theory (DFT) study²⁴³ of the mechanism of the GPx catalyzed H₂O₂ reduction by two glutathione molecules has revealed that the first elementary reaction of the process, (E–SeH) + H₂O₂ → (E–SeOH) + H₂O (step 1), proceeds via a stepwise pathway with the overall barrier

Chart 50



Scheme 96



of 17.1 kcal/mol, which is in good agreement with the experimental barrier of 14.9 kcal/mol. During this reaction, the Gln83 residue has been found to play a key role as a proton acceptor, which is consistent with experiments. The second elementary reaction, (ESeOH) + GSH \rightarrow (E–Se–SG) + H₂O (step 2), proceeds with the barrier of 17.9 kcal/mol. The last elementary reaction, (E–Se–SG) + GSH \rightarrow (E–SeH) + GSSG (step 3), is initiated with the coordination of the second glutathione molecule. The calculations clearly suggest that the amide backbone of the Gly50 residue directly participates in this reaction and that the presence of two water molecules is absolutely vital for the reaction to occur. This reaction proceeds with the barrier of 21.5 kcal/mol and is suggested to be a rate-determining step of the entire GPx-catalyzed reaction (eq 1). The results discussed in the study provide intricate details of every step of the catalytic mechanism of the GPx enzyme and are in good general agreement with the experimental findings and suggestions.

Several simple organoselenium compounds have been found to mimic the activity of glutathione peroxidases in vitro, and recently, much effort has been directed into this area of research. Various compounds having GPx activity have been reported including ebselen, the ebselen homologue, benzoselenazolinones, selenamides, α -phenylselenoketones, diaryl diselenides, and selenosubtilisin, an artificial selenoenzyme. These compounds can be classified into two major groups according to structure:

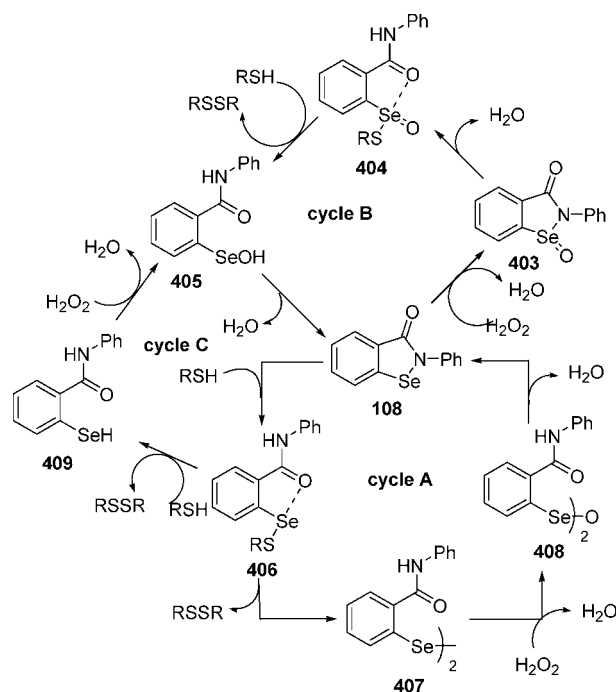
(1) Compounds having direct Se–N/Se–O bonds where the catalytically active species is formed from the cleavage of the Se–N/Se–O bond; and

(2) Compounds having a heteroatom (N, O) in close proximity to the selenium atom leading to the formation of weak Se \cdots N or Se \cdots O intramolecular nonbonded interactions.

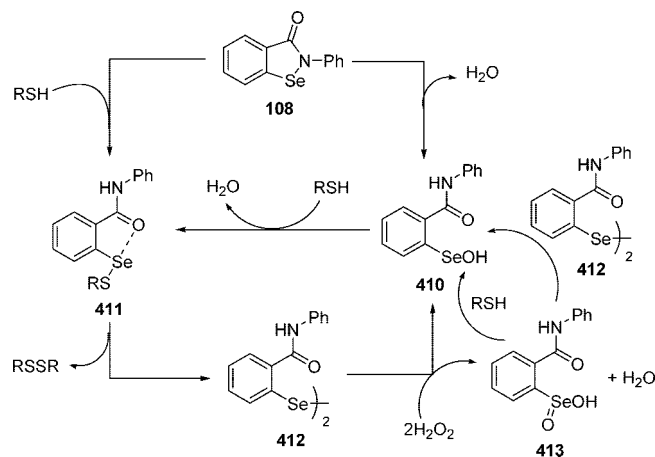
In this review, we will focus on compounds belonging to the latter category. Although the focus of this review is to delineate the structure–property correlation in GPx mimetics with intramolecular coordination, the chemistry of the ebselen derivatives, which are proposed to have intramolecular interaction at different steps of catalytic cycle, will also be discussed.

Ebselen (2-phenyl-1,2-benzisoselenazol-3(2*H*)-one), **111**, is a nontoxic, low molecular weight, selenium-containing heterocycle having anti-inflammatory, antiatherosclerotic, and cytoprotective properties²⁴⁴ and is thereby effective for treating diseases caused by cell damage due to the increased formation of active oxygen metabolites.²⁴⁵ These pharmacological properties of ebselen have been attributed to its ability to mimic the hydroperoxide reducing ability of glutathione peroxidase. Ebselen was first synthesized in 1924;^{245d} since then, many methods of preparation have been

Scheme 97



Scheme 98

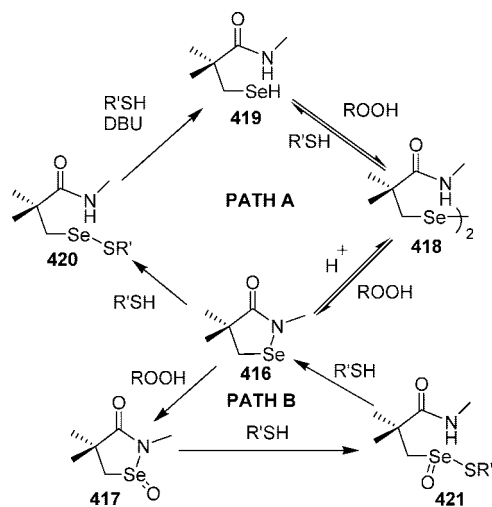


reported.²⁴⁶ Because of the exciting properties of this promising drug, several attempts have been made to develop new compounds in which the basic structure of ebselen is modified by the incorporation of different substituents and isoteric replacement.

According to the literature data,²⁴⁷ the first step in the catalytic mechanism of ebselen is the formation of a selenoxide (cycle B) or a selenenyl sulfide (cycle A), depending upon the relative concentration of thiol and peroxide (Scheme 97). It has been proposed that ebselen follows cycle B at higher peroxide concentrations, but under physiologically relevant conditions, that is, in the presence of an excess of thiol, cycle A may be operative.

A revised mechanism that accounts for the glutathione peroxidase (GPx)-like catalytic activity of ebselen was proposed through the formation of seleninic acid (Scheme 98).²⁴⁸ The reaction of ebselen with peroxides did not afford the selenoxide as previously postulated; instead, the formation of seleninic acid **413** was observed. The X-ray crystal structure of the seleninic acid shows Se \cdots O nonbonded interaction between the tetravalent selenium atom and the amide carbonyl moiety (Se–O distance, 2.46 Å). In the

Scheme 99



Oxidation-reduction chemistry of **416**.
Two mechanistic pathway **A** and **B** were postulated.

presence of excess thiol, the $\text{Se}\cdots\text{N}$ bond in ebselen is readily cleaved by the thiol to produce the corresponding selenenyl sulfide. The selenenyl sulfide thus produced undergoes a disproportionation in the presence of H_2O_2 to produce the diselenide, which, upon reaction with H_2O_2 , produces a mixture of selenenic and seleninic acids. The addition of thiol to the mixture containing selenenic and seleninic acids leads to the formation of the selenenyl sulfide. When the concentration of the thiol is relatively low in the reaction mixture, the selenenic acid undergoes a rapid cyclization to produce ebselen. The seleninic acid, on the other hand, reacts with the diselenide to produce ebselen as the final product. DFT calculations show that the cyclization of selenenic acids to the corresponding selenenyl amides is more favored than that of sulfenic acids to the corresponding sulfinyl amides. This indicates that the regeneration of ebselen under a variety of conditions protects the selenium moiety from irreversible inactivation, which may be responsible for the biological activities of ebselen.

In 1992, the ebselen homologue, **414**, was reported.²⁴⁹ It was thought that the presence of a direct $\text{Se}-\text{N}$ bond was responsible for the GPx-like activity. Several selenamide compounds have been reported that were also found to function in a similar manner to ebselen.^{247d,250} All these mimics were designed on the assumption that the $\text{Se}-\text{N}$ bond was essential for the GPx activity. This appeared to be proven when 1,3-benzoselazolinones, such as **415** containing Se and N atoms in the heterocycle but with no direct $\text{Se}-\text{N}$ bond, were prepared and tested.²⁵¹ These compounds were found to display no GPx-like activity, and compound **415** was found to have 0.033 times the activity of ebselen. Reich et al. reported that, under acid catalysis, the selenenamide, **416**, is in equilibrium with seleninamide **417** and diselenide **418** (Scheme 99).^{250a} It was also reported that oxidation of selenol, **419**, with *m*-chloroperoxybenzoic acid (mCPBA) led first to the diselenide **418** and then to the seleninamide **417**.

The observations that diselenide with suitably positioned donor groups plays an important role in the catalysis brought about an interest in the diselenides, which were more easily synthesized than the cyclic compounds and would function as effectively. The theory that a direct $\text{Se}-\text{N}$ bond was necessary for the GPx function was disproved by the observation that diphenyl diselenide **423** has GPx activity

Chart 51

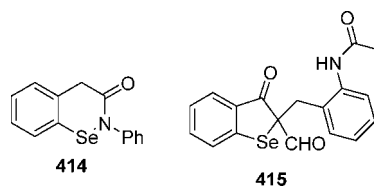
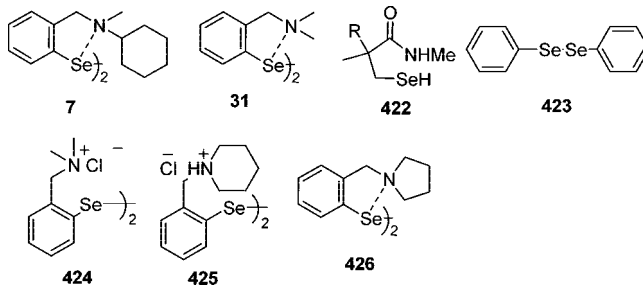


Chart 52

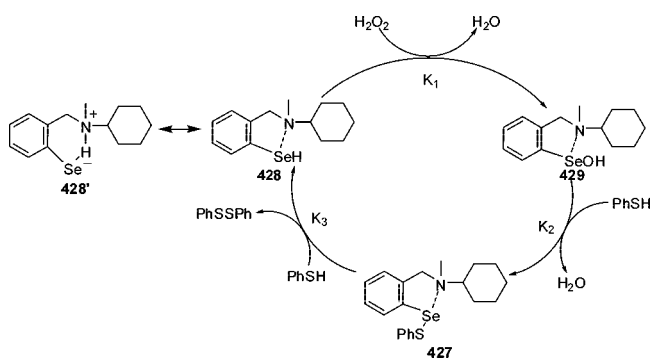


2-fold that of ebselen.^{251d} Compounds **424** and **425** were found to be 10 times more active than ebselen. It was proposed that, in order to display GPx-like activity, the disubstituted selenium must have at least one selenium–heteroatom bond, and as a result, several compounds containing $\text{Se}-\text{Se}$ bonds were developed.

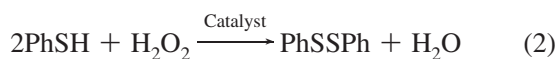
Wendel et al. suggested that amino acid residues in close proximity to the selenium atom in GPx may be involved in weak $\text{Se}\cdots\text{N}$ interactions that would be responsible for stabilizing the active site selenolate and enhancing the nucleophilic reactivity of selenium.^{237f} Hilvert et al. reported the preparation of the first artificial selenoenzyme, selenosubtilisin.²⁵² Selenosubtilisin was prepared using the semi-synthetic approach involving the chemical introduction of prosthetic groups into the active sites of enzymes. Selenocysteine was incorporated into the active site of the bacterial enzyme serine protease subtilisin (EC 3.4.21.14). The single atom change from oxygen to selenium in the active site serine of subtilisin was found to profoundly alter the enzyme's activity; the selenoenzyme was also found to mimic the catalytic behavior of GPx. The seleninic acid form of selenosubtilisin was found to be unusually stable, which was attributed to interactions of the enzyme-bound seleninic acid with the nearby oxyanion hole and His 64 preventing *syn*-elimination of β -hydrogens. This seems to again demonstrate the importance of the basic histidine residue at the active site of the enzyme. Flohé et al. have reported a simulation of the GPx catalytic cycle using computer-assisted molecular modeling.²⁵³ The X-ray structure of bovine GPx^{251d} was used as a base for the modeling. Force-field calculations and molecular dynamics were applied to kinetically defined intermediates and enzyme substrates. The results from this model implied the presence of weak interactions between selenium and the imino group of Trp 165 and the amido group of Gln 87; the $\text{Se}\cdots\text{N}$ distances were found to be 3.31 and 3.37 Å, respectively. This type of interaction was also seen in the crystal structure of human plasma GPx as determined by Ren et al.²⁴¹ Interactions between selenium and Gln 79 and Trp 153 were observed, and $\text{Se}\cdots\text{N}$ distances were found to be 3.5 and 3.6 Å, respectively. Following these observations, the GPx activities of other compounds containing Se and N in close proximity were explored by several groups.

Wilson et al. reported that protonated derivatives of diselenide **31** and **318** show strong GPx activity.^{251b} In both

Scheme 100



compounds, there is a basic amino nitrogen in close proximity to the selenium. Tomoda et al. carried out a study in order to investigate the mechanistic role of the amino nitrogens in the active center of GPx.⁸⁴ The GPx model used in this study was di-2-(*N*-cyclohexyl,*N*-(methylamino)-methyl)phenyl diselenide, **7**, and it was used to catalyze the following reaction (eq 2).



Each nitrogen atom present in **7** can directly interact with the nearest selenium, thus forming a five-membered ring; this has been revealed by X-ray analysis.¹⁹ Scheme 100 depicts the proposed mechanism of the reaction.

Intermediates **427**, **428'**, and **429** were characterized by ⁷⁷Se NMR spectroscopy. From the results of this investigation, three roles of the proximate nitrogen on GPx-like activity were proposed:

(1) Both theory (MO calculation) and experiment (⁷⁷Se NMR) suggested that the proximate nitrogen base activated the selenol intermediate, **428**, into the corresponding selenolate anion **428'**, thereby playing a key role in accelerating the catalytic cycle.

(2) The proximate nitrogen moiety stabilized the selenenic acid intermediate **429**. It appeared that intramolecular Se···N interaction in **429** prevented its destruction by further oxidation in the catalytic system.

(3) The formation of Se–N hypervalent bonding was observed in the low-temperature dynamic ¹H NMR spectrum of the selenenyl sulfide intermediate **427**; thus, it was expected that the nucleophilic attack of benzenethiol (PhSH) should occur preferentially at the sulfur atom of **427**, thereby allowing efficient production of **428'** in the catalytic cycle.

It, therefore, seemed that the presence of a basic amino group was indispensable for a GPx model compound. This theory was further supported by Reich et al.^{237c} because of the fact that the diselenide **418** and the selenosulfide **420**, both prepared from selenamide **416**, reacted with thiol only when a strong base was present. Singh et al. reported on the thiol peroxidase-like activity of the chiral diferrocenyl diselenides **198a** and **198b**.¹⁷⁷ These redox-active compounds synthesized by *ortho*-lithiation methodology showed excellent GPx activity. X-ray crystallographic data showed that **198** did not have any Se···N interactions in the solid state; the Se···N bond lengths (3.967 and 4.296 Å for **198a** and 3.98 and 4.12 Å for **198b**¹⁴⁴) were greater than the sum of the corresponding van der Waals radii (3.54 Å), but it was suggested that the nitrogen may come closer to the selenium atom in solution. Compound **431** without basic amino

Table 5. Initial Reduction Rates (v_0) of H_2O_2 with PhSH in the Presence of Various Selenium Catalysts Obtained by Lineweaver–Burk Plots

catalyst	relative GPx activity ($v_0 \mu\text{M}^{-1}\text{min}^{-1}$)
none	0.15 (0.04) ^a
31	28.38 (3.88)
42	inactive
198a	574.01 (23.98)
198b	466.49 (28.26)
423	0.55 (0.18)
431	3.39 (0.37)
432	inactive
433	inactive
434	5.32 (0.58)
435	36.10 (0.12)
436	0.35 (0.09)
437	3.16 (0.52)

^a Standard deviations shown in parentheses.

nitrogen displayed a low GPx activity. Compounds **42**, **432**, and **433** did not show any significant GPx activity; these compounds contain strong nonbonded intramolecular Se···N interactions (2.705, 2.891 Å for **432**, 2.778, 2.794 Å for **433**, and 2.628, 2.652 Å for **42**). It was, therefore, concluded that the presence of a proximate heteroatom is important provided the Se···N interaction is not too strong. Singh et al. also undertook a mechanistic study of compounds with GPx-like activity to investigate the importance of the amino group and to ascertain its role in the catalytic cycle.^{186a} The relative GPx activities are summarized in Table 5. The uncatalyzed reaction was very slow and was greatly increased by the simple diselenide **423**. Diselenides **435**, **436**, and **42** having strong Se···N interactions were inactive as previously discussed. Compound **82** containing a strong electron-donating *para*-substituent was also found to be inactive. The low GPx activity of compound **436** may be due to the presence of the secondary amino group in the *ortho*-position, which could lead to the formation of a cyclic selenamide and then a stable selenenyl sulfide reacting with thiol very slowly to give disulfide.²⁵³ The high catalytic activities of compounds **198a** and **198b** were proposed to be due to the synergistic effects of amino substituents and the redox-active ferrocenyl groups. The lower activity of the similar compound **435** suggested that stabilizing Se···N interactions may differ during the catalytic cycle. This study demonstrated that *N,N*-dimethylaminoethylferrocene derived diselenides were more effective catalysts than oxazoline based diselenides and Wilson's catalyst. The GPx activities were attributed to the strength of Se···N interactions in the catalytic intermediates. In the compounds showing low GPx activity, the nitrogen interacts with the selenium atom in all three intermediates in the catalytic cycle (selenol, selenenic acid, and selenenyl sulfide), whereas in more active compounds, the nitrogen interacts with selenium in order to stabilize only selenol and selenenic acid derivatives. It was, therefore, postulated that it is the reactivity of the selenenyl sulfide toward thiol which determines the GPx like catalytic behavior of the compounds.

The location of the basic nitrogen atom was important for three reasons. It should be positioned so that it can

(1) Abstract H^+ from RSeH and activate selenol into the reactive selenolate anion;

(2) Interact strongly with Se in selenol in order to increase its stability against further oxidation and to increase nucleophilic attack of thiol at selenium; and

Chart 53

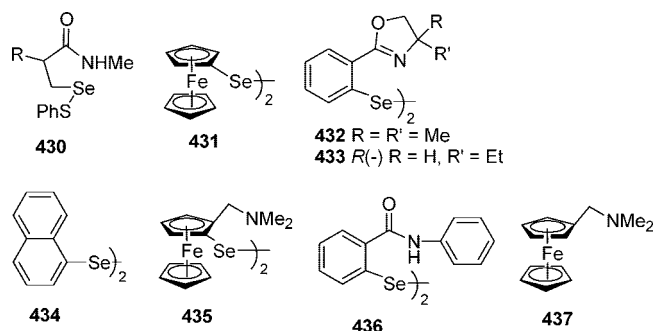
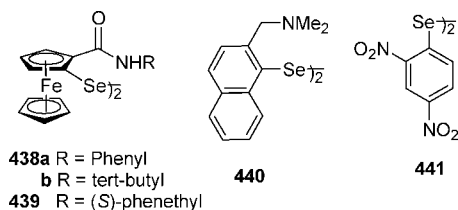


Chart 54



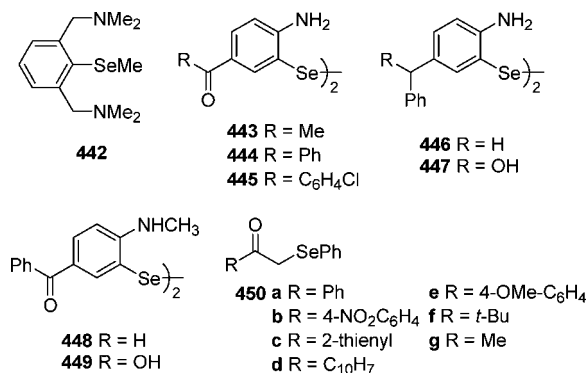
(3) Deprotonate the thiol sulphydryl group, providing a high local concentration of the nucleophilic thiolate anion.

The newly synthesized ferrocenecarboxamide based diselenides **438a**, **438b**, and **439**, amonomethylnaphthyl based diselenide **440**, and bis(2,4-dinitrophenyl) diselenide **441** have been investigated as GPx mimics using the thiol assay.²⁵⁴ The diselenides **438a**, **438b**, and **439** showed 40-fold lower activity compared to that for the ferrocene based diselenides **198a** and **198b**.^{254,255} However, these diselenides are better catalysts than simple ferrocenyl diselenides and benzamide based diselenide, which is inactive. Diselenide **440**, with a basic amino group, was found to be an efficient catalyst and showed 10-fold higher activity than that of corresponding phenyl based diselenide **31**.²⁵⁵ Interesting, naphthyl diselenide **42**, having an amino group at the *peri*-position, is inactive, which has shown strong Se \cdots N interactions in solid-state single-crystal X-ray structure. The considerably high activity of diselenide **441** can be attributed to the influence of the electronic effect on selenium by the interactions of nitro groups.

Fujihara and co-workers reported that aryl alkyl selenides may have GPx activity if the selenide is converted into a reactive cationic species.⁶³ For example, when compound **442** was treated with *t*-BuOCl to produce the selenium cation **100**, it was found to display catalytic activity. Compound **100** has two neighboring amino groups, and although no interaction between counteranion and counteranion was seen from X-ray data, intramolecular contacts of 2.154 and 2.180 Å were observed, which were considerably shorter than the sum of van der Waals radii for the two atoms. Galet et al. decided to compare the GPx activities of the diselenides with their cyclic counterparts.^{251a} Diselenides **443–450** were synthesized and their GPx activities were tested and compared with their cyclic analogues, the substituted benzose-lenazolinones such as **108**. As previously discussed, these compounds displayed no catalytic activity, whereas the diselenides showed catalytic activity of up to three times that of ebselen. This was probably due to the fact that cyclic compounds cannot be opened by thiol in vitro; however, acyclic derivatives can react with peroxides.

Glutathione peroxidase-like activity has also been observed in compounds containing oxygen as the heteroatom, for

Chart 55



Scheme 101

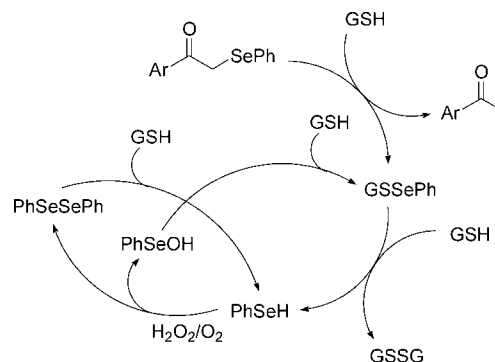


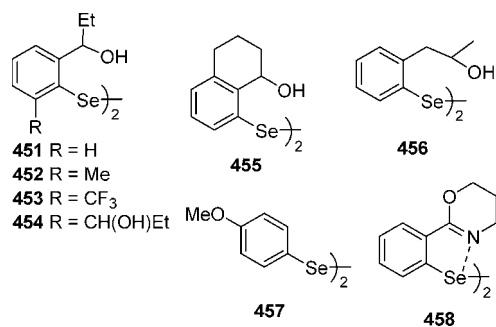
Table 6. GPx Activities of Compounds 451–458

diselenide	GPx activity (20 μ M Se equiv) [nmol of NADPH \cdot min ⁻¹] 100 μ M H ₂ O ₂
451	26.6
452	20.2
453	8.7
454	18.8
455	14.5
456	27.5
457	17.9
458	30.2

example, the α -(phenylselenenyl)ketones **450a–450g**.²⁵⁶ Compound **450b** with an electron-withdrawing group in the acetophenone moiety showed good catalytic activity; however, **450e** with an electron-donating substituent had reduced activity. Substitution of the acetophenone aryl group for alkyls in compounds **450f** and **450g** also led to decreased activity. A catalytic cycle was postulated (Scheme 101). It was concluded that the GPx activity of the (phenylselenenyl) ketones was due to cleavage of the C–Se bond of the catalyst and generation of C–Se $^-$ in situ.

Wirth reported on the glutathione peroxidase activity of oxygen-containing diselenides.²⁵⁷ Eight novel diselenides **78** and **451–457** were prepared that contained an oxygen atom in close proximity to selenium. Asymmetric induction was observed and was ascribed to Se \cdots O interaction. The GPx activities of compounds **78** and **451–457** are summarized in Table 6. Although all the diselenides displayed GPx activity, compounds **451**, **454**, and **457** are the most active. The bis-*ortho*-substituted diselenides, **452–454**, displayed lower activity. Compound **453** seems to confirm the idea that an electron-withdrawing substituent has an adverse effect on the GPx activity. Compound **78**, which contains a methoxy group rather than a hydroxy group, displayed one-half of the activity of diselenide **451**. The low activity of

Chart 56



diselenide **456** may be an indication of a less favorable interaction between selenium and oxygen. The highest activity was seen in compound **457**. The GPx activity of unsubstituted benzyl alcohol diselenide **135e** is comparable to the substituted derivatives and 2.5 times higher than bis(2-formylphenyl)diselenide, where stronger Se···O interactions were observed compared to the benzyl alcohol diselenide.⁹² This observation is in line with previous studies^{177a} on organoselenium compounds having Se···N nonbonded interactions that moderate interactions enhance the GPx like activity of the intramolecularly coordinated organoselenium compounds compared to those having stronger such interactions.

Singh et al. recently reported GPx-like activity of diselenide **458** and triselenide **65** having an oxazine ring *ortho* to selenium.³⁹ Triselenide **65** was found to be 12 and 3 times more efficient than the diselenide analogue **458** and Wilson's catalyst [bis{2-(*N,N*-dimethylbenzylamine)} diselenide] **31**, respectively, in the coupled reductase assay. The better catalytic activity of triselenide **65** can be ascribed to the formation of more reactive intermediates like RSeSeSPh and RSeSeH, which have been stabilized by strong Se···N interaction. Formation of an intermediate like RSeSPh has been confirmed by electrospray mass spectrometry (ES-MS) and single-crystal X-ray crystallographic studies.

The novel cyclic selenenate ester **139** and its precursor diselenide **138** showed significant GPx-like activities.⁹³ Almost 7- and 6-fold enhancement in the initial reduction rate (ν_0) has been observed for diselenide **138** and selenenate **139** compared to the Wilson's catalyst [bis{2-(*N,N*-dimethylbenzylamine)}diselenide] **31**, respectively. The mechanistic pathway has been discussed for the catalytic cycle of the selenenate ester on the basis of ⁷⁷Se NMR studies and the previous reported mechanism for selenenate ester by Back et al.²⁵⁸ (Scheme 102). These results corroborated the observations made by Back et al. that compounds containing Se···O bonds can be equally effective catalysts as the commonly studied Se···N derivatives. The azaselenonium chloride **149a** displayed significant glutathione peroxidase-like catalytic activity compared to ebselen in an assay with benzyl thiol and either hydrogen peroxide or *tert*-butyl hydroperoxide.⁹⁸

Singh et al. have studied the ebselen derivatives **116a–116c** as GPx mimics.⁷⁷ Enhancement in the catalytic activity of ebselen derivatives **116b** and **116c** was observed and compared to the parent ebselen, which can be ascribed to the presence of Se···O interaction in these compounds. However, phenyl derivative **116a** was found to be less active than the parent ebselen. This may be due to the poor solubility of compound **116a**. Mugesh and co-workers have prepared a series of ebselen analogues as GPx mimics and

Scheme 102

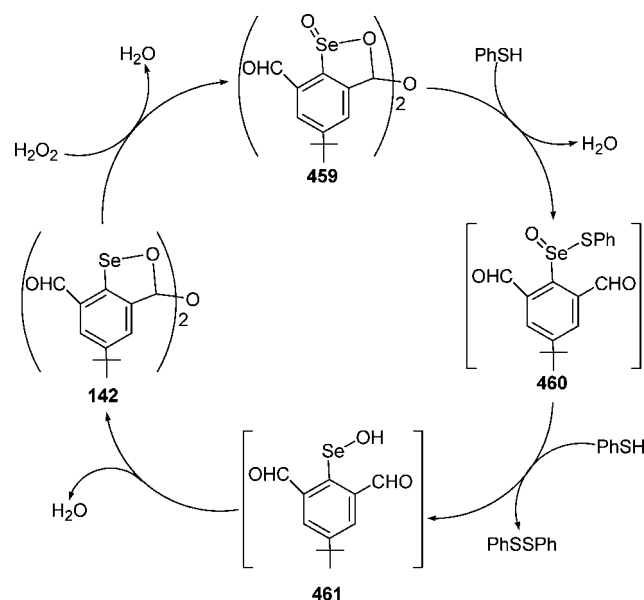
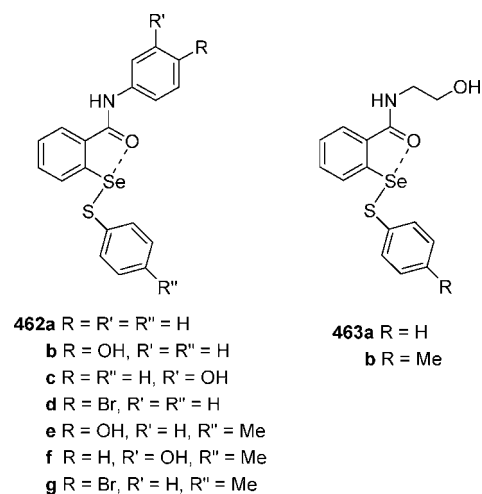
Proposed catalytic cycle for the GPx like activity of **142**

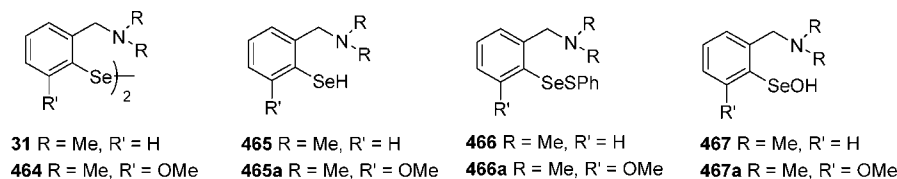
Chart 57



correlated their Se···O intramolecular interactions with the observed catalytic activities. As in the case of ebselen, the relatively low catalytic activity observed in the aromatic thiol assays can be attributed to the presence of strong Se···O noncovalent interactions in the selenenyl sulfide intermediates, which prevents the regeneration of catalytically active selenol species because of an undesired thiol exchange reaction at the selenium center. The presence of such interactions was confirmed by DFT studies, which suggest that the strong nonbonding Se···O interactions increase the nucleophilic attack at the selenium atoms and that the strength of these interactions depends upon the substituents attached to the phenyl ring of ebselen. The selenenyl sulfide **462a** derived from ebselen and the other selenenyl sulfides (**462b–d** and **463a**) showed strong Se···O interactions (Chart 57). This observation was further confirmed on the basis of a large downfield shift observed in ⁷⁷Se NMR spectra of **462e–462g** and **463b** compared with PhSeSPh, thus supporting the results of the DFT calculations. Consequently, the nature of the thiol shows a dramatic effect on the catalytic activity of ebselen and its analogues.²⁵⁹

In the related investigation, Bhabak and Mugesh studied a series of secondary and tertiary amide-substituted dis-

Chart 58



elenides **145** and **146**, as GPx mimics.⁹⁷ It was observed that substitution at the free $-NH$ group significantly enhances the GPx-like activities of the *sec*-amide based diselenides (**145**) mainly by reducing the $Se\cdots O$ nonbonded interactions. The reduction in the strength of $Se\cdots O$ interaction upon introduction of *N,N*-dialkyl substituents enhances the GPx activity by (i) preventing the undesired thiol exchange reactions and (ii) reducing the stability of selenenyl sulfide intermediates. This leads to a facile disproportionation of the selenenyl sulfide to the corresponding diselenide, which enhances the catalytic activity. A comparison of the catalytic cycles of *sec*- and *tert*-amide-substituted diselenides **145** and **146** reveals that the mechanisms are very similar for these two classes of compounds except that the selenenic acids such as **147a** having *sec*-amide substituents undergo a cyclization reaction to produce the corresponding selenenyl amides.

In continuation, Muges et al. have explored in detail the correlation between the selenium-heteroatom nonbonding interactions and the GPx activity by considering the example of the 2,6-disubstituted diselenide **464**.²⁶⁰ It is shown that the incorporation of 6-OMe group in amino substituted GPx mimics like **31** is a simple and efficient strategy to enhance the activity. The 6-OMe group reduces $Se\cdots N$ interactions and enhances the zwitterionic characters of the resulting selenol. The methoxy substituents also protect the selenium in the selenenic acid intermediates from overoxidation to seleninic acids or irreversible inactivation to selenonic acid derivatives. Additionally, the 6-OMe substituent prevents thiol exchange reactions at the selenenyl sulfide intermediate and shifts the course of reaction toward formation of selenol. The relatively weak interactions are sufficient for the reduction of the diselenide bond by a thiol. The ⁷⁷Se NMR spectra showed the upfield shift for the intermediate selenosulfides **466a** compared to **466** by 130 ppm. DFT calculation showed a longer $Se\cdots N$ distance in **466a** compared to that of **466**. The NBO analysis showed more positive charge on sulfur in **466a** than in **466**. Also the DFT calculations revealed that the zwitterionic form of selenol **465a** is relatively more stable by 4 kcal/mol compared to that of **466**. Further, the DFT calculations on the selenenic and seleninic acids have revealed that the introduction of methoxy substituents at 6-positions prevents the overoxidation of the selenenic acids to the corresponding seleninic acids.

These studies have revealed that the presence of basic amino groups in close proximity to selenium in diselenides possessing tertiary amino groups play a more positive role when methoxy groups are present at the 6-positions. The modified role of tertiary amino substituents in proximity of selenium in GPx mimics should be reconsidered as (i) it should not be involved in any $Se\cdots N$ interactions in the selenols, but should be sufficiently basic to deprotonate the selenols to produce more reactive selenolates, (ii) should not participate in strong interactions with selenium in the selenenyl sulfide intermediates, and (iii) should exhibit some

Chart 59

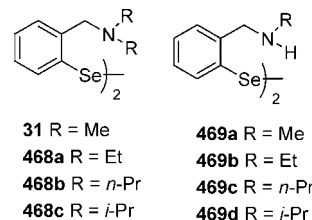
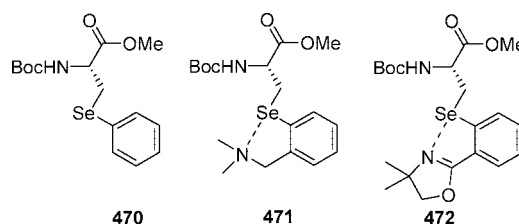


Chart 60

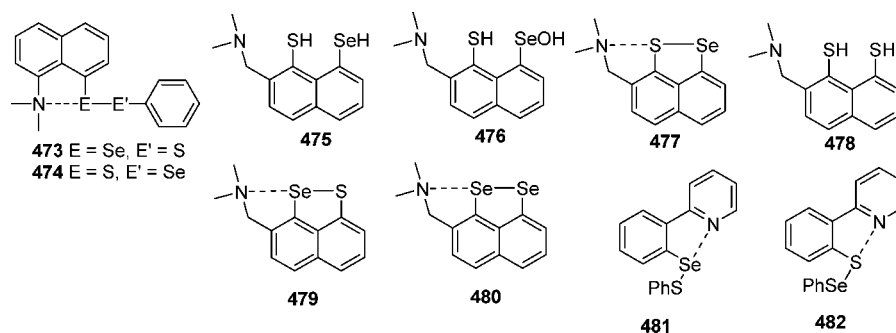


noncovalent interactions with selenium in the selenenic acid intermediates to increase the electrophilic reactivity of selenium.

Muges and Bhabak showed that replacement of the *tert*-amino groups in benzylamine based diselenides **31** and **468** with *sec*-amino moieties drastically enhances the catalytic activities in both the aromatic thiol (PhSH) and GSH assay systems.²⁶¹ Particularly, the *N*-propyl- and *N*-isopropylamino-substituted diselenides **469c** and **469d** are 8–18 times more active than the corresponding *N,N*-dipropyl- and *N,N*-diisopropylamine diselenides **468b** and **468c** in all three peroxide systems when GSH is used as the thiol cosubstrate. Although the catalytic mechanism of *sec*-amino-substituted diselenides is similar to that of the *tert*-amine-based compounds, differences in the stability and reactivity of some of the key intermediates account for the differences in the GPx-like activities. It is observed that the *sec*-amino groups are better than the *tert*-amino moieties for generating the catalytically active selenols. This is due to the absence of any significant thiol-exchange reactions in the selenenyl sulfides derived from *sec*-amine based diselenides. A comparison of the activities of *sec*-amino-substituted compounds with that of *sec*-amide based diselenides indicates that the *sec*-amino-substituted compounds are more sensitive to the nature of the peroxide than the *sec*-amide based compounds. Furthermore, the seleninic acids ($RSeO_2H$) derived from the *sec*-amine based compounds are more stable toward further reactions with peroxides than their *tert*-amine based analogues.

Suitable selenocystein derivatives with in situ formation of internally chelated active selenol capability by oxidative elimination of capped biogenic moiety should prove to be interesting candidates for biological applications. In this regard, Phadnis and Muges have synthesized phenyl, benzylamine, and phenyloxazoline based selenocystein derivatives (**470**–**472**, Chart 60).²⁶² The GPx activity of the phenyl derivative **470** was only marginally higher than that

Chart 61



of ebselen; however, benzylamine derivative **471** exhibited an almost 16-fold increase in the GPx activity as compared with ebselen due to the presence of $\text{Se}\cdots\text{N}$ intramolecular interactions. Thus, selenocystein capped benzylamine derivative acts as a procatalyst for generating catalytically active selenol stabilized by $\text{Se}\cdots\text{N}$ intramolecular interaction.

Peroxynitrite Scavenger

Peroxynitrite anion (ONOO^-) is a potent cytotoxic agent and has attracted great attention over the past decades. The recent theoretical studies on ebselen derivatives as peroxynitrite scavengers reveal that the weak $\text{Se}\cdots\text{N}$ interaction may facilitate the peroxynitrite nitrate isomerization.²⁶³ Kumar et al. studied protection against peroxynitrite mediated nitration reaction (PN assay) by diorganoselenides/-sulfides (with and without intramolecular coordination).⁹⁶ The PN assay data of diorganoselenides reveal that the selenides, having a basic amino group ($\text{sp}^3\text{-N}$ donor) in close proximity of selenium, are more active compared to the diorganoselenides having an imino group ($\text{sp}^2\text{-N}$ donor) and also show much higher protective action than the diorganoselenides without such interactions. This study reveals that the selenides having basic amino groups with weak intramolecular $\text{Se}\cdots\text{N}$ interaction are more active than the selenides having imino groups with strong $\text{Se}\cdots\text{N}$ interaction against PN-mediated nitration reactions. Intramolecularly coordinated diaryl selenoxides lacking an α -hydrogen do not undergo any selenoxide elimination reaction. The absence of selenoxide elimination reactions may help in recycling the selenoxides back to selenides without loss of any activity.

Inhibition of Iodothyronine Deiodinase

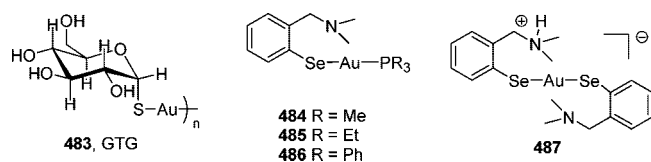
Recently, the mechanism for the inhibition of iodothyronine deiodinase by thiourea based drugs has been experimentally verified by utilizing selenenyl iodide **50** as enzyme mimetic substrate (ESeI) stabilized by internal chelation.²⁶⁴ Treatment of these compound with aromatic thiols in the presence of NEt_3 afford areneselenenyl sulfide during the reduction of selenenyl iodide by thiol and its possible relevance to the iodothyronine deiodinase. Catalytic cycle has been demonstrated. Furthermore, selenenyl halide **50** has been studied as a new substrate for mammalian thioredoxin reductase (TrxR)²⁶⁵ and in the bioimplication of a nitrosation reaction of selenol and homolysis of Se -nitroselenol.²⁶⁶ Recent studies are focusing on the other selenium-containing selenoenzymes such as iodothyronine deiodinase (ID) and thioredoxin reductase (TrxR) and mimicking the action of these enzymes by incorporating active selenium residue, selenocystein (Sec), into proteins²⁶⁷ and by using small selenium compounds having $\text{Se}\cdots\text{N}$ interactions.²⁶⁸

Thioredoxin Reductase Mimics

Mugesh et al. have described the roles of built-in thiol cofactors and the basic histidine (His) residues in the active site of mammalian thioredoxin reductases (TrxRs) with the help of experimental and density functional theory calculations on small-molecule model compounds.²⁶⁹ The reduction of selenenyl sulfides by thiols in selenoenzymes such as glutathione peroxidase (GPx) and TrxR is crucial for the regeneration of the active site. The nucleophilic attack of thiols takes place at the selenium center in the selenenyl sulfides. These thiol-exchange reactions would hamper the regeneration of the active species selenol. Therefore, the basic His residues are expected to play crucial roles in the selenenyl sulfide state of TrxR . The basic His residues may play important roles by deprotonating the thiol moiety in the selenenic acid state and by interacting with the sulfur atom in the selenenyl sulfide state to facilitate the nucleophilic attack of thiol at sulfur rather than at selenium, thereby generating the catalytically active species selenol.⁷⁷ ^{77}Se NMR spectroscopic studies as well as reverse-phase high-performance liquid chromatography (HPLC) experiment strongly suggest that strong $\text{Se}\cdots\text{N}$ interactions in the selenenyl sulfide state lead to thiol-exchange reactions, which hamper the regeneration of the active species selenol.

The DFT calculations also show that the ^{77}Se NMR chemical shift (573 ppm) of **473** is much downfield shifted compared to that of **474** (424 ppm), indicating the presence of an $\text{Se}\cdots\text{N}$ interaction in **473** and an $\text{S}\cdots\text{N}$ interaction in **474** (Chart 61). The calculations show that the nitrogen atom in **474** interacts with the sulfur ($\text{S}\cdots\text{N}$, 2.59 Å), leading to an elongation of the $-\text{S}-\text{Se}-$ bond ($\text{Se}-\text{S}$, 2.27 Å). The NBO second-order perturbation energy for the $\text{S}\cdots\text{N}$ interaction ($E_{\text{S}\cdots\text{N}}$) in **474** is calculated to be 11.35 kcal/mol. The calculated ^{77}Se NMR chemical shift for **474** (424 ppm) also shows a large upfield shift compared to that of **473** (573.0 ppm), confirming the expected decrease in the electrophilic character of selenium. NBO analysis showed that the nonbonded interactions with sulfur in the selenenyl sulfide intermediate not only increase the electropositive character of sulfur but also decrease the electrophilic character of selenium. In other words, the $\text{S}\cdots\text{N}$ interactions would certainly enhance the possibility of the thiol attack at sulfur rather than at selenium. To apply these findings to the mammalian TrxR catalytic cycle, model studies have been carried on theoretical models **475**–**482** for the anti-oxidant properties of the mammalian TrxR using DFT calculations at the B3LYP/6-31G(d) level of theory. Similar results were obtained for these model compounds. These studies on small-model selenenyl sulfides show that the mammalian TrxR may use internal cysteines mainly to overcome the thiol-exchange reactions and to enhance the

Chart 62



reduction of the selenenyl sulfide intermediate. The His residues (His108 and His472) that are very close to the cysteine and Sec residues in the active site may play crucial roles by (i) deprotonating the thiol to enhance the nucleophilic attack of the thiolate in the selenenic acid intermediate and (ii) interacting with sulfur in the selenenyl sulfide to facilitate a thiol attack at sulfur rather than at selenium.

Inhibition of the glutathione peroxidase activity of two synthetic organoselenium compounds, bis[2-(*N,N*-dimethylamino)benzyl]diselenide (**31**) and related monoselenide, bis[2-(*N,N*-dimethylamino)benzyl]selenide ((2-Me₂NCH₂-C₆H₄)₂Se), by antiarthritic gold compounds gold(I) thioglucose (**483**), chloro(triethylphosphine)gold(I), chloro(trimethylphosphine)gold(I), and chloro(triphenylphosphine)gold(I) was reported recently.²⁷⁰ The inhibition was found to be competitive with respect to a peroxide (H₂O₂) substrate and noncompetitive with respect to a thiol (PhSH) cosubstrate. The diselenide **31** reacts with PhSH to produce the corresponding selenol **466**, which upon treatment with 1 equiv of gold(I) chlorides produces the corresponding gold selenolate complexes 2-Me₂NCH₂C₆H₄AuPR₃ (**484**, R = Me; **485**, R = Et; and **486**, R = Ph). However, the addition of 1 equiv of selenol **465** to complexes leads to the formation of bis-selenolate complex **487** by ligand-displacement reactions involving the elimination of phosphine ligands. The phosphine ligands eliminated from these reactions were further converted to the corresponding phosphine oxides (R₃P=O) and selenides (R₃P=Se). In addition to the replacement of the phosphine ligand by selenol **465**, an interchange between two different phosphine ligands was also observed. The reactivity of selenol **465** toward gold(I) phosphines was found to be similar to that of selenocysteine.

6. Theoretical Models for Interpretation of Nonbonding Interactions

The discussions thus far on a large variety of compounds have formed the premise for the existence of nonbonding interactions in organochalcogens. Nonbonding interactions have been unequivocally established with the help of a wide range of experimental methods, particularly using the X-ray diffraction studies.^{12,19,21,22,84} Structural characterizations of a number of novel compounds have indeed contributed to establishing the importance of ubiquitous nonbonding interaction involving pseudo-hypervalent chalcogens. The widely accepted geometrical criteria for the existence of nonbonding interaction have been based on the contact distance between chalcogens and the other heteroatoms.¹⁰² Nuclear magnetic resonance techniques are becoming increasingly popular as a probe to study nonbonding interactions.^{79,271} The basic factors responsible for the origin and magnitude of such nonbonding interaction evidently demands an explicit understanding of the electronic interactions. A number of models focusing on the role of orbital as well as electrostatic effects are proposed toward this goal. Computational methods have been very effective in gaining valuable insights on nonbonding interaction in a multitude of interesting mol-

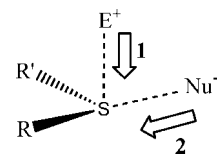


Figure 18. Preferred direction of approach for electrophiles and nucleophiles for divalent sulfur center.

ecules. Our objective at this juncture is mainly to summarize the generally accepted models based on electronic structure calculations, in identifying and interpreting nonbonding interactions.

Goldstein et al. proposed that the Se···O nonbonding interaction exhibits predominantly electrostatic character in selenazofurans.^{48b,49,272} Barton et al. have highlighted the involvement of a three-center four-electron (3c,4e) interaction based on their study on selenoiminoquinones.⁷¹ These early conjectures that the intramolecular nonbonding interactions could exhibit ionic or covalent characteristics have provided the impetus for further studies toward understanding the nature of nonbonding interactions. In their study, Parthasarathy et al. have established the directional features of nonbonded atomic contacts involving divalent sulfur atoms based on their analyses of crystal structures of a large group of compounds. They found that the electrophiles and nucleophiles tend to interact with the bivalent sulfur, respectively, through the HOMO and LUMO orbitals as shown in Figure 18.²⁰ The direction of preferred contact for an electrophile (E⁺) is nearly perpendicular to the plane of R-S-R' (*direction-1*, Figure 18), guided by the interaction of filled HOMO with the unfilled orbital on the electrophile. In the case of interaction with a nucleophile, the donation of electron from the nucleophile to the σ^* antibonding orbital of the Se-R (or Se-R') (*direction-2*, Figure 18) is important. These generalizations were proposed based on a large number of compounds having predominantly intermolecular interactions. The scenario is more interesting when intramolecular variants of such interactions are considered. The inherent structural features in such molecules could be sensitive to the nature of nonbonding interactions.

These observed directional features in intermolecular interactions are reminiscent of covalent binding. Subsequently, it has been identified that one of the driving forces in promoting nonbonding interaction is the electron delocalization between orbitals of comparable energies. Different scenarios can be envisaged based on the geometrical disposition as well as the nature of the donor-acceptor orbitals. The *filled-unfilled* interaction between suitably aligned orbitals leads to net stabilization. Such a donor-acceptor orbital interaction model, which provided a good conceptual framework in understanding nonbonding interactions in organochalcogens, will be discussed in the following sections.

Tomoda and others have employed electron delocalization as a model framework toward understanding the origin of intramolecular nonbonding interaction in organochalcogens.^{84,91b,115,117} The analyses using the natural bond orbital (NBO) have contributed in establishing a conceptually simpler approach based on electron delocalizations. In the case of intramolecular chalcogen···chalcogen interactions, the lone pair electron on the electron-rich chalcogen atom was found to delocalize into the suitably positioned σ^* orbital of the adjacent bond (acceptor bond). A representative example depicting the $n_{\text{O}}-\sigma^*_{\text{Se-Cl}}$ stabilizing interaction in an *ortho*-substituted arylselenide is shown in Figure 19. It

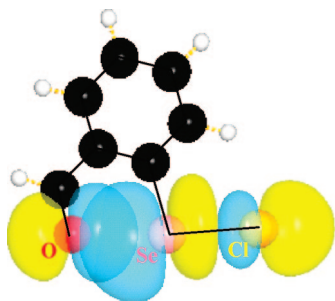


Figure 19. Natural bond orbital overlap between the oxygen lone pair (n_{O}) and the antibonding orbital of the Se–Cl ($\sigma^*_{\text{Se-Cl}}$).

Table 7. Summary of Calculations Performed at the B3LYP/6-31H Level^a for Compounds

compd	X	computed structural parameters		$E_{\text{Se}\cdots\text{O}}$ (kcal/mol)
		$R_{(\text{Se}\cdots\text{O})}$	$\theta_{(\text{O}\cdots\text{Se}\cdots\text{X})}$	
134a	Cl	2.305	176.4	36.07
134b	Br	2.336	177.6	33.80
134c	CN	2.594	171.9	11.33
134d'	SMe	2.644	176.4	10.72
134e'	SeMe	2.661	177.4	10.66
134f	Me	2.758	173.9	6.19
135a	Cl	2.567	175.2	14.80
135b	Br	2.604	157.7	13.61
135c	CN	2.787	170.9	5.95
135d'	SMe	2.873	174.5	4.71
135e'	SeMe	2.901	175.1	4.46
135f	Me	3.005	171.0	2.57
137a	Cl	2.555	175.5	14.38
137b	Br	2.596	175.9	13.17
137c	CN	2.795	170.9	4.86
137d'	SMe	2.876	175.2	4.21
137e'	SeMe	2.912	175.2	3.87
137f	Me	3.007	171.3	2.26

^a Values taken from ref 91b.

is evident from the overlap between the natural bond orbitals that the delocalization of oxygen lone pair into the $\sigma^*_{\text{Se-Cl}}$ is quite effective. The orbital interaction of this kind would have direct influence on the geometry of molecules possessing such intramolecular interactions. For instance, the Se–Cl bond in the present case tends to remain planar with respect to the aryl ring and collinear to the donor oxygen atom. It has been reported using the density functional theory calculations that the orthogonal orientation of the Se–Cl bond leads to a higher-energy conformer for the same molecule.^{115,273}

The second-order perturbation energies obtained using the natural bond orbital (NBO) analysis are commonly used toward quantifying the efficiency of electron delocalizations responsible for nonbonding interactions.^{91b,274,275} A compilation of second-order perturbation energies, along with the corresponding nonbonding interaction distances for a representative set of molecules calculated using the DFT method, is provided in Table 7. In a series of *ortho*-substituted arylselenenides, the most significant delocalization has been reported to be between the oxygen lone pair (n_{O}) and the antibonding orbital of the Se–X ($\sigma^*_{\text{Se-X}}$). For instance, depending on the nature of the X group in the Se–X acceptor bond, as in **134a**–**134f**, the second-order perturbation stabilization energy ($E_{\text{Se}\cdots\text{O}}$) values exhibited large variation from 6.2 to 36.1 kcal mol^{−1}. For other compounds such as **135a**–**135f** as well as in **137a**–**137f**, the corresponding values are, respectively, found to be in the range 2.6–14.8 kcal mol^{−1} and 2.3–14.4 kcal mol^{−1}. The $n_{\text{O}} \rightarrow \sigma^*_{\text{Se-X}}$ orbital interaction energies were found to be the

highest when X = Cl and lowest for X = Me for the group in compounds such as **134**, **135**, and **137**. It is, therefore, evident that the estimated second-order perturbation energies reflect the strength of secondary bonding interaction between the oxygen donor atom and the acceptor selenium center. Further, the contact distance between Se and O atoms showed a good correlation with the computed $E_{\text{Se}\cdots\text{O}}$ values, indicating that orbital interaction is a key factor contributing to the stability of the Se \cdots O interactions.

Another widely used protocol within the NBO framework toward identifying the orbital interaction contributions in nonbonding interactions is *orbital deletion* procedure. The deletion energy (ΔE_{del}) is the loss of stabilization energy due to the selective removal of the acceptor orbital participating in the nonbonding interaction.²⁷⁶ Iwaoka and Tomoda have used NBO deletion method to establish the role of orbital interaction in Se \cdots N nonbonding interaction in a group of 2-selenobenzylamines (**11**–**17**).¹² It was found that the ΔE_{del} values correlate quite well with the strength of nonbonding interaction estimated using the ¹⁵N NMR technique. In another study on *o*-hydroxymethylphenyl chalcogens exhibiting intramolecular Se \cdots O as well as Te \cdots O nonbonding interactions, Singh and co-workers effectively used NBO deletion method to compare the relative strengths of nonbonding interactions between selenium and tellurium atoms.⁹²

The nature of Se \cdots O nonbonding interaction in the above compounds has been studied in order to understand the contributions from electrostatic and covalent interactions. The density functional theory calculations at the B3LYP level suggest that the correlation between the charges on selenium and oxygen with the Se \cdots O interaction distances is not good in a series of 2-substituted benzeneselenenyl derivatives having oxygen as the donor atom and Se–X as the acceptor bond (X = Cl, Br, CN, SPh, SeAr, and Me). Tomoda and co-workers have proposed that the nature of the Se \cdots O interaction cannot be entirely explained using electrostatic considerations. Reed et al. have proposed a dimensionless covalency ratio for characterizing the nature of binding in van der Waals complexes.^{274,277} The covalency factor defined in terms of the covalent as well as van der Waals bonding distances has also been used as an indicator of covalent contributions in intramolecularly bound organochalcogen compounds. Sadekov et al. employed *covalency factor* in a number of tellurium compounds exhibiting nonbonding interactions in order to evaluate the extent of covalent contribution.²⁷⁸ In another study, Singh and co-workers have found that the percentage covalent contribution in 2-dichalcogenobenzylalcohols is relatively higher with ditellurides than the corresponding diselenides (**135e** and **137e**).⁹²

A more refined method based on the quantum theory of atoms and molecule, proposed by Bader, has been widely used for probing the nonbonding interactions in organochalcogens. The method known as atoms in molecules (AIM) involves the topological analysis of the electron density.²⁷⁹ In practice, the starting point for an AIM calculation demands the optimized wave function at any appropriate level of theory. In AIM formalism, the interatomic interaction is characterized by the presence of a bond path and a corresponding (3, −1) bond critical point (bcp). A representative example depicting the Se \cdots O nonbonding interaction is provided in Figure 20. It can be easily noticed that there are distinct bond critical points for all the bonded as well as nonbonded pairs of interacting atoms. While the primary indicator for the existence of nonbonding interac-

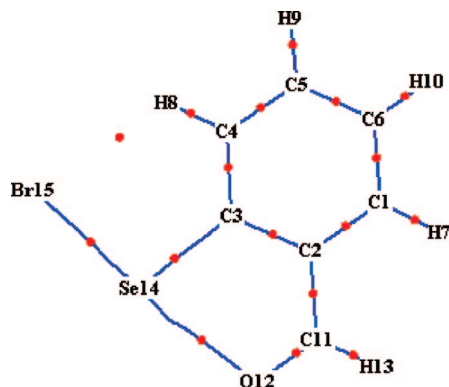


Figure 20. Molecular plot showing the $\text{Se}\cdots\text{O}$ bond critical point (between Se_{14} and O_{12}) in *ortho*-formyl arylselenenylbromide **101**. Intramolecular nonbonding interaction is characterized by a bond path (blue lines) as well as the bond critical point (red dots) between formyl oxygen (donor) and selenium (Se—Br bond acts as the acceptor). The topological analysis performed at the BHANDHLYP/cc-pVDZ//cc-pVDZ level of theory.²⁸²

tion is the presence of a bcp, other topological properties such as the gradient of the electron density at the bcp ($\nabla^2\rho(r_c)$) and the total energy density (H) are proposed to be more reliable indicators characterizing the nature of interaction.²⁸⁰ For instance, the information on whether the electron density at the bcp is locally dense or depleted can be obtained by examining the value of $\nabla^2\rho(r_c)$. The value of $\nabla^2\rho(r_c)$ less than zero implies a shared electron interaction characteristic of a covalent bond, and if $\nabla^2\rho(r_c)$ is greater than zero, it indicates a closed-shell or electrostatic interaction. The total energy density (H) at the bcp is reported to be more reliable in identifying whether the interaction is electrostatic or covalent.²⁸¹

In an interesting study, Tomoda and co-workers have effectively utilized AIM analyses²⁸² on formyl as well as benzyl (alcohol and either) substituted arylselenenyls (**134**, **135**, and **137**) toward concluding that the $\text{Se}\cdots\text{O}$ interaction is predominantly covalent rather than electrostatic.⁹¹ The $\text{Se}\cdots\text{O}$ nonbonding distances were reported to exhibit better correlation with the total energy density at the bcp for these compounds. Since the nonbonding interaction involves delocalization into the $\sigma^*_{\text{Se-X}}$ bond, the acceptor ability of the Se—X bond will have a direct bearing on the strength of these interactions. In fact, the highest and lowest values for the H_{bcp} were found to be for X = Cl and X = Me, respectively. Following Tomoda's proposal on the importance of topological analyses in gaining better insights on the nature of nonbonding interactions in organochalcogens, several other related applications have also appeared in the literature.^{283,284}

Although there are large numbers of examples on the identification of $\text{Se}\cdots\text{N}$, $\text{Se}\cdots\text{O}$, and $\text{Se}\cdots\text{X}$ (X = F, Cl, and Br) interactions, the first experimental effort toward quantifying intramolecular nonbonding interactions in organochalcogens was reported by Tomoda and co-workers. They have employed variable-temperature NMR techniques to quantify weak intramolecular $\text{Se}\cdots\text{N}$ as well as $\text{Se}\cdots\text{F}$ interactions in a series of *ortho*-selenobenzyl amino and *ortho*-selenobenzyl fluoride derivatives.^{12,114a} The estimated $\text{Se}\cdots\text{F}$ interaction energy in 2-(fluoromethyl)phenylselenenyl cyanate (**165a**, Chart 26) is $1.23 \text{ kcal mol}^{-1}$. When the group attached to the selenium is SeAr, i.e., in the corresponding diselenide, the interaction energy is found to be only $0.85 \text{ kcal mol}^{-1}$. The interactions were found to be much stronger

in 2-selenobenzylamine derivatives. For instance, the $\text{Se}\cdots\text{N}$ interaction is estimated to be more than $18.8 \text{ kcal mol}^{-1}$, when Se—Cl, Se—Br, and Se—OAc act as the acceptor Se—X bond. Additional ^{77}Se experiments with ^{15}N -labeled compounds exhibited a large downfield shift of ^{15}N NMR and a significant enhancement of $J_{\text{Se}\cdots\text{N}}$ coupling constants. These observations could be readily rationalized with the help of assuming a covalent character for the $\text{Se}\cdots\text{N}$ interaction primarily contributed by $n_{\text{N}} \rightarrow \sigma^*_{\text{Se-X}}$ delocalization.

The importance of theoretical chemistry in rationalizing experimental observations is quite well-known. It is intuitively appealing to predict quantities that are amenable to immediate experimental verification. One such quantity widely employed in examining intramolecular nonbonding interaction in chalcogenic systems is the NMR chemical shift (δ) and coupling constant (J). Minor accuracy issues in the computed values with respect to the experimentally determined values arising as a result of varying degrees of approximation should not be a major concern as the ^{77}Se ($I = 1/2$) nuclei enjoys a wider range of chemical shifts ($\sim 2000 \text{ ppm}$).^{132,285} Parallel to the experimental studies, a good number of theoretical methods based on the “gauge-including atomic orbitals” (GIAO) formalism have received wider acceptance.²⁸⁶ In a very recent study, Iwaoka et al. have successfully demonstrated how ^{17}O as well as ^{77}Se NMR techniques could be employed to gain further insights on $\text{Se}\cdots\text{O}$ nonbonding interactions.⁹¹ For example, in all the model compounds **134**–**136** (Chart 17), the most stable conformer is predicted to maintain an intramolecular $\text{Se}\cdots\text{O}$ interaction at the B3LYP level of theory. This was found to be in good accordance with the chemical shift values of the donor oxygen atom. In the case of ^{17}O -enriched aldehydes (**134a**) an upfield shift (δ_{O}) relative to benzaldehyde, where the —SeX group is absent, was noticed. Similar chemical shift variations have also been observed for ^{77}Se (δ_{Se}) in the same series of compounds. The magnitude of chemical shift is found to be dependent on the nature of substituent attached to the selenium atom, opening up a useful way to quantify intramolecular nonbonding interactions. In another report, Bayse has elegantly established the correlation between the theoretically predicted chemical shifts with that obtained experimentally in a series of simple organoselenium compounds. In particular, the chemical shift values (δ_{Se}) calculated at the MP2/GIAO level using double as well as triple ζ -quality basis sets with added polarization and diffuse functions were found to give improved estimates. Further, the difference between the computed and experimental chemical shift values obtained from biochemical studies was found to be only within about 15–30 ppm. It is proposed that accurate prediction of chemical shift will facilitate studies on selenoproteins and their mimics by helping to assign unknown resonances as well as through detection of intramolecular interactions.²⁸⁷ In general, the MP2 method in conjunction with triple- ζ or higher quality basis sets exhibited superior performance as compared to other DFT methods, such as the B3LYP, B3P86, and mPW1PW91, for small organoselenium compounds. In systems involving (3c,4e) bonding, diffuse functions are recommended toward improving the predicted chemical shift values.²⁸⁸ The most interesting point pertaining to the present discussion is the changes in the chemical shift upon variations in the immediate coordination environment around the selenium nuclei. Such chemical shift variations could be used as an effective

Table 8. Nonbonding Interaction Energies (in kcal/mol) Calculated Using the Homodesmotic Reaction and *Ortho-Para* Method^a

mol.	type of interaction	homodesmotic reaction			<i>ortho-para</i> method		
		CCSD(T)	MP2	KMLYP	CCSD(T)	MP2	KMLYP
134a	O⋯Se–Cl	5.1	5.9	6.8	6.9	7.5	8.5
134c	O⋯Se–CN	2.8	3.2	3.5	2.8	2.7	5.4
134f	O⋯Se–Me	0.2	0.5	0.8	0.1	0.4	0.1

^a Interaction energy values are adopted from ref 284.

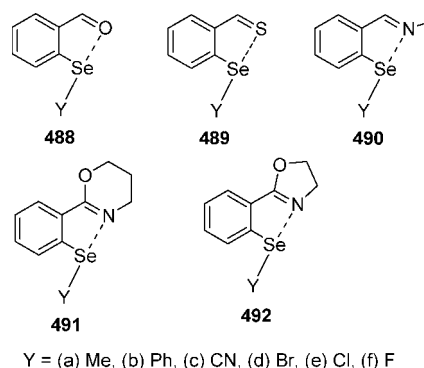
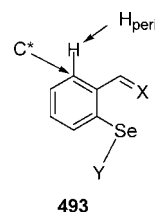
indicator for the existence of intramolecular interaction in organochalcogens.

As described in the earlier sections, nonbonding interactions in organochalcogens are unequivocally established with the help of structural elucidation in conjunction with theoretical support. The preliminary indicator for the existence of nonbonding interaction is based on the distance criteria that the interaction distance should be less than the sum of van der Waals radii of the interacting atoms. While simple distance-based criteria along with the efficiency of delocalization using the NBO formalism continue to help gain semiquantitative estimates on the strength of interaction, explicit quantification of the strength intramolecular interactions in organochalcogens is not widely reported. In a very recent study, Roy et al. have proposed schemes based on computed thermochemical values toward quantification of intramolecular interactions.^{273,284} Ab initio and density functional theory was employed to estimate the energies of suitably designed homodesmotic reactions. Alternatively, in the *ortho-para* method, the energy differences between *ortho* and *para* isomers, in which the nonbonding interactions are, respectively, turned on and turned off, were taken as a measure of the strength of stabilizing nonbonding interaction. A representative group of compounds and their quantified interaction energies are provided in Table 8. Both homodesmotic and *ortho-para* methods were reported to be mutually consistent in terms of the quantified intramolecular interaction energies.²⁸⁴ The data evidently supported that the strength of nonbonding interaction is dependent on the nature of the acceptor bond as well as the donor atom.

Furthermore, the intramolecular nonbonding interaction energy (E_{NB}) in organoselenium compounds has been quantified using the nucleus-independent chemical shift (NICS(0)) and chemical shifts at C* and H_{peri} as property descriptors at DFT as well as ab initio levels (Chart 64).²⁸⁹ These values are compared with the values obtained by thermochemical methods such as homodesmotic reactions and *ortho-para* method. NICS is a quantitative measure of the ring current in individual rings in a polycyclic system. Isotropic NICS(0) values are influenced by their immediate electronic environment (σ as well as π).

Thus, the differences in electronic energies between the two isomeric disubstituted benzenes can be taken to be linearly proportional to the differences in their NICS(0) values. NICS(0) at the center of the aromatic ring as a property descriptor is expected to show subtle changes depending on (i) the variations in the substitution patterns, (ii) the presence or absence of nonbonding interactions, and (iii) the strength of nonbonding interactions.

The methyl and phenyls are weak acceptors (**488–492a** and **492b**), evidently due to lower accepting ability of a less polarized bond. The highest nonbonding interaction is found to be with the Se–F bond as the acceptor (species **488–492f**). In between, in general, are the cyano, bromo, and chloro species (**488–492b**, **492d**, and **492e**). This interaction order roughly corresponds to the electronegativity

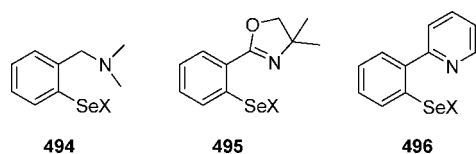
Chart 63**Chart 64**

ties of the affixed groups (Y) and to the generally understood stability of hypervalent species. The extent of nonbonding interaction evidently depends on the atom/group attached to the selenium (Y) as well as the nature of the donor atom (N, O, and S). When Y is an alkyl group, the interaction is found to be the weakest among the present series of compounds. The E_{NB} shows a gradual increase when the acceptor group is changed from Se–Cl to Se–F, consistent with the increased polarity of the Se–Cl/F bonds. The computed E_{NB} values reveal that N(sp²) is a better donor than O(sp²). This can be rationalized by considering the higher electronegativity and difficulty of ionization of the latter, leading to a larger energy difference between the lone pair bearing orbital on O and the antibonding Se–Y orbital.

The correlations between the changes in chemical shift values for C* as well as H_{peri} atoms and the computed strength of nonbonding interactions are found to be very good and comparable with the NICS(0) approach. More interesting correlations are also identified between the E_{NB} values calculated using the property descriptor (C* chemical shifts) and the corresponding values evaluated from homodesmotic reaction approach and *ortho-para* methods.

Sarma and Mughes have evaluated the effect of different donor nitrogen atoms on the strength and nature of intramolecular Se⋯N interaction by the quantum chemical calculations on three series of compounds 2-(dime)C₆H₄SeX (**494**, containing sp³ hybridized N), 2-(oxa)C₆H₄SeX (**495**, containing sp² hybridized N of nonaromatic ring), 2-(py)C₆H₄SeX (**496**, containing sp² hybridized N of aromatic ring); X = Cl, Br, OH, CN, SPh, SePh, CH₃ at B3LYP/6-31G(d) level.²⁹⁰ Natural bond orbital (NBO), NBO deletion, and atoms in molecules (AIM) analyses suggest that the nature

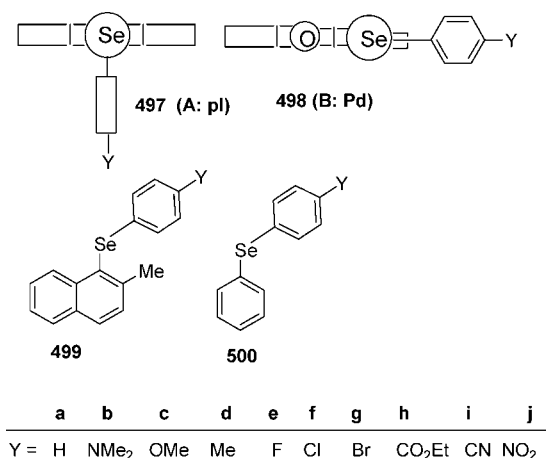
Chart 65



of $\text{Se}\cdots\text{N}$ interaction is predominantly covalent and involves $n_{\text{N}} \rightarrow \sigma^*_{\text{Se-X}}$ orbital interaction. In the three series of compounds, the strength of $\text{Se}\cdots\text{N}$ interaction decreases in the order **496** > **495** > **494** for a particular X and it decreases in the order $\text{Cl} > \text{Br} > \text{OH} > \text{SPh} \approx \text{CN} \approx \text{SePh} > \text{CH}_3$ for all three series (**494**–**496**). However, further analyses suggest that the differences in strength of $\text{Se}\cdots\text{N}$ interaction in **494**–**496** are predominantly determined by the distance between the Se and the N atom, which in turn is an outcome of specific structures of **494**, **495**, and **496**, and the nature of the donor nitrogen atoms involved has very little effect on the strength of $\text{Se}\cdots\text{N}$ interaction. It is also observed that $\text{Se}\cdots\text{N}$ interaction becomes stronger in polar solvent such as CHCl_3 as indicated by the shorter $r_{\text{Se}\cdots\text{N}}$ and higher $E_{\text{Se}\cdots\text{N}}$ values in CHCl_3 when compared to that observed in the gas phase. The strength of $\text{Se}\cdots\text{N}$ interaction in organoselenium compounds (RSeX) increases with an increase in the electrophilicity of selenium. The $\text{Se}\cdots\text{N}$ interactions are strong when $\text{X} = \text{Cl}$, Br , and OH ; intermediate for $\text{X} = \text{SPh}$, SePh , and CN ; and weak for $\text{X} = \text{Me}$. A detailed theoretical analysis of the interactions indicates that both electrostatic and covalent contributions are important for the stabilization. The contribution of electrostatic and covalent character depends not only on the substituent attached to the selenium atom but also on the distance of donor nitrogen atom from the selenium center. It should be noted that both electrostatic character and covalent character of $\text{Se}\cdots\text{N}$ interaction are somehow interconnected in a way that the strong electrostatic attraction favors the donation of electron density from the lone pair of nitrogen (n_{N}) to the antibonding orbitals of Se-X bond ($\sigma^*_{\text{Se-X}}$). The relatively strong $\text{Se}\cdots\text{N}$ interactions in compounds **496** may be ascribed to the planar pyridine ring, which brings the Se and the N atoms close together and favors an efficient orbital overlap between the lone pair on nitrogen (n_{N}) and the antibonding orbital of Se-X bond ($\sigma^*_{\text{Se-X}}$). This is reflected in the relatively high values of $E_{\text{Se}\cdots\text{N}}$, E_{del} , and χ for **496** as compared to those of **494** and **495**. When $r_{\text{Se}\cdots\text{N}}$ was kept constant, the slightly higher values of $E_{\text{Se}\cdots\text{N}}$ for **496** compared to **494** and **495** can be ascribed to the lower basicity of the pyridine group, which increases the donor ability of the pyridyl nitrogen atom. Furthermore, the negative values of local energy density ($H_{\text{Se}\cdots\text{N}}$) obtained for $\text{Se}\cdots\text{N}$ interaction by AIM analysis and the AIM dual-parameter analysis also suggest a dominant covalent character of the interaction. The plots of $E_{\text{Se}\cdots\text{N}}$, E_{del} , χ , and $H_{\text{Se}\cdots\text{N}}$ with the $\text{Se}\cdots\text{N}$ atomic distances ($r_{\text{Se}\cdots\text{N}}$) represent a single correlation curve irrespective of the nature of coordinating nitrogen atom.

The importance of the orientational effect on $\delta(\text{Se})$ of $p\text{-YC}_6\text{H}_4\text{SeR}$ (ArSeR), for the better structural analysis in solutions based on the chemical shifts, is discussed.²⁹¹ Two sets of $\delta(\text{H})$ and $\delta(\text{C})$ are proposed for each based on 9-(arylselanyl)anthracenes [9-($p\text{-YC}_6\text{H}_4\text{Se}$)Atc] **123** and 1-(arylselanyl)anthraquinones [1-($p\text{-YC}_6\text{H}_4\text{Se}$)Atq] **124**, where $\text{Y} = \text{H}$ (**a**), NMe_2 (**b**), OMe (**c**), Me (**d**), F (**e**), Cl (**f**), Br (**g**), COOEt (**h**), CN (**i**), and NO_2 (**j**), to analyze the structures

Scheme 103



of $p\text{-YC}_6\text{H}_4\text{SeR}$ (ArSeR) in solutions based on $\delta(\text{H})$ and $\delta(\text{C})$, together with $\delta(\text{Se})$. The structures of **123** and **124** are (**497 A: pl**) and (**498 B: pd**), respectively, for all Y examined in chloroform-*d* solutions. $\delta(\text{H: 497})$ and $\delta(\text{C: 497})$ are typical for (**A: pl**), and $\delta(\text{H: 498})$ and $\delta(\text{C: 498})$ are characteristic for (**B: pd**). Structures are analyzed for **162** [1-($p\text{-YC}_6\text{H}_4\text{Se}$)Nap], **499** [1-($p\text{-YC}_6\text{H}_4\text{Se}$)NapMe-2], and **161** [1-($p\text{-YC}_6\text{H}_4\text{Se}$)NapBr-8] in the chloroform-*d* solutions, by employing $\delta(\text{H, C: 497})$ and $\delta(\text{H, C: 498})$, after the elucidation of the behavior of $\delta(\text{H, C: 497})$ and $\delta(\text{H, C: 498})$. Although the structure of **499** remains in (**A: pl**) in the solutions, for all Y examined, that of **161** is (**B: pd**) in the solutions, except for Y (**i**) and (**j**) (Scheme 103). Although **161j** and **161i** are substantially in equilibrium between (**B: pd**) and (**A: pl**) in the solutions, **161h** exists almost predominantly in (**B: pd**). Very similar results are obtained for 1-(arylselanyl)-8-chloronaphthalenes. The energy-lowering effect of the $n_{\text{p}}(\text{X})-\delta^*(\text{Se-C})$ 3c-4e ($\text{X} = \text{Br}$ in **161**) seems not to be large enough to keep the structure (**B: pd**) for Y (**i**) and (**j**), whereas the $n_{\text{p}}(\text{O})-\delta^*(\text{Se-C})$ 3c-4e in **162** is strong enough for all Y examined. In the case of **499**, the structure is demonstrated to equilibrate between (**A: pl**) and (**B: pd**), and the equilibrium constants change from Y to Y in the solutions. Meanwhile, the contributions of (**B: pd**) and (**A: pl**) are shown to be predominant for **499b** and **499j**, respectively, based on the QC calculations containing the solvent effect of chloroform. $\delta(\text{H, C: 497})$ and $\delta(\text{H, C: 498})$, as well as $\delta(\text{Se})$, are demonstrated to be powerful tools as the standards to analyze the structures of $p\text{-YC}_6\text{H}_4\text{SeR}$ in solutions, if they are applied carefully.

Nuclear spin–spin coupling constants (J) provide highly important information about coupled nuclei that have strongly bonded and weakly interacting states. Values of $^nJ(\text{Se,Se})$ (number of bonds $n = 1-4$,) were analyzed as the first step to investigating the nature of bonded and nonbonded interactions between Se atoms through $^nJ(\text{Se,Se})$.²⁹² QC calculations were used for the analysis and interpretation of the J values obtained experimentally. $^nJ(\text{Se,Se})$ ($n = 1-4$) were analyzed by using MO theory. $^1J(\text{Se,Se})$ was calculated for the MeSeSeMe model compound, which showed a typical dependence on the torsion angle ($\phi(\text{CMeSeSeCMe})$). This dependence explains the small values (≤ 64 Hz) of $^1J_{\text{obsd}}(\text{Se,Se})$ observed for RSeSeR' and large values (330–380 Hz) of $^1J_{\text{obsd}}(\text{Se,Se})$ observed for 4-substituted naphtho[1,8-*c,d*]-1,2-diselenoles, which correspond to synperiplanar diselenides. The $\text{HOMO} \rightarrow \text{LUMO}$ and $\text{HOMO-1} \rightarrow \text{LUMO}$ transitions contribute the most to

$^1J_{\text{obsd}}(\text{Se}, \text{Se})$ at $\phi = 0$ and 180° to give large values of $^1J_{\text{obsd}}(\text{Se}, \text{Se})$, whereas various transitions contribute and cancel each other out at $\phi = 90^\circ$ to give small values of $^1J_{\text{obsd}}(\text{Se}, \text{Se})$. Large $^4J_{\text{obsd}}(\text{Se}, \text{Se})$ values were also observed in the nonbonded $\text{Se} \cdots \text{Se}$, $\text{Se} \cdots \text{Se}=\text{O}$, and $\text{O}=\text{Se} \cdots \text{Se}=\text{O}$ interactions at naphthalene 1,8-positions. The Fermi contact (FC) term contributes significantly to $^4J_{\text{obsd}}(\text{Se}, \text{Se})$, whereas the paramagnetic spin-orbit (PSO) term contributes significantly to $^1J_{\text{obsd}}(\text{Se}, \text{Se})$; $^2J_{\text{obsd}}(\text{Se}, \text{Se})$ and $^3J_{\text{obsd}}(\text{Se}, \text{Se})$ were analyzed in a similar manner; and a torsional angular dependence was confirmed for $^3J_{\text{obsd}}(\text{Se}, \text{Se})$. Depending on the structure, the main contribution to $^nJ_{\text{obsd}}(\text{Se}, \text{Se})$ ($n = 2, 3$) is from the FC term, with a lesser contribution from the PSO term. Analysis of each transition was done to visualize the origin and mechanism of the coupling.

Thus far, we have been able to summarize a number of modern tools, based on electronic structure calculations, in identifying nonbonding interactions in organochalcogens. The distinction between genuine nonbonding interactions and a relatively shorter atomic contacts arising due to packing effects needs to be clearly delineated. These could be achieved with the help of analyzing the molecular wave function besides experimental verification using X-ray crystallography and NMR methods. Recent literature on nonbonding interactions in organochalcogens conspicuously brings out the synergism between theory and experiment in understanding the interactions at the molecular level.

7. Summary

In this review, we have attempted to present the recent developments in the field of organoselenium chemistry with the major emphasis on the hypervalent nature of selenium. There are many known organoselenium compounds containing intramolecular selenium \cdots heteroatom interactions, and it is these interactions that define the stability and molecular conformation of the compounds. Many of the compounds have been analyzed using ^1H , ^{13}C , and ^{77}Se NMR and IR spectroscopy, mass spectrometry, molecular orbital analysis, natural bond orbital methods, atoms in molecule analyses, and X-ray diffraction studies. The results of these investigations have been presented as well as the application of this type of compound in the fields of ligand chemistry, organic synthesis, and biochemistry. It is hoped that this work will contribute to a greater understanding of the subject of hypervalency in organoselenium compounds and generate interest across the organoselenium community, stimulating further work in this area.

8. Acknowledgments

We are grateful to the Department of Science and Technology (DST), New Delhi, for the award of Ramanna Fellowship to H.B.S. R.B.S. acknowledges Dipankar Roy for his enthusiastic participation and contributions in preparing this manuscript.

9. References

- (1) Löwig, C. J. *Poggendorff's Ann. Phys.* **1836**, 37, 552.
- (2) Rathke, B. *Ann. Chem.* **1869**, 152, 211.
- (3) (a) Chivers, T. *A Guide to Chalcogen-Nitrogen Chemistry*; World Scientific Publishing: Singapore, 2005. (b) *Handbook of Chalcogen Chemistry*; Devillanova, F. A., Ed.; RSC Publishing: Cambridge, U.K., 2007. (c) Zeni, G.; Lüdtkke, D. S.; Panatieri, R. B.; Braga, A. L. *Chem. Rev.* **2006**, 106, 1032.

- (4) (a) Paulmier, C. *Selenium Reagents and Intermediates in Organic Synthesis*; Baldwin, J. E., Ed.; Pergamon Press: Oxford, U.K., 1986. (b) *Organoselenium Chemistry*; Liotta, D., Ed.; Wiley: New York, 1987. (c) *The Chemistry of Organic Selenium and Tellurium Compounds*; Patai, S.; Rappoport, Z., Eds.; Wiley: New York, 1986, Vol. 1; 1987, Vol. 2. (d) Krief, A.; Hevesi, L. *Organoselenium Chemistry*; Springer: Berlin, 1998. (e) *Organoselenium Chemistry—A Practical Approach*; Back, T. G., Ed.; Oxford University Press: Oxford, U.K., 1999. (f) *Organoselenium Chemistry—Modern Development in Organic Synthesis*. In *Topics in Current Chemistry*; Wirth, T., Ed. Springer-Verlag: Berlin, 2000; Vol. 208. (g) Wirth, T. *Tetrahedron* **1999**, 55, 1. (h) Wirth, T. *Angew. Chem., Int. Ed.* **2000**, 39, 3740. (i) Freudendahl, D. M.; Shahzad, S. A.; Wirth, T. *Eur. J. Org. Chem.* **2009**, 1649. (j) Freudendahl, D. M.; Santoro, S.; Shahzad, S. A.; Santi, C.; Wirth, T. *Angew. Chem., Int. Ed.* **2009**, 48, 8409.
- (5) (a) *Organic Selenium Compounds: Their Chemistry and Biology*; Klayman, D. L.; Günther, W. H. H., Eds.; Wiley Interscience: New York, 1973. (b) Shamberger, R. J. In *Biochemistry of Selenium*; EDS Plenum Press: New York, 1983. (c) Nicolaou, K. C.; Petasis, N. A. In *Selenium in Natural Product Synthesis*; CIS: Philadelphia, PA, 1984. (d) Mughesh, G.; du Mont, W.-W.; Sies, H. *Chem. Rev.* **2001**, 101, 2125. (e) Chasteen, T. G.; Bentley, R. *Chem. Rev.* **2003**, 103, 1. (f) Nogueira, C. W.; Zeni, G.; Rocha, J. B. T. *Chem. Rev.* **2004**, 104, 6255. (g) Zeni, G.; Lüdtkke, D. S.; Panatieri, R. B.; Braga, A. L. *Chem. Rev.* **2006**, 106, 1032.
- (6) Berger, S. B. *Phosphorus Sulfur* **1988**, 38, 375.
- (7) Bryce, M. R. *Chem. Soc. Rev.* **1991**, 20, 355.
- (8) (a) Kanatzidis, M. G.; Huang, S. *Coord. Chem. Rev.* **1994**, 130, 509. (b) Hitchman, M. L.; Jenson, K. F. *Chemical Vapour Deposition: Principles and Applications*; Academic Press: London, 1993; p 677. (c) Stringfellow, G. B. *Organometallic Vapour Phase Epitaxy: Theory and Practice*; Academic Press: New York, 1989.
- (9) (a) Gysling, H. In *The Chemistry of Organic Selenium and Tellurium Compounds*; Patai, S.; Rappoport, Z., Eds.; John Wiley & Sons: New York, 1986; Vol. 1, p 221. (b) Gysling, H. J. *Coord. Chem. Rev.* **1982**, 42, 133. (c) Hope, E. G.; Levason, W. *Coord. Chem. Rev.* **1993**, 122, 109. (d) Levason, W.; Orchard, S. D.; Reid, G. *Coord. Chem. Rev.* **2002**, 225, 159. (e) Levason, W.; Reid, G. In *Handbook of Chalcogen Chemistry*; Devillanova, F. A., Ed.; RSC Publishing: Cambridge, U.K., 2007; p 81. (f) Panda, A. *Coord. Chem. Rev.* **2009**, 253, 1056. (g) Panda, A. *Coord. Chem. Rev.* **2009**, doi:10.1016/j.ccr.2009.03.025. (h) Singh, A. K.; Sharma, S. *Coord. Chem. Rev.* **2000**, 209, 49. (i) Arnold, J. *Prog. Inorg. Chem.* **1995**, 43, 353. (j) Englich, U.; Ruhlandt-Senge, K. *Coord. Chem. Rev.* **2000**, 210, 135.
- (10) (a) Coles, M. P. *Curr. Org. Chem.* **2006**, 10, 1993. (b) Iwaoka, M.; Tomoda, S. *Yuki Gosei Kagaku Kyokaiishi* **2005**, 63, 911–920.
- (11) (a) Vargas-Baca, I.; Chivers, T. *Phosphorus, Sulfur Silicon Relat. Elem.* **2000**, 164, 207. (b) Mughesh, G.; Singh, H. B. *Acc. Chem. Res.* **2002**, 35, 226. (c) Alcock, N. W. *Adv. Inorg. Chem. Radiochem.* **1972**, 15, 1. (d) Landrum, G. A.; Hoffmann, R. *Angew. Chem., Int. Ed.* **1998**, 37, 1887.
- (12) Iwaoka, M.; Tomoda, S. *J. Am. Chem. Soc.* **1996**, 118, 8077.
- (13) Sudha, N.; Singh, H. B. *Coord. Chem. Rev.* **1994**, 135/136, 469.
- (14) McWhinnie, W. R.; Sadekov, I. D.; Minkin, V. I. *Sulfur Rep.* **1996**, 18, 295.
- (15) Christaens, L.; Luxen, A.; Evers, M.; Thibault, Ph.; Mbuyi, M. *Chem. Scr.* **1984**, 24, 178.
- (16) Mbogo, S. A.; McWhinnie, W. R.; Lobana, T. S.; Tiekink, E. R. T. *J. Organomet. Chem.* **1990**, 388, 273.
- (17) Al-Salim, N.; West, A. A.; McWhinnie, W. R.; Hamor, T. A. *J. Chem. Soc., Dalton Trans.* **1988**, 2363.
- (18) Pauling, L. *The Nature of the Chemical Bond*, 3rd ed.; Cornell University Press: Ithaca, NY, 1960.
- (19) Iwaoka, M.; Tomoda, S. *Phosphorus, Sulfur Silicon Relat. Elem.* **1992**, 67, 125.
- (20) Ramasubbu, N.; Parthasarathy, R. *Phosphorus Sulfur* **1987**, 31, 221.
- (21) Iwaoka, M.; Tomoda, S. *J. Org. Chem.* **1995**, 60, 5299.
- (22) Iwaoka, M.; Tomoda, S. *J. Chem. Soc., Chem. Commun.* **1992**, 1165.
- (23) Kaur, R.; Singh, H. B.; Patel, R. P. *J. Chem. Soc., Dalton Trans.* **1996**, 2719.
- (24) Luthra, N. P.; Odom, J. D. In *The Chemistry of Organic Selenium and Tellurium Compounds*; Patai, S.; Rappoport, Z., Eds.; Wiley: New York, 1986; Vol. 1, p 189.
- (25) Kulcsar, M.; Silvestru, A.; Silvestru, C.; Drake, J. E.; Macdonald, C. L. B.; Hursthouse, M. B.; Light, M. E. *J. Organomet. Chem.* **2005**, 690, 3217.
- (26) (a) Kaur, R.; Menon, S. C.; Panda, S.; Singh, H. B.; Patel, R. P.; Butcher, R. J. *Organometallics* **2009**, 28, 2363. (b) Kaur, R.; Singh, H. B.; Patel, R. P.; Kulshreshtha, S. K. *J. Chem. Soc., Dalton Trans.* **1996**, 461.
- (27) Shimizu, T.; Enomoto, M.; Taka, H.; Kamigata, N. *J. Org. Chem.* **1999**, 64, 8242.

- (28) Klapötke, T. M.; Krumm, B.; Polborn, K. *J. Am. Chem. Soc.* **2004**, *126*, 710.
- (29) (a) Ostrowski, M.; Wagner, I.; du Mont, W.-W.; Jones, P. G.; Jeske, J. Z. *Anorg. Allg. Chem.* **1993**, *619*, 1693. (b) Klapötke, T. M.; Krumm, B.; Polborn, K. *Eur. J. Inorg. Chem.* **1999**, 1359. (c) Klapötke, T. M.; Krumm, B.; Mayer, P.; Piotrowski, H.; Vogt, M. *Z. Anorg. Allg. Chem.* **2003**, *629*, 1117.
- (30) Klapötke, T. M.; Krumm, B.; Scherr, M. *Inorg. Chem.* **2008**, *47*, 4712.
- (31) Panda, A.; Mughesh, G.; Singh, H. B.; Butcher, R. J. *Organometallics* **1999**, *18*, 1986.
- (32) Fujihara, H.; Tanaka, H.; Furukawa, N. *J. Chem. Soc., Perkin Trans. 1* **1995**, 2375.
- (33) Mughesh, G.; Panda, A.; Singh, H. B.; Butcher, R. J. *Chem.—Eur. J.* **1999**, *5*, 1411.
- (34) Mughesh, G.; Singh, H. B.; Butcher, R. J. *Tetrahedron: Asymmetry* **1999**, *10*, 237.
- (35) Roy, G.; Nethaji, M.; Mughesh, G. *J. Am. Chem. Soc.* **2004**, *126*, 2712.
- (36) Kumar, S.; Kandasamy, K.; Singh, H. B.; Butcher, R. J. *New J. Chem.* **2004**, *28*, 640.
- (37) Kumar, S.; Panda, S.; Singh, H. B.; Wolmershäuser, G.; Butcher, R. J. *Struct. Chem.* **2007**, *18*, 127.
- (38) Kandasamy, K.; Kumar, S.; Singh, H. B.; Butcher, R. J.; Holman, K. T. *Eur. J. Inorg. Chem.* **2004**, 1014.
- (39) Kumar, S.; Kandasamy, K.; Singh, H. B.; Wolmershäuser, G.; Butcher, R. J. *Organometallics* **2004**, *23*, 4199.
- (40) Ishii, A.; Matsubayashi, S.; Takahashi, T.; Nakayama, J. *J. Org. Chem.* **1999**, *64*, 1084.
- (41) Sladky, F.; Bildstein, B.; Rieker, C.; Gieren, A.; Betz, H.; Hübner, T. *J. Chem. Soc., Chem. Commun.* **1985**, *24*, 1800.
- (42) Goto, K.; Naga-hama, M.; Mizushima, T.; Shimada, K.; Kawashima, T.; Okazaki, R. *Org. Lett.* **2001**, *3*, 3569.
- (43) Jones, P. G.; Ramirez de Arellano, M. C. *Chem. Ber.* **1995**, *128*, 741.
- (44) Panda, S.; Zade, S. S.; Singh, H. B.; Wolmershäuser, G. *J. Organomet. Chem.* **2005**, *690*, 3142.
- (45) Kulcsar, M.; Beleaga, A.; Silvestru, C.; Nicolescu, A.; Deleanu, C.; Todasca, C.; Silvestru, A. *Dalton Trans.* **2007**, 2187.
- (46) Beleaga, A.; Kulcsar, M.; Deleanu, C.; Nicolescu, A.; Silvestru, C.; Silvestru, A. *J. Organomet. Chem.* **2009**, *694*, 1308.
- (47) (a) Uneyama, K.; Kanai, M. *Tetrahedron Lett.* **1990**, *31*, 3583. (b) Uneyama, K.; Hiraoka, S.; Amii, H. *J. Fluorine Chem.* **2000**, *102*, 215. (c) Lermontov, S. A.; Zavorin, S. I.; Pushin, A. N.; Chekhlov, A. N.; Zefirov, N. S.; Stang, P. J. *Tetrahedron Lett.* **1993**, *34*, 703. (d) Chekhlov, A. N.; Lermontov, S. A.; Zavorin, S. I.; Zefirov, N. S. *Dokl. Akad. Nauk* **1993**, *332*, 198. (e) Laali, K. K.; Fiedler, W.; Regitz, M. *Chem. Commun.* **1997**, 1641. (f) Poleschner, H.; Heydenreich, M.; Spindler, K.; Haufe, G. *Synthesis* **1994**, 1043. (g) Poleschner, H.; Heydenreich, M.; Schilde, U. *Liebigs Ann.* **1996**, 1187. (h) Poleschner, H.; Schilde, U. *Acta Crystallogr., Sect. C* **1996**, *52*, 644.
- (48) (a) Uneyama, K.; Asai, H.; Dan-oh, Y.; Matta, H. *Electrochim. Acta* **1997**, *42*, 2005. (b) Uneyama, K.; Asai, H.; Dan-oh, Y.; Funatsuki, H. *Phosphorus, Sulfur Silicon Relat. Elem.* **1997**, *120–121*, 395.
- (49) Poleschner, H.; Heydenreich, M.; Schilde, U. *Eur. J. Inorg. Chem.* **2000**, 1307.
- (50) Poleschner, H.; Seppelt, K. *J. Chem. Soc., Perkin Trans. 1* **2002**, 2668.
- (51) (a) Tomoda, S.; Usuki, Y. *Chem. Lett.* **1989**, 1235. (b) Usuki, Y.; Iwaoka, M.; Tomoda, S. *Chem. Lett.* **1992**, 1507.
- (52) McCarthy, J. R.; Matthews, D. P.; Barney, C. L. *Tetrahedron Lett.* **1990**, *31*, 973.
- (53) Nicolaou, K. C.; Petasis, N. A.; Claremon, D. A. *Tetrahedron* **1985**, *41*, 4835.
- (54) (a) Saluzzo, C.; Alvernhe, G.; Anker, D.; Haufe, G. *Tetrahedron Lett.* **1990**, *31*, 663. (b) Saluzzo, C.; Alvernhe, G.; Anker, D.; Haufe, G. *Tetrahedron Lett.* **1990**, *31*, 2127. (c) Saluzzo, C.; La Spina, A.-M.; Picq, D.; Alvernhe, G.; Anker, D.; Wolf, D.; Haufe, G. *Bull. Soc. Chim. Fr.* **1994**, *131*, 831.
- (55) Poleschner, H.; Seppelt, K. *Chem.—Eur. J.* **2004**, *10*, 6565.
- (56) Back, T. G.; Moussa, Z.; Parvez, M. *Phosphorus, Sulfur Silicon Relat. Elem.* **2004**, *179*, 2569.
- (57) Gushwa, A. F.; Richards, A. F. *Eur. J. Inorg. Chem.* **2008**, 728. (b) Gushwa, A. F.; Karlin, J. G.; Fleischer, R.; Richards, A. F. *J. Organomet. Chem.* **2006**, *691*, 5069. (c) Gushwa, A. F.; Karlin, J. G.; Fleischer, R.; Richards, A. F. *J. Organomet. Chem.* **2007**, *692*, 1173.
- (58) Mima, H.; Fujihara, H.; Furukawa, N. *Tetrahedron* **1998**, *54*, 743.
- (59) Fujihara, H.; Mima, H.; Ikemori, M.; Furukawa, N. *J. Am. Chem. Soc.* **1991**, *113*, 6337.
- (60) Akiba, K.; Takee, K.; Ohkata, K.; Iwasaki, F. *J. Am. Chem. Soc.* **1983**, *105*, 6965.
- (61) Fujihara, H.; Mima, H.; Erata, T.; Furukawa, N. *J. Chem. Soc., Chem. Commun.* **1991**, 98.
- (62) Fujihara, H.; Mima, H.; Erata, T.; Furukawa, N. *J. Am. Chem. Soc.* **1993**, *115*, 9826.
- (63) Fujihara, H.; Mima, H.; Furukawa, N. *J. Am. Chem. Soc.* **1995**, *117*, 10153.
- (64) Baiwir, M.; Llabrès, G.; Dideberg, O.; Dupont, L.; Piette, J. L. *Acta Crystallogr.* **1975**, *B31*, 2188.
- (65) Atkinson, A.; Brewster, A. G.; Ley, S. V.; Osborn, R. S.; Rogers, D.; Williams, D. J.; Woode, K. A. *J. Chem. Soc., Chem. Commun.* **1977**, 325.
- (66) Close, R.; Cagniant, D.; Le Coustumer, G.; Andrieu, C.; Mollier, Y. *J. Chem. Res.* **1978**, 4.
- (67) Roesky, R. W.; Weber, K. L.; Seseke, U.; Pinkert, W.; Noltemeyer, M.; Clegg, W.; Sheldrick, G. M. *J. Chem. Soc., Dalton Trans.* **1985**, 565.
- (68) Tomoda, S.; Iwaoka, M. *J. Chem. Soc., Chem. Commun.* **1990**, 231.
- (69) Goldstein, B. M.; Kennedy, S. D.; Hennen, W. J. *J. Am. Chem. Soc.* **1990**, *112*, 8265.
- (70) Burling, F. T.; Goldstein, B. M. *J. Am. Chem. Soc.* **1992**, *114*, 2313.
- (71) Barton, D. H. R.; Hall, M. B.; Lin, Z.; Perekh, S. I.; Riebenspies, J. *J. Am. Chem. Soc.* **1993**, *115*, 5056.
- (72) Panda, A.; Menon, S. C.; Singh, H. B.; Butcher, R. J. *J. Organomet. Chem.* **2001**, *623*, 87.
- (73) Bourland, T. C.; Carter, R. G.; Yokochi, A. F. T. *Org. Biomol. Chem.* **2004**, *2*, 1315.
- (74) (a) Parnham, M. J.; Biederman, J.; Bittner, C.; Dereu, N.; Leyck, S.; Wetzig, H. *Agents Actions* **1989**, *27*, 306. (b) Peng, Y. S.; Xu, H. S.; Naumov, P.; Raj, S. S. S.; Fun, H.-K.; Razak, I. A.; Ng, S. W. *Acta Crystallogr., Sect. C* **2000**, *56*, 1386.
- (75) Dupont, L.; Dideberg, O.; Sbit, M.; Dereu, N. *Acta Crystallogr., Sect. C* **1988**, *44*, 2159.
- (76) (a) Kersting, B.; DeLion, M. Z. *Naturforsch., B* **1999**, *54*, 1042. (b) Kersting, B. Z. *Naturforsch., B* **2002**, *57*, 1115.
- (77) Zade, S. S.; Panda, S.; Tripathi, S. K.; Singh, H. B.; Wolmershäuser, G. *Eur. J. Org. Chem.* **2004**, 3857.
- (78) Nakanishi, W.; Hayashi, S.; Itoh, N. *Chem. Commun.* **2003**, 124.
- (79) Nakanishi, W.; Hayashi, S.; Shimizu, D.; Hada, M. *Chem.—Eur. J.* **2006**, *12*, 3829.
- (80) Nakamoto, T.; Hayashi, S.; Nakanishi, W. *J. Org. Chem.* **2008**, *73*, 9259.
- (81) Fujihara, H.; Nakahodo, T.; Furukawa, N. *Chem. Commun.* **1996**, 311.
- (82) (a) Behaghel, O.; Müller, W. *Ber. Dtsch. Chem. Ges.* **1935**, *68*, 1540. (b) Rheinboldt, H.; Giesbrecht, E. *Chem. Ber.* **1955**, *88*, 1037. (c) Rheinboldt, H.; Giesbrecht, E. *Chem. Ber.* **1955**, *88*, 1974.
- (83) (a) Behaghel, O.; Müller, W. *Ber. Dtsch. Chem. Ges.* **1934**, *67*, 105. (b) Jenny, W. *Helv. Chim. Acta* **1958**, *41*, 317. (c) Rheinboldt, H.; Giesbrecht, E. *Chem. Ber.* **1956**, *89*, 631. (d) Reich, H. J.; Hoeger, C. A.; Willis, W. W., Jr. *J. Am. Chem. Soc.* **1982**, *104*, 2936.
- (84) Iwaoka, M.; Tomoda, S. *J. Am. Chem. Soc.* **1994**, *116*, 2557.
- (85) Reich, H. J.; Willis, W. W., Jr.; Wollowitz, S. *Tetrahedron Lett.* **1982**, *23*, 3319.
- (86) Saiki, T.; Goto, K.; Okazaki, R. *Angew. Chem., Int. Ed.* **1997**, *36*, 2223.
- (87) Bondi, A. J. *Phys. Chem.* **1964**, *68*, 441.
- (88) Sureshkumar, D.; Ganesh, V.; Chandrasekaran, S. *J. Org. Chem.* **2007**, *72*, 5313.
- (89) Fragale, G.; Neuberger, M.; Wirth, T. *J. Chem. Soc., Chem. Commun.* **1998**, 1867.
- (90) Wirth, T.; Fragale, G.; Spichty, M. *J. Am. Chem. Soc.* **1998**, *120*, 3376.
- (91) (a) Komatsu, H.; Iwaoka, M.; Tomoda, S. *J. Chem. Soc., Chem. Commun.* **1999**, 205. (b) Iwaoka, M.; Komatsu, H.; Katsuda, T.; Tomoda, S. *J. Am. Chem. Soc.* **2004**, *126*, 5309.
- (92) Tripathi, S. K.; Patel, U.; Roy, D.; Sunoj, R. B.; Singh, H. B.; Wolmershäuser, G.; Butcher, R. J. *J. Org. Chem.* **2005**, *70*, 9237.
- (93) Zade, S. S.; Singh, H. B.; Butcher, R. J. *Angew. Chem., Int. Ed.* **2004**, *43*, 4513.
- (94) Zade, S. S.; Panda, S.; Singh, H. B.; Sunoj, R. B.; Butcher, R. J. *J. Org. Chem.* **2005**, *70*, 3693.
- (95) Wada, M.; Nobuki, S.; Tenkyuu, Y.; Natsume, S.; Asahara, M.; Erabi, T. *J. Organomet. Chem.* **1999**, *580*, 282.
- (96) Kumar, S.; Singh, H. B.; Wolmershäuser, G. *Organometallics* **2006**, *25*, 382.
- (97) Bhabak, K. P.; Mughesh, G. *Chem. Asian J.* **2009**, *4*, 974.
- (98) Kuzma, D.; Parvez, M.; Back, T. G. *Org. Biomol. Chem.* **2007**, *5*, 3213.
- (99) Klapötke, T. M.; Krumm, B.; Scherr, M. *Eur. J. Inorg. Chem.* **2008**, 4413.
- (100) (a) Klapötke, T. M.; Krumm, B.; Mayer, P.; Piotrowski, H.; Schwab, I.; Vogt, M. *Eur. J. Inorg. Chem.* **2002**, 2701. (b) Klapötke, T. M.;

- Krumm, B.; Mayer, P.; Piotrowski, H.; Polborn, K.; Schwab, I. Z. *Anorg. Allg. Chem.* **2002**, 628, 1831.
- (101) Iwaoka, M.; Tomoda, S. *J. Am. Chem. Soc.* **1994**, 116, 4463.
- (102) Iwaoka, M.; Komatsu, H.; Tomoda, S. *Bull. Chem. Soc. Jpn.* **1996**, 69, 1825.
- (103) Wu, R.; Hernández, G.; Odom, J.; Dunlap, R.; Silks, L. *J. Chem. Soc., Chem. Commun.* **1996**, 1125.
- (104) Narayanan, S.; Sridevi, B.; Chandrashekar, T.; Vij, A.; Roy, R. *Angew. Chem., Int. Ed.* **1998**, 37, 3394.
- (105) Silks, R.; Wu, R.; Dunlap, R.; Odom, J. *Phosphorus, Sulfur Silicon Relat. Elem.* **1998**, 136, 137, & 138, 209.
- (106) Okamura, T.; Taniuchi, K.; Lee, K.; Yamamoto, H.; Ueyama, N.; Nakamura, A. *Inorg. Chem.* **2006**, 45, 9347.
- (107) Hope, H. *Acta Crystallogr.* **1965**, 18, 259.
- (108) Bensch, W.; Näther, C.; Schur, M. *J. Chem. Soc., Chem. Commun.* **1997**, 1773.
- (109) Sarkar, B.; Fang, C.-S.; You, L.-Y.; Wang, J.-C.; Liu, C. W. *New J. Chem.* **2009**, 33, 626.
- (110) (a) Nakanishi, W.; Hayashi, S.; Sakaue, A.; Ono, G.; Kawada, Y. *J. Am. Chem. Soc.* **1998**, 120, 3635. (b) Nakanishi, W.; Hayashi, S. *J. Org. Chem.* **2002**, 67, 38.
- (111) Hayashi, S.; Wada, H.; Ueno, T.; Nakanishi, W. *J. Org. Chem.* **2006**, 71, 5574.
- (112) Yamane, K.; Hayashi, S.; Nakanishi, W.; Sasamori, T.; Tokitoh, N. *Polyhedron* **2008**, 27, 2478.
- (113) Yamane, K.; Hayashi, S.; Nakanishi, W.; Sasamori, T.; Tokitoh, N. *Polyhedron* **2008**, 27, 3557.
- (114) (a) Iwaoka, M.; Komatsu, H.; Katsuda, T.; Tomoda, S. *J. Am. Chem. Soc.* **2002**, 124, 1902. (b) Iwaoka, M.; Katsuda, T.; Tomoda, S.; Harada, J. *Chem. Lett.* **2002**, 578.
- (115) Iwaoka, M.; Katsuda, T.; Komatsu, H.; Tomoda, S. *J. Org. Chem.* **2005**, 70, 321.
- (116) Iwaoka, M.; Komatsu, H.; Tomoda, S. *Chem. Lett.* **1998**, 969.
- (117) Iwaoka, M.; Komatsu, H.; Tomoda, S. *J. Organomet. Chem.* **2000**, 611, 164.
- (118) du Mont, W.-W.; Bätcher, M.; Daniliuc, C.; Devillanova, F. A.; Druckenbrodt, C.; Jeske, J.; Jones, P. G.; Lippolis, V.; Ruthe, F.; Seppälä, E. *Eur. J. Inorg. Chem.* **2008**, 4562.
- (119) (a) Tiecco, M.; Testaferri, L.; Bagnoli, L.; Marini, F.; Temperini, A.; Tomassini, C.; Santi, C. *Tetrahedron Lett.* **2000**, 41, 3241. (b) Tiecco, M.; Testaferri, L.; Santi, C.; Tomassini, C.; Marini, F.; Bagnoli, L.; Temperini, A. *Chem.—Eur. J.* **2002**, 8, 1118. (c) Tiecco, M.; Testaferri, L.; Santi, C.; Tomassini, C.; Bonini, R.; Marini, F.; Bagnoli, L.; Temperini, A. *Org. Lett.* **2004**, 6, 4751. (d) Tiecco, M.; Testaferri, L.; Santi, C.; Tomassini, C.; Marini, F.; Bagnoli, L.; Temperini, A. *Angew. Chem., Int. Ed.* **2003**, 42, 3131. (e) Tiecco, M.; Testaferri, L.; Bagnoli, L.; Marini, F.; Santi, C.; Temperini, A.; Scarponi, C.; Sternativo, S.; Terlizzi, R.; Tomassini, C. *ARKIVOC* **2006**, 186.
- (120) Tiecco, M.; Testaferri, L.; Santi, C.; Tomassini, C.; Santoro, S.; Marini, F.; Bagnoli, L.; Temperini, A.; Costantino, F. *Eur. J. Org. Chem.* **2006**, 4867.
- (121) Fujihara, H.; Akaishi, R.; Erata, T.; Furukawa, N. *J. Chem. Soc., Chem. Commun.* **1989**, 1789.
- (122) Ritch, J. S.; Chivers, T.; Eisler, D. J.; Tuononen, H. M. *Chem.—Eur. J.* **2007**, 13, 4643.
- (123) Fujihara, H.; Yabe, M.; Chiu, J.; Furukawa, N. *Tetrahedron Lett.* **1991**, 34, 4345.
- (124) Fujihara, H.; Saito, R.; Yabe, M.; Furukawa, N. *Chem. Lett.* **1992**, 1437.
- (125) Hayashi, S.; Nakanishi, W. *Bull. Chem. Soc. Jpn.* **2008**, 81, 1605.
- (126) Fujihara, H.; Mima, H.; Erata, T.; Furukawa, N. *J. Am. Chem. Soc.* **1992**, 114, 3117.
- (127) Nakahodo, T.; Takahashi, O.; Horn, E.; Furukawa, N. *J. Chem. Soc., Chem. Commun.* **1997**, 1767.
- (128) Nakanishi, W.; Hayashi, S.; Toyota, S. *Chem. Commun.* **1996**, 371.
- (129) Nakanishi, W.; Hayashi, S.; Yamaguchi, H. *Chem. Lett.* **1996**, 947.
- (130) Nakanishi, W.; Hayashi, S.; Yamaguchi, H. *J. Org. Chem.* **1998**, 63, 8790.
- (131) Nakanishi, W.; Hayashi, S.; Morinaka, S.; Sasamori, T.; Tokitoh, N. *New J. Chem.* **2008**, 32, 1881.
- (132) Nakanishi, W.; Hayashi, S.; Itoh, N. *J. Org. Chem.* **2004**, 69, 1676.
- (133) Dyker, G.; Hagel, M.; Henkel, G.; Köckerling, M.; Näther, Ch.; Petersen, S.; Schiemenz, G. P. Z. *Naturforsch., B: Chem. Sci.* **2001**, 56, 1109.
- (134) Kienitz, C.; Thöne, C.; Jones, P. G. *Inorg. Chem.* **1996**, 35, 3990.
- (135) (a) Bochmann, M. *Chem. Vap. Deposition* **1996**, 2, 85. (b) Park, H. S.; Mokhtari, M.; Roesky, H. W. *Chem. Vap. Deposition* **1996**, 2, 135. (c) Manasevit, H. W.; Simpson, W. I. *J. Electrochem. Soc.* **1971**, 118, 644.
- (136) Bierbach, U.; Reedijk, J. *Angew. Chem., Int. Ed.* **1994**, 33, 1632.
- (137) Lai, C.; Naiini, A.; Brubaker, C., Jr. *Inorg. Chim. Acta* **1989**, 164, 205.
- (138) Nishibayashi, Y.; Singh, J. D.; Segawa, K.; Fukuzawa, S.; Uemura, S. *J. Chem. Soc., Chem. Commun.* **1994**, 1375.
- (139) Nishibayashi, Y.; Singh, J. D.; Fukuzawa, S.; Uemura, S. *Tetrahedron Lett.* **1994**, 35, 3115.
- (140) Nishibayashi, Y.; Segawa, K.; Ohe, K.; Uemura, S. *Organometallics* **1995**, 14, 5486.
- (141) Nishibayashi, Y.; Uemura, S. *Synlett* **1995**, 79.
- (142) Bolm, C.; Kesselgraber, M.; Grenz, A.; Hermanns, N.; Hildebrand, J. *New J. Chem.* **2001**, 13.
- (143) You, S.-L.; Hou, X.-L.; Dai, L.-X. *Tetrahedron: Asymmetry* **2000**, 11, 1495.
- (144) Nishibayashi, Y.; Segawa, K.; Singh, J. D.; Fukuzawa, S.; Ohe, K.; Uemura, S. *Organometallics* **1996**, 15, 370.
- (145) Nishibayashi, Y.; Singh, J. D.; Fukuzawa, S.; Uemura, S. *J. Org. Chem.* **1995**, 60, 4114.
- (146) Nishibayashi, Y.; Singh, J. D.; Fukuzawa, S.; Uemura, S. *J. Chem. Soc., Perkin Trans. 1* **1995**, 2871.
- (147) Khanna, A.; Bala, A.; Khandelwal, B. L. *J. Organomet. Chem.* **1995**, 494, 199.
- (148) Jones, P.; Ramírez de Arellano, M. C. *J. Chem. Soc., Dalton Trans.* **1996**, 2713.
- (149) Mautner, H.; Chu, S.; Lee, C. *J. Org. Chem.* **1962**, 27, 3671.
- (150) Ehara, H.; Noguchi, M.; Sayama, S.; Onami, T. *J. Chem. Soc., Perkin Trans. 1* **2000**, 1429.
- (151) Apte, S. D.; Zade, S. S.; Singh, H. B.; Butcher, R. J. *Organometallics* **2003**, 22, 5473.
- (152) Hiroi, K.; Suzuki, Y.; Abe, I. *Tetrahedron: Asymmetry* **1999**, 10, 1173.
- (153) Enders, D.; Peters, R.; Lochtmann, R.; Raabe, G. *Angew. Chem., Int. Ed.* **1999**, 38, 2421.
- (154) (a) Ulman, A.; Manassen, J.; Frolow, F.; Rabinovich, D. *Tetrahedron Lett.* **1978**, 19, 167. (b) Hill, R. L.; Gouterman, M.; Ulman, A. *Inorg. Chem.* **1982**, 21, 1450. (c) Stein, P.; Ulman, A.; Spiro, T. G. *J. Phys. Chem.* **1984**, 88, 369. (d) Vogel, E.; Röhrig, P.; Sicken, M.; Knipp, B.; Herrmann, A.; Pohl, M.; Schmickler, H.; Lex, J. *Angew. Chem., Int. Ed. Engl.* **1989**, 28, 1651. (e) Vogel, E.; Fröde, C.; Breihan, A.; Schmickler, H.; Lex, J. *Angew. Chem. Int. Ed. Engl.* **1997**, 36, 2609. (f) Ulman, A.; Manassen, J.; Frolow, F.; Rabinovich, D. *J. Am. Chem. Soc.* **1979**, 101, 7055. (g) Ulman, A.; Manassen, J.; Frolow, F.; Rabinovich, D. *Inorg. Chem.* **1981**, 20, 1987.
- (155) Lisowski, J.; Sessler, L.; Lynch, V. *Inorg. Chem.* **1995**, 34, 3567.
- (156) Srinivasan, A.; Pushpan, S. K.; Ravikumar, M.; Chandrashekar, T. K.; Roy, R. *Tetrahedron* **1999**, 55, 6671.
- (157) Panda, A.; Menon, S. C.; Singh, H. B.; Morley, C. P.; Bachman, R.; Cocker, T. M.; Butcher, R. J. *Eur. J. Inorg. Chem.* **2005**, 1114.
- (158) Patel, U.; Singh, H. B.; Butcher, R. J. *Eur. J. Inorg. Chem.* **2006**, 5089.
- (159) Panda, S.; Zade, S. S.; Singh, H. B.; Butcher, R. J. *Eur. J. Inorg. Chem.* **2006**, 172.
- (160) Panda, S.; Singh, H. B.; Butcher, R. J. *Chem. Commun.* **2004**, 322.
- (161) Panda, S.; Singh, H. B.; Butcher, R. J. *Inorg. Chem.* **2004**, 43, 8532.
- (162) (a) Steigerwald, M. L.; Sprinkle, C. R. *J. Am. Chem. Soc.* **1987**, 109, 7200. (b) Steigerwald, M. L. *Chem. Mater.* **1989**, 1, 52.
- (163) (a) Aso, Y.; Yamashita, H.; Otsubu, T.; Ogura, F. *J. Org. Chem.* **1989**, 54, 5627. (b) Inokuch, T.; Kusumoto, M.; Torii, S. *J. Org. Chem.* **1990**, 55, 1548.
- (164) Gornitzka, H.; Besser, S.; Herbst-Irmer, R.; Kilimann, U.; Edelmann, F. T. *Angew. Chem., Int. Ed. Engl.* **1992**, 31, 9.
- (165) Crespo, O.; Gimeno, M. C.; Laguna, A.; Kulcsar, M.; Silvestru, C. *Inorg. Chem.* **2009**, 48, 4134.
- (166) Mugesh, G.; Singh, H. B.; Patel, R. P.; Butcher, R. J. *Inorg. Chem.* **1998**, 37, 2663.
- (167) Mugesh, G.; Singh, H. B.; Butcher, R. J. *Eur. J. Inorg. Chem.* **1999**, 1229.
- (168) Kandasamy, K.; Singh, H. B.; Kulshreshtha, S. K. *J. Chem. Sci.* **2009**, 121, 293.
- (169) Mugesh, G.; Singh, H. B.; Butcher, R. J. *J. Chem. Res. (S)* **1999**, 416.
- (170) Kandasamy, K.; Singh, H. B.; Wolmershäuser, G. *Inorg. Chim. Acta* **2005**, 358, 207.
- (171) (a) Dey, S.; Jain, V. K.; Chaudhury, S.; Knoedler, A.; Lissner, F.; Kaim, W. *J. Chem. Soc., Dalton Trans.* **2001**, 723. (b) Dey, S.; Jain, V. K.; Chaudhury, S.; Knoedler, A.; Kaim, W. *Polyhedron* **2003**, 22, 489. (c) Dey, S.; Jain, V. K.; Knoedler, A.; Klein, A.; Kaim, W.; Zalis, S. *Inorg. Chem.* **2002**, 41, 2864. (d) Dey, S.; Jain, V. K.; Knoedler, A.; Klein, A.; Kaim, W.; Zalis, S. *Eur. J. Inorg. Chem.* **2001**, 2965. (e) Dey, S.; Jain, V. K.; Knoedler, A.; Kaim, W. *Inorg. Chim. Acta* **2003**, 349, 104. (f) Dey, S.; Jain, V. K.; Klein, A.; Kaim, W. *Inorg. Chem. Commun.* **2004**, 7, 601.
- (172) Dey, S.; Kumbhare, L. B.; Jain, V. K.; Schurr, T.; Kaim, W.; Klein, A.; Belaj, F. *Eur. J. Org. Chem.* **2004**, 4510.
- (173) Proctor, D. J. *J. Chem. Soc., Perkin Trans. 1* **1999**, 641.

- (174) (a) Nishibayashi, Y.; Uemura, S. *Top. Curr. Chem.* **2000**, 208, 201, and references therein.
- (175) (a) Kshirsagar, T.; Moe, S.; Portoghese, P. *J. Org. Chem.* **1998**, 63, 1704. (b) Reich, H. J.; Yelm, K. E.; Wollowitz, S. *J. Am. Chem. Soc.* **1983**, 105, 2503. (c) Komatsu, N.; Nishibayashi, Y.; Uemura, S. *Tetrahedron Lett.* **1993**, 34, 2339.
- (176) (a) Davis, F. A.; Reddy, R. T. *J. Org. Chem.* **1992**, 57, 2599. (a) Reich, H. J.; Yelm, K. E. *J. Org. Chem.* **1991**, 56, 5672.
- (177) (a) Mughesh, G.; Panda, A.; Singh, H. B.; Puneekar, N. S.; Butcher, R. J. *Chem. Commun.* **1998**, 2227. (b) Mughesh, G.; Panda, A.; Singh, H. B.; Puneekar, N. S.; Butcher, R. J. *J. Am. Chem. Soc.* **2001**, 123, 839.
- (178) Chiba, T.; Nishibayashi, Y.; Singh, J. D.; Ohe, K.; Uemura, S. *Tetrahedron Lett.* **1995**, 36, 1519.
- (179) Nishibayashi, Y.; Chiba, T.; Ohe, K.; Uemura, S. *J. Chem. Soc., Chem. Commun.* **1995**, 1243.
- (180) Kurose, N.; Takahashi, T.; Koizumi, T. *J. Org. Chem.* **1996**, 61, 2932.
- (181) Miyake, Y.; Oda, M.; Oyamada, A.; Takada, H.; Ohe, K.; Uemura, S. *J. Organomet. Chem.* **2000**, 611, 475.
- (182) (a) Schmidt, G. H.; Garratt, D. G. In *The Chemistry of Double-Bonded Functional Groups*; Patai, S., Ed.; Wiley: London, 1977. (b) Garratt, D. G.; Kabo, A. *Can. J. Chem.* **1980**, 58, 1030.
- (183) Tomoda, S.; Iwaoka, M. *Chem. Lett.* **1988**, 1895.
- (184) Tomoda, S.; Fujita, K.; Iwaoka, M. *J. Chem. Soc., Chem. Commun.* **1990**, 129.
- (185) Fujita, K.; Iwaoka, M.; Tomoda, S. *Chem. Lett.* **1994**, 923.
- (186) (a) Fujita, K.; Murata, K.; Iwaoka, M.; Tomoda, S. *Tetrahedron Lett.* **1995**, 36, 5219. (b) Fujita, K.; Murata, K.; Iwaoka, M.; Tomoda, S. *J. Chem. Soc., Chem. Commun.* **1995**, 1641.
- (187) Fukuzawa, S.; Kasugahara, Y.; Uemura, S. *Tetrahedron Lett.* **1994**, 35, 9403.
- (188) Fukuzawa, S.; Takahashi, K.; Kato, H.; Yamazaki, H. *J. Org. Chem.* **1997**, 62, 7711.
- (189) (a) Wirth, T. *Angew. Chem., Int. Ed. Engl.* **1995**, 34, 1726. (b) Wirth, T.; Fragale, G. *Chem.—Eur. J.* **1997**, 3, 1894.
- (190) Burgler, F. W.; Gragale, G.; Wirth, T. *ARKIVOC* **2007**, 21.
- (191) Déziel, R.; Malenfant, E.; Belanger, G. *J. Org. Chem.* **1996**, 61, 1875.
- (192) Déziel, R.; Goulet, S.; Grenier, L.; Bordeleau, J.; Bernier, J. *J. Org. Chem.* **1993**, 58, 3619.
- (193) Déziel, R.; Malenfant, E.; Thibault, C.; Frechette, S.; Gravel, M. *Tetrahedron Lett.* **1997**, 38, 4753.
- (194) Fujita, K.; Murata, K.; Iwaoka, M.; Tomoda, S. *Tetrahedron* **1997**, 53, 2029.
- (195) (a) Fragale, G.; Neuberger, M.; Wirth, T. *J. Chem. Soc., Chem. Commun.* **1998**, 3625. (b) Uehlin, L.; Fragale, G.; Wirth, T. *Chem.—Eur. J.* **2002**, 8, 1125.
- (196) Wirth, T.; Kulicke, K.; Fragale, G. *Helv. Chim. Acta* **1996**, 79, 1957.
- (197) Santi, C.; Fragale, G.; Wirth, T. *Tetrahedron: Asymmetry* **1998**, 9, 3625.
- (198) (a) Back, T. G.; Dyck, B.; Nan, S. *Tetrahedron* **1999**, 55, 3191. (b) Back, T. G.; Moussa, Z.; Parvez, M. *J. Org. Chem.* **2002**, 67, 499.
- (199) (a) Tiecco, M.; Testaferri, L.; Santi, C.; Marini, F.; Bagnoli, L.; Temperini, A. *Tetrahedron Lett.* **1998**, 39, 2809. (b) Tiecco, M.; Testaferri, L.; Santi, C.; Marini, F.; Bagnoli, L.; Temperini, A.; Tomassini, C. *Eur. J. Org. Chem.* **1998**, 2275.
- (200) Tiecco, M.; Testaferri, L.; Marini, F.; Santi, C.; Bagnoli, L.; Temperini, A. *Tetrahedron: Asymmetry* **1999**, 747.
- (201) Poleschner, H.; Seppelt, K. *Angew. Chem., Int. Ed.* **2008**, 47, 6461.
- (202) Denmark, S. E.; Collins, W. R.; Cullen, M. D. *J. Am. Chem. Soc.* **2009**, 131, 3490.
- (203) Wang, X.; Houk, K. N.; Spichty, M.; Wirth, T. *J. Am. Chem. Soc.* **1999**, 121, 8567.
- (204) Spichty, M.; Fragale, G.; Wirth, T. *J. Am. Chem. Soc.* **2000**, 122, 10914.
- (205) Wang, H.-Y.; Yang, F.; Li, X.-L.; Yan, X.-M.; Huang, Z.-Z. *Chem.—Eur. J.* **2009**, 15, 3784.
- (206) Tiecco, M.; Testaferri, L.; Santi, C.; Tomassini, C.; Marini, F.; Bagnoli, L.; Temperini, A. *Tetrahedron: Asymmetry* **2000**, 11, 4645.
- (207) Santi, C.; Tiecco, M.; Testaferri, L.; Tomassini, C.; Santoro, S.; Bizzoca, G. *Phosphorus, Sulfur Silicon Relat. Elem.* **2008**, 183, 956.
- (208) Uchiyama, M.; Satoh, S.; Ohta, A. *Tetrahedron Lett.* **2001**, 42, 1559.
- (209) Uchiyama, M.; Oka, M.; Harai, S.; Ohta, A. *Tetrahedron Lett.* **2001**, 42, 1931.
- (210) Pedrosa, R.; Andrés, C.; Arias, R.; Mendiguchía, P.; Nieto, J. *J. Org. Chem.* **2006**, 71, 2424.
- (211) (a) Tiecco, M.; Tingoli, M.; Testaferri, L. *Pure Appl. Chem.* **1993**, 65, 715. (b) Tiecco, M.; Testaferri, L.; Tingoli, M.; Chianelli, D.; Bartoli, D. *J. Org. Chem.* **1991**, 56, 4529. (c) Tiecco, M.; Testaferri, L.; Tingoli, M.; Bartoli, D. *J. Org. Chem.* **1990**, 55, 4523. (d) Tiecco, M.; Testaferri, L.; Tingoli, M.; Bartoli, D.; Marini, F. *J. Org. Chem.* **1991**, 56, 5207. (e) Tiecco, M.; Testaferri, L.; Tingoli, M.; Bagnoli, L.; Luana, S. *J. Chem. Soc., Chem. Commun.* **1993**, 637. (f) Tiecco, M.; Testaferri, L.; Tingoli, M.; Bagnoli, L.; Santi, C. *Synlett* **1993**, 798. (g) Tiecco, M.; Testaferri, L.; Santi, C. *Eur. J. Org. Chem.* **1999**, 797.
- (212) Wirth, T.; Hauptli, S.; Leuenberger, M. *Tetrahedron: Asymmetry* **1998**, 9, 547.
- (213) (a) Browne, D. M.; Niyomura, O.; Wirth, T. *Org. Lett.* **2007**, 9, 3169. (b) Browne, D. M.; Niyomura, O.; Wirth, T. *Phosphorus, Sulfur Silicon Relat. Elem.* **2008**, 183, 1026.
- (214) Okamoto, K.; Nishibayashi, Y.; Uemura, S.; Toshimitsu, A. *Angew. Chem., Int. Ed.* **2005**, 44, 3588.
- (215) Nishibayashi, Y.; Srivastava, S.; Takada, H.; Fukuzawa, S.; Uemura, S. *J. Chem. Soc., Chem. Commun.* **1995**, 2321.
- (216) Ley, S. V. In *Organoselenium-Mediated Cyclisation Reactions in Organic Synthesis*. Papers presented at a meeting of the Fine Chemicals Group of the SCI, London, 1984.
- (217) Campos, M. D. M.; Petragiani, N. *Chem. Ber.* **1960**, 93, 317.
- (218) Takada, H.; Nishibayashi, Y.; Uemura, S. *J. Chem. Soc., Perkin Trans 1* **1999**, 1511.
- (219) Back, T. G.; Dyck, B. *P. Chem. Commun.* **1996**, 2567.
- (220) Fragale, G.; Wirth, T. *Eur. J. Org. Chem.* **1998**, 1361.
- (221) Déziel, R.; Malenfant, E.; Thibault, C. *Tetrahedron Lett.* **1998**, 39, 5493.
- (222) Tiecco, M.; Testaferri, L.; Bagnoli, L.; Scarponi, C.; Purgatorio, V.; Temperini, A.; Marini, F.; Santi, C. *Tetrahedron: Asymmetry* **2005**, 16, 2429.
- (223) Fujihara, H.; Mima, H.; Furukawa, N. *Tetrahedron* **1996**, 52, 10375.
- (224) Wirth, T.; Kulicke, K.; Fragale, G. *J. Org. Chem.* **1996**, 61, 2686.
- (225) Wirth, T. *Leibigs, Ann./Rec.* **1997**, 1155.
- (226) Wirth, T. *Tetrahedron Lett.* **1995**, 36, 7849.
- (227) Bolm, C.; Kesselgraber, M.; Grehz, A.; Hermanns, N.; Hilderbrand, J. P. *New J. Chem.* **2001**, 13.
- (228) Okoroafor, M.; Shen, L.; Honeychuck, R.; Brubaker, C., Jr. *Organometallics* **1988**, 7, 1297.
- (229) (a) Drake, M. D.; Bateman, M. A.; Detty, M. R. *Organometallics* **2003**, 22, 4158. (b) Drake, M. D.; Bright, F. V.; Detty, M. R. *J. Am. Chem. Soc.* **2003**, 125, 12558.
- (230) Goodman, M. A.; Detty, M. R. *Organometallics* **2004**, 23, 3016.
- (231) Cooper, M.; Ward, D. *Tetrahedron Lett.* **1995**, 36, 2327.
- (232) (a) Tiecco, M.; Testaferri, L.; Santi, C.; Tomassini, C.; Bonini, R.; Marini, F.; Bagnoli, L.; Temperini, A. *Org. Lett.* **2004**, 6, 4751. (b) Santi, C.; Tiecco, M.; Testaferri, L.; Tomassini, C.; Marini, F.; Bagnoli, L.; Temperini, A. *Phosphorus, Sulfur Silicon Relat. Elem.* **2005**, 180, 1071. (c) Santi, C.; Santoro, S.; Tomassini, C.; Pascolini, F.; Testaferri, L.; Tiecco, M. *Synlett* **2009**, 743.
- (233) Ceccherelli, P.; Curini, M.; Epifano, F.; Marcotullio, M.; Rosati, O. *Tetrahedron: Asymmetry* **1998**, 9, 919.
- (234) Ceccherelli, P.; Curini, M.; Epifano, F.; Marcotullio, M.; Rosati, O. *Tetrahedron Lett.* **1995**, 36, 5079.
- (235) Wirth, T.; Fragale, G. *Synthesis* **1998**, 2, 162.
- (236) Miyake, Y.; Oda, M.; Oyamada, A.; Takada, H.; Ohe, K.; Uemura, S. *J. Organomet. Chem.* **2000**, 611, 475.
- (237) (a) Flohé, L. Glutathione Peroxidase Brought into Focus. In *Free Radicals in Biology*; Pryor, W. A., Ed.; Academic Press: 1982. (b) Flohé, L.; Loschen, G.; Günzler, W. A.; Eichelle, E. *Z. Physiol. Chem.* **1972**, 353, 987. (c) *Selenium in Biology and Human Health*; Burk, R. F., Ed.; Springer-Verlag: New York, 1994. (d) Flohé, L. *Curr. Top. Cell. Regul.* **1985**, 27, 473. (e) Tappel, A. L. *Curr. Top. Cell. Regul.* **1984**, 24, 87. (f) Epp, O.; Ladenstein, R.; Wendel, A. *Eur. J. Biochem.* **1983**, 133, 51.
- (238) Ladenstein, R.; Epp, O.; Bartels, K.; Jones, A.; Huber, R.; Wendel, A. *J. Mol. Biol.* **1979**, 134, 199.
- (239) Forstrom, J. W.; Zakowski, J. J.; Tappel, A. L. *Biochemistry* **1978**, 17, 2639.
- (240) Böck, A.; Forchhammer, K. J. H.; Baron, C. *TIBS*, 16 December, 1991.
- (241) Ren, B.; Huang, W.; Åkesson, B.; Ladenstein, R. *J. Mol. Biol.* **1997**, 268, 869.
- (242) Mughesh, G.; Singh, H. B. *Chem. Soc. Rev.* **2000**, 29, 347.
- (243) Prabhakar, R.; Vreven, T.; Morokuma, K.; Musaev, D. G. *Biochemistry* **2005**, 44, 11864.
- (244) Schewe, T. *Gen. Pharmacol.* **1995**, 26, 1153.
- (245) (a) Müller, A.; Cadenas, E.; Graf, P.; Sies, H. *Biochem. Pharmacol.* **1984**, 33, 3235. (b) Wendel, A.; Fausel, M.; Safayhi, H.; Tiegs, G.; Otter, R. *Biochem. Pharmacol.* **1984**, 33, 3241. (c) Parnham, M.; Graf, E. *Biochem. Pharmacol.* **1987**, 36, 3095. (d) Lesser, R.; Weiss, B. *Ber. Dtsch. Chem. Ges.* **1924**, 57, 1077.
- (246) (a) Lambert, C.; Hilbert, M.; Christaens, L.; Dereu, N. *Synth. Commun.* **1991**, 21, 85. (b) Ruwet, A.; Renson, M. *Bull. Soc. Chim. Belg.* **1969**, 78, 571. (c) Weber, R.; Renson, M. *Bull. Soc. Chim. Fr.* **1976**, 1124. (d) Engman, L.; Hallberg, A. *J. Org. Chem.* **1989**, 54, 2964. (e) Fong, M. C.; Schiesser, C. H. *Tetrahedron Lett.* **1995**, 36, 7329. (f) Fong, M. C.; Schiesser, C. H. *J. Org. Chem.* **1997**, 62, 3103.

- (247) (a) Fischer, H.; Dereu, N. *Bull. Soc. Chim. Belg.* **1987**, *96*, 757. (b) Engman, L.; Stern, D.; Cotgreave, I. A.; Andersson, C. M. *J. Am. Chem. Soc.* **1992**, *114*, 9737. (c) Maiorino, M.; Roveri, A.; Coassin, M.; Ursini, F. *Biochem. Pharmacol.* **1988**, *37*, 2267. (d) Back, T. G.; Dyck, B. P. *J. Am. Chem. Soc.* **1997**, *119*, 2079. (e) Pearson, J. K.; Boyd, R. J. *J. Phys. Chem. A* **2006**, *110*, 8979.
- (248) Sarma, B. K.; Mughesh, G. *Chem.—Eur. J.* **2008**, *14*, 10603.
- (249) Jacquemin, P. V.; Christaens, L. E.; Renson, M. J.; Evers, M. J.; Dereu, N. *Tetrahedron Lett.* **1992**, *33*, 3863.
- (250) (a) Reich, H. J.; Jasperse, C. P. *J. Am. Chem. Soc.* **1987**, *109*, 5549. (b) Chaudiere, J.; Erdelmeier, I.; Moutet, M.; Yadan, J. C. *Phosphorus, Sulfur Silicon Relat. Elem.* **1998**, *136–138*, 467.
- (251) (a) Galet, V.; Bernier, J. L.; Hénichart, J. P.; Lesieur, D.; Abadie, C.; Rochette, L.; Lindenbaum, A.; Chalas, J.; Renaud de la Faverie, J. F.; Pfeiffer, B.; Renard, P. *J. Med. Chem.* **1994**, *37*, 2903. (b) Wilson, S. R.; Zucker, P. A.; Huang, R. C.; Spector, A. J. *Am. Chem. Soc.* **1989**, *111*, 5936. (c) Wu, Z. P.; Hilvert, D. J. *Am. Chem. Soc.* **1989**, *111*, 4513. (d) Wu, Z. P.; Hilvert, D. J. *Am. Chem. Soc.* **1990**, *112*, 5647.
- (252) (a) House, K. L.; Dunlap, R. B.; Odom, J. D.; Wu, Z. P.; Hilvert, D. J. *Am. Chem. Soc.* **1992**, *114*, 8573. (b) Bell, I. M.; Hilvert, D. *Biochemistry* **1993**, *32*, 13969. (c) Syed, R.; Wu, Z. P.; Hogle, J. M.; Hilvert, D. *Biochemistry* **1993**, *32*, 6157. (d) Bell, I. M.; Fisher, M. L.; Wu, Z. P.; Hilvert, D. *Biochemistry* **1993**, *32*, 3754. (e) House, K. L.; Garbe, A. R.; Dunlap, R. B.; Odom, J. D.; Hilvert, D. *Biochemistry* **1993**, *32*, 3468. (f) Peterson, E. B.; Hilvert, D. *Tetrahedron* **1997**, *53*, 12311.
- (253) Aumann, K. D.; Bedorf, N.; Brigelius-Flohe, R.; Schomburg, D.; Flohé, L. *Biomed. Environ. Sci.* **1997**, *10*, 136.
- (254) Parnham, M. J.; Kindt, S. *Biochem. Pharmacol.* **1984**, *33*, 3247.
- (255) Kumar, S.; Singh, H. B. *J. Chem. Sci.* **2005**, *117*, 621.
- (256) Engman, L.; Andersson, C.; Morgenstern, R.; Cotgreave, I. A.; Anderson, C. M.; Hallberg, A. *Tetrahedron* **1994**, *50*, 2929.
- (257) Wirth, T. *Molecules* **1998**, *3*, 164.
- (258) (a) Back, T. G.; Moussa, Z. J. *Am. Chem. Soc.* **2002**, *124*, 12104. (b) Back, T. G.; Moussa, Z. J. *Am. Chem. Soc.* **2003**, *125*, 13455. (c) Back, T. G.; Moussa, Z.; Parvez, M. *Angew. Chem.* **2004**, *116*, 1288. *Angew. Chem., Int. Ed.* **2004**, *43*, 1268.
- (259) Bhabak, K. P.; Mughesh, G. *Chem.—Eur. J.* **2007**, *13*, 4594.
- (260) Bhabak, K. P.; Mughesh, G. *Chem.—Eur. J.* **2008**, *14*, 8640.
- (261) Bhabak, K. P.; Mughesh, G. *Chem.—Eur. J.* **2009**, *15*, 9846.
- (262) Phadnis, P. P.; Mughesh, G. *Org. Biomol. Chem.* **2005**, *3*, 2476.
- (263) Musaev, D. G.; Geletii, Y. V.; Hill, C. L.; Hirao, K. J. *Am. Chem. Soc.* **2003**, *125*, 3877.
- (264) (a) du Mont, W.-W.; Mughesh, G.; Wismach, C.; Jones, P. G. *Angew. Chem., Int. Ed.* **2001**, *40*, 2486. (b) Mughesh, G.; du Mont, W.-W.; Wismach, C.; Jones, P. G. *ChemBioChem* **2002**, *3*, 440.
- (265) Mughesh, G.; Klotz, L.-O.; du Mont, W.-W.; Becker, K.; Sies, H. *Org. Biomol. Chem.* **2003**, *1*, 2848.
- (266) Wismach, C.; du Mont, W.-W.; Jones, P. G.; Ernst, L.; Papke, U.; Mughesh, G.; Kaim, W.; Wanner, M.; Becker, K. D. *Angew. Chem., Int. Ed.* **2004**, *43*, 3970.
- (267) Roy, G.; Sarma, B. K.; Phadnis, P. P.; Mughesh, G. *J. Chem. Sci.* **2005**, *117*, 287.
- (268) Roy, G.; Mughesh, G. *J. Am. Chem. Soc.* **2005**, *127*, 15207.
- (269) Sarma, B. K.; Mughesh, G. *Inorg. Chem.* **2006**, *45*, 5307.
- (270) Bhabak, K. P.; Mughesh, G. *Inorg. Chem.* **2009**, *48*, 2449.
- (271) (a) Tormena, C. F.; Dias, L. C.; Rittner, R. J. *Phys. Chem. A* **2005**, *109*, 6077. (b) Nakanishi, W.; Hayashi, S.; Hada, M. *Chem.—Eur. J.* **2007**, *13*, 5282. (c) Cmoch, P.; Urbańczyk-Lipkowska, Z.; Petrosyan, A.; Stepień, A.; Staliński, K. *J. Mol. Struct.* **2005**, *733*, 29. (d) Tokunaga, T.; Seki, H.; Yasuike, S.; Ikoma, M.; Kurita, J.; Yamaguchi, K. *Tetrahedron Lett.* **2000**, *41*, 1031.
- (272) Franchetti, P.; Cappellacci, L.; Sheikha, G. A.; Jayaram, H. N.; Gurudutt, V. V.; Sint, T.; Schneider, B. P.; Jones, W. D.; Goldstein, B. M.; Perra, G.; De Montis, A.; Loi, A. G.; La Colla, P.; Grifantini, M. *J. Med. Chem.* **1997**, *40*, 1731.
- (273) Roy, D.; Sunoj, R. B. *J. Mol. Struct.: THEOCHEM* **2007**, *809*, 145.
- (274) Reed, A. E.; Curtiss, L. A.; Weinhold, F. *Chem. Rev.* **1988**, *88*, 899.
- (275) The donor–acceptor interactions lead to a departure from idealized Lewis structure description of a molecule by losing occupancy from the localized Lewis type NBOs into the empty non-Lewis orbitals (delocalization). For each donor NBO (i) and the acceptor NBO (j), the stabilization energy (ES) associated with delocalization is estimated as $ES = E_{ij} = q_i[F(i,j)/2(j-i)]$ where q_i is the donor orbital occupancy, i and j are orbital energies, and $F(i,j)$ is the off-diagonal elements of NBO Fock matrix.
- (276) (a) Giuffreda, M. G.; Bruschi, M.; Luthi, H. P. *Chem.—Eur. J.* **2004**, *10*, 56718. (b) Bruschi, M.; Giuffreda, M. G.; Luthi, H. P. *Chem.—Eur. J.* **2002**, *8*, 4216.
- (277) The covalency factor (χ) for the $A \cdots B$ interaction can be estimated by the following equation $\chi = [(R_A + R_B)_{\text{vdw}} - d_{AB}]/[(R_A + R_B)_{\text{vdw}} - (r_A + r_B)_{\text{cov}}]$ where R and r are the van der Waals and covalent radii, respectively, and d is the distance between the two interacting atoms.
- (278) Sadekov, I. D.; Minkin, V. I.; Zakharov, A. V.; Starikov, A. G.; Borodkin, G. S.; Aldoshin, S. M.; Tkachev, V. V.; Shilov, G. V.; Berry, F. J. J. *Organomet. Chem.* **2005**, *690*, 103.
- (279) (a) Bader, R. F. W. *Atoms in Molecules. A Quantum Theory*; Oxford University Press: Oxford, U.K., 1990. (b) Bader, R. F. W.; Matta, C. F.; Cortés-Guzmán, F. *Organometallics* **2004**, *23*, 6253.
- (280) (a) Arnold, W. D.; Oldfield, E. J. *Am. Chem. Soc.* **2000**, *122*, 12835. (b) Jenkins, S.; Morrison, I. *Chem. Phys. Lett.* **2000**, *317*, 97.
- (281) Rozas, I.; Alkorta, I.; Elguero, J. *J. Am. Chem. Soc.* **2000**, *122*, 11154.
- (282) Biegler-König, F.; Schonbohm, J.; Bayles, D. *J. Comput. Chem.* **2001**, *22*, 545.
- (283) Nakanishi, W.; Nakamoto, T.; Hayashi, S.; Sasamori, T.; Tokitoh, N. *Chem.—Eur. J.* **2007**, *13*, 255.
- (284) Roy, D.; Sunoj, R. B. *J. Phys. Chem. A* **2006**, *110*, 5942.
- (285) (a) Nakanishi, W.; Hayashi, S.; Uehara, T. *J. Phys. Chem. A* **1999**, *103*, 9906. (b) Nakanishi, W.; Hayashi, S. *J. Phys. Chem. A* **1999**, *103*, 6074. (c) Hayashi, S.; Wada, H.; Ueno, T.; Nakanishi, W. *J. Org. Chem.* **2006**, *71*, 5574.
- (286) Wolinski, K.; Hilton, J. F.; Pulay, P. *J. Am. Chem. Soc.* **1990**, *112*, 8251.
- (287) (a) Bayse, C. A. *Inorg. Chem.* **2004**, *43*, 1208. (b) Bayse, C. A. *J. Chem. Theory Comput.* **2005**, *1*, 1119.
- (288) (a) Rasul, G.; Prakash, G. K. S.; Olah, G. A. *J. Phys. Chem. A* **2004**, *108*, 8456. (b) Zhao, Y.; Houk, K. N.; Rechavi, D.; Scarso, A.; Rebek, J., Jr. *J. Am. Chem. Soc.* **2004**, *126*, 11428. (c) Hayashi, S.; Nakanishi, W. *J. Org. Chem.* **1999**, *64*, 6688.
- (289) Roy, D.; Patel, C.; Liebman, J. F.; Sunoj, R. B. *J. Phys. Chem. A* **2008**, *112*, 8797.
- (290) Sarma, B. K.; Mughesh, G. *ChemPhysChem* **2009**, *10*, 3013.
- (291) Hayashi, S.; Yamane, K.; Nakanishi, W. *J. Org. Chem.* **2007**, *72*, 7587.
- (292) Nakanishi, W.; Hayashi, S. *Chem.—Eur. J.* **2008**, *14*, 5645.

CR900352J